

# Three new and one little-known species of Hypogastruridae (Collembola) from Russia's northeast

Anatoly Babenko<sup>1</sup>, Boris Efeykin<sup>1,2</sup>, Mikhail Bizin<sup>1</sup>

**1** Severtsov Institute of Ecology & Evolution, Russian Academy of Sciences, Leninski pr. 33, 119071, Moscow, Russia **2** Kharkevich Institute for Information Transmission Problems, Russian Academy of Sciences, Bol'shoi Karetnyi per. 19, 127051, Moscow, Russia

Corresponding author: Anatoly Babenko ([lsrc@mail.ru](mailto:lsrc@mail.ru))

---

Academic editor: L. Deharveng | Received 29 May 2020 | Accepted 30 November 2020 | Published 18 December 2020

<http://zoobank.org/D58975C5-29E7-45B0-B564-65E379C1EED7>

---

**Citation:** Babenko A, Efeykin B, Bizin M (2020) Three new and one little-known species of Hypogastruridae (Collembola) from Russia's northeast. ZooKeys 1005: 1–20. <https://doi.org/10.3897/zookeys.1005.54882>

---

## Abstract

Three new species, *Hypogastrura variata* **sp. nov.**, *Xenylla aculeata* **sp. nov.**, and *X. arnei* **sp. nov.**, are described based on material from coastal communities of the Sea of Okhotsk, northeast Russia. Taxonomic remarks concerning a little-known species, *H. yosii* Stach, 1964, found in coastal wrack sediments on Kunashir Island, Kuriles are also given. COI sequences of the above species are analysed, thus allowing for their species statuses to be confirmed.

## Keywords

$\alpha$ -taxonomy, coastal communities, DNA sequencing, East Palaearctic, *Hypogastrura*, springtails, *Xenylla*

## Introduction

The first information concerning the collembolan faunas of the Far Eastern regions of Russia was obtained during the expedition of N.A.E. Nordenskjöld aboard the 'Vega' along the northern coasts of Eurasia to the Commander Islands (1878–1879). The material collected by that expedition on the northern coast of Chukotka was published by Schött (1893), who recorded slightly fewer than 20 species of Collembola from the region. Currently, this number totals 466 species (Kuprin and Potapov 2018) and

continues to increase. This paper is devoted to descriptions of three new species of the family Hypogastruridae from the coastal communities in the northern part of the Sea of Okhotsk. Moreover, their statuses are confirmed using both morphological and molecular studies.

## Abbreviations

<b>Abd.1–6</b>	abdominal segments;
<b>A1, A7</b>	tenent seta in distal whorl of setae on tibiotarsi;
<b>a-, m-, p-setae</b>	setae of anterior, medial, and posterior rows on terga, respectively;
<b>A–E papillae and a-, b-, d-, e-guards</b>	labial papillae and associated guards on the labial palp, according to Fjellberg (1999);
<b>Ant.1–4</b>	antennal segments;
<b>L.1–6</b>	maxillary lamellae;
<b>l.p.</b>	lateral process on the labial palp;
<b>MSPU</b>	Zoology and Ecology Department of the Moscow State Pedagogical University;
<b>ms</b>	microsensillum/-a;
<b>or</b>	organite on antennal tip;
<b>PAO</b>	postantennal organ;
<b>S3, S7–S9</b>	antennal sensilla;
<b>VT</b>	ventral tube;
<b>U<sub>3</sub></b>	unguis of leg 3.

## Methods of molecular analysis

DNA was isolated from specimens fixed in 96% ethanol using Holterman's technique (Holterman et al. 2006), with the addition of proteinase K and mercaptoethanol in the lysing solution. Sequences of the cytochrome oxidase subunit I (COI) gene were amplified using an EncycloPlus PCR Kit (Evrogen, Russia) with primers from the Table 1. The standard PCR reaction protocol of the Canadian Center for DNA Barcoding was used for amplifications (<http://www.dnabarcodes2011.org/conference/preconference/CCDB-Amplification-animals.pdf>). Polymerase chain reaction (PCR) products were visualised in gel, cut out, and cleaned using the SV Gel and PCR CleanUp System kit (Evrogen, Russia). DNA sequencing was performed at the Genome Centre for Collective Use in the Severtsov Institute of Ecology and Evolution of Russian Academy of Science (Moscow, Russia). The sequences were combined and aligned using ClustalX software after the addition of sequences from the GenBank. Distance analyses were performed with MEGA6 (Tamura et al. 2013) with the Kimura-2 parameter model (Kimura 1980) to estimate genetic distances. All sequences were deposited into the GenBank.

**Table 1.** Species used for molecular study, primers, and GenBank accession numbers of the sequences.

Species	Forward primer	Reverse primer	COI sequence number	Sequence size
<i>Hypogastrura variata</i> sp. nov.	colfol-for: ttccaacaatcataargayatygg	colfol-rev: taaacttcnggrtgncaaaaaatca	KY066780 KY066781 KY066782 KY066783	660 bp
<i>Hypogastrura yosii</i> Stach, 1964	colfol-for: ttccaacaatcataargayatygg	colfol-rev: taaacttcnggrtgncaaaaaatca	KY066784 KY066785 KY066786	660 bp
<i>Xenylla arnei</i> sp. nov.	LCO1490_t1: tgtaaacgacggccagtg tccaacaatcataagatattgg	HCO2198_t1: caggaaacagctatgactaaacttc agggtgaccaaaaaatca	KY066787 KY066788 KY066789	652 bp

## Species descriptions

### *Hypogastrura variata* sp. nov.

<http://zoobank.org/28CCD965-FD16-4F17-9817-C1FA1A773A51>

Figs 1–23

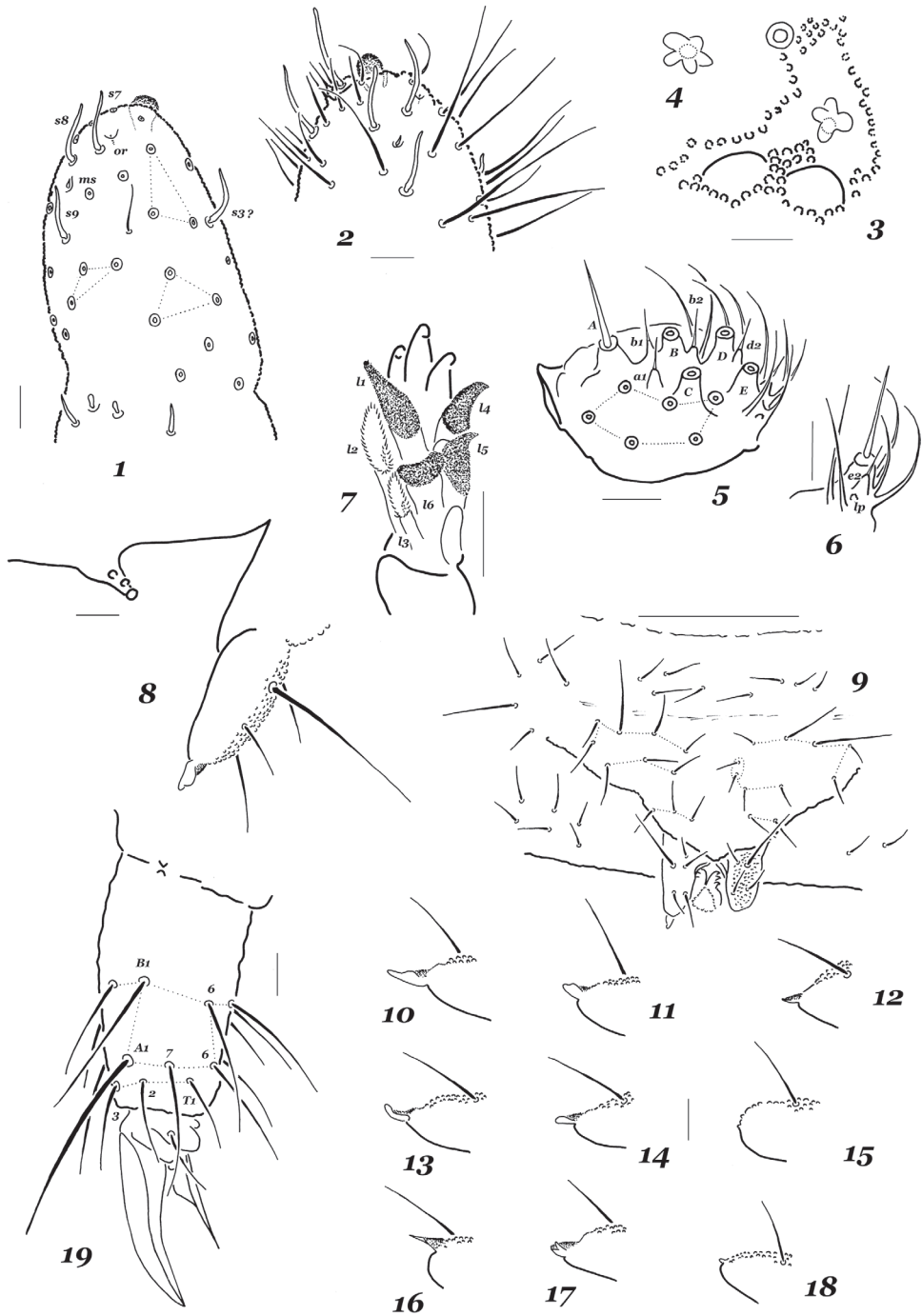
**Type material.** *Holotype* RUSSIA, North-East • ♂; Magadan Province, Ola; 59°36.19'N, 151°21.72'E; maritime marsh with *Carex subspataceae*; July 2017; M. Bizin and B. Efevkin leg.

**Paratypes** RUSSIA, North-East • ♀; same data as for holotype • 13 ♀♀, 6 ♂♂ and 10 juveniles; same region, but Tauisk; 59°44.07'N, 149°23.32'E; maritime marsh with *Puccinellia phryganodes*; July 2017; M. Bizin and B. Efevkin leg. The types are deposited in MSPU.

**Additional material.** more than 300 specimens (alcohol), mainly from the *P. phryganodes* plant association of the same region. Several specimens from this material were sequenced (Table 1). Their partial COI genes were amplified and deposited in the GenBank under the sample ID: KY066780–KY066783.

**Diagnosis.** A species of the genus *Hypogastrura* Bourlet, 1839, with four weakly differentiated, curved, sensory setae (one dorsal and three external) on Ant.4, the relatively clearly differentiated dorsal setae, the tridentate retinaculum, the basal lamella on the unguiculus, one tenent seta on all tibiotarsi, the partly reduced furca with four or five posterior setae, and the highly variable shape of the mucro.

**Description.** Length of males 1.2–1.5 mm, females 1.2–1.8 mm, holotype 1.41 mm long. Colour dark, bluish black, not paler ventrally. Granulations fine and uniform, with 14–18 granules between setae p1 on Abd.5. Ant.4 with a simple apical bulb and four weakly differentiated, curved, sensory setae (one dorsal [S3 ?] and three external [S7, S8, and S9], subapical organite (or) and microsensillum (ms) present as usual (Figs 1, 2). Ant.3 organ typical of the genus, with all usual sensorial elements: two outer guards, two inner sensilla and a lateral microsensillum. Ant.1 and Ant.2 with seven and 13 setae, respectively. Head with 8+8 virtually equal ocelli. PAO slightly smaller than nearest ocelli, usually with four subequal lobes (range 3–6), an



**Figures 1–19.** *Hypogastrura variata* sp. nov. **1** sensory equipment of Ant.3 and Ant.4 **2** tip of Ant.4 **3** PAO and nearest ocelli **4** PAO, different specimen **5** labial palp **6** labial papilla **7** maxillary head **8** furca and retinaculum, lateral view **9** sternum of Abd.4 **10–18** mucro, different specimens **19** tip of leg 3. Scale bars: 0.1 mm (**9**), 0.01 mm (**1–8, 10–19**).

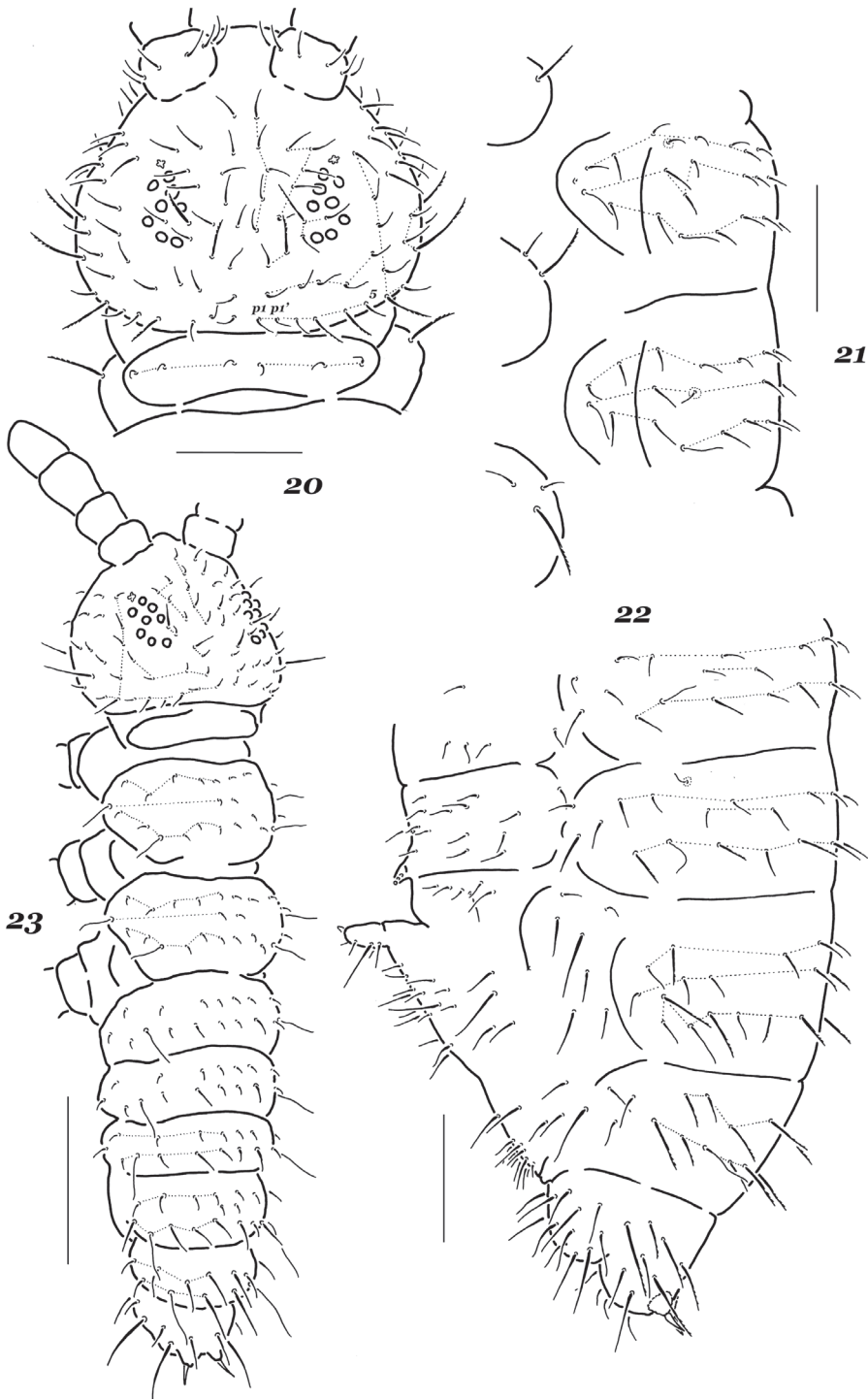
accessory boss not developed (Figs 3, 4). Distal edge of labrum with six low papillae, setal formula of labrum, 4/554. Labium typical of the genus, with all common papillae (A–E), 14 guards (a1, b1, b2, d2, and e2 shorter and set on low papillae) and six proximal setae, lateral process (lp) rudimentary (Figs 5, 6). Basomedial field of labium (submentum) with four setae, basolateral field (mentum) with five setae, as usual. Head with 3+3 postlabial setae present along ventral line. Maxillary head unmodified, of general generic type, L.1 hardly longer than maxillary teeth, L.2 and L.3 with short marginal filaments and usually few denticles, all other lamellae densely covered with fine denticles (Fig. 7), outer lobe simple, with two sublobal hairs.

*Dorsal chaetotaxy* typical of the genus (Figs 20–23). Most dorsal setae stout and finely serrate, those on abdominal tip (Abd.5 and Abd.6) clearly longer and rougher, sensorial setae thin and not especially long compared to ordinary ones. Main characteristics: detectible differentiation into micro- and meso- or macrosetae on all terga including head in adults (Figs 20–22) and, especially, juveniles (Fig. 23), usual presence of an additional seta in p-row on head (six p-setae totally) and abnormal variability (unusual shapes, absence or doubling of certain setae). Chaetotaxy of legs 1–3 as follows: upper subcoxae – 1, 2, 3 (among them, one macroseta on each subcoxa); lower subcoxae – 0, 3, 3; coxae – (2)3, 3, 3; trochanters – 7(8), 7(8), 7; femora – 13–14, 13–14, 12–14; tibiotarsi – 19, 19, 18 setae, respectively. Tenent tibiotarsal setae (A1) of moderate length, ~ as long as 1.1–1.5 inner unguis edge, truncate or indistinctly clavate. Unguis slender and usually toothless, rarely an indistinct tooth present in midsection of inner edge. Unguiculus with a clear basal lamella, its apical filament reaching the middle of inner unguis edge or slightly above (Fig. 19). Ventral tube with 4+4 distal setae. Retinaculum with 3+3 teeth. Furca short (Figs 8, 9), mucro rudimentary, sometimes completely absent (often asymmetrically), its shape highly variable (Figs 10–18). Manubrial field with 10–12+10–12 ventral setae including one or two basolateral macrosetae (Fig. 9). Dens usually with four or five posterior setae (whole range 2–6), one of which ~ as long as dens+mucro or even longer (ratio = 0.9–1.2:1). Mucrodens slightly longer than inner edge of hind unguis (1.0–1.3 ×). Anal spines rather strong and slightly curved, set on high contiguous papillae.

**Variability.** One of the most characteristic features of the new species is its high-level variability of such important morphological traits as the number of PAO lobes and dental setae, as well as the shape and presence of a mucro (Table 2). This may be assumed as a direct consequence of rather severe conditions of boreal maritime marshes.

**Table 2.** Variation of some important morphological characters in *Hypogastrura variata* sp. nov.

Number of dental setae	%		presence of a mucro	%		PAO lobes	%	
	adults	juveniles		adults	juveniles		adults	juveniles
3+3	–	20	0+0	10	20	4+3	12	–
3+4	3	40	1+0	47	30	4+4	28	70
4+4	30	40	1+1	43	50	4+5	56	30
4+5	37	–				5+6	4	–
5+5	27	–						
5+6	3	–						
Number of specimens studied	30	10		30	10		25	10



**Figures 20–23.** *Hypogastrura variata* sp. nov. **20** chaetotaxy of head and Th.1 **21** chaetotaxy of Th.2 and Th.3, lateral view **22** chaetotaxy of Abd.2–6, lateral view **23** chaetotaxy of juvenile, I instar. Scale bars: 0.1 mm.

**Etymology.** The name of the new species is intended to reflect the morphological variability.

**Affinities.** Apart from the new species, there are only four congeners known in the world fauna that are characterised by a shortened furca with five or fewer dental setae, coupled with a tridentate retinaculum and only one tenent seta on each leg: *H. oreophila* Butschek, 1948, *H. exigua* Gisin, 1958, *H. mongolica* (Nosek, 1976), and *H. magistri* Babenko, 1994. The first two species are from high-montane habitats in the European Alps, and both have been recently redescribed (Skarżyński 2011). They are much smaller than *H. variata* sp. nov. (0.8 mm vs. 1.2–1.8 mm) and have short, undifferentiated, dorsal setae and a longer furca (dens+mucro/ $U_3$  with ratio  $\sim 2$  vs. 1.0–1.3 in *H. variata* sp. nov.). In addition, *H. oreophila* is characterised by the presence of m-setae on Abd.5, a broadened maxillary L.1, an inner tooth on the unguis and a hook-like mucro with a broad outer lamella, whereas *H. exigua* shows a larger PAO ( $\sim 1.5$  ocellus) and more numerous setae on VT (5+5 vs. 4+4 in *H. variata* sp. nov.).

The two other similar species, *H. mongolica* and *H. magistri*, are known from mountainous regions of Central Asia (northern Mongolia and western Tuva). Of these, *H. magistri* can easily be distinguished due to the presence of six or seven curved sensilla on Ant.4 (vs. four in *H. variata* sp. nov.) and the presence of additional setae on Abd.4 and Abd.5. As regards *H. mongolica*, its comparison with *H. variata* sp. nov. is impossible, because the holotype, the only known specimen, of *H. mongolica* was immature (Skarżyński 2011). According to the original description (Nosek 1976) and re-description of the type (Skarżyński 2011), *H. mongolica* differs from *H. variata* sp. nov. in being smaller (0.6 mm long) and lighter in colouration, the “body clothed sparsely with short setae”, long tergal sensilla and an inner tooth on the unguis, but at least some of these characters may reflect its immature status. Nevertheless, *H. mongolica* and *H. variata* sp. nov. are unlikely to be synonymous from an ecological point of view alone, because their habitat preferences are drastically different: litter of a mountain forest vs. a saline maritime marsh.

There are another four known Palearctic congeners which may be related to the above group: *H. capitata* Cassagnau & Delamare, 1955 (Lebanon), *H. verruculata* Rusek, 1967 (China), *H. ramia* Lee & Choe, 1979 (South Korea), and *H. pizzoci* Fanciulli & Dallai, 2008 (Italy). All of them are also characterised by the presence of a single tenent seta on each leg, and the unguiculus with a basal lamella and a tridentate retinaculum, but they all share a complete, less strongly reduced furca with six posterior setae.

**Molecular data.** Unfortunately, the GenBank does not contain sequences of any of the above-mentioned species. Therefore, the isolated position of *H. variata* sp. nov. among fifteen taxonomic units of *Hypogastrura* present in the GenBank is not particularly surprising and may well serve as an additional confirmation of its independent status. Molecular data have shown that the divergences between all units considered are rather high (Table 3). The average interspecific divergence between all species is 26.3% (ranging from 15.9 to 36.4%), while it is 26.7% for *H. variata* sp. nov. and the other fourteen species (ranging from 23.0 to 31.4%). Nevertheless, it seems noteworthy

**Table 3.** K2P distances in *Hypogastrura* species from GenBank and our sequences, measured in %.

Species	Region	1	2	3	4	5	6	7	8	9	10	11	12	13	14
1 <i>H. arcandria</i>	Ontario														
2 <i>H. assimilis</i>	Ontario	20.2													
3 <i>H. yosii</i>	Kunashir	22.2	25.2												
4 <i>H. concolor</i>	Ontario	25.6	26.3	23.8											
5 <i>H. distincta</i>	Ontario	19.2	26.1	24.2	22.5										
6 <i>H. helena</i>	Alaska	25.7	28.2	28.5	23.5	21.5									
7 <i>H. macrotuberculata</i>	Ontario	22.7	29.9	29.4	29.3	21.1	28.6								
8 <i>H. socialis</i>	Estonia	23.0	26.8	26.9	29.0	24.3	24.3	27.7							
9 <i>H. reticulata</i>	Japan	30.3	34.8	34.2	32.2	26.3	28.4	28.4	31.4						
10 <i>H. sensilis</i>	Ontario	23.6	28.0	25.6	18.9	23.7	23.0	28.8	26.9	35.4					
11 <i>H. variata</i> sp. nov.	Magadan	23.0	26.8	26.9	29.0	24.3	24.3	27.7	25.2	31.4	26.9				
12 <i>H. subboldorii</i>	France	21.4	28.3	23.3	23.6	24.0	24.9	24.4	26.2	34.2	22.6	26.2			
13 <i>H. wooliki</i>	Alberta	26.6	28.3	27.6	25.0	28.3	26.0	28.3	27.2	28.3	25.4	27.2	26.1		
14 <i>H. vernalis</i>	France	27.0	24.6	25.3	26.2	26.5	27.7	23.8	28.7	36.6	23.9	28.7	27.6	27.6	
15 <i>H. viatica</i>	Churchill	24.2	26.2	24.8	18.1	23.4	25.3	31.4	26.6	36.4	15.9	26.6	22.7	30.0	26.0

that the molecular trees obtained fail to fully reflect the relationships within the genus *Hypogastrura* based on morphological evidence alone. The most apparent assumption explaining this fact is that the molecular data are still too scant to realistically construct reliable trees that would adequately reflect the real phylogenetic relationships within the genus.

**Distribution and ecology.** *Hypogastrura variata* sp. nov. was collected in two neighbouring sites located on the northern shore of the Sea of Okhotsk, both in the vicinity of Magadan. It seems to inhabit a narrow belt of mudflat maritime marshes, i.e., a monodominant plant association *Puccinellietum phryganodis*, where it achieves very high abundance levels and is the most common collembolan species. Its occurrence in all other types of marsh in the study area was sporadic.

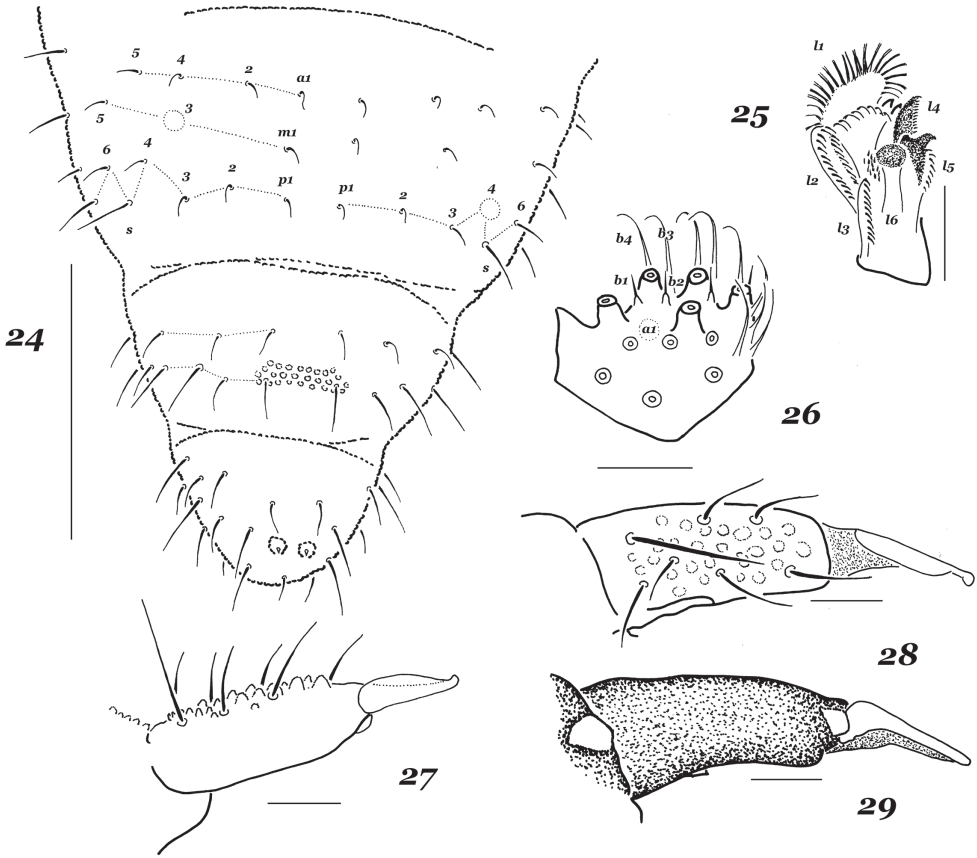
### *Hypogastrura yosii* Stach, 1964

Figs 24–29

Syn.: *Hypogastrura sheyangensis* Jiang, Tang & Chen, 2007.

**Material.** RUSSIA • 3 ♂♂, 9 ♀♀ (slides) and ~ 50 specimens (alcohol); Kuril Islands, Kunashir; 43°42.91'N, 145°33.20'E; wrack beds; August 2017; K. Makarov leg. Several specimens from this material were sequenced (Table 1). Their partial COI genes were amplified and deposited in the GenBank under the sample ID: KY066784–KY066786.

**Taxonomic remarks.** Stach's (1964) original description of *H. yosii* was based on two specimens collected in forest sites in eastern China. Its real position within the genus had remained unclear until it was recently redescribed from the types (Jia et al. 2011) and synonymised with *H. sheyangensis* Jiang, Tang & Chen, 2007. The latter species was known from the coastal wetlands of the same region. Specimens



**Figures 24–29.** *Hypogastrura yosii* Stach, 1964 **24** dorsal chaetotaxy of Abd.4–6 **25** maxillary head **26** labial palp **27** dens and mucro, lateral view **28** dens and mucro, dorsal view **29** dens and mucro, ventral view. Scale bars: 0.1 mm (**24**), 0.01 mm (**25–29**).

from Kunashir Island fit rather well with the existing descriptions, but are significantly smaller, 0.7–0.9 mm vs. “up to 1.5 mm” in Chinese specimens.

Both recent descriptions (Jiang et al. 2007; Jia et al. 2011) considered *H. yosii* as being most similar to two Nearctic species, viz. *H. matura* (Folsom, 1916) and *H. utahensis* (Wray, 1953) (now a junior synonym of *H. promatro* (Wray, 1950) [see Bernard 2015]). This opinion was mainly based on the absence of seta p4 on Abd.4. In fact, this seta, set anteriorly to the p-row (almost aligned with m-setae), may occasionally be absent on one or both sides in many species of the *manubrialis*-group. This is also rather frequent in specimens of *H. yosii* from Kunashir Island (Fig. 24). In our view, *H. yosii* is closely related to the widespread *H. manubrialis* (Tullberg, 1869). Apart from the absence of a seta m2 on Th.2 (one of the most notable peculiarities of *H. manubrialis*), the similar number of sensilla on Ant.4, the relatively large PAO with secondary projections at the base of the lobes, and the short anal spines, both species are characterised by an almost identical structure of the maxillary head (except for lam.6, which

in *H. manubrialis* has no denticles in the central part) (Fig. 25) and the absence of a a1 guard on the labial palp (Fig. 26). This short guard is present in most congeners studied, but not in the *manubrialis* group, in which it is present in only some species: *H. arctandria* Fjellberg, 1988, *H. assimilis* (Krausbauer, 1898), *H. vernalis* (Carl, 1901), and *H. promatro*, but it is absent from others: *H. manubrialis*, *H. yosii*, *H. serrata* (Ågren, 1904), and *H. rangkuli* Martynova in Martynova and Chelnokov 1975. Meaningful differences between *H. yosii* and *H. manubrialis* appear to be limited by maxillary lam.6 (see above), the presence of seta p' on Ant.1 in *H. yosii* (a variable character in specimens from Kunashir, where only six of ten specimens examined show p' seta on at least one antenna) and a characteristic mucro shape, i.e., a long and slender mucro without clear lateral lamellae in *H. manubrialis* or a mucro with an “upturned apex and [clear] outer lamella” in *H. yosii* (Figs 27–29).

***Xenylla aculeata* sp. nov.**

<http://zoobank.org/AC26673B-7C17-4B16-B800-9700FC9906BF>  
Figs 30–35

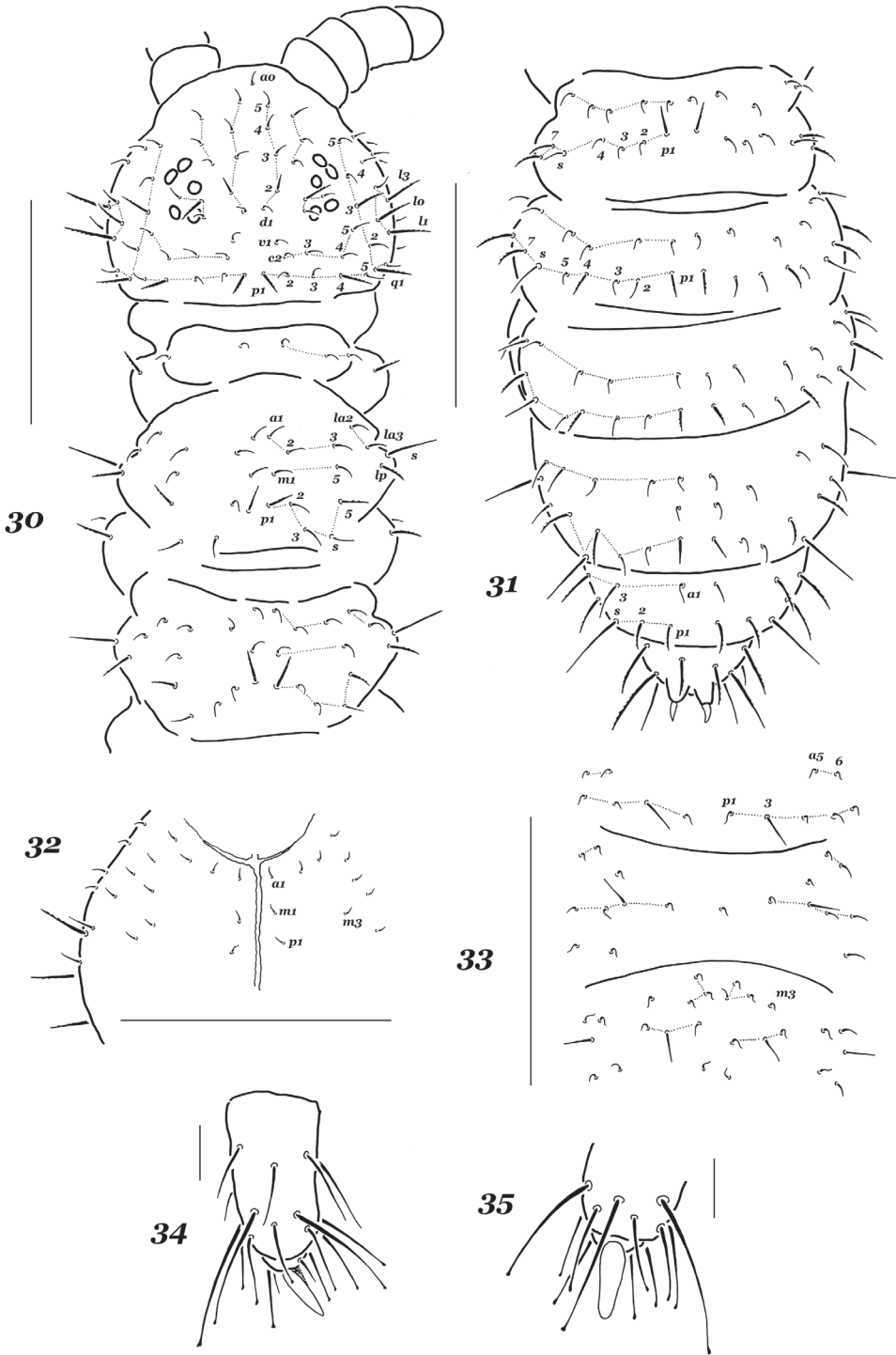
**Type material. Holotype** RUSSIA, North-East • ♂; Magadan Province, “Magadan–Ola Road (closer to Ola) [~ 59°35.25'N, 151°08.00'E]; treeless bog with *Ledum*, *Arctostaphylos*, *Empetrum*, and *Betula* vegetation (sample taken in *Carex* and moss), 20.07.1979”; V. Behan leg. The type is deposited in MSPU.

**Diagnosis.** A species of chaetotaxic group VI (b) of the genus *Xenylla* Tullberg, 1869, characterised by the presence of one sublobal seta on the maxillary outer lobe and a complete reduction of both furca and retinaculum.

**Description.** *Holotype* length 0.67 mm. Intravital colour unknown, holotype stored in alcohol for more than 30 years completely lacks dark pigment even on the eye fields. Tegument granulations rather fine and uniform. Ant.4 with a simple apical vesicle and four blunt sensilla (one dorsal and three lateral), rather short and subequal in size, both subapical microsensillum and organite invisible due to the poor condition of the slide. AO typical of the genus, outer sensilla rather short. Ant.1 and Ant.2 with seven and eleven setae, respectively.

*Head* with 5+5 subequal ocelli, as usual. Buccal cone typical of the genus, not elongate. Setal formula of labrum, 4/554, setae of distal row clearly thickened. Labium with all common papillae (A–E), 9 guards (five long and four short, truncate and papillate) and six proximal setae. Basomedial field of labium (submentum) with four setae, basolateral field (mentum) with five setae, as usual. Maxillary outer lobe simple, with one sublobal seta.

*Most dorsal setae* stout, finely ciliate and clearly differentiated into finer microsetae and subspiniform macrosetae, sensilla usually long and straight, especially on abdominal tip and laterally on Th.2 and Th.3 (Figs 30–31). Head with all usual dorsal setae present, except for c1 [b]; setae p1, p4, d2, oc2, q1, q3, l0, l1, and l3 more or less clear macrosetae, l1 only slightly longer than l3 (ratio = 1.1–1.2/1). Th.2 and Th.3 with seta a2 in a posterior position compared to a1 [h1], both p1 and p2 setae set in front of p3,



**Figures 30–35.** *Xenylla aculeata* sp. nov. **30** dorsal chaetotaxy of head and thorax **31** dorsal chaetotaxy of abdomen **32** ventral chaetotaxy of head **33** ventral chaetotaxy of Abd.2–4 **34, 35** tip of tibiotarsus, different views. Scale bars: 0.1 mm (**30–33**), 0.01 mm (**34, 35**).

setae la1 and m3 absent [i and k]; setae p1, p5 and p6 being macrosetae, lateral sensilla long, but dorsal ones rather short (Fig. 30). Chaetotaxy of abdominal terga as follows: Abd.1 without p5, m3 setae absent from Abd.4 [o] and a2 from Abd.5 [q] (Fig. 31). Ventral chaetotaxy: head with setae p1 and m3 (Fig. 32), Th.2 and Th. 3 with 1+1 axial setae, abdominal sterna as in Fig. 34, Abd.2 with p1, but without p2, Abd.3 with a medial unpaired seta, Abd.4 with only one m-seta (m1 and m2 absent [a4 and a5]). General code of chaetom: bh<sub>1</sub>ikoqa<sub>4</sub>a<sub>5</sub>.

*Ventral tube* with 4+4 setae. furca and retinaculum completely absent. Tibiotarsi of legs 1–3 with 19, 19, and 18 setae, respectively; all setae of distal whorls (A+T) more or less clearly clavate (Figs 34, 35). Anal spines rather long and set on subequal cuticular papillae (Fig. 31).

**Etymology.** The name of the new species is derived from the Latin *aculeata*, meaning spiny, to reflect the shape of the dorsal macrosetae characteristic of *X. aculeata* sp. nov.

**Affinities.** The chaetotaxic pattern of *X. aculeata* sp. nov. allows us to include it into group VI (b), although a forward position of both p1 and p2 on Th. 2 and Th.3 appears to be unique to the new species. There is only one other species in the group that has neither a furca nor a retinaculum, viz. *X. osetica* Stebaeva & Potapov, 1994. Yet the latter species can easily be distinguished from *X. aculeata* sp. nov. by the presence of three sublobal setae on the maxillary outer lobe (vs. one in *X. aculeata* sp. nov.) and a complete chaetotaxy of Th.2 and Th.3 with setae al1 and m3 being present (absent in *X. aculeata* sp. nov.). Thus latter character (the absence of setae) seems to point to the relations between *X. aculeata* sp. nov. and several other congeners of the same group that share a functional furca with one (*X. betulae* Fjellberg, 1985) or two dental setae (*X. corticalis* Börner, 1901, *X. grisea* Axelson, 1900, *X. hexagona* Fjellberg, 1992, and *X. laurisilvae* Fjellberg, 1992). Among these species, only *X. betulae* has hitherto been known from the region under study. It appears to be rather similar to the new species in having an identical dorsal chaetotaxy including such fine characters as short sensilla in p-row on Th.2–Abd.1 and the usual absence of setae p5 from Abd.1 and of setae p7 from Abd.4. Ventral chaetotaxy (the absence of p2 from Abd.2 and of some m-setae from Abd.4, the presence of axial unpaired setae on Abd.3), the rather strong anal spines, and the long stout setae on the abdominal tip are also similar. Apart from the complete absence of a furca, *X. aculeata* sp. nov. differs from *X. betulae* in having much finer tegument granulation, coarser and more clearly differentiated dorsal setae, only one sublobal seta on the maxillary outer lobe (vs. two sublobals in *X. betulae*), p1-setae in an anterior position on Th.2 and Th.3, and numerous clavate setae on tibiotarsi (vs. 2–2–2 in *X. betulae*). The latter character appears to be unique in the genus, but needs verification based on fresh material.

**Distribution and ecology.** The only known specimen of *X. aculeata* sp. nov. was found in a typical swampy association of the region, but a search in similar communities in the same area failed to reveal additional material. Taking this into account, as well as some morphological traits of the new species, namely the complete reduction of a furca and the presence of numerous clavate tibiotarsal setae, *X. aculeata* sp. nov. can be assumed to rather represent a corticolous, not hygrophilous, species.

***Xenylla arnei* sp. nov.**

http://zoobank.org/4BB2F510-C7FE-4BDD-9412-7076B364C4D8

Figs 36–47

**Type material.** *Holotype* RUSSIA, North-East • ♂; Magadan Province, Tauisk; 59°43.66'N, 149°21.85'E; coastal meadow; July 2017; M. Bizin and B. Efevkin leg.

*Paratypes* RUSSIA, North-East • 5 ♀♀ and 5 ♂♂, same data as for holotype. The types are deposited in MSPU.

**Additional material.** more than 500 specimens (alcohol), mainly from the holotype locality; Several specimens from this material were sequenced (Table 1). Their partial COI genes were amplified and deposited in the GenBank under the sample ID: KY066787–KY066789; 9 specimens; same region, AF-51/79: “Geartner Bay, steep slope down to beach with *Artemisia*, *Sedum*, *Saxifraga*, *Potentilla*, grasses, 20.07.1979”; A. Fjellberg leg.

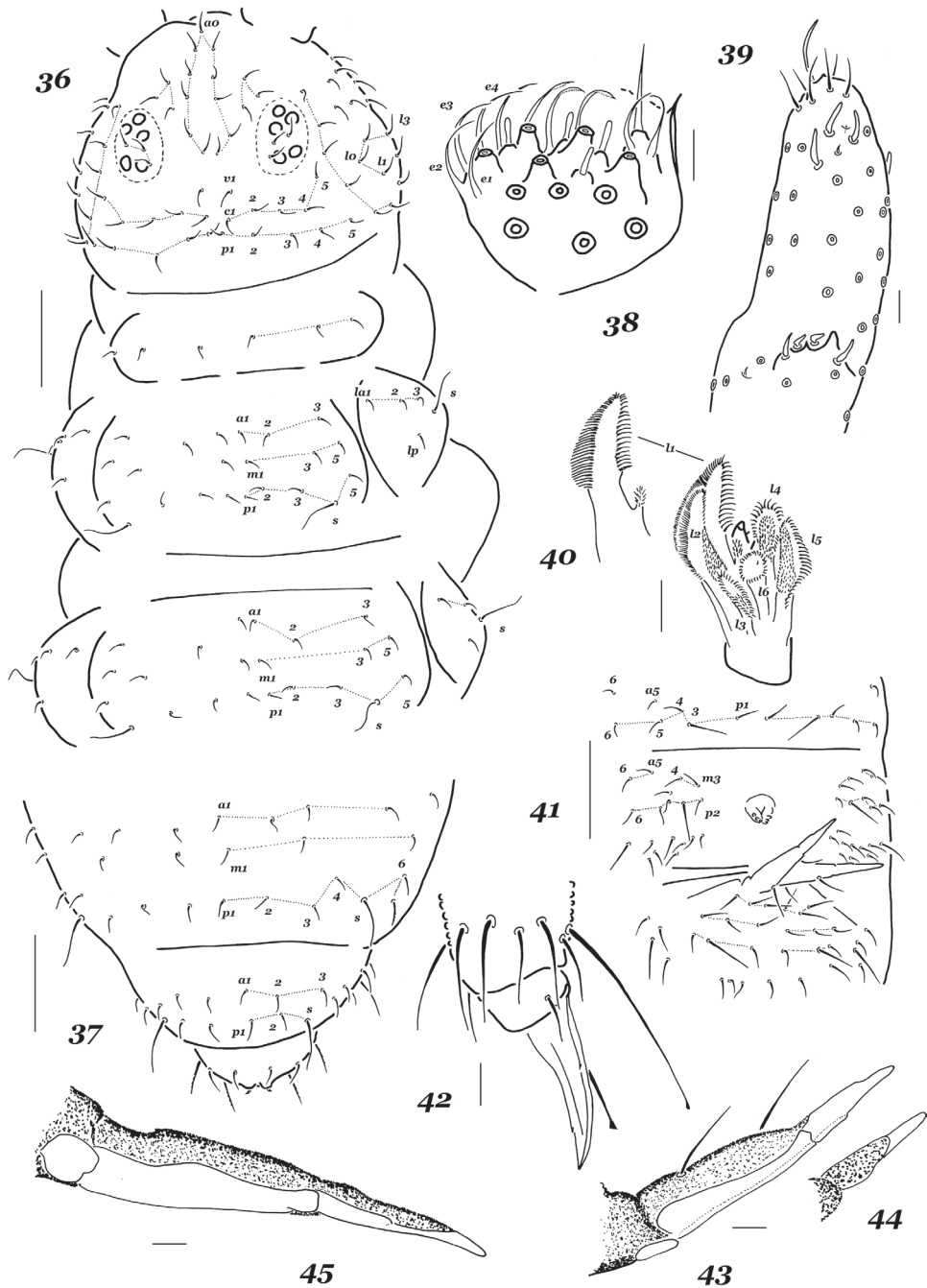
**Diagnosis.** A species from chaetotaxic group II of the genus *Xenylla* with a general chaetotaxic code of  $h_1rt$ , characterised by a light brownish colour, non-differentiated dorsal setae, and the absence of a prominent cuticular lobe from the subcoxae of hind legs.

**Description.** Length 1.4–1.7 mm. Colour rather light, yellow-brown (chamois), with patches of diffuse darker pigmentation, ocular field and antennal tip dark, ventral side usually paler. Tegument granulation fine and almost uniform. Ant.4 with a simple apical vesicle and four blunt sensilla (one dorsal [S3 or S4?] and three lateral [S7–S9]), relatively short and subequal in size, both a subapical microsensillum and an organite are present. AO typical of the genus, outer sensilla thinner than subapical ones, but not especially short (1:1.2–1.8, Fig. 39). Ant.1 and Ant.2 with seven and 12 or 13 setae, respectively.

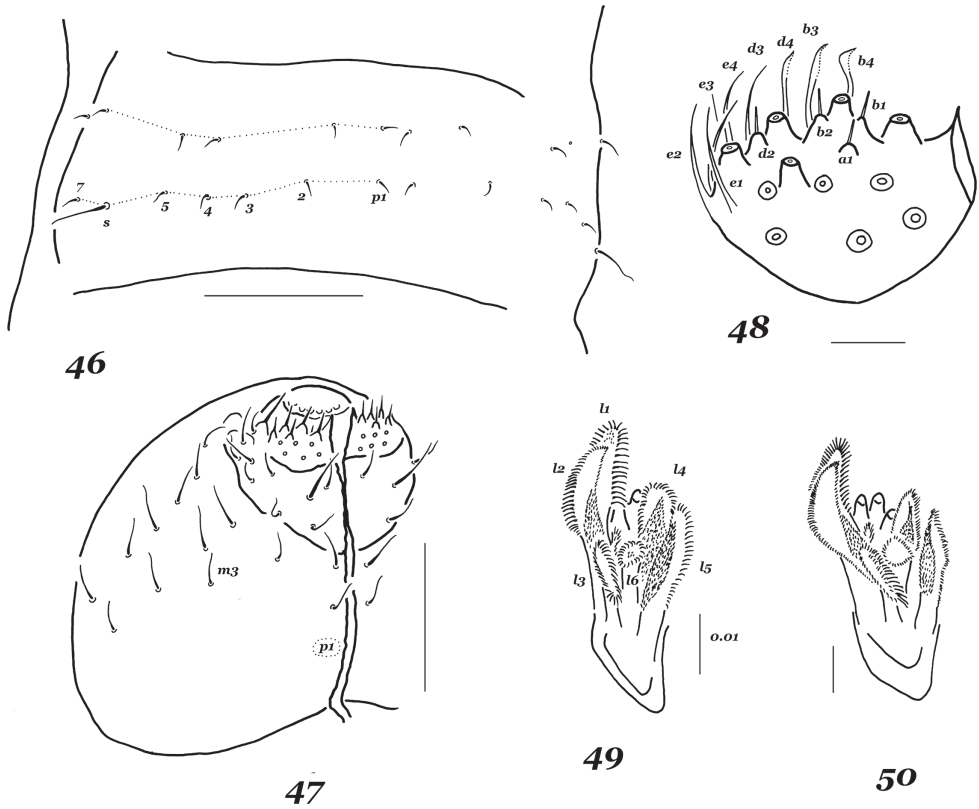
*Head* with 5+5 subequal ocelli, as usual. Buccal cone typical of the genus, not elongate. Setal formula of labrum, 4/554, setae of distal row clearly thickened. Labium with all common papillae (A–E), 12 guards (eight long and four short, rhabdoid, papillate) and six proximal setae (Fig. 38). Basomedial field of labium (submentum) with four setae, basolateral field (mentum) with five setae, as usual. Maxillary outer lobe simple, with three sublobal setae.

*Dorsal setae* fine, thin, and barely differentiated (except for those on Abd.6), tergal sensilla clearly longer than ordinary setae (~ 3.2–3.4:1), dorsal and lateral sensilla on Th.2 and Th.3 subequal. Head with a basic set of setae (Fig. 37), lateral setae not differentiated. Th.2 and Th.3 also with all usual setae, a2 in a posterior position compared to a1 [h1] only on Th.3, p2 seta set aligned with p1 and p3 (Fig. 36). Abdominal terga also with basic set of setae (Fig. 37), p-row on Abd.1–3 with p5 present, s = p6 (Fig. 46). Ventral chaetotaxy: head with 2+2 setae along midline (p1 absent [r]), m3 present (Fig. 48), Th.2 and Th.3 without axial setae [t]. Abdominal sterna as in Fig. 41: Abd.2 with p1 but without p2, Abd.3 without medial unpaired seta above retinaculum. General chaetotaxic code as  $h_1rt$ .

*Ventral tube* with 4+4 setae. Retinaculum with 3+3 teeth. Furca complete, both dens and mucro thin, long, and clearly separated ventrally. Mucrodens/ $U_3$  ratio as 2.6–2.9:1. Dens with two dorsal setae (Fig. 43), ventral side of dens and mucro com-



**Figures 36–45.** *Xenylla arnei* sp. nov. **36** dorsal chaetotaxy of head and thorax **37** dorsal chaetotaxy of Abd.4–6 **38** labial palp **39** sensorial equipment of Ant.3 and Ant.4 **40** maxillary head **41** ventral chaetotaxy of Abd.2 and Abd.3 **42** tip of leg 3 **43** dens and mucro, lateral view **44** mucro, dorsal view **45** dens and mucro, ventral view. Scale bars: 0.1 mm (**36**, **37**, **41**), 0.01 mm (**38–40**, **42–45**).



**Figures 46–50.** *Xenylla arnei* sp. nov. (46, 47) and *X. humicola* (48–50) 46 dorsal chaetotaxy of Abd.1 47 ventral chaetotaxy of head 48 labial palp 49 maxillary head, specimen from Kola Peninsula 50 maxillary head, specimen from Chukotka. Scale bars: 0.1 mm (46, 47), 0.01 mm (48–50)

pletely smooth, without primary granulations (Figs 44, 45). Mucro shorter than dens (0.7–0.8:1), with a low outer lamella, ventral thickening neither prominent nor with a clear tooth. Chaetotaxy of legs 1–3 usually as follows: upper subcoxae – 1, 3, 3; lower subcoxae – 0, 3, 3; coxae – 3, 8, 8; trochanters – 6, 6, 6; femora – 13, 12, 11; tibiotarsi – 19, 19, 18 setae, respectively. Tibiotarsal setae A1 and A7 on all legs as long as 1.5–1.7 inner edge of unguis, clearly clavate. Unguis with a pair of lateral teeth and usually with a small tooth in upper third of inner edge. Anal spines short, usually curved and set on tiny cuticular papillae.

**Etymology.** The new species is named after the famous Norwegian collembologist, Arne Fjellberg, who discovered it in the Magadan Region more than 40 years ago.

**Affinities.** Using the most recent key to the Asiatic species of the genus (Jia and Skarżyński 2019), *X. arnei* sp. nov. keys out to *X. humicola* (Fabricius, 1790), because their general chaetotaxic codes [h<sub>1</sub>rt] are identical. Moreover, both species are similar in many other important morphological traits, namely the labial palp is with four e-

**Table 4.** K2P distances in *Xenylla* species from GenBank and our sequences, measured in %.

Species	Region	1	2	3	4	5	6	7	8	9	10	11	12	13
1 <i>X. humicola</i>	Magadan													
2 <i>X. humicola</i>	Vaigach	0.6												
3 <i>X. humicola</i>	Estonia	0.9	1.2											
4 <i>X. betulae</i>	Ontario	28.0	27.9	30.1										
5 <i>X. boeneri</i>	UK	25.0	25.4	23.1	28.6									
6 <i>X. brevisimilis</i>	Ontario	27.5	27.1	26.4	24.8	25.8								
7 <i>X. canadensis</i>	Ontario	30.4	30.8	28.8	26.2	31.2	30.7							
8 <i>X. grisea</i>	Antarctica	25.7	25.4	24.0	32.3	23.7	26.1	26.7						
9 <i>X. maritima</i>	Ontario	22.3	22.7	21.1	34.9	18.8	30.3	34.5	27.4					
10 <i>X. mediterranea</i>	Ontario	28.1	28.5	26.2	27.9	30.4	29.1	27.2	23.9	26.3				
11 <i>X. pomorskii</i>	Poland	28.6	28.2	29.5	24.6	25.7	24.7	28.7	28.7	29.6	27.1			
12 <i>X. szepteyckii</i>	Poland	22.7	23.1	24.6	30.0	23.7	28.0	33.5	24.7	22.2	28.9	28.7		
13 <i>X. arnei</i> sp. nov.	Magadan	22.9	22.6	23.4	29.1	22.2	22.9	25.9	25.2	26.1	26.7	24.4	25.3	
14 <i>X. tullbergi</i>	France	22.4	22.8	23.1	28.7	24.5	27.7	31.0	24.7	22.1	27.8	28.3	19.1	22.7

guards (cf. Fig. 38 and Fig. 48), which is not typical of the genus [see Fjellberg (1999)], the virtually identical maxillae (cf. Fig. 40 and Figs 49, 50), three sublobes on the maxillary outer lobe, a retinaculum with 3+3 teeth, a long dens with two setae and a narrow straight mucro. Nevertheless, several fine morphological differences between *X. arnei* sp. nov. and *X. humicola* are traceable. Apart from the different colouration, the non-differentiated setae l1 and l3 on the head (vs. similar in size, but spine-like setae in *X. humicola*) and the absence of subcoxal lobes from Th.3 in *X. arnei* sp. nov. (variable in shape, but always present in *X. humicola*) seem to be the most sound. In addition, the species status of *X. arnei* sp. nov. is well confirmed by molecular evidence (Table 4).

*Xenylla arnei* sp. nov., together with the widespread *X. humicola* and the Japanese *X. brevispina* Kinoshita, 1916 [h<sub>1</sub>r<sub>1</sub>t<sub>1</sub>s<sub>1</sub>v], represent the only known Holarctic members of the species group II (Stebaeva and Potapov 1994). There is also one more form, *X. convexopyga* Lee, Park & Park, 2005, from the Korean Peninsula, in which the chaetotaxy is rather similar. The chaetotaxic code given for this species in the original description is as follows: k<sub>1</sub>r<sub>1</sub>t<sub>1</sub>s<sub>1</sub>v. This code is likely to be not fully correct. The absence of a m<sub>3</sub> seta from Th.2 [k] contradicts to fig. 1A in Lee et al. (2005), where this seta is present, albeit marked as m<sub>4</sub> (a situation unknown within the genus). In our view, the species rank of *X. convexopyga* and its separation from *X. brevispina* need confirmation.

All other species of this group, viz. *X. yukatana* Mills, 1938 [h<sub>1</sub>t<sub>1</sub>q<sub>1</sub>a<sub>3</sub>a<sub>4</sub>], *X. gamae* Cardoso, 1968 [h<sub>1</sub>t<sub>1</sub>q<sub>1</sub>], *X. nigeriana* Gama & Lasebikan, 1976 [h<sub>1</sub>t<sub>1</sub>q<sub>1</sub>soa<sub>3</sub>], *X. brasiliensis* Gama, 1978 [h<sub>1</sub>r<sub>1</sub>l<sub>1</sub>q<sub>1</sub>], and *X. niraе* Gama & Oliveira, 1994 [h<sub>1</sub>r<sub>1</sub>l<sub>1</sub>q<sub>1</sub>iomu], are characterised by more strongly reduced chaetotaxy patterns and inhabit various tropical regions.

**Molecular data.** GenBank currently contains COI sequences for only eleven species of the genus (of 140 species known worldwide). The obtained interspecific divergences (Table 4) between all of them, together with *X. arnei* sp. nov., range between 18.8 to 34.9% (mean 26.5%). Analogous data for *X. arnei* sp. nov. are 22.2–29.1% (mean 24.9%), which can be considered as an additional argument in favour of its specific status. Nevertheless, such a scant amount of primary data does not allow for

any serious statements to be made, but a trend to the absence of parallelisms in molecular and morphological evolution can be traced quite clearly.

**Distribution and ecology.** *Xenylla arnei* sp. nov. was collected in two neighbouring sites located on the northern shore of the Sea of Okhotsk, in the vicinity of Magadan. In this region, it was mainly found in various herbaceous meadows at some distance off the coastal line, where its abundance may be very high. Its occurrence in all other types of coastal plant associations in the study area was rather sporadic.

## Acknowledgements

We would like to express our sincere gratitude to D. Berman (IBPN RAS) and N. Petrunina, without whose help our work in the Magadan Region would have been much more difficult. We are also much indebted to K. Makarov (MSPU), A. Fjellberg (Norway), and V. Behan-Pelletier (Canada) for the loan of material and to S. Golovatch (IPEE RAS) for his editing of the English.

The paper has been supported through the Programs “Biodiversity and Natural Resources of Russia” and “Biosphere evolution” of the Presidium of the Russian Academy of Sciences.

## References

- Ågren H (1904) Lappländische Collembola. Arkiv för zoologi 2(1): 1–29. <https://doi.org/10.5962/bhl.part.4541>
- Axelson WM (1900) Vorläufige Mittheilung über einige neue Collembolen-Formen aus Finnland. Meddelanden af Societatis pro Fauna et Flora Fennica 26: 105–123. <https://doi.org/10.5962/bhl.part.26726>
- Axelson WM (1905) Einige neue Collembolen aus Finnland. Zoologischer Anzeiger 28(24/25): 788–794.
- Babenko AB (1994) The genus *Hypogastrura* Bourlet, 1839. In: Chernova NM (Ed.) Opre-delitel kollembol fauny Rossii i sopredelnykh stran. Semeistvo Hypogastruridae. Nauka, Moscow, 30–194. [in Russian]
- Bernard EC (2015) Redescriptions of Hypogastruridae and Onychiuridae (Collembola) described by David L. Wray. Zootaxa 3918(3): 301–338. <https://doi.org/10.11646/zootaxa.3918.3.1>
- Börner C (1901) Neue Collembolenformen und zur Nomenclatur der Collembola Lubb. Zoologischer Anzeiger 24(657/658): 696–712.
- Börner C (1903) Neue altweltliche Collembolen, nebst Bemerkungen zur Systematik der Isotominen und Entomobryinen. Sitzungsberichten der Gesellschaft naturforschender Freunde zu Berlin 1903: 129–182. <https://doi.org/10.5962/bhl.part.29866>
- Bourlet A (1839) Mémoires sur les Podures. Mémoires de la Société Royale des Sciences de l'Agriculture et des Arts de Lille 1: 377–417.

- Butschek E (1948) Einige neue und wenig bekannte Collembolen aus den Nordostalpen. *Zeitschrift der Wiener Entomologischen Gesellschaft* 33: 25–34.
- Cardoso MA (1968) Una nova espécie de Colêmbolos de Moçambique, *Xenylla gisini* n. sp. *Revista de Ciências Biológicas* 1: 1–8.
- Carl J (1901) Zweiter Beitrag zur Kenntnis der Collembolafauna der Schweiz. *Revue suisse de Zoologie* 9: 243–278. <https://doi.org/10.5962/bhl.part.20304>
- Carpenter GH (1900) Collembola from Franz-Josef Land (collected by Mr. W.S. Bruce, 1896–1897). *Proceedings of the Royal Dublin Society, New Series* 9 (3): 271–276.
- Cassagnau P, Delamare Deboutteville Cl (1955) Mission Henri Coiffait au Liban (1951). 3. Collemboles. *Biospeologica* 65: 365–395.
- Christiansen K, Bellinger P (1980) The Collembola of North America, north of the Rio Grande (1<sup>st</sup> edn.). Parts 1–3. Grinnell College, Grinnell, 1042 pp.
- Delamare Deboutteville C, Jacquemart S (1962) Un Collembole nouveau des Pyrénées-Orientales *Hypogastrura subboldorii* n. sp. *Vie et Milieu* 12(4): 667–671.
- Fabricius O (1780) *Fauna Groenlandica: systematice sistens animalia Groenlandiae occidentalis hactenus indagata, quoad nomen specificum, triviale, vernaculumque: synonyma auctorum plurium, descriptionem, locum, victum, generationem, mores, usum, capturamque singuli, prout detegendi occasio fuit: maximaque parte secundum proprias observations. Hafniae, Impensis Ioannis Gottlob Rothe, 450 pp.* <https://www.biodiversitylibrary.org/page/13442285>
- Fanciulli PP, Dallai R (2008) Three new species of Collembola from north-east Italy. *Zootaxa* 1701: 15–28. <https://doi.org/10.11646/zootaxa.1701.1.2>
- Fjellberg A (1985) Arctic Collembola. I. Alaskan Collembola of the families Poduridae, Hypogastruridae, Odontellidae, Brachystomellidae and Neanuridae. *Entomologica Scandinavica, Suppl.* 21, 126 pp.
- Fjellberg A (1988) Six new species of Collembola from North Norway (Hypogastruridae, Odontellidae, Onychiuridae, Isotomidae). *Fauna Norvegica, Series B* 35: 35–41.
- Fjellberg A (1992) Collembola of the Canary Islands. I. Introduction and survey of the family Hypogastruridae. *Entomologica Scandinavica* 22: 437–456. <https://doi.org/10.1163/187631291X00246>
- Fjellberg A (1999) The labial palp in Collembola. *Zoologischer Anzeiger* 237: 309–330.
- Folsom JW (1916) North American collembolous insects of the subfamilies Achorutinae, Neanurinae, Podurinae. *Proceedings of the U.S. National Museum* 50: 477–525. <https://doi.org/10.5479/si.00963801.50-2134.477>
- Folsom JW (1919) Collembola of the Canadian Arctic Expedition, 1913–1918. *Report of the Canadian Arctic Expedition* 3: 1A–29A.
- Hammer M (1953) Investigations on the microfauna of Northern Canada. II. Collembola. *Acta Arctica* 6, 108 pp.
- Holterman M, Van Der Wurff A, Van Den Elsen S, Van Megen H, Bongers T, Holovachov O, Bakker J, Helder J (2006) Phylum-wide analysis of SSU rDNA reveals deep phylogenetic relationships among nematodes and accelerated evolution toward crown clades. *Molecular Biology and Evolution* 23: 1792–1800. <https://doi.org/10.1093/molbev/msl044>

- Gama MM da (1964) Collembolos de Portugal continental. Memórias e Estudos do Museu Zoológico Universidade da Coimbra 292: 1–252.
- Gama MM da (1978) Systématique évolutive des *Xenylla*. X. Espèces provenant du Brésil, du Vietnam et de Madagascar (Insecta: Collembola). Ciência Biológica (Portugal) 4: 45–48.
- Gama MM da, Lasebikan BA (1976) Systématique évolutive des *Xenylla*. IX. Espèces provenant du Nigeria (Insecta: Collembola). Ciência Biológica (Portugal) 1: 131–137.
- Gama MM da, Oliveira EP (1994) Systématique évolutive des *Xenylla*. XVI. Description d'une nouvelle espèce provenant d'Amazonie (Insecta: Collembola). Amazoniana 13: 205–208.
- Gisin H (1958) Quatre espèces nouvelles de collemboles (Insectes, Aptérygotes), récoltes par M. Marcuzzi dans les Dolomites italiennes. Atti dell'Istituto Veneto di scienze, lettere ed arti 116: 85–91.
- Jia J, Skarżyński D, Konikiewicz M (2011) A taxonomic study on *Hypogastrura* Bourlet, 1839 (Collembola, Hypogastruridae) from China. Zootaxa 2981: 56–62. <https://doi.org/10.11646/zootaxa.2981.1.5>
- Jia J, Skarżyński D (2019) A new species of *Xenylla* Tullberg, 1869 (Collembola: Hypogastruridae) from China, with a key to Asian species of the genus. Zootaxa 4608 (3): 579–585. <https://doi.org/10.11646/zootaxa.4608.3.11>
- Jiang J, Tang B, Chen JX (2007) A new species of the genus *Hypogastrura* from coastal wetlands of East China (Collembola: Hypogastruridae). Zootaxa 1630: 63–68. <https://doi.org/10.11646/zootaxa.1630.1.6>
- Kimura M (1980) A simple method for estimating evolutionary rates of base substitutions through comparative studies of nucleotide sequences. Journal of Molecular Evolution 16: 111–120. <https://doi.org/10.1007/BF01731581>
- Kinoshita S (1916) On the Japanese Collembola. Zoological Magazine, Tokyo (Dobutsugaku zasshi) 28: 494–498. [in Japanese]
- Krausbauer Th (1898) Neue Collembola aus der Umgebung von Weilburg a. Lahn. Zoologischer Anzeiger 21(568): 501–504.
- Kuprin AV, Potapov MB (2018) The history of study of springtails' fauna (Collembola) of the Russian Far East. In: A.I. Kurentsov's Annual Memorial Meetings 29: 23–31. <https://doi.org/10.25221/kurentzov.29.2> [in Russian]
- Lee BH, Choe YS (1979) A study of the Collembola fauna of Korea. VIII. Two new species of *Hypogastrura* with some notes on additional collections of Neanuridae and Tomoceridae. Korean Journal of Entomology 9(2): 1–8.
- Lee BH, Park KH, Park NY (2005) Four new species of *Xenylla* (Collembola: Hypogastruridae) from Korea. Entomological Research 35: 265–275. <https://doi.org/10.1111/j.1748-5967.2005.tb00168.x>
- Lubbock J (1870) Notes on the Thysanura. Part III. Transactions of the Linnean Society of London 26: 295–304. <https://doi.org/10.1111/j.1096-3642.1968.tb00508.x>
- Martynova EF, Chelnokov VG (1975) Collembola of the East Pamirs. The families Onychiuridae and Hypogastruridae. Zoologicheskyy Zhurnal 54(3): 464–470. [in Russian]
- Mills HD (1938) Collembola from Yucatan caves. In: Pearse AS (Ed.) Fauna of the caves of Yucatan. Carnegie Institution of Washington 491: 183–190.

- Nosek J (1976) A new species of springtail from the northern Mongolia *Mesogastrura mongolica* sp. n. (Collembola, Hypogastruridae). *Biologia (Bratislava)* 31: 825–828.
- Rusek J (1967) Beitrag zur Kenntnis der Collembola (Apterygota) Chinas. *Acta entomologica bohemoslovaca* 64: 186–189.
- Schött H (1893) Zur Systematik und Verbreitung paläarktischen Collembola. *Kongliga Svenska Vetenskaps-Akademiens Handlingar* B25(11): 1–100. <https://doi.org/10.5962/bhl.title.8645>
- Skarżyński D (2011) A taxonomic study on some Alpine *Hypogastrura* Bourlet, 1839 (Collembola, Hypogastruridae). *Zootaxa* 2786: 62–68. <https://doi.org/10.11646/zootaxa.2786.1.5>
- Skarżyński D, Piwnik A, Porco D (2018) Integrating morphology and DNA barcodes for species delimitation within the species complex *Xenylla maritima* (Collembola: Hypogastruridae). *Arthropod Systematics and Phylogeny* 76(1): 31–43.
- Stach J (1949) The Apterygotan fauna of Poland in relation to the world-fauna of this group of insects. Families: Neogastruridae and Brachystomellidae. *Acta Monographica Musei Historiae Naturalis, Kraków*, 341 pp.
- Stach J (1964) Materials to the knowledge of Chinese Collembolan fauna. *Acta zoologica cracoviensia* 9: 1–26.
- Stamatakis A (2014) RAxML Version 8: A tool for Phylogenetic Analysis and Post-Analysis of Large Phylogenies. *Bioinformatics* 7: 5–12. <https://doi.org/10.1093/bioinformatics/btu033>
- Stebaeva SK, Potapov MB (1994) The genus *Xenylla* Tullberg, 1869. In: Chernova NM (Ed.) *Opredelitel kollembol fauny Rossii i soprodelnykh stran. Semeistvo Hypogastruridae*. Nauka, Moscow, 250–305. [in Russian]
- Tamura K, Stecher G, Peterson D, Filipski A, Kumar S (2013) Mega6: Molecular evolutionary genetics analysis version 6.0. *Molecular Biology and Evolution* 30: 2725–2729. <https://doi.org/10.1093/molbev/mst197>
- Tullberg T (1869) Om skandinaviska Podurider af underfamiljen Lipurinae. *Akademisk Afhandling, Uppsala*, 21 pp.
- Tullberg T (1871) Förteckning öfver Svenska Podurider. Öfersigt af Kongliga Vetenskaps-Akademiens Förhandlingar 28: 143–155.
- Tullberg T (1872) Sveriges Podurider. *Kongliga Svenska Vetenskaps-Akademiens Handlingar* 10(10): 4–70.
- Wray DL (1950). Some new Collembola from Utah and Idaho. *Bulletin of the Brooklyn Entomological Society* 45 (3): 91–95. <https://doi.org/10.1155/1950/65134>
- Wray DL (1953) Some new species of springtail insects (Collembola). *Occasional Papers, Nature Notes, Raleigh North Carolina* 1: 1–7.

# †*Camelosphecia* gen. nov., lost ant-wasp intermediates from the mid-Cretaceous (Hymenoptera, Formicoidea)

Brendon E. Boudinot<sup>1,2</sup>, Vincent Perrichot<sup>3</sup>, Júlio C. M. Chaul<sup>4</sup>

**1** Department of Entomology & Nematology, University of California, Davis, One Shields Ave, Davis, CA 95616, USA **2** Friedrich-Schiller-Universität Jena, Institut für Zoologie und Evolutionsforschung, 1 Erbertstraße, 07743 Jena, Thüringen, Germany **3** Univ. Rennes, CNRS, Géosciences – UMR 6118, F-35000, Rennes, France **4** Pós-Graduação em Ecologia, Departamento de Biologia Geral, Universidade Federal do Viçosa, 36570-900, Viçosa, MG, Brazil

Corresponding author: Brendon E. Boudinot ([boudinotb@gmail.com](mailto:boudinotb@gmail.com))

Academic editor: M. Borowiec | Received 14 August 2020 | Accepted 14 November 2020 | Published 18 December 2020

<http://zoobank.org/B9954463-1D57-46C3-AB90-751157C9D0B5>

**Citation:** Boudinot BE, Perrichot V, Chaul JCM (2020) †*Camelosphecia* gen. nov., lost ant-wasp intermediates from the mid-Cretaceous (Hymenoptera, Formicoidea). ZooKeys 1005: 21–55. <https://doi.org/10.3897/zookeys.1005.57629>

## Abstract

Fossils provide primary material evidence for the pattern and timing of evolution. The newly discovered “beast ants” from mid-Cretaceous Burmite, †*Camelosphecia* gen. nov., display an exceptional combination of plesiomorphies, including absence of the metapleural gland, and a series of unique apomorphies. Females and males, represented by †*C. fossor* sp. nov. and †*C. venator* sp. nov., differ in a number of features which suggest distinct sexual biologies. Combined-evidence phylogenetic analysis recovers †*Camelosphecia* and †*Camelomecia* as a clade which forms the extinct sister group of the Formicidae. Notably, these genera are only known from alate males and females; workers, if present, have yet to be recovered. Based on ongoing study of the total Aculeata informed by the beast ant genera, we provide a brief diagnosis of the Formicoidea. We also provide the first comprehensive key to the major groupings of Mesozoic Formicoidea, alongside a synoptic classification in which †Zigrasimeciinae stat. nov. and †*Myanmyrma maraudera* comb. nov. are recognized. Finally, a brief diagnosis of the Formicoidea is outlined.

## Keywords

classification, identification key, Mesozoic revision, morphology, paleontology, phylogeny, taxonomic synopsis

## Introduction

Ants are the dominant lineage of surface-dwelling eusocial insects, filling tropical canopies, permeating leaf litter, and shaping ecosystems through predation, granivory, herbivory, and a plethora of other means (Hölldobler and Wilson 1990). The fossil record of ants spans more than 100 million years of geological time, with hundreds of species attributed to modern taxa in the Cenozoic (e.g., Mayr 1868; Wheeler 1915; LaPolla et al. 2013), and a Mesozoic fauna with over 50 known species (e.g., Barden 2017; Barden and Engel 2019). It is the Mesozoic fossils which have imparted the deepest insight into ant evolution, from the first description of a stem-ant species which refined our knowledge of the ant ground plan (Wilson et al. 1967a, b), to the first Cretaceous crown ants (Grimaldi and Agosti 2000, McKellar et al. 2013a) which have informed our chronological estimates of ant origins (e.g., Brady et al. 2006; Moreau et al. 2006; Borowiec et al. 2019). Some of the most remarkable specimens, however, have been representatives of a lost fauna of highly modified top predators, including the so-called “hell ants” (†Haidomyrmecinae, e.g., Barden et al. 2020; Perrichot et al. 2020) and “iron-maiden ants” (†Zigrasimeciinae stat. nov., e.g., Cao et al. 2020).

Here, we report and describe a new genus of singularly bizarre “beast ants” from mid-Cretaceous Burmite, †*Camelosphecia* gen. nov., which combines novel autapomorphies with critical plesiomorphies of the ancestral Aculeata, such as absence of the metapleural gland. Based on phylogenetic analysis of genomic and morphological data spanning the total Aculeata (Boudinot et al. 2020a), we have found that †*Camelosphecia* is closely related to the hitherto unplaced genus †*Camelomecia*, with the two forming a clade which is sister to the Formicidae. The †*Camelomecia* clade informs the polarization of character states throughout the total Formicidae and foreshadows the discovery of other illuminating fossils. In order to contextualize the description of this new genus, we synthesize the systematics and morphology of the Cretaceous ant fauna as a synoptic classification and provide the first key to the major groups of Formicoidea.

## Materials and methods

Morphological observations which formed the foundation of this study were made via comparison of dry-mounted extant specimens, hand-cut amber fossils, digital photomicrographs from several sources (particularly AntWeb.org), and graphic representations in the literature. Several microscopes were used for examining physical material, with primary reliance on a Leica MZ 12A with fluorescent and fiber-optic lighting. Photomicrographs were taken with a variety of equipment, including a JVC KY-F57U digital camera mounted on a Leica MZ 16A microscope, a Canon 1100D digital camera mounted on a Leica S8APO, and a Olympus BX60 microscope equipped with fluorescent light source, with resultant z-stacks processed via Auto-Montage Pro (Synoptics Ltd. Cambridge England) or Zerene Stacker (Zerene Systems LLC). Figures were processed with Adobe Photoshop 2020 and Illustrator 2020 (Adobe Systems Inc. California, U.S.A.). Measurements were taken from photomicrographs using Photoshop.

## Terminology

Morphological terminology follows Richter et al. (2020) for the cranium and its appendages, Boudinot (2015) for the mesosoma and legs, Brown and Nutting (1950) for the abscissae of the wing veins, Bolton (1990) and Keller (2011) for the metasoma, and Harris (1979) for surface sculpture. However, we have found that it was necessary to further differentiate among structures and their corresponding terms based on further study of development and anatomy. In the present work, we refer to the “pronotal rim” of †*Camelosphecia*, which is the carina which margins the disc of the pronotum ventrally, and which should not be confused with the anteromedian lobe (“neck”) of the pronotum. We also refer to the “lateral pronotal lobes”, which correspond to the paired posterolateral extensions of the pronotum which conceal the mesothoracic spiracle, as is used for Apoidea.

Generally, the antenna is considered to comprise three segments, the scape, pedicel, and multi-annulate flagellum (Snodgrass 1935; Goulet and Huber 1993). However, we distinguish between the *radicle* and the *scape* based on molecular developmental study demonstrating correspondence between the radicle with the coxa plus trochanter, the scape with the femur, the pedicel with the tibia, and the multi-annulate flagellum with the tarsus (Toegel et al. 2009). The subdivisions of the radicle are recognized as the “bulbus” and “bulbus neck” in the ant literature (e.g., Keller 2011), and we employ those terms here where appropriate. We do note that Toegel et al. (2009) mislabeled the radicle as the antennifer, which is the condyle of the cranium articulating with the antenna (Snodgrass 1935).

Regarding setation, “hairs” are properly considered as mechanosensory *sensilla trichodea* (Chapman 2012), with three forms commonly expressed among Hymenoptera: *s. trichodea fliformis*, or setae in the strict sense, i.e., non-tapering or very narrowly-tapering setae; *s. trichodea chaetiformis*, or chaetae (“traction setae”), i.e., tapering or conical setae; and *s. trichodea psammochaetis*, or psammochaetae (“fossorial chaetae”), i.e., large, flattened, and often longitudinally-grooved setae. Regardless of form, *sensilla trichodea* on contact surfaces such as on the tibiae and tarsi are functionally significant as they provide traction in addition to sensory information (see references in Boudinot et al. 2020b). Chaetae occur most often on the tarsi, although they may be present on the tibiae, femora, and on the perioral sclerites. For example, the “traction setae” on the meso- and metatibiae of *Cryptopone*, *Centromyrmex*, and other Ponerinae (e.g., Bolton and Fisher 2008; Schmidt and Shattuck 2014) are chaetae used for gaining traction in soil tunnels, and the “spicules” or “clypeal” and “labral pegs” of various Leptanillinae, Amblyoponinae, and stem ants (e.g., Boudinot 2015) are short, stout chaetae. With respect to the labral chaetae of taxa treated in this study, we clarify that the terms “above”, “below”, dorsal, and ventral should be avoided, as the chaetae are only expressed on the aboral face of the labrum, and which have locations that are described by the lateromedial and proximodistal coordinate axes on the sclerite. Finally, we note that psammochaetae are widespread in fossorial Aculeata, often occurring in stereotyped positions on the legs of Tiphioidea, Thynnoidea, Pompilidae, Mutillidae, Bradynobaenidae, Scoliidae, and spheciform Apoidea.

**Measurement abbreviations (all in mm):**

- A1L** Antennomere I length. Length of the main body of the scape, excluding the radicle.
- A2L** Antennomere II length. Length of the main body of the pedicel.
- A3L** Antennomere III length. Length of the first flagellar antennomere.
- CL** Cranium length. As measured in profile view, the length of head from posteriormost head margin as would be observed in full-face view to anteriormost discernible margin.
- CW** Clypeus width. Maximum measurable width of the clypeus in the most full-face view perspective achievable.
- EL** Eye length. Maximum measurable length of the compound eye.
- HL** Head length. As measured in profile view, the length of the head from the posteriormost head margin as for CL to the apicalmost point of the mandibles.
- HW** Head width. Maximum width of the cranium as measured in dorsal view.
- LW** Lateral ocellus width. Maximum measurable width of one of the lateral ocelli; note: lateral ocellus length measured for male due to specimen orientation.
- MsL** Mesoscutellum length. Maximum length of the mesoscutellum in dorsal view.
- MsW** Mesoscutellum width. Maximum width of the mesoscutellum in dorsal view.
- MtL** Mesoscutum length. Maximum length of the mesoscutum in dorsal view.
- MtW** Mesoscutum width. Maximum width of the mesoscutum in dorsal view.
- MW** Median ocellus width. Maximum measurable width of the median ocellus.
- PnL** Pronotal medial length. Length of the pronotum along its midline in dorsal view (note: measured in profile view for the male diagonally from the anterior pronotal margin to the posteriormost point of the medial margin).
- PnLm** Pronotal maximal length. Maximum length of the pronotum as measured between the pronotal lobes to the anteriormost discernible point (note: measured in profile view for the male diagonally from the anterior pronotal margin to the posteriormost point of the lateral pronotal lobe).
- PnW** Pronotal width: Maximum measurable width of the pronotum in dorsal view.
- PtL** Petiole length. Maximum discernible length of the petiole.
- WL** Mesosoma length. Diagonal length of the mesosoma as measured from the anteriormost pronotal angle to the posteriormost apex of the propodeal projection in dorsal view.
- WLa** Mesosoma length, alternative. Diagonal length of mesosoma as measured in profile view from the pronotal inflection to the posteriormost point of the propodeal projection.
- VBL** Vertexal bulge length, male specimen. As measured in profile view and in the same line as CL, the length of the vertexal bulge of the male from the occipital carina to the dorsal point of the cranium, excluding the ocelli.

**Repositories of material examined for specific results here reported**

**AMNH** American Museum of Natural History, New York, New York, USA;

- BEBC** Brendon E. Boudinot collection, University of California, Davis, CA, USA. and Friedrich-Schiller-Universität Jena, Thüringen, Germany;
- CNUC** Key Lab of Insect Evolution and Environmental Changes, College of Life Sciences, Capital Normal University, Beijing, China;
- DZUP** Coleção Entomológica Padre Jesus Santiago Moure, Universidade Federal do Paraná, Curitiba, Paraná, Brazil;
- JCMC** Júlio C. M. Chaul collection, Universidade Federal de Viçosa, Minas Gerais, Brazil;
- NIGP** Nanjing Institute of Geology and Palaeontology, Chinese Academy of Sciences, Nanjing, China;
- PSWC** Philip S. Ward collection, University of California, Davis, CA, USA;
- UCDC** Bohart Museum of Entomology, University of California, Davis, CA, USA.

## Results

### Hymenoptera Linnaeus, 1758

#### Apocrita Latreille, 1810

#### Aculeata Latreille, 1802

#### Formicoidea Latreille, 1809

**Definition.** Detailed study of the †*Camelomecia* clade has redefined the Formicoidea and refined our understanding of the definition and evolutionary patterning of the total and crown Formicidae (Boudinot et al. 2020a). Formicoids, we now know, are a clade of Formicapoidina (sister to Apoidea: Johnson et al. 2013; Branstetter et al. 2017; Peters et al. 2017) defined by positive (i.e., non-“absence” character) morphological synapomorphies most of which form an innovation suite for cursorial or surface-based predation, including: (1) prognathy and elongation of the postgenal bridge (Figs 13A, 14B); (2) enlargement of the dorsal (cranial) mandibular condyle (Fig. 13A); (3) rotation of the antennal toruli laterad in females (Fig. 13A, B); (4) elongation of the procoxae (Figs 14A, 15A); (5) partial to complete enclosure of the proximal protrochanteral articulations within the distal procoxal foramina (Figs 14E, 15A, 16E); (6) internalization of the proximal meso- and metacoxal articulations within the mesosoma (Figs 14B, 15A, 16); (7) petiolation of the first metasomal segment (Figs 14A, 15A, 16A, D, E); (8) gain of the anteroventral process of the petiolar sternum (Fig. 16A); (9) buttressing of the metasomal waist through gain of the prora (an anteroventral process of the second metasomal sternum) (Figs 15A, 16A, D); plus (10) an angled juncture between the first free abscissae of Rs and M in the fore wing (Figs 15A, 16A, D). The †*Camelomecia* clade, in contrast to the total clade of the Formicidae, probably lack the metapleural gland and apterous workers altogether, while also being defined by a combination of derived and plesiomorphic features (see, e.g., the key below). Based on direct examination of the unique specimen (holotype) of †*Camelomecia janovitzii* (BEB at the AMNH, 2017), presence of this gland is uncertain and requires further scrutiny.

## Extended definition of diagnostic states

To ensure maximal clarity for the definition provided for the Formicoidea above, we provide further definition of these conditions here:

- (1) Prognathy in ants is achieved through elongation of the postgenal bridge, i.e., the sclerotization between the occipital and oral foramina (Richter et al. 2019, 2020). This condition has arisen independently in a number of other Aculeata, including the Bethyridae, Dryinidae, Sclerogibbidae, a few Tiphioidea, some Mutillidae, Philanthidae, and Ampulicidae. This was recognized as a synapomorphy of the Formicidae by Bolton (2003).
- (2) The dorsal mandibular condyle—also known as the “cranial condyle” or “anterior mandibular condyle” in hypognathous taxa (Snodgrass 1935, 1956) and more recently labeled the “dorsal mandibular articulation” (Richter et al. 2019, 2020, Klunk et al. 2020)—is an outgrowth of the cranium which articulates with the mandible via the mandibular acetabulum, forming the second functional condyle defining the Dicondylia. In ants, this condyle is much enlarged, allowing for a wider gape via a slide-locking mechanism. The form is variable among and often within the crown ant subfamilies, and the enlarged condition is a strong diagnostic feature of the Formicoidea, with limited similarity among other Aculeata.
- (3) Torular orientation is mechanically significant and has consequences for the radicle form. The ancestral condition of the Aculeata is to have the toruli directed anteriorly away from the cranium (assuming hypognathy), such that the foramina are aligned with the plane of the cranium, nearly perpendicular to the long axis of the head. In the majority of Formicoidea, the medial rims of the toruli are raised dorsally (assuming prognathy), such that they are above the lateral rims when viewed in profile; when viewed anteriorly, the foramina of the toruli are clearly directed laterally. This condition has arisen in a number of other Aculeata, so the diagnostic value of this is limited to that of the cranial condyle.
- (4) Procoxal elongation is observed in ants when compared to other Aculeata, as recognized by Liu et al. (2019). Specifically, the procoxae are ca. 2 × as long dorsoventrally as they are wide in anteroposterior diameter. This is another strong diagnostic feature as the procoxae of most other Aculeata are generally more globular or are somewhat wedge-shaped in profile view, with lengths sometimes only slightly exceeding widths, even in lineages with apterous females.
- (5) Distal protrochanteral closure is the condition in which the coxotrochanteral articulation is concealed within the procoxa, such that the membrane is completely hidden (Boudinot 2015). This is observed in all living ants, including males and deformed inquilines, and was confirmed for all amber taxa for which the condition could be evaluated, including stem Formicidae plus the †*Camelomecia* group. In a number of fossils examined, the articulation of the procoxa and trochanter is decayed, giving the appearance of a partially open cavity. In these cases, the strong constriction and curvature of the protrochanter are observable and indicative of a tighter articulation prior to death. Among all Aculeata, protrochanteral closure

is only observed in some species of *Myrmosa* (Mutillidae), but these insects are otherwise grossly distinct from Formicoidea.

- (6) Closure of the meso- and metathoracicocoxal articulations is the condition in which the proximal articular structures of the coxae are completely internalized within the mesosoma, resulting in total concealment of the articular membranes. This is distinct from closure of the metacoxal cavity by a ring of sclerite, which relates to the separation or lack thereof from the propodeal foramen (Bolton 2003, Keller 2011). The proximal coxal articulations are further modified as ball-like structures, while the thoracic foramina are oriented parallel to the ground (Boudinot 2015, Liu et al. 2019). Closure of these thoracicocoxal articulations is much more frequently observed among Aculeata than closure of the distal procoxal articulation and is widespread among those taxa with apterous females.
- (7) Petiolation of the first metasomal segment is the condition in which the posterior foramen is constricted, and in ants is associated with the formation of a distinct posterior face of the muscular dorsal node. This was recognized as a synapomorphy of the Formicidae by Bolton (2003). It should be noted that petiolation of the second metasomal segment is observed as a spectrum, with varying degrees of constriction and reduction in size.
- (8) The subpetiolar process is a cuticular projection of the petiolar sternum which articulates between the metacoxae when the metasoma is completely down-flexed. The process is present in the majority of the Formicoidea, and similar structures have been gained in some non-ant Aculeata, including a few Chrysididae, a few Tiphioidea, some Ampulicidae, some Bembicidae, and some Philanthidae. The subpetiolar process was intuitively inferred to be absent in the ancestral formicid by Bolton (2003, p. 289), whereas it is robustly supported a synapomorphy of the superfamily in our work.
- (9) The prora is an anteroventral thickening of the second metasomal sternum that buttresses the segment during strong ventral flexion of the abdomen. Presence of the prora has not been previously recognized as a defining feature of the ants, and similar developments are observed in only a few other Aculeata, such as Brachycistidinae (Tiphidae), *Chyphotes* (Chyphotidae), and *Dolichurus* (Ampulicidae). Loss of the prora has occurred sporadically among the crown Formicidae, and defines, for example, the Formicinae as well as the Aneuretinae + Dolichoderinae clade.
- (10) An angled juncture of Rsf1 and Mf1 is observed with some frequency among other Aculeata and has been reversed or otherwise modified in various crown Formicidae. Among venational features, Bolton (2003) recognized loss of 3rs-m and 2m-cu as synapomorphies of the Formicidae; these are observed to be present in some but not all †*Camelomecia* group species, indicating tendency for parallel loss.

### Synopsis of Formicoidea emphasizing Mesozoic taxa

**Note.** Only taxa known from the Mesozoic are listed. For a complete subfamily-level classification of crown Formicidae as stands, see AntCat.org. †Armaniinae Dlussky, 1983 and other compression-fossil taxa are treated in a forthcoming phylogenetic study, as will

the Burmite fossil †*Burmomyrma rossi* Dlussky, 1996, which was recently transferred from the Formicidae to the †Falsiformicidae by Lucena and Melo (2018) without morphological justification. Note that the revised diagnosis of †*Myanmyrma* is provided in the key, particularly couplet 10. Elevation of the †Zigrasimeciinae stat. nov. is justified by their morphological distinctness from all other Formicidae and uncertain relationship with other stem groups (see the key and Cao et al. 2020). Moreover, this action stabilizes the formalization of stem subfamilies, following the similar elevation of †Haidomyrmecinae by Perrichot et al. (2020). Given the expanding knowledge of haidomyrmecines, recognition of a tribal system may be worthwhile. Regarding the poorly preserved fossils attributed to †*Cretomyrma*, we have made this transfer based on the results of Boudinot et al. (2020a); for which a refined explanation will be provided soon. Bracketed abbreviations in the list below indicate sex or caste: f = female/gyne, m = male, w = worker.

#### †*Camelomecia* clade

- 1• †*Camelomecia* Barden & Grimaldi, 2016
  1. †*Cm. janovitzi* Barden & Grimaldi, 2016 [f, Burmese amber]
- 2• †*Camelosphecia* gen. nov.
  2. †*Cs. fossor* sp. nov. [f, Burmese amber]
  3. †*Cs. venator* sp. nov. [m, Burmese amber]

#### Total clade Formicidae Latreille, 1809

##### Stem Formicidae *incertae sedis*

- 3• †*Baikuris* Dlussky, 1987
  4. †*Ba. casei* Grimaldi et al., 1997 [m, Raritan amber]
  5. †*Ba. mandibularis* Dlussky, 1987 [m, Taimyr amber]
  6. †*Ba. maximus* Perrichot, 2015 [m, Charentese amber]
  7. †*Ba. mirabilis* Dlussky, 1987 [m, Taimyr amber]
- 4• †*Cretomyrma* Dlussky, 1975 subfam. transfer
  8. †*Cr. arnoldii* Dlussky, 1975 [w, Taimyr amber]
  9. †*Cr. unicornis* Dlussky, 1975 [w, Taimyr amber]
- 5• †*Dlusskyidris* Bolton, 1994
  10. †*Dl. zherichini* Bolton, 1994 [m, Taimyr amber]

#### Clade †Sphecomyrmines nom. nov.

†Haidomyrmecinae Bolton, 2003 (see Barden et al. 2020; Perrichot et al. 2020)

##### †*Aquilomyrmex* clade

- 6• †*Aquilomyrmex* Perrichot et al., 2020
  11. †*A. huangi* Perrichot et al., 2020 [f, Burmese amber]
- 7• †*Chonidris* Perrichot et al., 2020
  12. †*Ch. insolita* Perrichot et al., 2020 [f, Burmese amber]
- 8• †*Dhagnathos* Perrichot et al., 2020
  13. †*Dh. autokrator* Perrichot et al., 2020 [f, Burmese amber]

##### †*Haidomyrmex* group (newly recognized)

- 9• †*Dilobops* Lattke & Melo, 2020

14. †*Di. bidentata* Lattke & Melo, 2020 [w, Burmese amber]
- †*Haidomyrmex* clade
- †*Ceratomyrmex* subclade
- 10• †*Ceratomyrmex* Perrichot et al., 2016
15. †*Ce. ellenbergeri* Perrichot et al., 2016 [w, Burmese amber]
16. †*Ce. planus* Lattke & Melo, 2020 [w, Burmese amber]
- 11• †*Linguamyrmex* Barden & Grimaldi, 2017
17. †*L. brevicornis* Perrichot et al., 2020 [f, w, Burmese amber]
18. †*L. rhinocerus* Miao & Wang, 2019 [w, Burmese amber]
19. †*L. vladi* Barden & Grimaldi, 2017 [w, Burmese amber]
- 12• †*Protoceratomyrmex* Perrichot et al., 2020
20. †*Pc. revelatus* Perrichot et al., 2020 [w, Burmese amber]
- †*Haidomyrmex* subclade
- 13• †*Haidomyrmex* Dlussky, 1996
21. †*Hx. cerberus* Dlussky, 1996 [w, Burmese amber]
22. †*Hx. davidbowiei* Lattke & Melo, 2020 [w, Burmese amber]
23. †*Hx. scimitarus* Barden & Grimaldi, 2012 [f, Burmese amber]
24. †*Hx. zigasi* Barden & Grimaldi, 2012 [f, Burmese amber]
- 14• †*Haidomyrmodes* Perrichot et al., 2008
25. †*Hd. mammothus* Perrichot et al., 2008 [f, w, Charentese amber]
- 15• †*Haidoterminus* McKellar et al., 2013b
26. †*Ht. cippus* McKellar et al., 2013b [w, Medicine Hat amber]
- †Zigrasimeciinae Borysenko, 2017 stat. nov. (see also Cao et al. 2020)
- 16• †*Boltonimecia* Borysenko, 2017
27. †*Bo. canadensis* (Wilson, 1985) [w, Medicine Hat amber]
- 17• †*Protozigrasimecia* Cao et al., 2020
28. †*Pz. chauli* Cao et al., 2020 [w, Burmese amber]
- 18• †*Zigrasimecia* Barden & Grimaldi, 2013 (gynes known, see also Cao et al. 2020)
29. †*Z. ferox* Perrichot, 2014 [w, Burmese amber]
30. †*Z. hoelldobleri* Cao et al., 2020 [w, Burmese amber]
31. †*Z. tonsora* Barden & Grimaldi, 2013 [w, Burmese amber]
- †*Sphecomyrminae* Wilson & Brown, 1967 *sensu stricto*
- 19• †*Gerontoformica* Nel & Perrault, 2004 (see Barden and Grimaldi 2014)
- †*Gerontoformica orientalis* species group (newly recognized; †*Gerontoformica sensu stricto*)
32. †*G. cretatica* Nel & Perrault, 2004 [w, Charentese amber]
33. †*G. gracilis* (Barden & Grimaldi, 2014) [w, Burmese amber]
34. †*G. occidentalis* (Perrichot et al., 2008) [w, Charentese amber]
35. †*G. orientalis* (Engel & Grimaldi, 2005) [w, Burmese amber]
- (Note: †*G. orientalis* is the type species of †*Sphecomyrmodes* Engel & Grimaldi, 2005)
36. †*G. robusta* (Barden & Grimaldi, 2014) [w, Burmese amber]
37. †*G. spiralis* (Barden & Grimaldi, 2014) [w, Burmese amber]

38. †*G. subcuspis* (Barden & Grimaldi, 2014) [w, Burmese amber]  
 †*Gerontofornica pilosa* species group (newly recognized)  
 39. †*G. contega* (Barden & Grimaldi, 2014) [w, Burmese amber]  
 40. †*G. magna* (Barden & Grimaldi, 2014) [w, Burmese amber]  
 41. †*G. pilosa* (Barden & Grimaldi, 2014) [w, Burmese amber]  
 †*Gerontofornica* species newly recognized as unplaceable due to preservation  
 42. †*G. rugosa* (Barden & Grimaldi, 2014) [w, Burmese amber]  
 43. †*G. tendir* (Barden & Grimaldi, 2014) [w, Burmese amber]  
 20• †*Myanmyrma* Engel & Grimaldi, 2005  
 • (Note: The diagnosis of †*Myanmyrma* is revised via the key below, see particularly couplet 10)  
 44. †*M. gracilis* Engel & Grimaldi, 2005 [w, Burmese amber]  
 45. †*M. maraudera* (Barden & Grimaldi, 2014) comb. nov. [w, Burmese amber]  
 21• †*Sphecomyrma* Wilson & Brown, 1967  
 46. †*S. freyi* Wilson & Brown, 1967 [w, Raritan amber]  
 47. †*S. mesaki* Engel & Grimaldi, 2005 [w, Raritan amber]

Clade Antennoclypeata nom. nov.

†Brownimeciinae Bolton, 2003

- 22• †*Brownimecia* Grimaldi et al., 1997  
 48. †*Br. clavata* Grimaldi et al., 1997 [w, Raritan amber]

Crown clade Formicidae Latreille, 1809

Ponerinae Lepeletier de Saint-Fargeau, 1835

- Kachin and Tilin burmite deposits (Zheng et al. 2018, unpubl. data).

Dolichoderinae Forel, 1878

- 23• †*Chronomyrmex* McKellar et al., 2013a  
 49. †*Cx. medicinehatensis* McKellar et al., 2013a [w, Medicine Hat amber]  
 • Kachin and Tilin burmite deposits (Zheng et al. 2018, unpubl. data).

Formicinae Latreille, 1809

- 24• †*Kyromyrma* Grimaldi & Agosti, 2000  
 50. †*K. neffi* Grimaldi & Agosti, 2000 [w, Raritan amber]  
 • Kachin and Tilin burmite deposits (Zheng et al. 2018, unpubl. data).

Additional crown taxa:

- 25• †*Canapone* Dlussky, 1999 (“Ponerinae” *sensu* Wilson, Brown, and others)  
 51. †*Cp. dentata* Dlussky, 1999 [w, Medicine Hat amber]  
 26• †*Cananeuretus* Engel & Grimaldi, 2005 (Aneuretinae Emery, 1913)  
 52. †*Cn. occidentalis* Engel & Grimaldi, 2005 [w, Medicine Hat amber]

## Diagnostic key to the major groupings of Mesozoic Formicoidea

**Note.** †Armaniinae and other compression fossil taxa are not included in this key due to a lack of preserved detail. Additionally, †*Burmomyrma* and †*Cretomyrma* are excluded from this key as both fossils are missing their anterior halves. Comprehensive review of all Mes-

ozoic male Formicoidea is necessary before †*Baikuris* and †*Dlusskyidris* can be considered specifically identifiable. For detailed keys to the genera and species of †Haidomyrmecinae, we refer the readers to Perrichot et al. (2020); in distinction to the former publication, we include †*Dilobops* which was published soon thereafter (Lattke and Melo 2020).

- 1 Mandibles of both sexes cup-shaped, being strongly bowed in lateral view (Figs 1A, 2). Masticatory margins of mandibles in both sexes always elongate (white triangle, Fig. 1A). Entire body of clypeus projecting anteriorly away from remainder of cranium (black triangle, Fig. 1A) (weakly so in males). Anterior clypeal margin always lacking chaetae (“traction setae”, “spicules”, “pegs”). Frontal carinae (paired median, longitudinal ridges) between antennal toruli always absent. Face always without anterior or dorsomedian projections .....2 (†*Camelomecia* clade)
- Mandibles not cup-shaped (Fig. 1B, C). Masticatory margins of mandibles short (white triangle, Fig. 1B) or elongate (white triangle, Fig. 1C). Body of clypeus not projecting anteriorly away from remainder of cranium, rather being tightly integrated and surrounded laterally by the malar area. Anterior clypeal margin with or without chaetae (arrows, Fig. 1B, C). Frontal carinae usually present .....3 (**Formicidae Latreille, 1809**)

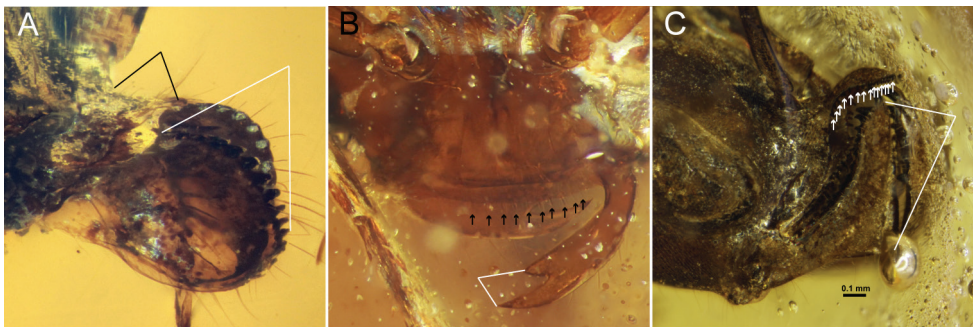


**Figure 1.** Mandibles of representative Formicoidea **A** †*Camelosphecia fossor* gen. et sp. nov. holotype female, lateral oblique (ANTWEB1038930) **B** †*Gerontoformica* species, male, dorsal or full-face view (ANTWEB1032638) **C** †*Chonidris insolita* holotype female, anterolateral oblique (FANTWEB00022, AntWeb: Vincent Perrichot).

- 2 Masticatory mandibular margins of both sexes multidentate, with ten or more well-defined teeth (Fig. 2A). Anterior clypeal margin of female produced anteriorly as thin, laminar sheet (black triangle, Fig. 1A). Female anterior clypeal margin medially bidentate (white curve and arrows, Fig. 2A). Disc (i.e., dorsal surface) of female labrum with several very large, stout, and curved chaetae (black asterisks, Fig. 2A). Compound eyes of female massive, taking up most of cranium laterally. Female profemora massively enlarged. Second protarsomere of female margined with conspicuous psammochaetae (“fossorial setae”)....†***Camelosphecia* gen. nov.**
- Masticatory mandibular margins of both sexes edentate, or if teeth present, these very fine, representing mere crenulation (Fig. 2B). Anterior clypeal margin not produced anteriorly as thin laminar process. Anterior clypeal margin edentate, but may be medially emarginate (white curve, Fig. 2B). Disc of female labrum

glabrous, lateral margins with sprays of thin setae (white asterisks, Fig. 2B). Female compound eyes comparatively small, not taking up entire lateral side of cranium. Female profemora thin, twig-like. Second protarsomere of female lacking psammochaetae..... †*Camelomecia* Barden & Grimaldi, 2016

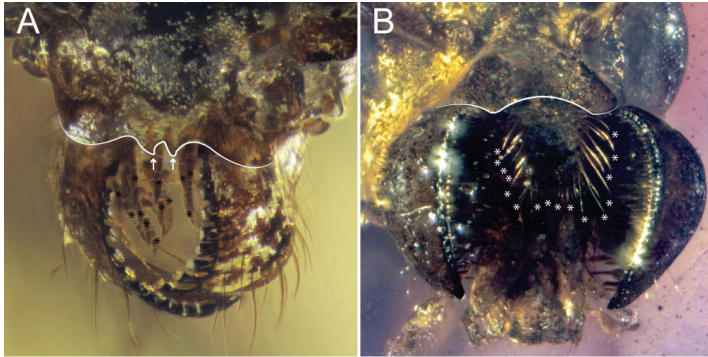


**Figure 2.** Mouthparts of †*Camelomecia* clade genera **A** †*Camelosphesia fossor* gen. et sp. nov. holotype female, dorsolateral oblique (ANTWEB1038930) **B** †*Camelomecia janovtzi* holotype female, anterolateral oblique (AMNH-BUTJ003, AntWeb: Phil Barden).

- 3 Basal angle or tooth of mandible (i.e., the juncture between the basal and masticatory margins) directed posterodorsally (black curve on mandible, Fig. 3A), whether as an elongate process or simply due to rotation of the mandibles. Clypeus or anterior region of face distinctly produced, either bearing a tubercle or laminar or linear processes (white curve on clypeus, Fig. 3A). Elongate (trigger) setae present or absent on face projecting into active area of mandibles (black arrows, Fig. 3A). (Note: Males unknown.)..... 4 (†*Haidomyrmecinae* Bolton, 2003; see Barden et al. 2020 for phylogeny)
- Basal angle or tooth of mandible never directed posterodorsally (black curve on mandible, Fig. 3B). Clypeus or anterior head region not produced, nor bearing such processes (white curve on clypeus, Fig. 3B). Elongate setae absent. (Note: Males known.) ..... 7

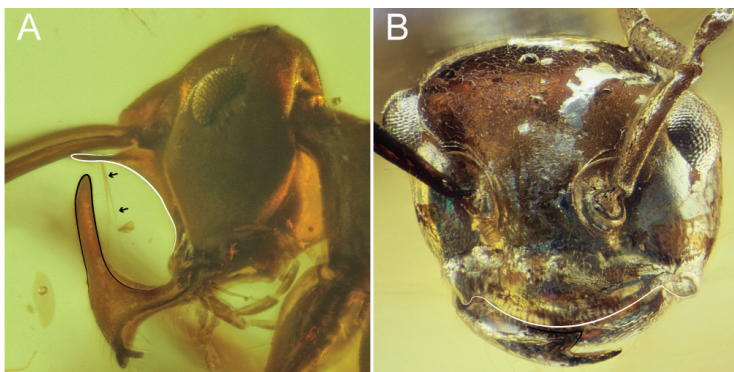


**Figure 3.** Cranium and mandibles of stem Formicidae **A** †*Linguamyrmex brevicornis*, worker, lateral view (FANTWEB00035, AntWeb: Vincent Perrichot) **B** †*Gerontiformica* species, worker, dorsolateral oblique (ANTWEB1032639).

- 4 Labrum large and exposed beneath clypeus (white curves, Fig. 4A, B) (ventral view or open mandibles sometimes necessary, as in Fig. 4B). Labrum with peg-like chaetae (natural black structures outside of white curve in Fig. 4A, inside curve in Fig. 4B). Median portion of clypeus ecarinate, i.e., lacking median longitudinal carina. Clypeus and labrum both concave in cross-section. Trigger hairs absent ..... †*Aquilomyrmex* clade (see couplet 9 of Perrichot et al. 2020 to distinguish among constituent genera)
- Labrum small and concealed in buccal cavity. Labrum without margin or field of peg-like chaetae. Median portion of clypeus with or without a median longitudinal carina. Clypeus and labrum not concave; clypeus flat to convex in cross-section (black curve beneath frontal process, Fig. 4C). Trigger hairs present as long, thin setae which project into the active area of the mouthparts (black arrow, Fig. 4C) ..... 5 (†*Haidomyrmex* group)



**Figure 4.** Cranial armaments of †Haidomyrmecinae **A** †*Chonidris insolita* female, dorsolateral oblique (FANTWEB00033, AntWeb: Vincent Perrichot) **B** †*Aquilomyrmex huangi* female, ventrolateral oblique (FANTWEB00023, AntWeb: Vincent Perrichot) **C** †*Linguamyrmex rhinocerus*, female, lateral (FANTWEB00016, AntWeb: Vincent Perrichot).

- 5 Clypeus with a dense brush of chaetae (brush indicated by white asterisk, Fig. 5A); brush located approximately in center of clypeus or more dorsally, just beneath the frontal tubercle.....6
- Clypeus without a dense brush of chaetae; frontal horn, if present, may bear long, thin setae or be apically margined by short, peg-like chaetae (short thick hairs outside of white curve in Fig. 5B) ..... †*Ceratomyrmex* subclade (see couplet 6 of Perrichot et al. 2020 to distinguish among constituent genera)

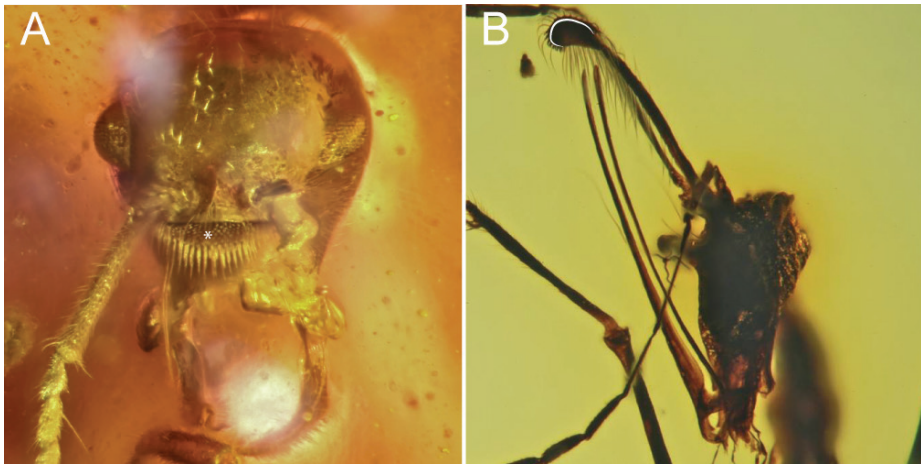


**Figure 5.** Facial seta and chaeta arrays of trigger-hair-bearing †Haidomyrmecinae **A** †*Haidomyrmex cerberus*, holotype worker, dorsolateral oblique (BMNHP20182, AntWeb: Vincent Perrichot) **B** †*Ceratomyrmex ellenbergeri*, worker, dorsal anterolateral oblique (FANTWEB00005, AntWeb: Vincent Perrichot).

- 6 Cranium highly modified: In profile view, cranium more-or-less teardrop-shaped (Fig. 6A); clypeal area dorsoventrally elongate, concave (black curve, Fig. 6A); mouthparts migrated posteroventrally, thus nearly in a hypognathous position. Anterolateral corners of cranium simple, without distinct triangular processes ..... †*Haidomyrmex* **subclade** (see couplet 2 of Perrichot et al. 2020 to distinguish genera of this group)
- Cranium not modified as above: cranium not teardrop-shaped; clypeal area not dorsoventrally elongate; and mouthparts not migrated posteroventrally. Anterolateral corners of cranium armed with distinct triangular processes (black angle, Fig. 6B)..... †*Dilobops* Lattke & Melo, 2020

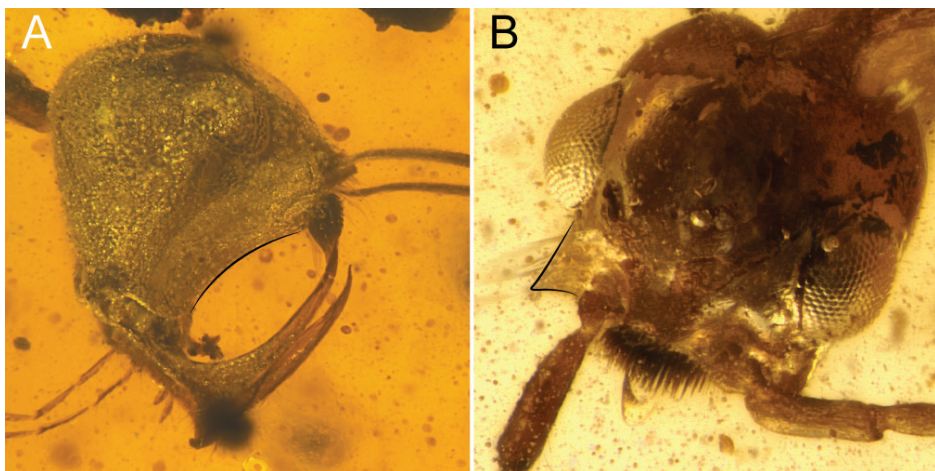


**Figure 6.** Cranial conformation of clypeal-brush-bearing †Haidomyrmecinae **A** †*Haidomyrmex cerberus* worker, lateral (FANTWEB000017, AntWeb: Vincent Perrichot) **B** †*Dilobops bidentata* worker holotype, dorsolateral oblique (FANTWEB000039, AntWeb: Gabriel Melo).

- 7 Clypeus extending posteriorly past the anterior margins of the antennal toruli (right torulus on left side, as shown, marked by white curve, Fig. 7A), thus having an elongate posteromedian strip between the antennal insertions (black curve, Fig. 7A); exceptions within the crown clade include Pseudomyrmecinae and many Formicinae (see Bolton 1994, 2003; Boudinot 2015 for identification). Anterolateral portions of clypeus **not** developed as lobate processes; anterolateral clypeal corners or malar area may be dentate. Mandibles edentate to many-dentate. Scape length  $> 4 \times$  scape width and  $\geq 1/2 \times$  head length .....**8 (Antennoclypeata)**
- Clypeus not extending posteriorly past anterior margins of the antennal toruli (right torulus on left side, as shown, marked by white curve, Fig. 7B), thus without an elongate posteromedian strip between the antennal insertions (black curve, Fig. 7B). Anterolateral portions of clypeus developed as broad and flat lobe-like processes overhanging or tightly fitting against mandibular bases (white arrows pointing at white curve, Fig. 7B). Mandibles uni- or bidentate (Fig. 7B). Scape length  $< 4 \times$  scape width and  $\leq 1/2 \times$  head length .....**9**

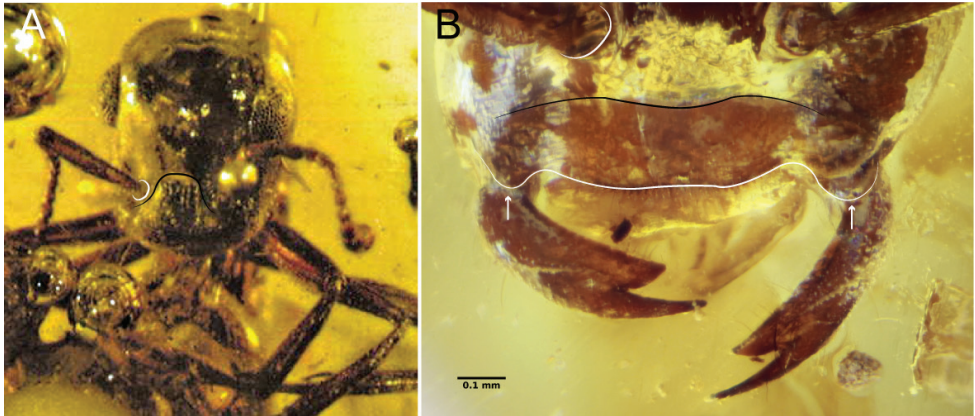


**Figure 7.** Clypeus and cranium of Antennoclypeata and †Sphecomyrmines **A** †*Brownimecia clavata* holotype worker, full-face (from Grimaldi and Engel 2005, used with permission of the publisher) **B** †*Geronotoformica* species, worker, dorsal (ANTWEB1032629).

- 8 Mandible unidentate. Cranium dome-shaped (deep black curve at back of head, Fig. 8A). Anterolateral corners of cranium (malar area) derived as pointed, triangular processes (black angle near front of head, Fig. 8A). Anterolateral margins of mesopectus evenly rounded, without longitudinal (epicnemial) carina. (Queens and males unknown.).....**†Brownimeciinae Bolton, 2003**
- Mandibles uni- or more dentate. Cranium not dome-shaped (shallow black curve at back of head, Fig. 8B). Anterolateral corners of cranium not (black curve near mandibles, Fig. 8B) or rarely derived as pointed, triangular processes (Amblyoponinae Forel, 1893). Anterolateral margins of mesopectus often angularly marked by longitudinal (epicnemial) carina (white curve, Fig. 8B). (Note: Queens and males known) ..... **crown clade Formicidae**

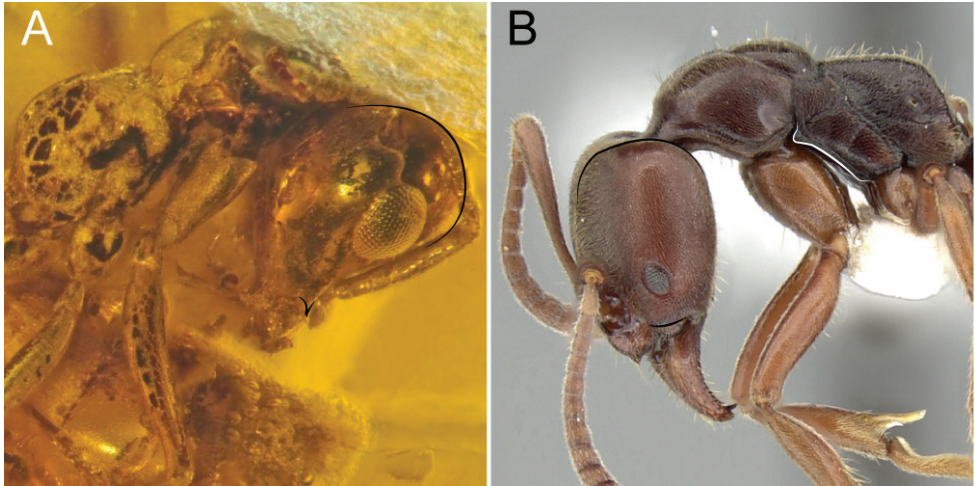


**Figure 8.** Cranial and mesosomal profiles of Antennoclypeata **A** †*Brownimecia clavata* holotype worker, lateral (AMNH-NJ667, AntWeb: Dave Grimaldi and Vincent Perrichot) **B** *Austroponera castanea* (Mayr, 1865) worker, lateral (CASENT0249168, AntWeb: Ryan Perry).

- 9 Clypeus transverse and arcuate; anterior clypeal margin broadly concave (Fig. 9B). Mandible rotated in socket with blade torqued such that the ventromedial mandibular margin is exposed in full-face view (black line exposed proximal to white curve of basal margin, Fig. 9A) (state unknown for †*Boltonimecia*). Ventral (inner) mandibular face with dense array of spiniform chaetae (state unknown for †*Boltonimecia*). Antennal toruli very wideset, being nearly situated beneath compound eyes in full-face view, approximately one scape length or more apart. Facial region of cranium in female castes with linear and diagonally oriented scrobes for reception of antennal scapes, extending from antennal toruli to anterior margins of compound eyes. (Note: Males unknown.) ..... †**Zigrasimeciinae** **Borysenko, 2017, stat. nov.** (see Cao et al. 2020 for key to constituent genera)
- Clypeus variable, usually shield like; anterior clypeal margin linear to convex (Fig. 9C) or medially emarginate. Mandible neither rotated in socket nor blade torqued; ventromedial margin of mandible only visible laterally (Fig. 9C). Antennal toruli close-set, positioned well medial to the compound eyes in full-face view, and distinctly less than one scape length apart. Facial region of cranium in female castes without diagonally oriented scrobes; if areas lateral to frontal carinae sulcate, these sulci are curved and ending medial to compound eye or posterior to compound eye anterior margin (†*Myanmyrma* is the exception, Fig. 10A). (Note: Males known.) ..... **10 (†Sphecomyrminae** **Wilson & Brown, 1967 sensu stricto**, including male-based taxa †*Baikuris* Dlussky, 1987 and †*Dlusskyidris* Bolton, 1994 [see also: Grimaldi et al. 1997, Perrichot 2015]; for putative male of †*Sphecomyrma* Wilson & Brown, 1967, see Grimaldi et al. 1997)



**Figure 9.** Facial views of †Zigrasimeciinae stat. nov. and †Sphecomyrminae *sensu stricto* **A** †*Zigrasimecia* species, worker, posterodorsal oblique (ANTWEB1032623) **B** †*Zigrasimecia* species, worker, anterodorsal oblique (ANTWEB1032660) **C** †*Gerontoformica* species, worker, dorsal (ANTWEB1032649).

- 10 Mandibles elongate, not fitting against clypeus snugly at rest. Frontal carinae robustly flanged, only weakly curved along their lengths, and ending posterior to anterior eye margin (white curve, Fig. 10A) (state not exactly known for †*M. gracilis*). Both clypeus and labrum bearing chaetae on their contact surfaces. (Note: Males unknown) ..... †*Myanmyrma* Engel & Grimaldi, 2005
- Mandibles short, fitting snugly against clypeus at rest. Frontal carinae finely carinate, strongly curved thus forming a distinct semicircle, and ending anterior the anterior eye margin (white curve, Fig. 10B). Rarely both clypeus and labrum with chaetae on their contact surfaces. (Note: Males known) ..... 11

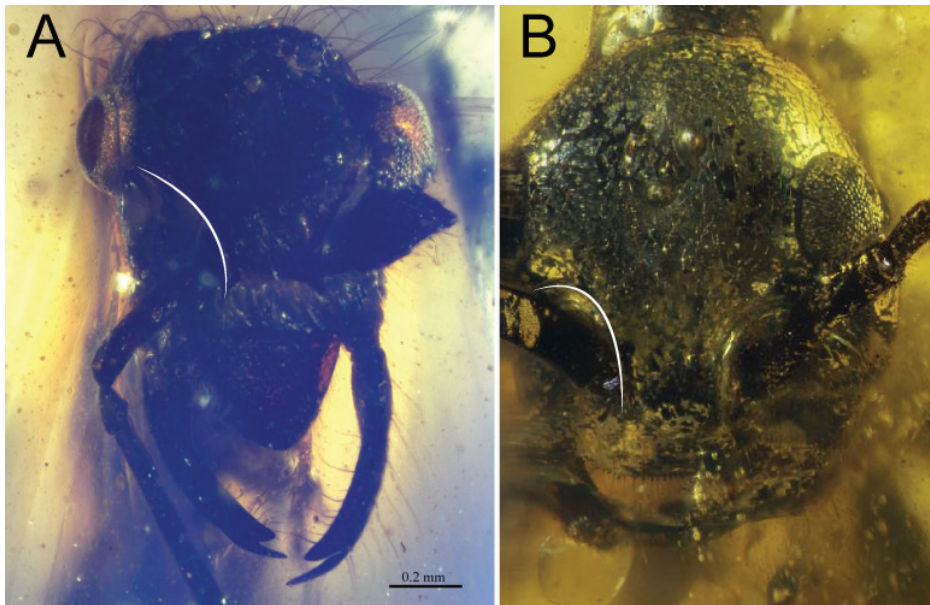


**Figure 10.** Cranial gestalts of †Sphecomyrminae *sensu stricto* **A** †*Myanmyrma maraudera* (Barden & Grimaldi, 2016) comb. nov., holotype worker, full-face (JZCBU1846, AntWeb: Phillip Barden) **B** †*Gerontoformica* species, worker, full-face (ANTWEB1038348).

- 11 Clypeus lacking chaetae. Clypeus bearing lateromedially narrow anteromedian lobate process which overhangs mandibles at mandibular closure (white curve, Fig. 11A). Abdominal segment III foreshortened....†*Sphecomyrma* Wilson & Brown, 1967
- Clypeus with chaetae. Clypeus more-or-less evenly convex, without a distinct anteromedian lobate process (white curve, Fig. 11B). Abdominal segment III foreshortened or not..... 12 (†*Gerontoformica* Nel & Perrault, 2004; see Barden and Grimaldi 2014 for key to species)

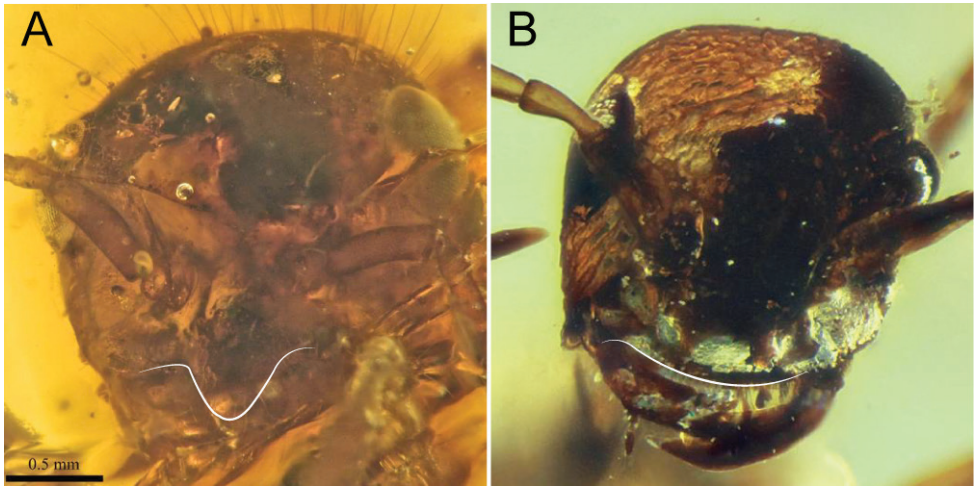


**Figure 11.** Facial views of †*Sphecomyrminae* which have short mandibles **A** †*Sphecomyrma mesaki* Engel & Grimaldi, 2005, holotype worker, anterodorsal oblique (AMNH-NJ1023, AntWeb: Dave Grimaldi and Vincent Perrichot) **B** †*Gerontoformica* species, worker, full-face (ANTWEB1032418).

- 12 Abdominal segment IV with tergum and sternum strongly differentiated into pre- and post-sclerites by sulci and a deep constriction ("cinctus") (Fig. 12A). Abdominal segment III not foreshortened; its anteroposterior length usually greater than that of petiole (Fig. 12A)..... †*Gerontoformica pilosa* species group
- Abdominal segment IV with tergum and sternum weakly or not at all differentiated into pre- and post-sclerites by sulci or a constriction (Fig. 12B). Abdominal segment III usually anteroposteriorly foreshortened; its anteroposterior length usually less than that of petiole (Fig. 12B)..... †*Gerontoformica sensu stricto*

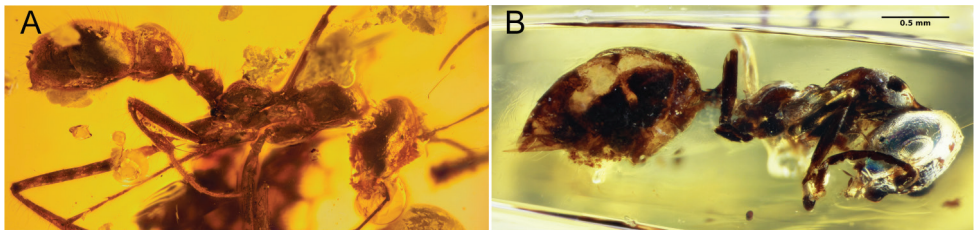


**Figure 12.** Body profiles of †*Gerontoformica pilosa* and *orientalis* species groups **A** †*Gerontoformica pilosa* Barden & Grimaldi, 2014, worker profile (ANTWEB1038931) **B** †*Gerontoformica* species, worker profile (ANTWEB1032649).

## New taxon definitions

### †*Camelosphecia* gen. nov.

<http://zoobank.org/5E38E92B-51D4-4B0B-B8DA-FAE77F7764B9>

Figs 1A, 2A, 13–16

**Type species.** †*Camelosphecia fossor* sp. nov., by present designation.

**Constituent species.** †*Cs. fossor* sp. nov., †*Cs. venator* sp. nov.

**Diagnosis.** Identifiable as members of the †*Camelomecia* clade by the bowed mandibles with elongate masticatory margins, projecting clypeus, and absence of clypeal chaetae, frontal carinae, and facial projections, as outlined in the key above.

Both sexes specifically differentiated from †*Camelomecia* by: (1) the conspicuously-developed mandibular teeth on the masticatory margin (versus teeth present as mere crenulation or absent altogether); (2) fore wing 1cu-a crossvein distant proximally from divergence of free M and Cu by at least one of its own lengths (the phrase “markedly prefurcal” is used to describe this condition throughout this work; versus 1m-cu proximal to M+Cu split by less than one 1m-cu length, or 1m-cu usually at or distal to split, as observed in all known †*Camelomecia* and †Haidomyrmecinae, for example); and (3) crossvein 2m-cu absent (versus 2m-cu present or absent).

Females further differentiated from those of †*Camelomecia* as follows: (4) occipital carina of female extending to hypostoma (versus not); (5) compound eyes of female massively enlarged, filling entire lateral portion of head in profile view and rendering malar space virtually absent (versus compound eyes smaller, malar space well-defined); (6) teeth of masticatory mandibular margins conspicuously developed (versus present as crenulation or absent altogether); (7) disc (main central region) of labrum in the female bearing massive, long, thick chaetae (versus such chaetae absent); (8) anterior clypeal margin bidentate medially (versus margin edentate); (9) notauli on mesoscutum absent (versus present); (10) fore femora powerfully enlarged (versus weak and thin); (11) protarsomeres I and II margined with an array of differentiated psammochaetae (versus such chaetae absent); (12) posterolateral corners of propodeum armed (versus denticles absent or present); (13) abdominal poststernite IV short relative to posttergite.

Males, as so far known for both genera, are further differentiated from †*Camelomecia* in having: (14) eyes medially binocular, i.e., with clypeus nearly concave and compound eyes massively, medially bulging such that medial-most ommatidia of each eye are directed toward one another.

**Etymology.** The root of the generic name, *camelo-*, is made in reference to †*Camelomecia*, the camel-faced ants; the second part of the name, *-sphaeria* emphasizes the waspiness of these intermediate formicoids.

†*Camelosphracia fossor* sp. nov.

<http://zoobank.org/E6AD4D2B-89FA-4A5D-AFCE-5C1FC207F8A7>

Figs 1A, 2A, 13–15

**Holotype.** Myanmar, Kachin State: Hukawng Valley [ANTWEB1038930, deposited in DZUP].

**Additional material examined.** Same as holotype [females: BALBuTJ-36, BAL-BuTJ-38, BALBuTJ-40 all in Janovitz collection]

**Diagnosis.** Recognizable as Formicoidea and †*Camelosphracia* as defined above. Distinguished from †*C. venator* by features listed in that species' diagnosis. In briefest, the most distinct features include massive compound eyes, huge and muscular profemora, and presence of psammochaetae on the protarsus.

**Measurements. Female.** CL 0.76; HL 0.94; WH 1.08; CW 0.46; EL 0.41; MW 0.07; LW 0.06; A1L 0.21; A2L 0.11; A3L 0.22; PnW 0.66; PL 0.83; PnLm 1.05; MtW 0.66; MtL 0.41; MsW 0.37; MsL 0.32; WL 1.83; PtL 0.63.

**Description. Female. Head.** Postgenal bridge elongate, thus head “prognathous”. Head posterior to clypeus strongly broadened (broader than long) and inflated, except for a pair of concavities lying over the posterolateral clypeal margin which accommodate the base of scapes. Mandibles cup-shaped, strongly bowed. Masticatory margin of mandibles with 13 teeth. Teeth, except the apical, truncate, gear-like; individual teeth short basally on masticatory margin and gradually increasing in length apically. Apical tooth (maybe apical and preapical) largest, pointed. Ventral surface of mandible without dense tuft of chaetae. Mandibles crossing apically, at full closure approximately half the masticatory margin would cross. Basolateral area of dorsal mandibular surface just beneath malar margin distinctly concave, contrasting to the remaining strongly convex, dome-shaped surface; the margin of this area just before meeting the cranium sinuous in profile view, appearing dentate. Labrum bilobed, its dorsum covered with ca. 24 long, stout chaetae with gently curved tips (chaetae somewhat shorter than 0.1 mm). Palps basally concealed by the labrum and mandibles, so that maxillary palpomeres total count is five or six and labial palpomeres are not visible. Maxillary palpomeres elongate. Clypeus having a basal section integrated with the cranium and an anteromedially projected over mandibles as a thin laminar platform, its maximum width ca. 0.4 × that of head. Clypeal platform having a pair of broad and low anterolateral lobes which curve into an anteromedial pair of close-set triangular teeth. In face view, considering the entire clypeus, the anterior clypeal margin bears two pairs of lobes and the medial pair of teeth, the lobes laterad corresponding to the actual anterolateral corners of the clypeus. Posterior to the platform, the remainder of the clypeus is rightly integrated into the cranium and confined to the anterior eighth of the head. The posterior margin of the clypeus is poorly marked medially, between the toruli, the margin slightly surpassing toruli anteriormost level, but not reaching their posteriormost level.

**Antennae.** Torulus laterally directed; posteromedian portion of torular arch slightly enlarged and covering part of bulbus. Bulbus and bulbus neck coplanar and angled in relation to scape. Antennae 12-merous, not clubbed. Longest antennomeres are I (scape) and III, these two being subequal in length. Antennomere II (pedicel) is small

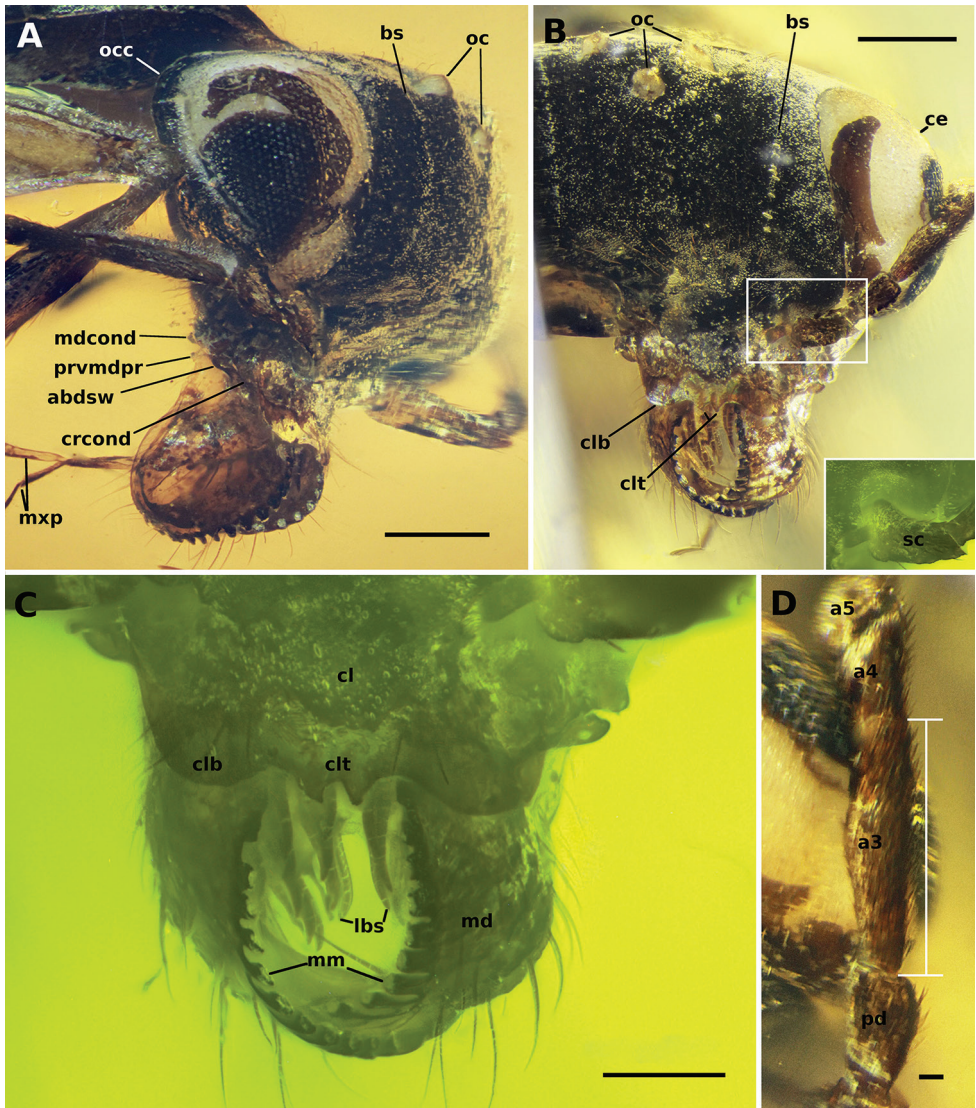


**Figure 13.** Holotype of †*Camelosphracia fossor* sp. nov. **A** lateral view of right side of head **B** full face view of head, right margin blurred on this view due to a folding of the facet. Box on bottom right evidencing scape under fluorescent microscopy **C** detail of clypeus, mandibles and labrum under fluorescent microscopy **D** posterodorsal view of anterior section of funiculus (pedicel plus flagellum), evidencing pedicel and antennomeres III and IV. Abbreviations: **a3–5**, antennomeres III–V; **abdswh**, abductor swelling; **bs**, bubble stream; **ce**, compound eye; **cl**, clypeus; **clb**, clypeal lobe; **clt**, clypeal teeth; **crcond**, cranial condyle; **md**, mandible; **mm**, masticatory margins; **lbs**, labral chaetae; **mdcond**, mandible condyle; **mxp**, maxillary palps; **oc**, ocelli; **occ**, occipital carina; **pd**, pedicel; **prvmdpr**, posteroventral mandible process; **sc**, scape. Scale bars: 0.2 mm (**A**, **B**); 0.1 mm (**C**); 0.02 mm (**D**).

and slightly inflated. Antennomere IV longer than V. Antennomeres V–XI more-or-less similar in size and shape. Apical antennomere not much longer than previous. Antennomeres dorsoventrally compressed (could be a taphonomic artifact). Frontal carinae ab-

sent. Eyes enormous, not bulging, length ca.  $2 \times$  the width in the full view of the eye; in full-face view, eye length ca.  $0.7 \times$  the length of head discounting clypeal projection. In full-face view, medial margin of compound eyes weakly concave, although not conspicuously notched. Ocelli relatively small and positioned high on dorsum of head, the lateral pair almost reaching the vertexal margin in full-face view. Vertexal margin slightly convex. Lateral margins almost entirely occupied by the compound eyes, except for anterior portions, which converge until meeting the outer margin of mandibles. Posterolateral and lateral occipital margin carinate, the margin poorly delimited posteromedially and anteromedially. Ventral surface of head flat to gently concave, with a slightly raised longitudinal median section corresponding in location with the postgenal ridge. Postgenal ridge with a small indentation at its posterior limit. Small, simple, suberect to recurved setae on dorsum of head, except for longer ones originating on the anterior edge of the clypeus and on the mandibles. Antennomeres II–XII covered on dense pubescence.

**Mesosoma.** Pronotum elongate, distinctly bell-shaped in dorsal view; posterior-most region transversely constricted. Pronotum without anterior fringe of setae which is observed in †*Camelomecia*; anterior margin of pronotum, however, with distinct “beading” or rim and sulcus which delimit the anteriormost region. In profile view, posterodorsal portion extended posteriorly as a lobe, with the lobe situated very close to the tegula (nearly contacting); posterior margin just below lobe apparently concave; posteroventral margin lobate, not extending medially posterior to fore coxae, as would be expected for Apoidea. Mesonotum (mesoscutum + mesoscutellum) length in dorsal view subequal to length of pronotum. Mesoscutum  $> 1.5 \times$  broader than long, more-or-less oval in shape. Axillae small. Scutoscutellar sulcus distinct and cross-ribbed, but not particularly deep. Mesoscutellum slightly longer than wide, tapering posterad and with an arched posterior margin. Mesopleuron bulging; oblique mesopleural sulcus present as a thin and poorly-marked line in the upper half of the mesopleural area posteriorly, separating the upper mesopleural area (erstwhile “anepisternum”) from the lower mesopleural area (erstwhile “katepisternum”); lower mesopleural area ca.  $4 \times$  longer than upper mesopleural area. Propodeal spiracle large, protruding from the cuticle, its opening slit and crescent-shaped and posteriorly oriented; spiracle positioned on the upper anterior region of the lateropropodeal surface. Lower metapleural area thin, delimited posteroventrally by carina. Upper metapleural area triangular, its margins approximately the same size. A small metanotal spiracle is apparently seen on the upper anterior corner of the left metapleural area. Propodeum with a subquadrate lamellate projection developed on the lower posterolateral mesosomal corner, projecting over the bases of the metacoxa and metasomal petiole. The anterior and posterior angles of the projection are sharply defined, and its dorsal surface is concave. Propodeum dorsal and declivous faces separated from the lateral face by a pair of ridges that are poorly marked anteriorly and strongly marked posteriorly, each reaching the metapleuropropodeal lamellate projection posteriorly; in the holotype, it appears that a pair of indentations on the upper portion of the propodeal ridges make the propodeum angled in profile view (at least on the left side of the specimen), whereas in the non-type specimens, these carinae toothed at the posterodorsal angle. Metapleural gland orifice absent, and there is no trace of a metapleural gland reservoir (bulla).

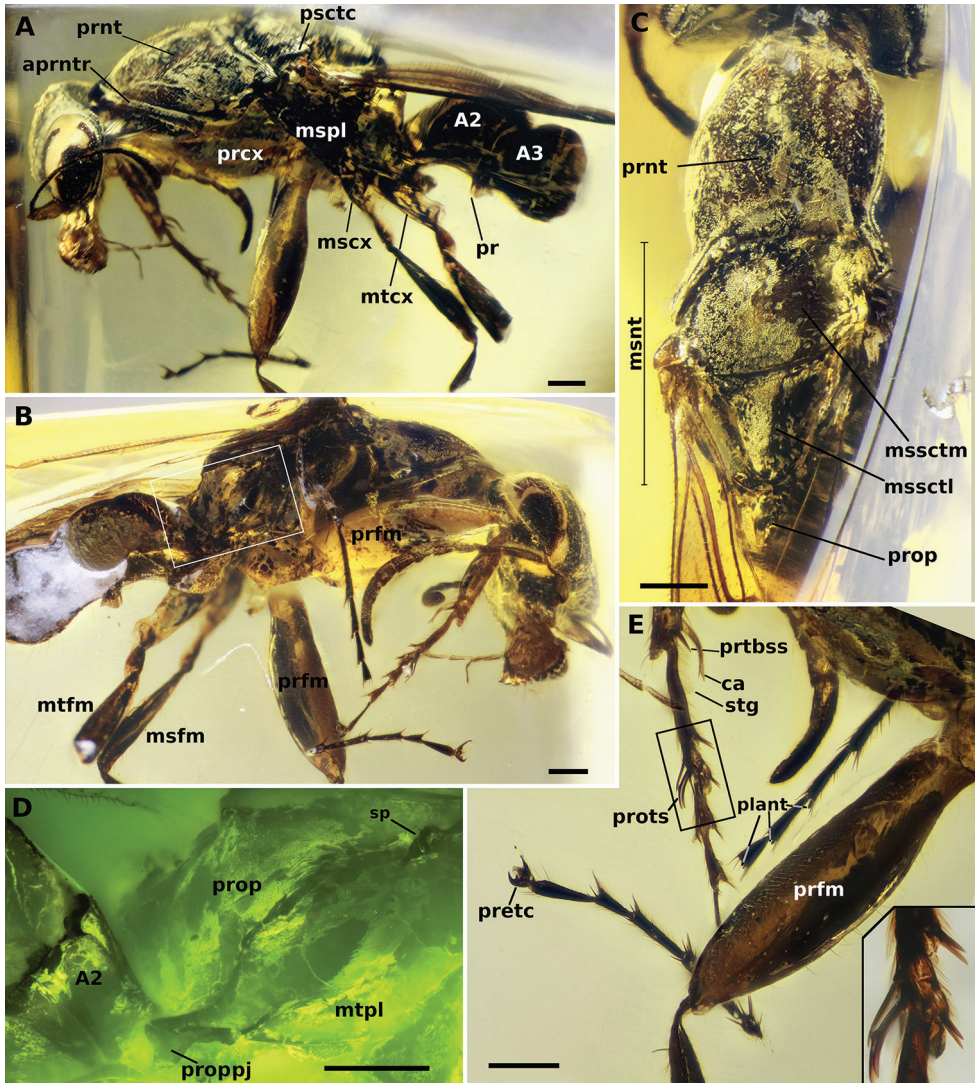


**Figure 14.** Holotype of †*Camelosphecia fossor* sp. nov. **A** profile of left side of body **B** profile of right side of body **C** dorsal view of mesosoma **D** delimited area of **C** under fluorescent light **E** details of the legs, especially the forelegs. Abbreviations: **A2–A3**; abdominal segments 2 and 3; **aprnt**, anterior pronotal rim; **ca**, calcar; **mscx**, mesocoxa; **msfm**, mesofemur; **msnt**, mesonotum; **mspl**, mesopleural region of mesopectus; **mssctm**, mesoscutum; **mssctl**, mesoscutellum; **mtcx**, metacoxa; **mtfm**, metafemur; **mtpl**, metapleural region of metapectus; **plant**, plantulae; **pr**, prora; **prcx**, procoxa; **pretc**, pretarsal claws; **prfm**, profemur; **prnt**, pronotum; **prop**, propodeum; **proppj**, propodeal projection; **prots**, protarsomeres I and II chaetae; **prtbs**, distal protibia stout chaeta; **psctc**, parascutal carina; **sp**, propodeal spiracle; **strg**, strigil. Scale bars: 0.2 mm.

**Legs.** Procoxa and profemur hypertrophied. Protibia bearing distally next to calcar a short, robust, spike-shaped chaeta. Calcar thin, curved, with bifid tip, without a distinct brush along its length, but having pubescence-like projections. Probasitarsal notch only gently concave, bearing the probasitarsal comb, but without any chaetae

next to it. Probasitarsus and protarsomere II forming a specialized structure consisting of long, curved, somewhat bluntly tipped, psammochaetae. Probasitarsus anterior surface having two of such specialized sensilla trichodea apically, projecting over protarsomere II and protarsomere II bearing three of such sensilla trichodea on its anterior surface. The five psammochaetae are very close together and probably form a digging apparatus in analogy to extant fossorial Aculeata. In addition to the specialized chaetae, a pair of spike-shaped chaetae is also present apically on the posterior surface of probasitarsus as well as a tiny, peg-like chaeta apicomediaally on the posterior surface. Protarsomere II has additionally a pair of small, spike-shaped chaetae on its posterior apical edge and an apicomedian, enlarged, blister-like, lobate chaeta on the posterior surface. Protarsomere II is short and slightly offset from the long axis of the probasitarsus. Protarsomeres III and IV each bearing two pairs of small, spike-shaped chaetae apicolaterally and with a lobate apicomedian chaeta in between them on the posterior surface, similar in shape but not as enlarged as that on protarsomere II. Spike-shaped chaetae and lobate chaeta apparently absent on protarsomere V. Pretarsal claws of proleg robust and curved, armed with a pair of teeth on their inner margins. Arolium slightly longer than half the length of claws. Mid and hind legs without any hypertrophied segment, although metatibiae apically clavate. Meso- and metatarsomeres I–IV similar in structure to protarsomeres III and IV, except for the apicomedian chaeta, which is not lobate and apparently rigid. These chaetae are also longer and more conspicuous on the mesotarsus than on the metatarsus. Paired mesotibial spurs present; spurs long and simple. Metatibial spurs not preserved, but from non-type material can be described as a pair of long and simple spurs similar but slightly longer than that on mesotibia.

**Metasoma.** In total, three metasomal segments of holotype preserved, corresponding to abdominal segments II–IV. Petiole (abdominal II) massive in dorsal view; posttergite II anteriorly broad (approximately as broad as the width at midlength of the mesoscutellum), broadly inserting into the lower propodeal declivous surface (propodeal foramen wide). Laterotergite of segment II well-defined and dorsoventrally broad. Posttergite II mildly constricted posteriorly and consequently, constriction between pre- and posttergite III also not strong, therefore, the abdominal segment II has only mild petiolation. Poststernite II V-shaped in ventral view, its lateral margins carinate (could be a taphonomic artifact), tapering anteriorly until meeting and forming a small subpetiolar process (in profile largely obliterated by the metacoxae). Entire posttergite II and anterior portion of posttergite III laterally carinated. Anterior process on poststernite III, the prora, subrectangular; its anterior angle round and the posterior angle pointy and inclined ventrally. Abdominal segment IV, as determined from non-type specimens, with slight constriction corresponding to transverse sulci which delimit the pre- and post-sclerites of the tergum and sternum; lateral margins of tergum and sternum IV aligned for their whole length. Sclerites of abdominal segments V, VI, and VII telescoped internally, their tergal margins apparently overlap the sterna laterally.

**Wing venation.** (Determined from non-type specimens.) Costal vein (C), subcostal-radial-radial-sector complex vein (Sc+R+Rs), and first free abscissa of the Radius (Rf1) present and tubular, enclosing costal cell. Pterostigma well-developed, situated

near the apical third of the fore wing, but exact position difficult to ascertain. Rf distal to pterostigma present, meeting the free Radial Sector (Rsf) and enclosing third radial cell (3R1, or “first marginal cell”, 1MC). Cell 3R1 ca. 4 × as long proximodistally as wide anteroposteriorly; apex of cell rounded and considerably distant from apex of wing. The first free abscissa of the Radial Sector (Rsf1) splitting from Sc+R+Rs proximal to the pterostigma, but separated by ca. 1 of its lengths; Rsf1 directed posterobasally. The mediocubital complex vein (M+Cu) present; free Media (Mf) and Cubitus (Cuf) splitting near midlength of wing. First free abscissa of Media (Mf1) short, with a length subequal to that of the first cubitoanal crossvein (1cu-a). Rsf1 and (Mf1) meeting at a very oblique angle, nearly parallel; Radial-Sector-Media composite abscissa (Rs+M) tubular, directed posterodistally, and nearly orthogonal to main axis of Rsf1 and Mf1; Rs+M length subequal to that of Rsf1; split of Rs and M distal to anterior juncture of first mediocubital crossvein (1m-cu), thus Rs+M comprising two abscissae (Rs+M1, Rs+M2), and 1m-cu “prefurcal” in general aculeate terminology. 1m-cu short, subequal in length to Mf1. Rsf immediately distal to split of Rs+M, with apex of kink marked by flexion line, thus Rsf2 and Rsf3 defined; flexion line spectral, thus first radiosectoral crossvein (1r-rs) “absent”. Second radiosectoral crossvein (2r-rs) tubular, situated at approximately pterostigma midlength, directed slightly posterodistally, and short (length subequal to Mf1, 1cu-a). Rsf distal to 2r-rs divided into two remaining abscissae (Rsf4, Rsf5) by second sectoriomedial crossvein (2rs-m) [*note*: 1rs-m always absent in Hymenoptera due to fusion of Rsf and Mf which forms Rs+M]; Rsf4 longer than 2r-rs but shorter than Rf1, 2rs-m. Mf, distal to Rs+M, straight and divided into two abscissae by 2rs-m (Mf2, Mf3); Mf2 longer than Rs+M but shorter than Rsf5; Mf3 tubular but becoming spectral well before apex of wing. Two “submarginal cells” enclosed by tubular abscissae; third “submarginal cell” undefined due to absence of third sectoriomedial crossvein (3rs-m). First medial cell (1M, or “discal cell 1”) rhomboidal, ca. 4 × as long proximodistally as wide anteroposteriorly; Mf1 and 1m-cu parallel; Rs+M and first free cubital abscissa (Cuf1) parallel. Second medial cell (2M, or “discal cell 2”) undefined due to absence of the second mediocubital crossvein (2m-cu). The second free cubital abscissa (Cuf2) evenly and shallowly curved until its apex is directed posteriorly; Cuf2 apparently reaching first anal vein (1A); cubitus distal to Cuf nebulous to spectral and curved. 1cu-a situated considerably proximad M+Cu split, being distant by at least twice its length, hence 1cu-a “very prefurcal”. 1A tubular, although full extend uncertain. Hind wing venation not evaluated due to lack of appropriate preserved views.

**Preservation. Holotype.** The body parts of the holotype that have suffered considerable distortion inside the amber matrix are the left procoxa, left mesopleuron and left mesocoxa, left and right metapleura and metacoxae, and the propodeum. Propodeal and metathoracic regions are considerably distorted, so much so that it is impossible to determine on which side the morphology has been better preserved. For example, on the right side, the propodeal spiracle is positioned at the same level of the mesocoxa in an anteroposterior axis, and the distance between the spiracle and the metapleural posteroventral corner is 0.43 mm. On the left side, it is positioned slightly



**Syninclusions.** One nematoceran fly, which remains in the same amber piece with the holotype. Two staphylinid beetles, which were separated from the holotype in other amber pieces after the preparation (JCCamb00051 and JCCamb00052, both in JCMC).

**Etymology.** The specific epithet emphasizes the digging adaptations of the species; the name is treated as a noun in apposition.

**Comments.** Four additional specimens of †*Camelosphecia*, three females (Fig. 15) and one male (Fig. 16), were studied based on images only. Among the females, two specimens (BALBuTJ\_36 and BALBuTJ\_40) are probably conspecifics to †*C. fossor* and one of them (BALBuTJ\_38) probably represents another species. BALBuTJ\_36 (Fig. 15A) is particularly interesting for its exceptional preservation. No significant differences were found between †*C. fossor* holotype and BALBuTJ\_36, and the fossil was used to complete the description of †*C. fossor*, as most of the metasoma of the holotype was missing and its propodeum very distorted. BALBuTJ\_40 (Fig. 15C) is a fossil difficult to interpret for containing a lot of debris and internal fractures around the inclusion. We doubtfully consider it conspecific to †*C. fossor*. A more thorough examination of the specimen can change this interpretation. BALBuTJ\_38 almost certainly is a different species which we do not describe here. It differs from †*C. fossor* for having abundant thick, long and flexuous setae dorsally on mesosoma; unarmed, block-like propodeum; and an even thicker profemur.

†*Camelosphecia venator* sp. nov.

<http://zoobank.org/00B043E6-1956-4EC6-A567-6186222B0280>

Fig. 16

**Holotype.** Myanmar, Kachin State: Hukawng Valley [NIGP163574, deposited in NIGP].

**Diagnosis.** Identifiable as Formicoidea based on the definition given for the superfamily above. Associated with †*Camelosphecia* females by the multidentate mandibles, the shape of the clypeus, and the markedly prefurcal 1cu-a. †*Camelosphecia venator* differs substantially from †*C. fossor* and is undoubtedly a new species based on the following features: (1) “marginal cell” very short, area approximately equal to that of pterostigma; (2) 1m-cu “postfurcal”, or joining Mf distal to split of Rs+M; (3) 2r-rs joining Rsf proximal to 2r-rs; (4) “discal cell” wider; (5) “subdiscal cell” (enclosed by Cu, A, and 1cu-a) shorter; (6) petiolar node very well-defined, hump-like; and (7) prora (anteroventral keel of abdominal sternum III) shelf-like, strongly projecting. The male-based species differs from †*C. fossor* and †*C. cf. fossor* (BALBuTJ\_38) by additional features which are expected due to sexual dimorphism, including having a distinct eye shape, shorter pronotum, twig-like profemora, and lack of the psammochaetae.

**Measurements. Male.** CL 0.98; VBL 0.21; HL 1.34; EL 0.58; LW 0.16; A1L 0.20; A2L 0.09; A3L 0.39; PnL 0.48; PnLm 0.68; WL 1.76; WLa 1.62; PtL 0.42. (Note: due to preservation and orientation, could not measure HW, CW, MW, PnW, MtW, MtL, MsW, and MsL.)

**Description. Male. Head.** Cranium “male-like” for Formicoidea, particularly stem Formicidae and taxa of the ponerine clade (i.e., the “poneroids” of Bolton 2003): Cranium more-or-less hypognathous despite elongate postgenal bridge; compound eyes bulging, medially emarginate; vertex (bearing ocelli) produced dorsally. Features differing from expectation: Mandibles distinctly multidentate, with eleven teeth as determined from the holotype; masticatory mandibular margin elongate; mandibles bowed, as observed in the female; cranial mandibular condyle small; clypeus reduced, concave, reminiscent of male Ponerini; compound eyes “binocular” in that anterior medialmost ommatidia with direct line of sight across the clypeus; antennal toruli close-set and dorsally directed (distinct from female); ocelli hypertrophied (suggesting nocturnal flight); occipital carina incomplete, possibly encircling occipital foramen but definitely not extending to mandibular base. Antenna 13-merous. Scape short, ca. 3–4 × as long as broad. Main body of pedicel approximately as broad as long. Flagellum elongate, each flagellomere several times longer than broad.

**Mesosoma.** Pronotum short but muscular, with distinct bulge in profile view between “neck” and posterior “collar”; lateral face of mesopleuron broadly and deeply concave; concavity oriented dorsoventrally, apparently for reception of leg when fore leg completely retracted up to body; pronotum posterodorsally produced as lobe, lobe contacting fore wing tegulum; pronotum not forming ring posterior to fore coxae. Mesoscutum with deep and convergent notauli. Oblique mesopleural sulcus of mesopectus extending completely from anterior (“epicnemial”) margin to posterior (“mesepimeral”) margin. Mesothorax distinct laterally. Propodeum with dorsal and posterior faces curving into one another in profile view, apparently without distinct angular marking; posterolateral portion of propodeum, i.e., the area corresponding to the propodeal lobe, produced posteriorly, but not apparently in subrectangular form. Propodeal spiracle apparently situated high and anterior on segment, subtending metapleuron.

**Legs.** Legs, overall, thin and without notable setal armament. Long setae not discernible. Protibial calcar apparently bifurcate apically. Mesotibia apparently with two ventroapical spurs, the anterior of which is thick compared to a seta and is barbirulate (*sensu* Bolton 2003). Metatibial spurs and tarsi not preserved in holotype.

**Metasoma.** Abdominal segment II with distinct petiolar node which is strong and convex; anterolateral corners carinate; form of subpetiolar process uncertain. Helcium (articulatory portion of abdominal segment II) well-defined, axial (situated at approximately segment midheight), and broad dorsoventrally and lateromedially. Prora (keel of abdominal sternum II) robust and triangular in profile view.

**Wing venation.** Veins tubular as in female †*Camelosphecia*. Differing as follows: 1Rsf situated ca. 2 × its length from pterostigma, nearly perpendicular to proximodistal length of wing; juncture of 1Rsf and Mf1 more distinctly angular; 1m-cu “postfurcal”, i.e., joining M distal to split of Rs+M; 2r-rs somewhat more proximal; “marginal cell” small, curve of posterior margin (as defined by Rsf) parallel to pterostigma; 2rs-m “pre-furcal”, with anterior juncture proximal to 2r-rs; tubular portion of Mf distal to 2r-rs very short; “discal cell” pentagonal and less than 1.5 × as long proximodistally as broad anteroposteriorly; 1cu-a joining M+Cu ca. 1 × of its lengths proximal to split of Rs+M.

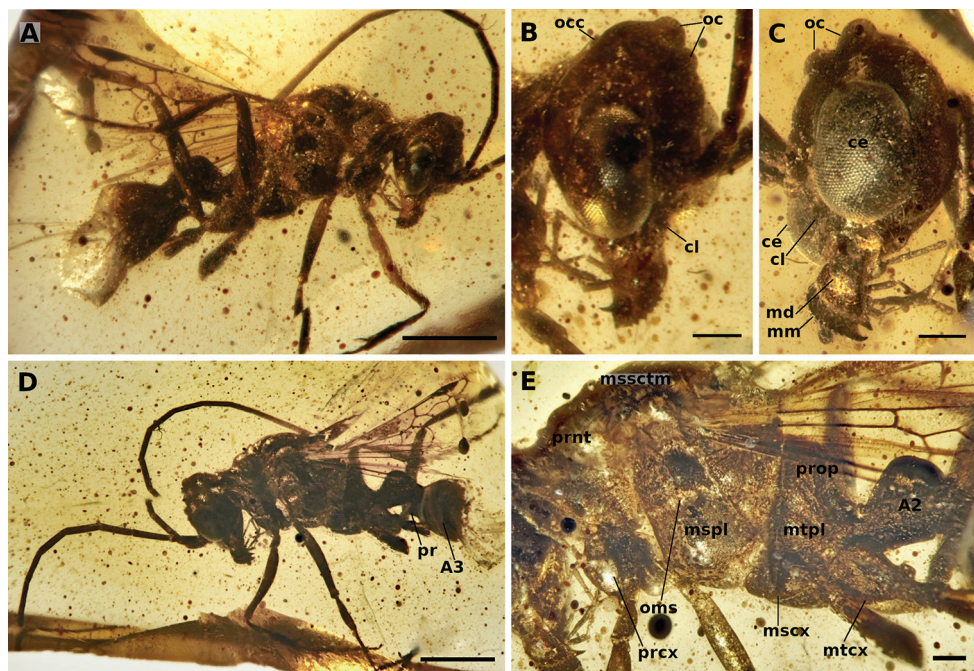


**Figure 16.** †*Camelosphecia venator* sp. nov. holotype (NIGP163574) **A, D** right and left profile view of body, respectively **B, C** right and left profile view of head, respectively **E** left mesosoma zooming. Abbreviations: **ce**, compound eye; **cl**, clypeus; **md**, mandible; **mm**, masticatory margins; **oc**, ocelli; **occ**, occipital carina; **A2–A3**; abdominal segments 2 and 3; **mscx**, mesocoxa; **mspl**, mesopleural area of mesopectus; **mssctm**, mesoscutum; **mtcx**, metacoxa; **mtpl**, metapleural area of mesopectus; **oms**, oblique mesopleural sulcus; **pr**, prora; **prcx**, procoxa; **prnt**, pronotum; **prop**, propodeum. Note that indication of clypeus in **C** is exactly at its margin as seen in profile, which is concave, and should not be confused with convex right compound eye margin, also indicated. Clypeal concave shape is better evidenced in figure **B**. Also in **C**, mm indicated is from the right mandible, while mandible indicated is that of the left side. Scale bars: 1 mm (**A, D**); 0.2 mm (**B, C, E**).

**Preservation.** Amber matrix filled with uniformly distributed dark spheres. Mesosoma from posterior portion of abdominal segment III, left meso- and meta-femora and distal segments, and right metatarsus removed due to specimen preparation. Hind wings not easily visible due to taphonomy. Specimen does not appear dehydrated or otherwise compressed or distorted.

**Etymology.** The specific epithet suggests the likely predatory habits of the unknown female, while also highlighting the visual acuity of the male probably required for mate-seeking.

**Comments.** We recognize that providing formal names to unassociated males risks inflating species-based biodiversity measures and runaway “parallel taxonomy” between sexes, as seen in various Dorylinae (e.g., *Neivamyrmex*) and Leptanillinae (e.g., *Leptanilla*). However, we are confident of the male-female pairing here due to the uniquely diagnostic mandibular conformation and markedly prefurcal 1cu-a crossvein.

Moreover, the distinct wing venation and petiolar node of †*Cs. venator* provides both strong evidence of non-conspicuity with †*Cs. fossor*, and ample detail to associate unidentified females. For these reasons, we strongly recommend that any female which has a similar venational pattern and especially a nodiform petiole be considered conspecific with †*Cs. venator*, at least until further evidence accrues.

The marked reduction of the male's cranium and pronotum coupled with hypertrophied or bulging eyes compared to the female strongly suggests specialized and sex-specific life histories. Among extant Formicidae, similarly enlarged eyes are often associated with nocturnal flights. At light sheets, such bug-eyed males are often observed *en masse*, without presence of conspecific females, suggesting either limited flights by females or the female-calling syndrome. Unfortunately, the genitalia of the unique specimen were lost during specimen preparation, thus the presence of copulatory specializations remains unknown. However, it is apparent from other male Formicoidea from Burmite and other ambers that a wide array of sexual modifications are known.

## Acknowledgments

For museums access, BEB thanks: Dave Grimaldi (AMNH), Taiping Gao and Huijia Cao (CNUC), Bo Wang (NIGP), Philip Ward (PSWC), and Lynn Kimsey and Steve Heydon (UCDC). For collaboration and discussion over the years, we heartily thank Philip Barden, Bo Wang, Roberto Keller; we especially thank Christine Sosiak for help with the description of the female beast ant. For access to images of material in the Janovitz collection, we thank Philip Barden again. We thank Barry Bolton for encouraging the separate description of the new genus, Phil Ward for persistent and positive guidance, and Marek Borowiec and an anonymous reviewer for critical feedback. For AntWeb and AntCat, we thank Brian Fisher, Michele Esposito, and Barry Bolton. Finally, we thank Nathalie Yonow for careful copy-editing during the proof stage. We acknowledge funding from Conselho Nacional de Desenvolvimento Científico e Tecnológico (CNPq) and the Coordenação de Aperfeiçoamento de Pessoal de Nível Superior (CAPES) for JCMC; and from Jastro-Shields Research Grants (UC Davis, 2014, 2015), a McBeth Scholarship (UC Davis, 2015), and two Ernst Mayr Grants from the Museum of Comparative Zoology (2013, 2016) for BEB. BEB further acknowledges an Alexander von Humboldt Foundation Postdoctoral Research Fellowship, and support from the NSF grants DEB-1345996 and DEB-1932405 awarded to P. Ward (UC Davis). We declare no competing interests.

## References

- Barden P (2017) Fossil ants (Hymenoptera: Formicidae): ancient diversity and the rise of modern lineages. *Myrmecological News* 24: 1–30. [https://doi.org/10.25849/myrmecol.news\\_024:001](https://doi.org/10.25849/myrmecol.news_024:001)
- Barden P, Engel MS (2019) Fossil social insects. *Springer Nature*, Switzerland, 21 pp. [https://doi.org/10.1007/978-3-319-90306-4\\_45-1](https://doi.org/10.1007/978-3-319-90306-4_45-1)

- Barden P, Grimaldi DA (2012) Rediscovery of the bizarre Cretaceous ant *Haidomyrmex* Dlussky (Hymenoptera: Formicidae), with two new species. *American Museum Novitates* 3755: 1–16. <https://doi.org/10.1206/3755.2>
- Barden P, Grimaldi DA (2013) A new genus of highly specialized ants in Cretaceous Burmese amber (Hymenoptera: Formicidae). *Zootaxa* 3681: 405–412. <https://doi.org/10.11646/zootaxa.3681.4.5>
- Barden P, Grimaldi DA (2014) A diverse ant fauna from the mid-Cretaceous of Myanmar (Hymenoptera: Formicidae). *PLoS ONE* 9(4): e93627. <https://doi.org/10.1371/journal.pone.0093627>
- Barden P, Grimaldi DA (2016) Adaptive radiation in socially advanced stem-group ants from the Cretaceous. *Current Biology* 26: 515–521. <https://doi.org/10.1016/j.cub.2015.12.060>
- Barden P, Grimaldi DA (2017) A new genus of hell ants from the Cretaceous (Hymenoptera: Formicidae: Haidomyrmecini) with a novel head structure. *Systematic Entomology* 42: 837–846. <https://doi.org/10.1111/syen.12253>
- Barden P, Perrichot V, Wang B (2020) Specialized predation drives aberrant morphological integration and diversity in earliest ants. *Current Biology* 30: 3818–3824. <https://doi.org/10.1016/j.cub.2020.06.106>
- Bolton B (1990) Abdominal characters and status of the cerapachyine ants (Hymenoptera, Formicidae). *Journal of Natural History* 24: 53–68. <https://doi.org/10.1080/00222939000770051>
- Bolton B (1994) Identification guide to the ant genera of the world. Harvard University Press, Cambridge, 222 pp.
- Bolton B (2003) Synopsis and classification of Formicidae. *Memoirs of the American Entomological Institute* 71: 1–370.
- Bolton B, Fisher BL (2008) Afrotropical ants of the ponerine genera *Centromyrmex* Mayr, *Promyopias* Santschi gen. rev. and *FerAPONERA* gen. n., with a revised key to genera of African Ponerinae (Hymenoptera: Formicidae). *Zootaxa* 1929: 1–37. <https://doi.org/10.11646/zootaxa.1929.1.1>
- Borowiec ML, Rabeling C, Brady SG, Fisher BL, Schultz TR, Ward PS (2019) Compositional heterogeneity and outgroup choice influence the internal phylogeny of the ants. *Molecular Phylogenetics & Evolution* 134: 111–121. <https://doi.org/10.1016/j.ympev.2019.01.024>
- Borysenko LH (2017) Description of a new genus of primitive ants from Canadian amber, with the study of relationships between stem- and crown-group ants (Hymenoptera: Formicidae). *Insecta Mundi* 570: 1–57. <https://doi.org/10.1101/051367>
- Boudinot BE (2015) Contributions to the knowledge of Formicidae (Hymenoptera, Aculeata): a new diagnosis of the family, the first global male-based key to subfamilies, and a treatment of early branching lineages. *European Journal of Taxonomy* 120: 1–62. <https://doi.org/10.5852/ejt.2015.120>
- Boudinot BE, Khouri, Z, Richter A, van de Kamp T, Barden P, Chaul JCM (2020a) Chapter II. The evolution of the ants: Extinct ant sister-group illuminates eusociality origin and post-K/Pg persistence. In: Boudinot BE 2020. *Systematic and Evolutionary Morphology: Case Studies on Formicidae, Mesozoic Aculeata, and Hexapodan Genitalia*. Ph. D. Dissertation, University of California, Davis, 174–393.
- Boudinot BE, Beutel RG, Gorb SN, Polilov AA (2020b) Functional diversity of attachment and grooming leg structures is retained in all but the smallest insects. *Journal of Zoology* (London). <https://doi.org/10.1111/jzo.12840>

- Brady SG, Schultz TR, Fisher BL, Ward PS (2006) Evaluating alternative hypotheses for the early evolution and diversification of ants. *Proceedings of the National Academy of Sciences of the United States of America* 103: 18172–18177. <https://doi.org/10.1073/pnas.0605858103>
- Branstetter MG, Danforth BN, Pitts JP, Faircloth BC, Ward PS, Buffington ML, Gates MW, Kula RR, Brady SG (2017) Phylogenomic insights into the evolution of stinging wasps and the origins of ants and bees. *Current Biology* 27: 1019–1025. <https://doi.org/10.1016/j.cub.2017.03.027>
- Brown Jr WL, Nutting WL (1950) Wing venation and the phylogeny of the Formicidae. *Transactions of the American Entomological Institute* 75: 113–132.
- Cao H, Boudinot BE, Wang Z, Miao X, Shih C, Ren D, Gao T (2020) Two new iron maiden ants from Burmese amber (Hymenoptera: Formicidae: †Zigrasimeciini). *Myrmecological News* 30: 161–173.
- Chapman RF (2012) *The Insects: Structure and Function* (Fifth Edition). Cambridge University Press, Cambridge, 929 pp.
- Dlussky GM (1975) Superfamily Formicoidea Latreille, 1802. Family Formicidae Latreille, 1802 [in Russian]. In: Rasnitsyn AP (Ed.) *Hymenoptera Apocrita of Mesozoic* (in Russian). *Trudy Paleontologicheskogo Instituta. Akademiya Nauk SSSR* 147: 1–134.
- Dlussky GM (1983) A new family of Upper Cretaceous Hymenoptera: an “intermediate link” between the ants and the scolioids [in Russian]. *Paleontologicheskii Zhurnal* 1983(3): 65–78.
- Dlussky GM (1987) New Formicoidea (Hymenoptera) of the Upper Cretaceous [in Russian]. *Paleontologicheskii Zhurnal* 1987(1): 131–135.
- Dlussky GM (1996) Ants (Hymenoptera: Formicidae) from Burmese amber. *Paleontological Journal* 30: 449–454.
- Engel MS, Grimaldi DA (2005) Primitive new ants in Cretaceous amber from Myanmar, New Jersey, and Canada (Hymenoptera: Formicidae). *American Museum Novitates* 3485: 1–23. [https://doi.org/10.1206/0003-0082\(2005\)485\[0001:PNAICA\]2.0.CO;2](https://doi.org/10.1206/0003-0082(2005)485[0001:PNAICA]2.0.CO;2)
- Forel A (1878) Études myrmécologiques en 1878 (première partie) avec l’anatomie du gésier des fourmis. *Bulletin de la Société Vaudoise des Sciences Naturelles* 15: 337–392.
- Goulet H, Huber JT (1993) *Hymenoptera of the World: An Identification Guide to Families*. Canada Communications Group Publishing, Ottawa, 668 pp.
- Grimaldi D, Agosti D, Carpenter JM (1997) New and rediscovered primitive ants (Hymenoptera: Formicidae) in Cretaceous amber from New Jersey, and their phylogenetic relationships. *American Museum Novitates* 32081: 1–43.
- Grimaldi D, Agosti D (2000) A formicine in New Jersey Cretaceous amber (Hymenoptera: Formicidae) and early evolution of the ants. *Proceedings of the National Academy of Sciences of the United States of America* 97: 13678–13683. <https://doi.org/10.1073/pnas.240452097>
- Grimaldi D, Engel M (2005) *Evolution of the Insects*. Cambridge University Press, Cambridge, 772 pp.
- Harris RA (1979) A glossary of surface sculpturing. *Occasional Papers in Entomology* 28: 1–31.
- Hölldobler B, Wilson EO (1990) *The Ants*. Cambridge, Harvard University Press, 732 pp. <https://doi.org/10.1007/978-3-662-10306-7>

- Johnson BR, Borowiec ML, Chiu JC, Lee EK, Atallah J, Ward PS (2013) Phylogenomics resolves evolutionary relationships among ants, bees, and wasps. *Current Biology* 23: 2058–2062. <https://doi.org/10.1016/j.cub.2013.08.050>
- Keller RA (2011) A phylogenetic analysis of ant morphology (Hymenoptera: Formicidae) with special reference to the poneromorph subfamilies. *Bulletin of the American Museum of Natural History* 355: 1–90. <https://doi.org/10.1206/355.1>
- Klunk CL, Argenta MA, Casadei-Ferreira A, Economo EP, Pie MR (2020) Mandibular morphology, task specialization, and bite mechanics in *Pheidole* ants (Hymenoptera: Formicidae). *BioRxiv*. <https://doi.org/10.1101/2020.11.16.385393>
- Latreille PA (1802) *Histoire naturelle générale et particulière des crustacés et des insectes*. Tome 3. Familles naturelles des genres. F. Dufart, Paris, 467 pp.
- Latreille PA (1809) *Genera crustaceorum et insectorum secundum ordinem naturalem in familias disposita iconibus exemplisque plurimis explicata*. Tomus 4. A. Koenig, Parisiis et Argentorati, 399 pp.
- Latreille PA (1810) *Considérations générales sur l'ordre naturel des animaux composant les classes des crustacés, des arachnides et des insectes; avec un tableau méthodique de leurs genres, disposés en familles*. F. Schoell, Paris, 444 pp. <https://www.biodiversitylibrary.org/page/27543876>
- Lattke JE, Melo GAR (2020) New haidomyrmecine ants (Hymenoptera: Formicidae) from mid-Cretaceous amber of Northern Myanmar. *Cretaceous Research* 114: e104502. <https://doi.org/10.1016/j.cretres.2020.104502>
- Lepeletier de Saint-Fargeau A (1835 “1836”) *Histoire naturelle des insectes*. Hyménoptères. Tome I. Roret, Paris, 547 pp. <https://doi.org/10.5962/t.173542>
- Linnaeus C (1758) *Systema naturae per regna tria naturae, secundum classes, ordines, genera, species, cum characteribus differentiis, synonymis, locis*. Tomus I. Editio decima, reformata. Salvii, Holmiae, 824 pp.
- Liu S-P, Richter A, Stoessel A, Beutel RG (2019) The mesosomal anatomy of *Myrmecia nigrocincta* workers and evolutionary transformations in Formicidae (Hymenoptera). *Arthropod Systematics & Phylogeny* 77: 1–19. <https://doi.org/10.26049/ASP77-1-2019-01>
- Lucena DAA, Melo GAR (2018) Chrysidid wasps (Hymenoptera: Chrysididae) from Cretaceous Burmese amber: Phylogenetic affinities and classification. *Cretaceous Research* 89: 279–291. <https://doi.org/10.1016/j.cretres.2018.03.018>
- Mayr G (1865) Formiciden. In: *Novara Expedition 1865. Reise der Österreichischen Fregatte ‘Novara’ um die Erde in den Jahren 1857, 1858, 1859. Zoologischer Theil*. Bd. II. Abt. 1. K. Gerold's Son, Wien, 119 pp.
- Mayr G (1868) Die Ameisen des baltischen Bernsteins. *Beiträge zur Naturkunde Preussens* 1: 1–102.
- McKellar RC, Glasier JRN, Engel MS (2013a) New ants (Hymenoptera: Formicidae: Dolichoderinae) from Canadian Late Cretaceous amber. *Bulletin of Geosciences* 88: 583–594. <https://doi.org/10.3140/bull.geosci.1425>
- McKellar RC, Glasier JRN, Engel MS (2013b) A new trap-jawed ant (Hymenoptera: Formicidae: Haidomyrmecini) from Canadian Late Cretaceous amber. *Canadian Entomologist* 145: 454–465. <https://doi.org/10.4039/tce.2013.23>

- Miao Z, Wang M (2019) A new species of hell ants (Hymenoptera: Formicidae: Haidomyrmecini) from the Cretaceous Burmese amber. *Journal of the Guangxi Normal University (Natural Science Edition)* 37: 139–142. <https://doi.org/10.16088/j.issn.1001-6600.2019.02.017>
- Moreau CS, Bell CD, Vila R, Archibald SB, Pierce NE (2006) Phylogeny of the ants: diversification in the age of angiosperms. *Science* 312: 101–104. <https://doi.org/10.1126/science.1124891>
- Nel A, Perrault G, Perrichot V, Néraudeau D (2004) The oldest ant in the Lower Cretaceous amber of Charente-Maritime (SW France) (Insecta: Hymenoptera: Formicidae). *Geologica Acta* 2: 23–29. <https://doi.org/10.1344/105.000001630>
- Perrichot V (2014) A new species of the Cretaceous ant *Zigrasimecia* based on the worker caste reveals placement of the genus in Sphecomyrminae (Hymenoptera: Formicidae). *Myrmecological News* 19: 165–169.
- Perrichot V (2015) A new species of *Baikuris* (Hymenoptera: Formicidae: Sphecomyrminae) in mid-Cretaceous amber from France. *Cretaceous Research* 52: 585–590. <https://doi.org/10.1016/j.cretres.2014.03.005>
- Perrichot V, Nel A, Néraudeau D, Lacau S, Guyot T (2008) New fossil ants in French Cretaceous amber (Hymenoptera: Formicidae). *Naturwissenschaften* 95: 91–97. <https://doi.org/10.1007/s00114-007-0302-7>
- Perrichot V, Wang B, Engel MS (2016) Extreme morphogenesis and ecological specialization among Cretaceous basal ants. *Current Biology* 26: 1468–1472. <https://doi.org/10.1016/j.cub.2016.03.075>
- Perrichot V, Wang B, Barden P (2020) New remarkable hell ants (Formicidae: Haidomyrmecinae stat. nov.) from mid-Cretaceous amber of Northern Myanmar. *Cretaceous Research* 109: e104381. <https://doi.org/10.1016/j.cretres.2020.104381>
- Peters RS, Krogmann L, Mayer C, Donath A, Gunkel S, Meusemann K, Kozlov A, Podsiadlowski L, Petersen M, Lanfear R, Diez PA, Heraty J, Kjer KM, Klopstein S, Meier R, Polidori C, Schmitt T, Liu S, Zhou X, Wappler T, Rust J, Misof B, Niehuis O (2017) Evolutionary history of the Hymenoptera. *Current Biology* 27: 1013–1018. <https://doi.org/10.1016/j.cub.2017.01.027>
- Richter A, Keller RA, Rosumek FB, Economo EP, Hita Garcia F, Beutel RG (2019) The cephalic anatomy of workers of the ant species *Wasmannia affinis* (Formicidae, Hymenoptera, Insecta) and its evolutionary implications. *Arthropod Structure & Development* 49: 26–49. <https://doi.org/10.1016/j.asd.2019.02.002>
- Richter A, Hita Garcia F, Keller RA, Billen J, Economo EP, Beutel RG (2020) Comparative analysis of worker head anatomy of *Formica* and *Brachyponera* (Hymenoptera: Formicidae). *Arthropod Systematics & Phylogeny* 78: 133–170. <https://doi.org/10.26049/ASP78-1-2020-06>
- Schmidt CA, Shattuck SO (2014) The higher classification of the ant subfamily Ponerinae (Hymenoptera: Formicidae), with a review of ponerine ecology and behavior. *Zootaxa* 3817: 1–242. <https://doi.org/10.11646/zootaxa.3817.1.1>
- Snodgrass RE (1935) *Principles of Insect Morphology*. McGraw-Hill Book Company Inc., New York, 667 pp.
- Snodgrass RE (1956) *Anatomy of the Honey Bee*. Comstock Publishing Associates, Ithaca, 334 pp.

- Toegel JP, Wilmmmer EA, Prpic N-M (2009) Loss of *spineless* function transforms the *Tribolium* antenna into a thoracic leg with pretarsal, tibiotarsal, and femoral identity. *Development, Genes & Evolution* 219: 53–58. <https://doi.org/10.1007/s00427-008-0265-5>
- Wheeler WM (1915, “1914”) The ants of the Baltic amber. *Schriften der Physikalisch-Ökonomischen Gesellschaft zu Königsberg* 55: 1–142.
- Wilson EO, Carpenter FM, Brown Jr WL (1967a) The first Mesozoic ants, with the description of a new subfamily. *Psyche* (Cambridge) 74: 1–19. <https://doi.org/10.1155/1967/89604>
- Wilson EO, Carpenter FM, Brown Jr WL (1967b) The first Mesozoic ants. *Science* 157: 1038–1040. <https://doi.org/10.1126/science.157.3792.1038>
- Wilson EO (1985) Ants from the Cretaceous and Eocene amber of North America. *Psyche* (Cambridge) 92: 205–216. <https://doi.org/10.1155/1985/57604>
- Zheng D, Cheng S-C, Perrichot V, Dutta S, Rudra A, Mu L, Kelly RS, Li S, Zhang Q, Zhang Q, Zhang Q, Wong J, Wang J, Wang H, Fang Y, Zhang H, Wang B (2018) A Late Cretaceous amber biota from central Myanmar. *Nature Communications* 9: e3170. <https://doi.org/10.1038/s41467-018-05650-2>



# Complete mitochondrial genome of the freshwater fish *Onychostoma lepturum* (Teleostei, Cyprinidae): genome characterization and phylogenetic analysis

I-Chen Wang<sup>1\*</sup>, Hung-Du Lin<sup>2\*</sup>, Chih-Ming Liang<sup>1</sup>, Chi-Chun Huang<sup>3</sup>,  
Rong-Da Wang<sup>4</sup>, Jin-Quan Yang<sup>4</sup>, Wei-Kuang Wang<sup>1</sup>

**1** Department of Environmental Engineering and Science, Feng Chia University, Taichung 407, Taiwan **2** The Affiliated School of National Tainan First Senior High School, Tainan 701, Taiwan **3** Taiwan Endemic Species Research Institute, Nantou 552, Taiwan **4** Shanghai Universities Key Laboratory of Marine Animal Taxonomy and Evolution, Shanghai Ocean University, Shanghai 201306, China

Corresponding author: Wei-Kuang Wang ([wkwang@fcu.edu.tw](mailto:wkwang@fcu.edu.tw))

Academic editor: M.E. Bichuette | Received 13 August 2020 | Accepted 25 November 2020 | Published 18 December 2020

<http://zoobank.org/92DDFB54-0FC4-404D-BF2C-7C0B373E2992>

**Citation:** Wang I-C, Lin H-D, Liang C-M, Huang C-C, Wang R-D, Yang J-Q, Wang W-K (2020) Complete mitochondrial genome of the freshwater fish *Onychostoma lepturum* (Teleostei, Cyprinidae): genome characterization and phylogenetic analysis. ZooKeys 1005: 57–72. <https://doi.org/10.3897/zookeys.1005.57592>

## Abstract

The cyprinid genus *Onychostoma* Günther, 1896 consists of 24 valid species distributed in Southeast Asia, including Taiwan, Hainan, mainland China and the Indochina region. In the present study, we determined the complete mitochondrial genome of *O. lepturum*, which is 16,598 bp in length, containing 13 protein-coding genes, two rRNA genes, 22 tRNA genes and a typical control region (D-loop). To verify the molecular phylogeny of the subfamily Acrossocheilinae, we provide new insights to better understand the taxonomic status of *Acrossocheilus*, *Onychostoma* and *Folifer brevifilis*. The phylogenetic trees presented three major clades based on the 13 protein-coding genes from 28 Acrossocheilinae species. Clades I and II represent the *Onychostoma* and *Acrossocheilus* groups, respectively. Species of *Acrossocheilus*, *Onychostoma* and *F. brevifilis* are included in Clade III, which is considered as an ancestral group. This work provides genomic variation information and improves our understanding of the Acrossocheilinae mitogenome, which will be most valuable in providing new insights for phylogenetic analysis and population genetics research.

## Keywords

Cyprinid, mitogenome, *Onychostoma lepturum*, phylogeny, population genetics, Southeast Asia

\* These authors contributed equally to this work.

## Introduction

The cyprinid genus *Onychostoma* Günther, 1896 consists of 24 valid species distributed in Southeast Asia, including Taiwan, Hainan, mainland China and the Indochina region (Song et al. 2018; Froese 2019). *Onychostoma* is composed of mountain stream cyprinids that are characterized primarily by the possession of a sharp, cornified sheath cutting edge in the lower jaw and no fleshy lower lip (Shan et al. 2000). Among these species, four species are only distributed in the Indochina region, including Laos Vietnam and Thailand, eleven species are endemic to mainland China, one species is endemic to Taiwan island, and the remaining seven species are shared with mainland China and the Indochina region (Froese 2019). *Onychostoma lepturum* (Boulenger, 1900) is distributed in Laos and Vietnam and can also be found in the Yuanjiang River in mainland China and Hainan Island (Shan et al. 2000; Kottelat 2001).

The Cyprinidae family has the most species of any freshwater fish family. The family encompasses 11 subfamilies, with the genus *Onychostoma* belonging to the Acrossocheilinae subfamily (Yang et al. 2015). The taxonomic placement of the Asian genus *Onychostoma* has undergone many changes. *Onychostoma* was synonymized with the African genus *Varicorhinus* (e.g., Taki 1975), but recent studies demonstrate that *Onychostoma* and *Varicorhinus* fall in two distinct major clades in terms of chromosome numbers and molecular markers (Yang et al. 2015). According to previous studies, *Acrossocheilus* and *Onychostoma* were reported to be paraphyletic or polyphyletic (Yang et al. 2015; Wang et al. 2016; Zheng et al. 2016). Among these were Acrossocheilini, *Acrossocheilus*, *Onychostoma* and *Folifer brevifilis* (Peters, 1881), which formed a clade in the molecular analysis (Yang et al. 2015; Wang et al. 2016; Zheng et al. 2016). Three genera (*Acrossocheilus*, *Onychostoma* and *Folifer*) have been previously placed in different taxa together with many other cyprinines (Chen et al. 1984; Yue 2000). However, the phylogenetic relationships of these three genera, based on different molecular markers, has been controversial.

*Folifer brevifilis* is closely related to *O. simum* (Sauvage & Dabry de Thiersant, 1874) based on the mitochondrial and nuclear markers (Yang et al. 2015; Wang et al. 2016; Zheng et al. 2016). According to mitochondrial genomes, *O. simum* and *O. gerlachi* (Peters, 1881) were in sister groups (Zhang et al. 2018). The genus *Acrossocheilus* represents three separate lineages: the barred species (e.g., *A. beijiangensis* (Wu & Lin, 1977) and *A. iridescens* (Nichols & Pope, 1927)), non-barred species (e.g., *A. yunnanensis* (Regan, 1904) and *A. monticola* (Günther, 1888) based on mitochondrial DNA sequences (Zheng et al. 2016). However, Hou et al. (2020) reassigned species of the *Acrossocheilus* cluster into two separate clades: Clade I (an ancestral clade), including *A. monticola* and *A. yunnanensis*, and Clade II, which was further divided into two sublineages (subclades A and B) based on available whole mitochondrial genomes. Subclade B clustered with *A. longipinnis* (Wu, 1939), *A. iridescens* and *A. barbodon* (Nichols & Pope, 1927), and subclade A included other *Acrossocheilus* species (e.g., *A. parallens* (Nichols, 1931), *A. hemispinus* (Nichols, 1925), *A. jishouensis* (Zhao, Chen & Li, 1997) (Hou et al. 2020). Yang et al. (2015) and Zheng et al. (2016) proposed that members of *Onychostoma* be divided into three groups based on morphological and molecular data. Zhang et al. (2018) also showed that the

eight species of *Onychostoma* cluster into three separate lineages based on the whole mitochondrial genome sequence. However, similar research in Zhai et al. (2020) only identified two lineages among nine species of *Onychostoma* with the same molecular markers. Interestingly, Zhang et al. (2018) proposed that *O. rarum* (Lin, 1933) was the sister group of *O. alticorpus* (Oshima, 1920), but recently another study showed that *O. rarum* seems to be more closely related to *O. barbatulum* (Pellegrin, 1908) and *O. barbatum* (Lin, 1931) (Zhai et al. 2020). In the previous studies, the classification of the three groups was inconsistent (Yang et al. 2015; Zheng et al. 2016; Zhang et al. 2018). For example, *O. lepturum* (Boulenger, 1900) clustered together with *O. meridionale* (Kottelat, 1998) (Yang et al. 2015). In addition, Wang et al. (2016) and Zheng et al. (2016) proposed that *O. lepturum* was nested with *O. gerlachi*.

Recent population analyses suggested that the nucleotide diversity of cyprinids on Hainan Island was lower than that of cyprinids in mainland China (Zhou et al. 2017). A decline in freshwater fish resources has been observed due to the effects of overfishing, water pollution and environmental deterioration in China (Kang et al. 2013, 2014). The phylogenetic relationships among species in the genera *Onychostoma* and *Acrossocheilus* have been studied based on morphological data and on nuclear and mitochondrial genes (Wang et al. 2007; Xin 2008; Wang et al. 2016; Zheng et al. 2016). However, the current understanding among members of the genera *Onychostoma* and *Acrossocheilus* and their internal phylogenetic relationships remains confusing. The complete mitochondrial genome has alternative molecular markers for phylogenetic analysis capable of providing much more robust phylogenetic reconstructions than smaller portions of the mtDNA (Huang et al. 2017; Hou et al. 2020). Mitogenomes are thought to be reliable markers for reconstructing phylogenies in recent taxonomic and phylogenetic studies of cyprinids (Huang et al. 2017; Chung et al. 2020).

Previous studies suggest an inclusive phylogenetic clade including species from *Acrossocheilus*, *Onychostoma*, and *Folifer brevifilis* based on molecular markers (Yang et al. 2015; Zheng et al. 2016). Although a previous study has characterized the complete mitochondrial genome of *O. lepturum* (Zhai et al. 2020), the genome annotation, comparative analysis and the phylogenetic relationships of *Onychostoma* remain poorly understood due to the limited genomic data used. Our approach better informs the conservation of this species; thus, we determined the complete mitochondrial genome of *O. lepturum* based on next-generation sequencing data and assessed its phylogenetic relationships with another 11 available mitogenomes in the genus *Onychostoma* and 16 available mitogenomes in the genus *Acrossocheilus* and *F. brevifilis*, with an available mitogenome in *Spinibarbus hollandi* (Oshima, 1919) used as an outgroup.

## Materials and methods

### Sample and DNA extraction

The sample of *Onychostoma lepturum* was caught from the Lingshui River in Baoting County of Hainan in China (18°42'07"N, 109°40'44"E). Samples were collected from

the field sites with seines, fatally anesthetized with MS-222 (Sigma, St. Louis, MO) and fixed and stored in 100% ethanol. All specimens are lodged in the laboratory of Jin-Quan Yang, Shanghai Ocean University, Key Laboratory of Exploration and Utilization of Aquatic Genetic Resources. All animal experiments were carried out in accordance with the guidelines and with approval of the Animal Research and Ethics Committee of Shanghai Ocean University (permissions, SHOU-DW-2018-021). Total genomic DNA was extracted from muscle tissue using the Genomic DNA Purification Kit (Genra Systems, Valencia, CA) in the laboratory.

## Sequencing and genome annotation and analysis

The complete mitogenome of *O. lepturum* was obtained from high-throughput sequencing of whole-genome DNA with a HiSeqX Ten platform (Illumina, San Diego, CA) with a paired-end 150 bp approach. Next-generation sequencing (NGS) was used to perform low-coverage whole-genome sequencing to obtain the complete mitogenome according to a previous protocol (Chiu et al. 2018). By using commercial software (Geneious V9, Auckland, New Zealand), approximately 1.1% of raw reads (34,001 out of 29,140,518) were assembled de novo to produce a single, circular form of the complete mitogenome with an average coverage of 245 X. Compared to the corresponding complete mtDNA sequence of genus *Onychostoma*, 13 protein-coding genes and ribosomal RNA (rRNA) genes were identified using Clustal X 1.83 (<http://www.clustal.org/>). Codon usage, nucleotide substitution and base composition were determined using MEGA X (Kumar et al. 2018), and the skewing of the nucleotide composition was measured in terms of AT- and GC-skews according to the following formulas:  $AT\text{-skew} = (A - T)/(A + T)$  and  $GC\text{-skew} = (G - C)/(G + C)$  (Perna and Kocher 1995).

## Phylogenetic analysis

Phylogenetic analyses using a total of 11 mitogenomes of *Onychostoma* species, 16 mitogenomes of *Acrossocheilus* species and one mitogenome of *F. brevifilis* were performed based on Neighbor-joining (NJ), Maximum-likelihood (ML), and Bayesian (BI) methods, with *Spinibarbus hollandi* as the outgroup. Twenty-nine mitogenomes were downloaded from NCBI and were aligned using MEGA X (alignment with CLUSTALW) with default settings (Kumar et al. 2018). The best model GTR + G (General Time Reversible model with Gamma distributed rates among sites) was chosen based on the Akaike information criterion (AIC) using the smart model selection algorithm (Lefort et al. 2017), and the ML trees were constructed using PhyML 3.0 software (Guindon et al. 2010). The statistical confidences were assessed through the bootstrap test inferred from 1000 replicates. A NJ tree was constructed based on the Kimura 2-parameter model with 1000 bootstrap replicates using MEGA X (Kumar et al. 2018). The Bayesian inference (BI) tree was conducted using the GTR+G model strategy with MrBayes 3.2.6 (Ronquist and Huelsenbeck 2003), and two independent Markov Chains Monte Carlo (MCMC) chains were run for  $5 \times 10^7$  generations; the first 50,000 trees before stationarity were discarded as burn-in, and the remaining trees were used to construct

the majority-rule consensus trees. Effective sample size (ESS) values, as computed by plotting the log likelihood scores against the generation times using the program Tracer 1.7 (Rambaut et al. 2018), were above 200 for the convergence of MCMC runs.

## Results

### Mitochondrial genomic structure and composition

In the present study, the complete mitochondrial genome sequence of *O. lepturum* derived by NGS was found to be 16,598 bp and was deposited in GenBank (accession MT258556). The mitogenome contained 37 typical mitochondrial genes with 13 typical vertebrate protein-coding genes, 2 ribosomal RNA (rRNA) genes, 22 tRNAs, and a control region (D-Loop) (Fig. 1). Most of the *O. lepturum* mitochondrial genes were encoded on the H-strand, although the ND6 and eight tRNA genes (tRNA<sup>Gln</sup>, tRNA<sup>Ala</sup>, tRNA<sup>Asn</sup>, tRNA<sup>Cys</sup>, tRNA<sup>Tyr</sup>, tRNA<sup>Ser</sup>, tRNA<sup>Glu</sup> and tRNA<sup>Pro</sup>) were encoded on the L-strand (Fig. 1). The total length was found to be similar to that of the other *Onychostoma* sequences compared, differing from them by between 1 and 9 bp. The mitogenome base composition is 31.3% A, 16.2% G, 24.0% T, and 28.6% C, with a slight AT bias (55.3%). Eleven of thirteen protein-coding genes in *O. lepturum* started with a typical ATG codon, except for the COI and ATP6 genes, which were GTG. Seven protein-coding genes ended with the termination codon TAA (ND1, CO1, ATP8, ATP6, ND4L, ND5, and ND6), while the remaining six genes terminated with a single base T (Table 1). The 22 tRNA genes ranged in size from 67 to 76 bp, and the length of tRNA<sup>Cys</sup> gene (67 bp) was the shortest, whereas the longest were the tRNA<sup>Leu</sup> and tRNA<sup>Lys</sup> genes (76 bp). The noncoding control region (D-loop) is located between tRNA<sup>Phe</sup> and tRNA<sup>Pro</sup> and is 937 bp in length (Table 1). The genes in the *O. lepturum* mitogenome were closely arranged with overlapping and interval phenomena. There is a total of 22 bp in overlaps between six gene junctions, and each single overlap ranged in size from 1 to 7 bp, with the longest overlapping region (7 bp) located between ATP8/ATP6 and ND4L/ND4, 4 bp of overlapping regions between ND5 and ND6 and fewer than 2 bp at the remaining three positions (Table 1). However, there are 11 intergenic spacer regions ranging in size from 1 to 35 bp (67 bp in total), and the largest spacer (35 bp) is located between tRNA<sup>Asn</sup> and tRNA<sup>Cys</sup> (Table 1).

We assessed the amino acid (AA) codon usage by calculating the relative synonymous codon usage (RSCU) values in 13 PCGs, which are shown in Fig. 2a. A total of 3803 codons were encoded by 13 PCGs, and the most frequently used codons were CUA (4.7%), ACA (3.4%) and ACC (3.1%). In the PCGs of the *O. lepturum* mitogenome, the AA components and their codon usage reveal that one codon family (Trp) represents more than 100 codons per thousand codons (CDpT), three codon families (Cys, Met and Ser2) between 50 CDpT and 100 CDpT, and the other twenty codon families less than 50 CDpT (Fig. 2b).

Comparative analysis of nucleotide base composition showed that the composition of *O. lepturum* is identical to that of the other *Onychostoma* fishes, and most of the



**Table 1.** Organization of the mitochondrial genome of *Onychostoma lepturum*.

Locus	Position			Codon				strand'
	start	stop	size(bp)	start	stop	anti-codon	intergenic nucleotide'	
tRNA <sup>Phe</sup>	1	69	69			GAA	0	H
12s rRNA	70	1030	961				0	H
tRNA <sup>Val</sup>	1031	1102	72			TAC	0	H
16s rRNA	1103	2783	1681				0	H
tRNA <sup>Leu</sup>	2784	2859	76			TAA	0	H
<i>ND1</i>	2860	3834	975	ATG	TAA		0	H
tRNA <sup>Leu</sup>	3840	3911	72			GAT	4	H
tRNA <sup>Gln</sup>	3910	3980	71			TTG	-2	L
tRNA <sup>Met</sup>	3983	4051	69			CAT	2	H
<i>ND2</i>	4052	5096	1045	ATG	T-		0	H
tRNA <sup>Tyr</sup>	5097	5168	72			TCA	0	H
tRNA <sup>Ala</sup>	5171	5239	69			TGC	2	L
tRNA <sup>Asn</sup>	5241	5313	73			GTT	1	L
tRNA <sup>Cys</sup>	5349	5415	67			GCA	35	L
tRNA <sup>Tyr</sup>	5415	5486	72			GTA	-1	L
<i>COI</i>	5488	7038	1551	GTG	TAA		1	H
tRNA <sup>Ser</sup>	7039	7109	71			TGA	0	L
tRNA <sup>Asp</sup>	7113	7184	72			GTC	3	H
<i>COII</i>	7197	7887	691	ATG	T-		12	H
tRNA <sup>Lys</sup>	7888	7963	76			TTT	0	H
<i>ATP8</i>	7965	8129	165	ATG	TAG		1	H
<i>ATP6</i>	8123	8805	683	GTG	TA-		-7	H
<i>COIII</i>	8806	9590	785	ATG	TAA		0	H
tRNA <sup>Gly</sup>	9591	9662	72			TCC	0	H
<i>ND3</i>	9663	10011	349	ATG	T-		0	H
tRNA <sup>Arg</sup>	10012	10081	70			TCG	0	H
<i>ND4L</i>	10082	10378	297	ATG	TAA		0	H
<i>ND4</i>	10372	11752	1381	ATG	T-		-7	H
tRNA <sup>His</sup>	11753	11821	69			GTG	0	H
tRNA <sup>Ser</sup>	11822	11890	69			GCT	0	H
tRNA <sup>Leu</sup>	11892	11964	73			TAG	1	H
<i>ND5</i>	11965	13788	1824	ATG	TAA		0	H
<i>ND6</i>	13785	14306	522	ATG	TAG		-4	L
tRNA <sup>Glu</sup>	14307	14375	69			TTC	0	L
<i>Cytb</i>	14381	15521	1141	ATG	T-		5	H
tRNA <sup>Thr</sup>	15522	15594	73			TGT	0	H
tRNA <sup>Pro</sup>	15594	15663	70			TGG	-1	L
D-loop	15664	16598	935				0	H

**Table 2.** Nucleotide composition of the *Onychostoma lepturum* mitochondrial genome.

	Length (bp)	T%	C%	A%	G%	A+T%	AT-skew%	GC-skew%
Genome	16598	24	28.6	31.3	16.2	55.3	0.132	0.277
PCGs	11409	25.7	29.4	29	15.8	54.7	0.06	-0.3
1 <sup>st</sup> codon position	3807	20.3	27	26.8	25.8	47.1	0.138	-0.023
2 <sup>nd</sup> codon position	3802	40.1	27.7	18.6	13.6	58.7	-0.366	-0.341
3 <sup>rd</sup> codon position	3800	16.8	33.6	41.7	8	58.5	0.423	-0.615
rRNA	2642	19.1	25.8	34.5	20.6	53.6	0.287	-0.112
tRNA	1566	26.6	21.5	28.2	23.7	54.8	0.029	0.049
D-loop	935	32.5	20.3	34	13.2	66.5	0.022	-0.212

enome, except for tRNA which was positive (0.049) (Table 2). Strand asymmetry in nucleotide composition is usually reflected by AT and GC skews, which is a remarkable feature of animal mitochondrial genomes (Wei et al. 2010). The mitogenome contents of 11 *Onychostoma* species were calculated and showed an A+T bias, ranging

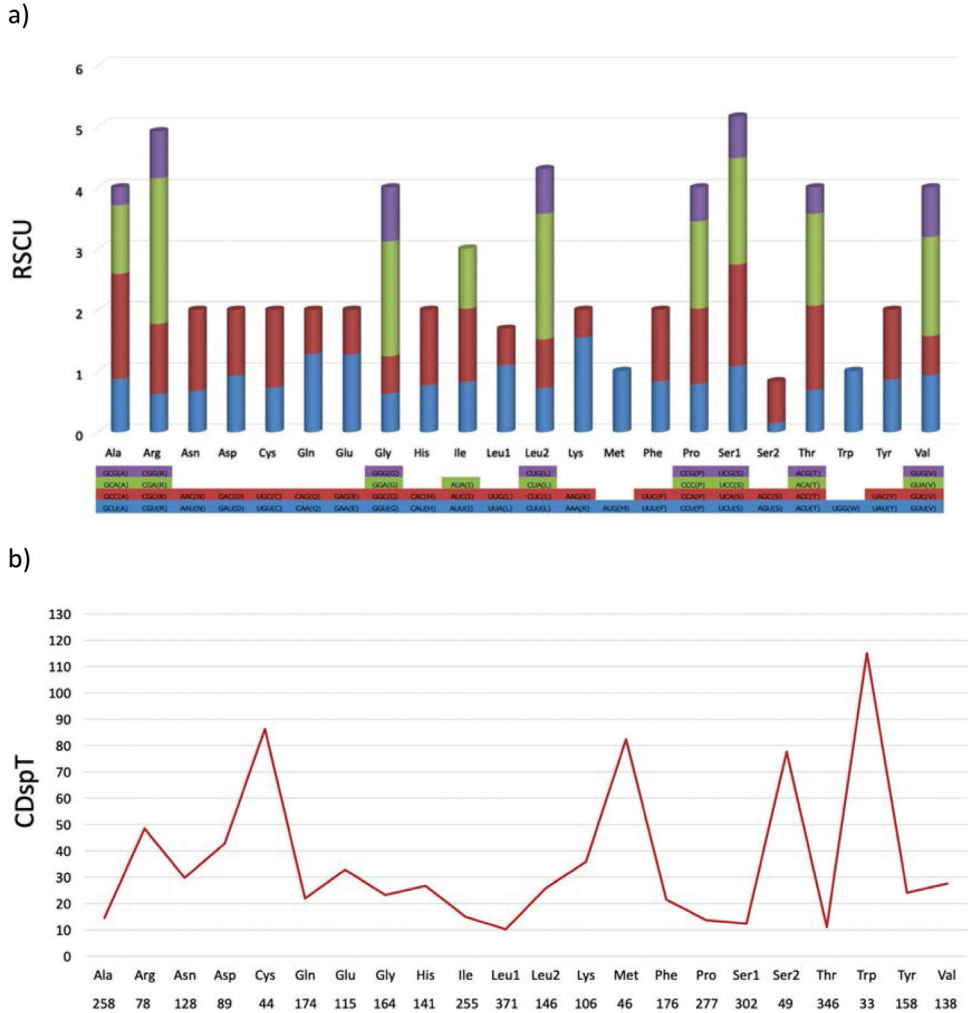


**Figure 2.** Comparison of codon usage in mitochondrial genomes of *Onychostoma lepturum* **a** Relative synonymous codon usage (RSCU) in the *Onychostoma lepturum* mitogenome. Codon families are provided on the X-axis, and the RSCU values, on the Y-axis **b** Codon distribution in the *Onychostoma lepturum* mitogenome. CDspT, codons per thousand codons. Codon families are provided on the X-axis.

from 55.3% (*O. lepturum*) to 56.6% (*O. barbatulum*) (Suppl. material 1: Table S1). The analysis of *Onychostoma* mitochondria populations showed distinct skew patterns, in which AT was positive and GC was negative (Suppl. material 1: Table S1).

The 22 tRNA genes in the *O. lepturum* mitogenome are interspersed between rRNA and protein-coding genes, with sizes ranging from 67 to 76 bp; tRNA<sup>Cys</sup> was the shortest (67 bp), while tRNA<sup>Leu</sup> and tRNA<sup>Lys</sup> were the longest (76 bp). The arrangement of 8 L-strand encoded and 14 H-strand-encoded tRNA genes is similar to the distributions observed in other *Onychostoma* species. Two rRNA genes were identified on the L-strand in *O. lepturum*, which is similar to the other *Onychostoma* species, with a total length of

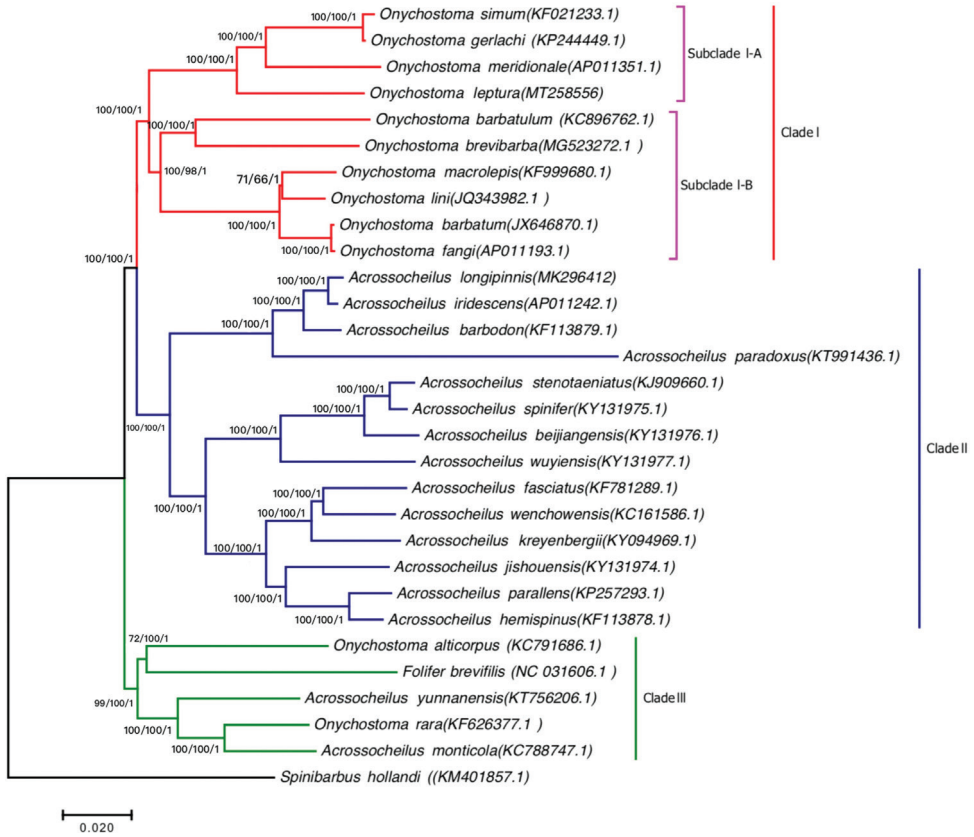


**Figure 3.** Phylogenetic trees derived from Maximum-Likelihood (ML) and Neighbor Joining (NJ) approaches based on whole mitochondrial genomes. The numbers on the nodes are the bootstrap values of ML/NJ. The number after the species name is the GenBank Accession Number.

2642 bp. The 16S rRNA is located between  $tRNA^{Val}$  and  $tRNA^{Leu}$ , with a length of 1681 bp, whereas the 12S rRNA is located between  $tRNA^{Phe}$  and  $tRNA^{Val}$ , with a length of 961 bp. Regarding the two rRNA genes, the GC-skew is slightly negative ( $-0.112$ ), but the AT-skew is strongly positive ( $0.287$ ). The total A+T content of the rRNA genes (53.1%) is lower than those of the total tRNA genes (55.0%) and the total PCG genes (55.6%).

### Phylogenetic analyses

To further investigate the phylogenetic position of *O. lepturum* within the genera *Acrossocheilus* and *Onychostoma*, the concatenated set of nucleotide sequences of available whole mitochondrial genomes from 10 *Onychostoma* species, 16 *Acrossocheilus* species and *F. brevivifilis* were derived for phylogenetic reconstruction, along with *S. hollandi* as an outgroup. The ML, NJ and BI analyses showed the same topology, representing the three main lineages (Clades I, II and III). The phylogenetic tree revealed that Clade I is the *Onychostoma* group, which can be separated into two subclades (subclades I-A and I-B) with strong support (Fig. 3). The phylogenetic po-

sition of *O. lepturum* is closer to that of *O. meridionale* than to that of *O. simum* and *O. gerlachi* in subclade I-A. Subclade I-B clusters with five species of *Onychostoma*, including *O. barbatulum*, *O. barbatum*, *O. fangi*, *O. lini* and *O. macrolepis*. Clade II is the *Acrossocheilus* group and includes 14 species, which is in accordance with traditional classifications based on morphology and previous phylogenetic studies based on whole mitochondrial genomes (Yuan et al. 2015; Hou et al. 2020). Species of *Acrossocheilus*, *Onychostoma* and *F. brevifilis* are included in Clade III, which is considered as an ancestral group, including *A. monticola*, *A. yunnanensis*, *O. rarum*, *O. alticorpus* and *F. brevifilis*.

## Discussion

### Mitochondrial genome of *O. lepturum*

The total length of the *Onychostoma* mitogenomes ranged between 16,590 (*O. rarum*) and 16,601 bp (*O. simum* and *O. gerlachi*), while that of the *O. lepturum* is a typical closed circular DNA molecule with a length of 16,598 bp (Fig. 1; GenBank No. MK296412), making it similar to other *Onychostoma* sequences, which differ by between 3 and 8 bp (16,590 bp for *O. rarum* and 16,601 bp for *O. simum*, *O. gerlachi*) (Suppl. material 1: Table S1). We suggest that the variability observed in closely related mitogenome length can be caused by variations in tandem repeat elements within the control region (D-Loop); differences in the lengths of intergenic regions are also a likely explanation for the gene overlaps (Fig. 1). The nucleotide composition of the *O. lepturum* mitogenome is highly biased toward A+T (55.3%), which is similar to the values in other *Onychostoma* species and displays strand skewness consistent with asymmetrical mutation pressure (Bielawski and Gold 2002) (Suppl. material 1: Table S1). Of the 22 identified tRNAs, the AT and GC skews were both positive in the *O. lepturum* mitogenome, which is common in *Onychostoma* mitogenomes. Comparative mitogenomic structure, organization and gene arrangement analyses of all *Onychostoma* mitogenomes are conserved without any structural rearrangement. Among *Onychostoma* fishes that also exhibited highly similar nucleotide compositions and codon usage patterns, a slight difference was also observed in some species. Ten of the thirteen total PCGs used ATG as the initiation codon (ND1, ND2, ND4, ND4L, ND5, ND6, COII, COIII, ATP8, and Cyt *b*), whereas the COI gene started with the GTG codon in all *Onychostoma* species. Most protein-coding genes started with a traditional ATG codon except for COI in *Onychostoma* mitogenomes, which is consistent with previous reports for other fish mitogenomes (Satoh et al. 2016). In the ATP6 gene, only *O. lepturum* was found with GTG as the initiation codon, and the other *Onychostoma* species used the typical ATG codon. In contrast, only ND3 held diverse start codons in *Onychostoma* mitogenomes. Five *Onychostoma* species were initiated by GTG, including *O. alticorpus*, *O. rarum*, *O. simum*, *O. gerlachi* and *O. meridionale*. The other *Onychostoma* species was initiated by ATG (Table 3). In addition, six PCGs

(ND1, COI, ATP8, ND4L, ND5 and ND6) harbored the typical termination codons (TAA and TAG) in the *Onychostoma* mitochondrial genome, and the remaining PCGs were terminated with incomplete codons (T- and TA-). The incomplete termination codon T in the *Onychostoma* mitochondrial genome was a common termination codon (ND2, ND3, ND4, COII and Cyt *b*), except for *O. alticorpus*, which was terminated by TAA in the ND3 gene (Table 3); however, the COI, ND4L and ND5 genes used TAA, the ATP8 gene used TAG, while ND1 and ND6 used TAG or TAA (Table 3). ND1 and ND6 are terminated with the codon TAA for most *Onychostoma* species, which is different from the termination codon (TAG) observed for ND1 in *O. barbatulum*, *O. simum* and *O. gerlachi* and ND6 in *O. lepturum*, *O. barbatulum*, *O. alticorpus*, *O. simum*, *O. gerlachi* and *O. meridionale* (Table 3). We suggest that ND1 and ND6 appear to have evolved relatively rapidly in these *Onychostoma* species, and a similar observation has also been reported in a previous study of *Acrossocheilus* mitogenomes (Hou et al. 2020).

### Molecular phylogeny of *Onychostoma*

Taki (1975) suggested that two groups were subgenera of the genus *Onychostoma*: *Onychostoma* and *Gymnostomus*. These two groups are divided based on their possession of osseous simple dorsal rays; the subgenus *Gymnostomus* includes those having non-osseous rays, while the subgenus *Onychostoma* includes those with osseous simple dorsal rays (Taki 1975). There are five species (*O. lepturum*, *O. barbatulum*, *O. barbatum*, *O. macrolepis* and *O. alticorpus*) belonging to the subgenus *Gymnostomus*, whereas the remaining species belongs to the subgenus *Onychostoma*. According to the mouth width, mouth-opening shape, and post-labial groove length, previous studies divided members of *Onychostoma* into three groups (Chen 1989; Xin et al. 2009). Our results showed that the *Onychostoma* with osseous simple dorsal rays (*O. simum*, *O. rara*, *O. lini*, *O. meridionale*, *O. gerlachi* and *O. fangi*) could not be successfully clustered together (Fig. 3). In addition, molecular evidence revealed that Clade I, including subclades I-A (*O. lepturum*, *O. meridionale*, *O. simum* and *O. gerlachi*) and subclade I-B (*O. barbatulum*, *O. barbatum*, *O. fangi*, *O. lini* and *O. macrolepis*), comprise a stable monophyletic group.

Comparison was made between the phylogenetic trees constructed by Yang et al. (2015), Wang et al. (2016) and Zheng et al. (2016), whereby input sequences such as mtDNA and nuclear sequences were used for phylogeny. One of the similarities between all studies is that Clade I in the *Onychostoma* group comprises a stable monophyletic group distinct from *Acrossocheilus* and *F. brevifilis*. Following our study, *O. simum* was consistently grouped closely with *O. gerlachi* in the *Onychostoma* group (Clade I-A), as in the previous study based on the mitogenome data (Zhang et al. 2018). However, one distinct difference among these above mentioned studies is that in the trees constructed by Yang et al. (2015), Wang et al. (2016) and Zheng et al. (2016) based on nuclear and mitochondrial genes, *O. simum* was found to be more closely related to *O. alticorpus* and *F. brevifilis*. *Onychostoma simum* was more closely related

**Table 3.** Composition and skewness in mitogenomes of 12 *Omychostoma* species.

Species	ND1	ND2	COI	COII	ATP8	ATP6	COIII	ND3	ND4L	ND4	ND5	ND6	Cytb	GenBank
<i>O. lepturum</i>	ATG/TAA	ATG/T-	GTG/TAA	ATG/T-	ATG/TAG	GTG/TA	ATG/TA	ATG/T-	ATG/TAA	ATG/T-	ATG/TAA	ATG/TAG	ATG/T-	MT258556
<i>O. macrolepis</i>	ATG/TAA	ATG/T-	GTG/TAA	ATG/T-	ATG/TAG	ATG/TA	ATG/TA	ATG/T-	ATG/TAA	ATG/T-	ATG/TAA	ATG/TAA	ATG/T-	KF999680.1
<i>O. lini</i>	ATG/TAA	ATG/T-	GTG/TAA	ATG/T-	ATG/TAG	ATG/TA	ATG/TA	ATG/T-	ATG/TAA	ATG/T-	ATG/TAA	ATG/TAA	ATG/T-	JQ343982.1
<i>O. barbatum</i>	ATG/TAA	ATG/T-	GTG/TAA	ATG/T-	ATG/TAG	ATG/TA	ATG/TA	ATG/T-	ATG/TAA	ATG/T-	ATG/TAA	ATG/TAA	ATG/T-	JX646870.1
<i>O. fangi</i>	ATG/TAA	ATG/T-	GTG/TAA	ATG/T-	ATG/TAG	ATG/TA	ATG/TA	ATG/T-	ATG/TAA	ATG/T-	ATG/TAA	ATG/TAA	ATG/T-	AP011193.1
<i>O. barbatulum</i>	ATG/TAG	ATG/T-	GTG/TAA	ATG/T-	ATG/TAG	ATG/TA	ATG/TA	ATG/T-	ATG/TAA	ATG/T-	ATG/TAA	ATG/TAG	ATG/T-	KC896762.1
<i>O. alticarpus</i>	ATG/TAA	ATG/T-	GTG/TAA	ATG/T-	ATG/TAG	ATG/TA	ATG/TA	GTG/TAA	ATG/TAA	ATG/T-	ATG/TAA	ATG/TAG	ATG/T-	KC791686.1
<i>O. narum</i>	ATG/TAA	ATG/T-	GTG/TAA	ATG/T-	ATG/TAG	ATG/TA	ATG/TA	GTG/T-	ATG/TAA	ATG/T-	ATG/TAA	ATG/TAA	ATG/T-	KF626377.1
<i>O. sinum</i>	ATG/TAG	ATG/T-	GTG/TAA	ATG/T-	ATG/TAG	ATG/TA	ATG/TA	GTG/T-	ATG/TAA	ATG/T-	ATG/TAA	ATG/TAG	ATG/T-	KF021233.1
<i>O. gerlachi</i>	ATG/TAG	ATG/T-	GTG/TAA	ATG/T-	ATG/TAG	ATG/TA	ATG/TA	GTG/T-	ATG/TAA	ATG/T-	ATG/TAA	ATG/TAG	ATG/T-	KP244449.1
<i>O. meridionale</i>	ATG/TAA	ATG/T-	GTG/TAA	ATG/T-	ATG/TAG	ATG/TA	ATG/TA	GTG/T-	ATG/TAA	ATG/T-	ATG/TAA	ATG/TAG	ATG/T-	AP011351.1
<i>O. brevisbarba</i>	ATG/TAA	ATG/T-	GTG/TAA	ATG/T-	ATG/TAG	ATG/TA	ATG/TA	ATG/T-	ATG/TAA	ATG/T-	ATG/TAA	ATG/TAG	ATG/T-	MG523272.1

to *O. gerlachi* and was distributed in the Lancang Jiang and Red River basins (Song et al. 2018), as described in a previous study based on the biogeography of *Onychostoma* (Zhang et al. 2018). The resulting relationships are not consistent with earlier conclusions based on morphological characteristics (Taki 1975; Xin et al. 2009) or on nuclear and mitochondrial genes (Wang et al. 2007; Yang et al. 2016; Zheng et al. 2016). However, the single-gene evolutionary tree of the COI gene is inconsistent with that of combined complete mitochondrial genome, suggesting that *O. simum* (KF021233.1) were incorrectly identified. According to NCBI data and Wang et al. (2013), specimens KF021233.1 did not have an associated collection site (and we suggest that specimens KF021233.1 were *O. gerlachi*). Our results show that *O. lepturum* was found to be more closely related to *O. meridionale* than *O. gerlachi*. *Onychostoma lepturum* and *O. meridionale* occur in Laos and Vietnam, while *O. lepturum* is distributed in the Yuanjiang River in mainland China and Hainan Island. According to the previous biogeographic studies, the Gulf of Tonkin once formed part of the coastal plain of mainland China and the River in Vietnam and Hainan Island drained into the Gulf of Tonkin during Pleistocene glaciations (Zhang et al. 2020).

Recent studies have revealed similar scenarios in the genetic patterns of *Garra orientalis* (Yang et al. 2016), *Aphyocypris normalis* (Huang et al. 2019) and *Opsariichthys hainanensis* (Zhang et al. 2020). Xin et al. (2009) proposed that *O. lini* and *O. barbata* were found to be related closer to *O. macrolepis* based on morphological characters. This result suggested that the phylogenetic relationship of subclade I-B are concordant with the molecular phylogenetic and morphological analyses. In addition, Clade II is the *Acrossocheilus* group, which includes 14 species, comprising a stable monophyletic group distinct from the *Onychostoma* group in the ML, NJ and BI trees (Fig. 3). The present study strongly supported that some species of *Acrossocheilus*, *Onychostoma* and *F. brevifilis* belong to the monophyletic group (Clade III), including *A. monticola*, *A. yunnanensis*, *O. rarum*, *O. alticorpus* and *F. brevifilis*. Interestingly, our results corroborate the previous finding that *O. rarum* is the sister group of *O. alticorpus* (Hoang et al. 2015; Song et al. 2018; Zhang et al. 2018), but Zhai et al. (2020) suggested that *O. rarum* appeared to be more closely related with *O. barbatulum* and *O. barbatum*. We suggested that the specimens of *O. rarum* (NC022869.1) were also misidentified. Moreover, all of these members were previously confirmed as a monophyletic group (Yuan et al. 2015; Hou et al. 2020). Overall, the complete mtDNA sequence of *O. lepturum* provides useful genetic data for addressing further questions in the systematics and evolutionary history of *Onychostoma*, for understanding its molecular diversity and for genetic conservation applications.

## Acknowledgements

This work was supported by grants from the Ministry of Science and Technology, Taiwan (MOST 108-2221-E-035-057 and MOST 109-2221-E-035-034). There are no conflicts of interest in this study.

## Reference

- Bielawski JP, Gold JR (2002) Mutation patterns of mitochondrial H-and L-strand DNA in closely related cyprinid fishes. *Genetics* 161: 1589–1597.
- Boulenger GA (1900) On the reptiles, batrachians, and fishes collected by the late Mr. John Whitehead in the interior of Hainan. In *Proceedings of the Zoological Society of London* 189: 956–962.
- Chen XL, Yue PQ, Lin RD (1984) Major groups within the family Cyprinidae and their phylogenetic relationships. *Acta zootaxonomica sinica* 9: 424–440.
- Chen Y (1989) Anatomy and phylogeny of the cyprinid fish genus *Onychostoma* Gunther, 1896. *Bulletin of British Museum Nature History (Zoology)* 55: 109–121.
- Chiu YW, Chang CW, Lin HD, Shen KN (2018) The complete mitogenome of the winged argonaut *Argonauta hians* and its phylogenetic relationships in Octopoda. *Conservation Genetics Resources* 10: 359–362. <https://doi.org/10.1007/s12686-017-0824-z>
- Chung HH, Kamar CKA, Lim LWK, Liao Y, Lam TT, Chong YL (2020) Sequencing and Characterisation of Complete Mitogenome DNA for *Rasbora hobelmani* (Cyprinidae) with Phylogenetic Consideration. *Journal of Ichthyology* 60: 90–98. <https://doi.org/10.1134/S0032945220010014>
- Froese RE (2019) FishBase. World Wide Web electronic publication. <http://www.fishbase.org>
- Guindon S, Dufayard J-F, Lefort V, Anisimova M, Hordijk W, Gascuel O (2010) New Algorithms and Methods to Estimate Maximum-Likelihood Phylogenies: Assessing the Performance of PhyML 3.0. *Systematic Biology* 59: 307–321. <https://doi.org/10.1093/sysbio/syq010>
- Hoang HD, Pha, HM, Tran NT (2015) Two new species of shovel-jaw carp *Onychostoma* (Teleostei: Cyprinidae) from southern Vietnam. *Zootaxa*, 3962: 123–138. <https://doi.org/10.11646/zootaxa.3962.1.6>
- Hou XJ, Lin HD, Tang WQ, Liu D, Han CC, Yang JQ (2020) Complete mitochondrial genome of the freshwater fish *Acrossocheilus longipinnis* (Teleostei: Cyprinidae): genome characterization and phylogenetic analysis. *Biologia* 75: 1871–1880. <https://doi.org/10.2478/s11756-020-00440-y>
- Huang SP, Wang FY, Wang TY (2017) Molecular phylogeny of the *Opsariichthys* group (Teleostei: Cypriniformes) based on complete mitochondrial genomes. *Zoological studies* 56: e40.
- Huang XX, Hsu KC, Kang B, Kuo PH, Tsai WH, Liang CM, Lin HD, Wang WK (2019) Population structure of *Aphyocypris normalis*: phylogeography and systematics. *ZooKeys* 872: 77–90. <https://doi.org/10.3897/zookeys.872.33105>
- Kang B, Deng J, Huang X, Chen L, Feng Y (2013) Explaining freshwater fish biogeography: history versus environment versus species personality. *Reviews in Fish Biology and Fisheries* 23: 523–536. <https://doi.org/10.1007/s11160-013-9314-x>
- Kang B, Deng J, Wu Y, Chen L, Zhang J, Qiu H, Lu Y, He D (2014) Mapping China's freshwater fishes: diversity and biogeography. *Fish and Fisheries* 15: 209–230. <https://doi.org/10.1111/faf.12011>
- Kottelat M (2001) Freshwater fishes of Northern Vietnam: a preliminary check-list of the fishes known or expected to occur in northern Vietnam with comments on systematics and nomenclature. Environment and Social Development Unit, East Asia and Pacific Region, World Bank, Washington, 184 pp.

- Kumar S, Stecher G, Li M, Knyaz C, Tamura K (2018) MEGA X: Molecular Evolutionary Genetics Analysis across Computing Platforms. *Molecular Biology and Evolution* 35: 1547–1549. <https://doi.org/10.1093/molbev/msy096>
- Lefort V, Longueville J-E, Gascuel O (2017) SMS: Smart Model Selection in PhyML. *Molecular Biology and Evolution* 34: 2422–2424. <https://doi.org/10.1093/molbev/msx149>
- Perna NT, Kocher TD (1995) Patterns of nucleotide composition at fourfold degenerate sites of animal mitochondrial genomes. *Journal of Molecular Evolution* 41: 353–358. <https://doi.org/10.1007/BF01215182>
- Rambaut A, Drummond AJ, Xie D, Baele G, Suchard MA (2018) Posterior Summarization in Bayesian Phylogenetics Using Tracer 1.7. *Systematic Biology* 67: 901–904. <https://doi.org/10.1093/sysbio/syy032>
- Ronquist F, Huelsenbeck JP (2003) MrBayes 3: Bayesian phylogenetic inference under mixed models. *Bioinformatics* 19: 1572–1574. <https://doi.org/10.1093/bioinformatics/btg180>
- Satoh TP, Miya M, Mabuchi K, Nishida M (2016) Structure and variation of the mitochondrial genome of fishes. *BMC Genomics* 17: e719. <https://doi.org/10.1186/s12864-016-3054-y>
- Shan X, Lin R, Yue P, Chu X (2000) *Onychostoma*. In: Yue P (Ed.) *Fauna Sinica, Osteichthyes*. Science Press, Beijing, Cypriniformes III, 126–147.
- Song X-L, Cao L, Zhang E (2018) *Onychostoma brevibarba*, a new cyprinine fish (Pisces: Teleostei) from the middle Chang Jiang basin in Hunan Province, South China. *Zootaxa* 4410: 147–163. <https://doi.org/10.11646/zootaxa.4410.1.8>
- Taki Y (1975) Cyprinid fishes of the genera *Onychostoma* and *Scaphiodonichthys* from Upper Laos, with remarks on the dispersal of the genera and their allies. *Japanese Journal of Ichthyology* 22: 143–150.
- Wang JP, Cheng CY, Ho CW, Ueng YT (2015) Complete mitochondrial DNA genome of *Onychostoma sima* (Cypriniformes: Cyprinidae). *Mitochondrial DNA* 26: 135–136. <https://doi.org/10.3109/19401736.2013.815173>
- Wang X, Li J, He S (2007) Molecular evidence for the monophyly of East Asian groups of Cyprinidae (Teleostei: Cypriniformes) derived from the nuclear recombination activating gene 2 sequences. *Molecular Phylogenetics and Evolution* 42: 157–170. <https://doi.org/10.1016/j.ympev.2006.06.014>
- Wang X, Gan X, Li J, Chen Y, He S (2016) Cyprininae phylogeny revealed independent origins of the Tibetan Plateau endemic polyploid cyprinids and their diversifications related to the Neogene uplift of the plateau. *Science China Life Sciences* 59: 1149–1165. <https://doi.org/10.1007/s11427-016-0007-7>
- Wei SJ, Shi M, Chen XX, Sharkey MJ, Achterberg C van, Ye GY, He JH (2010) New views on strand asymmetry in insect mitochondrial genomes. *PLoS ONE* 5(9): e12708. <https://doi.org/10.1371/journal.pone.0012708>
- Xin Q (2008) Taxonomic revision of species and phylogenetic analysis of interspecific relationships within the cyprinid genus *Onychostoma sensu lato* Günther, 1896. Dissertation. The Graduate School of Chinese Academy of Sciences.
- Xin Q, Zhang E, Cao WX (2009) *Onychostoma virgatum*, a new species of cyprinid fish (Pisces: Teleostei) from southern Anhui Province, South China. *Ichthyological Exploration of Freshwaters* 20: e255.

- Yang JQ, Hsu KC, Liu ZZ, Su LW, Kuo PH, Tang WQ, Zhou ZC, Liu D, Bao BL, Lin HD (2016) The population history of *Garra orientalis* (Teleostei: Cyprinidae) using mitochondrial DNA and microsatellite data with approximate Bayesian computation. *BMC Evolutionary Biology* 16: e.73. <https://doi.org/10.1186/s12862-016-0645-9>
- Yang L, Sado T, Vincent Hirt M, Pasco-Viel E, Arunachalam M, Li J, Wang X, Freyhof J, Saitoh K, Simons AM, Miya M, He S, Mayden RL (2015) Phylogeny and polyploidy: Resolving the classification of cyprinine fishes <https://doi.org/10.1016/j.ympev.2015.01.014> (Teleostei: Cypriniformes). *Molecular Phylogenetics and Evolution* 85: 97–116.
- Yuan LY, Liu XX, Zhang E (2015) Mitochondrial phylogeny of Chinese barred species of the cyprinid genus *Acrossocheilus Oshima*, 1919 (Teleostei: Cypriniformes) and its taxonomic implications. *Zootaxa* 4059: 151–168. <https://doi.org/10.11646/zootaxa.4059.1.8>
- Yue P (2000) *Fauna Sinica. Osteichthyes. Cypriniformes III*. Science Press. Beijing, 661 pp.
- Zhai D, Xie Z, Wang Y, Yu J, Chen Y, Xia M, Liu H, Xiong F (2020) Complete mitochondrial genome of *Onychostoma leptura* and phylogenetic analysis of *Onychostoma*. *Mitochondrial DNA Part B* 5: 2297–2298. <https://doi.org/10.1080/23802359.2020.1772692>
- Zhang C, Cheng Q, Geng H, Lin AH, Wang HY (2018) Molecular phylogeny of *Onychostoma* (Cyprinidae) based on mitochondrial genomes. *Acta Hydrobiologica Sinica* 42: 512–516.
- Zhang DX, Hewitt GM (1997) Insect mitochondrial control region: A review of its structure, evolution and usefulness in evolutionary studies. *Biochemical Systematics and Ecology* 25: 99–120. [https://doi.org/10.1016/S0305-1978\(96\)00042-7](https://doi.org/10.1016/S0305-1978(96)00042-7)
- Zhang WJ, Wang JJ, Li C, Chen JQ, Li W, Jiang SY, Hsu KC, Zhao M, Lin HD, Zhao J (2020) Spatial genetic structure of *Opsariichthys hainanensis* in South China. *Mitochondrial DNA Part A* 31: 98–107. <https://doi.org/10.1080/24701394.2020.1741564>
- Zheng LP, Yang JX, Chen XY (2016) Molecular phylogeny and systematics of the Barbinae (Teleostei: Cyprinidae) in China inferred from mitochondrial DNA sequences. *Biochemical Systematics and Ecology* 68: 250–259. <https://doi.org/10.1016/j.bse.2016.07.012>
- Zhou TQ, Lin HD, Hsu KC, Kuo PH, Wang WK, Tang WQ, Liu D, Yang JQ (2017) Spatial genetic structure of the cyprinid fish *Onychostoma lepturum* on Hainan Island. *Mitochondrial DNA Part A* 28: 901–908. <https://doi.org/10.1080/24701394.2016.1209193>

## Supplementary material I

### Table S1

Authors: I-Chen Wang, Hung-Du Lin, Chih-Ming Liang, Chi-Chun Huang, Rong-Da Wang, Jin-Quan Yang, Wei-Kuang Wang

Data type: DNA

Explanation note: Composition and skewness in the genus *Onychostoma* mitogenomes.

Copyright notice: This dataset is made available under the Open Database License (<http://opendatacommons.org/licenses/odbl/1.0/>). The Open Database License (ODbL) is a license agreement intended to allow users to freely share, modify, and use this Dataset while maintaining this same freedom for others, provided that the original source and author(s) are credited.

Link: <https://doi.org/10.3897/zookeys.1005.57592.suppl1>

# Description of a new horned toad of *Megophrys* Kuhl & Van Hasselt, 1822 (Amphibia, Megophryidae) from Zhejiang Province, China

Yanqing Wu<sup>1\*</sup>, Shize Li<sup>2\*</sup>, Wei Liu<sup>3</sup>, Bin Wang<sup>2</sup>, Jun Wu<sup>1</sup>

**1** Nanjing Institute of Environmental Sciences, Ministry of Ecology and Environment of China, Nanjing 210042, China **2** Chengdu Institute of Biology, Chinese Academy of Sciences, Chengdu 610041, China **3** Lishui Baiyun Ecological Forest Farm, Lishui 323000, China

Corresponding author: Jun Wu ([wujun@nies.org](mailto:wujun@nies.org)); Bin Wang ([wangbin@cib.ac.cn](mailto:wangbin@cib.ac.cn))

Academic editor: A. Ohler | Received 16 September 2020 | Accepted 24 November 2020 | Published 18 December 2020

<http://zoobank.org/EF069DEA-D4AB-458A-A828-A72402F98C58>

**Citation:** Wu Y, Li S, Liu W, Wang B, Wu J (2020) Description of a new horned toad of *Megophrys* Kuhl & Van Hasselt, 1822 (Amphibia, Megophryidae) from Zhejiang Province, China. ZooKeys 1005: 73–102. <https://doi.org/10.3897/zookeys.1005.58629>

## Abstract

A new species of the Asian horned toad genus *Megophrys* is described from Zhejiang Province, China, based on multiple data. Molecular phylogenetic analyses based on mitochondrial DNA indicated the new species as an independent clade deeply clustered into the *Megophrys* clade. The new species is identified from its congeners by a combination of the following characters: body size small (SVL 28.4–32.4 mm in males); vomerine teeth absent; tongue not notched behind; tympanum distinctly visible, oval; a small horn-like tubercle present at the edge of each upper eyelid; two metacarpal tubercles distinctly visible in hand; toes without webbing; heels overlapped when thighs are positioned at right angles to the body; tibiotarsal articulation reaching the level to middle of eye when leg stretched forward; an internal single subglular vocal sac in male; in breeding male, the nuptial pads present on the dorsal base of the first two fingers.

## Keywords

Molecular phylogenetic analyses, morphology, new species, taxonomy, toad

\* These authors have contributed equally to this work.

## Introduction

The Asian horned toad *Megophrys* Kuhl & Van Hasselt, 1822 (Anura: Megophryidae Bonaparte, 1850) is widely distributed in eastern and central China, throughout south-eastern Asia, and extending to the islands of the Sunda Shelf and the Philippines (Frost 2020). The generic assignment of species in the group has been controversial for decades (e.g., Tian and Hu 1983; Dubois 1987; Rao and Yang 1997; Lathrop 1997; Jiang et al. 2003; Delorme et al. 2006; Fei et al. 2009; Fei and Ye 2016; Chen et al. 2017; Deuti et al. 2017; Mahony et al. 2017; Li et al. 2020). Recent molecular phylogenetic studies proposed this group as a monophyletic group (Chen et al. 2017; Mahony et al. 2017; Li et al. 2018a; Liu et al. 2018; Liu et al. 2020; Wang et al. 2020), which was recognized as a big genus *Megophrys sensu lato* (Mahony et al. 2017; Li et al. 2018b; Liu et al. 2018; Liu et al. 2018; Liu et al. 2020; Lyu et al. 2020; Xu et al. 2020; Wang et al. 2020), though some studies still divided the taxa of the group into different genera and/or subgenera (Fei and Ye 2016; Chen et al. 2017; Deuti et al. 2017; Liu et al. 2018). The genus *Megophrys* currently contains 106 species, of which 52 species were described over the last decade (Frost 2020). A number of cryptic species were still indicated in the genus by molecular phylogenetic analyses (e.g., Chen et al. 2017; Liu et al. 2018).

Wuyi Mountain region, located in northern Fujian, southeastern Jiangxi and south Zhejiang provinces of China, is a biodiversity hotspot. In this region, four *Megophrys* species have been recorded, i.e., *M. boettgeri* (Boulenger, 1899), *M. kuatunensis* Pope, 1929, *M. ombrophila* Messenger & Dahn, 2019, and *M. lishuiensis* Wang, Liu & Jiang, 2017. However, many mountains in this region, especially in south Zhejiang Province, have been poorly investigated.

During field surveys in Qingyuan County, Zhejiang Province, China, we collected *Megophrys* specimens. Molecular phylogenetic analyses and morphological comparisons supported some of these specimens as an undescribed taxon that we describe herein as a new species.

## Materials and methods

### Sampling

A total of 15 specimens were sampled in this study: six adult males and one tadpole of the undescribed species and two adult males of *M. boettgeri* from Qingyuan County, Zhejiang Province, China, and one adult male of *M. ombrophila* and six adult males of *M. kuatunensis* from Wuyi Mountain, Fujian Province, China (Table 1; Fig. 1). The developmental stage of tadpole was identified following Gosner (1960). In the field, the toad and tadpole were euthanized using isoflurane, and the specimens were fixed in 75% ethanol. Tissue samples were taken and preserved separately in 95% ethanol prior to fixation. The specimens were deposited in Chengdu Institute of Biology, Chinese Academy of Sciences (CIB, CAS).

**Table 1.** Information for samples used in molecular phylogenetic analyses in this study.

ID	Species	Voucher number	Locality	GenBank accession number	
				16S	COI
1	<i>Megophrys baishanzuensis</i> sp. nov.	CIBQY20200719001	Baishanzu National Park, Qingyuan, Zhejiang, China	MW001150	MT998291
2	<i>Megophrys baishanzuensis</i> sp. nov.	CIBQY20200719002		MW001151	MT998292
3	<i>Megophrys baishanzuensis</i> sp. nov.	CIBQY20200719003		MW001152	MT998293
4	<i>Megophrys baishanzuensis</i> sp. nov.	CIBQY20200719004		MW001153	MT998294
5	<i>Megophrys baishanzuensis</i> sp. nov.	CIBQY20200719006		MW001154	MT998295
6	<i>Megophrys baishanzuensis</i> sp. nov.	CIBQY20200726001		MW001155	MT998296
7	<i>Megophrys baishanzuensis</i> sp. nov.	CIBQY20200726002		MW001156	MT998297
8	<i>Megophrys kuatunensis</i>	CIBWY18082407	Wuyi Shan, Fujian, China	MW001157	MT998298
9	<i>Megophrys kuatunensis</i>	CIBWY18082408		MW001158	MT998299
10	<i>Megophrys kuatunensis</i>	SYS a001579		KJ560376	–
11	<i>Megophrys lini</i>	SYS a002370	Suichuan, Jiangxi, China	KJ560412	–
12	<i>Megophrys xiangnanensis</i>	SYS a002874	Yangming Shan, Hunan, China	MH406713	MH406165
13	<i>Megophrys nanlingensis</i>	SYS a001959	Nanling Nature Reserve, Guangdong, China	MK524111	MK524142
14	<i>Megophrys dongguanensis</i>	SYS a001972	Yinping Shan, Guangdong, China	MK524098	MK524129
15	<i>Megophrys nankunensis</i>	SYS a004498	Nankun Shan, Guangdong, China	MK524108	MK524139
16	<i>Megophrys cheni</i>	SYS a001427	Jinggang Shan, Jiangxi, China	KJ560391	–
17	<i>Megophrys wugongensis</i>	SYS a002610	Wugongshan Scenic Area, Jiangxi, China	MK524114	MK524145
18	<i>Megophrys ombrophila</i>	KRM18	Wuyishan, Fujian, China	KX856404	–
19	<i>Megophrys ombrophila</i>	CIBWY18082308		MW001159	MT998300
20	<i>Megophrys obesa</i>	SYS a002272	Heishiding Nature Reserve, Guangdong, China	KJ579122	–
21	<i>Megophrys lishuiensis</i>	WYF00169	Lishui, zhejiang, China	KY021418	–
22	<i>Megophrys xianjuensis</i>	CIBXJ190505	Xianju, zhejiang, China	MN563753	MN563769
23	<i>Megophrys jinggangensis</i>	KIZ07132	Chashan Forest Farm, Jiangxi, China	KX811840	KX812108
24	<i>Megophrys boettgeri</i>	CIB20200718001	Baishanzu National Park, Qingyuan, Zhejiang, China	MW001160	MT998301
25	<i>Megophrys boettgeri</i>	CIB20200718002	Baishanzu National Park, Qingyuan, Zhejiang, China	MW001161	MT998302
26	<i>Megophrys boettgeri</i>	Tissue ID: YPXJK033	Wuyi Shan, Fujian, China	KX811814	KX812104
27	<i>Megophrys huangshanensis</i>	KIZ022004	Huang Shan, Anhui, China	KX811821	KX812107
28	<i>Megophrys liboensis</i>	GNUG:20160408003	Libo, Guizhou, China	MF285262	–
29	<i>Megophrys mufimontana</i>	SYS a006391	Mufu Shan, Hunan, China	MK524105	MK524136
30	<i>Megophrys wushanensis</i>	KIZ045469	Guangwu Shan, Sichuan, China	KX811838	KX812094
31	<i>Megophrys baolongensis</i>	KIZ019216	Baolong, Chongqing, China	KX811813	KX812093
32	<i>Megophrys tuberogranulata</i>	Tissue ID: YPX10987	Badagongshan Nature Reserve, Hunan, China	KX811823	KX812095
33	<i>Megophrys yangmingensis</i>	SYS a002877	Yangming Shan, Hunan, China	MH406716	MH406168
34	<i>Megophrys shimentaina</i>	SYS a002077	Shimentai Nature Reserve Guangdong, China	MH406655	MH406092
35	<i>Megophrys julianensis</i>	SYS a002107	Julian Shan, Jiangxi, China	MK524099	MK524130
36	<i>Megophrys shunhuangensis</i>	HNNU16SH02	Shunhuang Mountains, Hunan, China	MK836037	–
37	<i>Megophrys mirabilis</i>	SYS a002192	Huaping Nature Reserve, Guangxi, China	MH406669	MH406109
38	<i>Megophrys leishanensis</i>	CIBLS20171101001	Leigong Shan, Guizhou, China	MK005310	MK005306
39	<i>Megophrys omeimontis</i>	KIZ025765	Emei Shan, Sichuan, China	KX811884	KX812136
40	<i>Megophrys angka</i>	KIZ040591	Kiew Mae Pan nature trail, Chiang Mai, Thailand	MN508052	–
41	<i>Megophrys binchuanensis</i>	KIZ019441	Jizu Shan, Yunnan, China	KX811849	KX812112
42	<i>Megophrys palpebralespinosa</i>	KIZ011603	Pu Hu Nature Reserve, Thanh Hoa, Vietnam	KX811888	KX812137
43	<i>Megophrys spinata</i>	SYSa002227	Leigong Shan, Guizhou, China	MH406676	MH406116
44	<i>Megophrys sangzhiensis</i>	SYSa004307	Zhangjiajie, Hunan, China	MH406798	MH406260
45	<i>Megophrys binlingensis</i>	SYSa005313	Wawu Shan, Sichuan, China	MH406892	MH406354
46	<i>Megophrys wuliangshanensis</i>	KIZ046812	Huangcaoling, Yunnan, China	KX811881	KX812129
47	<i>Megophrys daweimontis</i>	KIZ048997	Dawei Shan, Yunnan, China	KX811867	KX812125

ID	Species	Voucher number	Locality	GenBank accession number	
				16S	COI
48	<i>Megophrys jingdongensis</i>	KIZ-LC0805067	Huanglianshan National Nature Reserve, Yunnan, China	KX811872	KX812131
49	<i>Megophrys fansipanensis</i>	VNMN 2018.01	Lao Cai, Sa Pa, Vietnam	MH514886	–
50	<i>Megophrys boanglienensis</i>	VNMN 2018.02	Lao Cai, Sa Pa, Vietnam	MH514889	–
51	<i>Megophrys minor</i>	KIZ01939	Qingcheng Shan, Sichuan, China	KX811896	KX812145
52	<i>Megophrys jiangi</i>	CIBKKS20180722006	Kuankuostui Nature Reserve, Guizhou, China	MN107743	MN107748
53	<i>Megophrys chishuiensis</i>	CIBCS20190518031	Chishui Nature Reserve, Guizhou, China	MN954707	MN928958
54	<i>Megophrys brachykolos</i>	ROM 16634	Hong Kong, China	KX811897	KX812150
55	<i>Megophrys acuta</i>	SYS a001957	Heishiding Nature Reserve, Guangdong, China	KJ579118	–
56	<i>Megophrys gerti</i>	ITBCZ 1108	Nui Chua National Park, Ninh Thuan, Vietnam	KX811917	KX812161
57	<i>Megophrys elfina</i>	ZMMU ABV-00454	Bidoup Mountain, Lam Dong, Vietnam	KY425379	–
58	<i>Megophrys synoria</i>	FMNH 262778	O'Reang, Mondolkiri, Cambodia	KY022198	–
59	<i>Megophrys hansi</i>	KIZ010360	Phong Dien Nature Reserve, Thua Thien Hue, Vietnam	KX811913	KX812155
60	<i>Megophrys microstoma</i>	KIZ048799	Xiaoqiaogou Nature Reserve, Yunnan, China	KX811914	KX812156
61	<i>Megophrys pachyproctus</i>	KIZ010978	Beibeng, Xizang, China	KX811908	KX812153
62	<i>Megophrys baluensis</i>	ZMH A13125	Gunung Kinabalu National Park, Kogopan Trail, Malaysia	KJ831310	–
63	<i>Megophrys stejnegeri</i>	KU 314303	Pasonanca Natural Park, Zamboanga, Philippines	KX811922	KX812052
64	<i>Megophrys ligayae</i>	ZMMU NAP-05015	Palawan, Philippines	KX811919	KX812051
65	<i>Megophrys kobayashii</i>	UNIMAS 8148	Gunung Kinabalu National Park, Sabah, Malaysia	KJ831313	–
66	<i>Megophrys nasuta</i>	KIZ019419	Malaysia	KX811921	KX812054
67	<i>Megophrys edwardinae</i>	FMNH 273694	Bintulu, Sarawak, Malaysia	KX811918	KX812050
68	<i>Megophrys aceras</i>	KIZ025467	Khao Nan National Park, Nakhon Si Thammarat, Thailand	KX811925	KX812159
69	<i>Megophrys maosonensis</i>	KIZ016045	Xiaoqiaogou Nature Reserve, Yunnan, China	KX811780	KX812080
70	<i>Megophrys mangshanensis</i>	KIZ021786	Nanling National Forest Park, Guangdong, China	KX811790	KX812079
71	<i>Megophrys flavipunctata</i>	SDBDU2009.297	East Khasi Hills dist., Meghalaya	KY022307	MH647536
72	<i>Megophrys glandulosa</i>	KIZ048439	Husa, Yunnan, China	KX811762	KX812075
73	<i>Megophrys medogensis</i>	KIZ06621	Beibeng, Xizang, China	KX811767	KX812082
74	<i>Megophrys periosa</i>	BNHS 6061	West Kameng dist., Arunachal Pradesh, IN	KY022309	MH647528
75	<i>Megophrys himalayana</i>	SDBDU2009.75	East Siang dist., Arunachal Pradesh, IN	KY022311	–
76	<i>Megophrys sanu</i>	K5198/ZSI11393	–	KX894679	–
77	<i>Megophrys zhangji</i>	KIZ014278	Zhangmu, Xizang, China	KX811765	KX812084
78	<i>Megophrys katabhako</i>	ZSIA11799	–	KX894669	–
79	<i>Megophrys major</i>	SYSa002961	Zhushihe, Yunnan, China	MH406728	MH406180
80	<i>Megophrys oreocrypta</i>	BNHS 6046	West Garo Hills dist., Meghalaya	KY022306	–
81	<i>Megophrys auralensis</i>	NCSM 79599	Aural, Kampong Speu, Cambodia	KX811807	–
82	<i>Megophrys parva</i>	SYSa003042	Zhushihe, Yunnan, China	MH406737	MH406189
83	<i>Megophrys dringi</i>	UNIMAS 8943	Gunung Mulu National Park, Sarawak, Malaysia	KJ831317	–
84	<i>Megophrys nankiangensis</i>	CIB ZYC517	Nanjiang, Sichuan, China	KX811900	–
85	<i>Megophrys wawuensis</i>	KIZ025799	Wawu Shan, Sichuan, China	KX811902	KX812062
86	<i>Megophrys gigantea</i>	SYSa003933	Wuliang shan, Yunnan, China	MH406775	MH406235
87	<i>Megophrys shapingensis</i>	KIZ014512	Liziping Nature Reserve, Sichuan, China	KX811904	KX812060
88	<i>Megophrys feae</i>	KIZ046706	Huangcaoling, Yunnan, China	KX811810	KX812056
89	<i>Megophrys chuannanensis</i>	CIB20050081	Hejiang, Sichuan, China	KM504261	–
90	<i>Megophrys carinense</i>	Tissue ID: YPX20455	Dayao Shan, Guangxi, China	KX811811	KX812057
91	<i>Megophrys popei</i>	SYS a000589	Naling Nature Reserve, Guangdong, China	KM504251	–

ID	Species	Voucher number	Locality	GenBank accession number	
				16S	COI
92	<i>Megophrys intermedia</i>	ZFMK 87596	U Bo, Phong Nha-Ke Bang NP, Vietnam	HQ588950	–
93	<i>Megophrys Montana</i>	LSUMZ 81916	Sukabumi, Java, Indonesia	KX811927	KX812163
94	<i>Megophrys lancip</i>	MZB: Amp:22233	–	KY679891	–
95	<i>Leptobranchium boringii</i>	Tissue ID: YPX37539	Emei Shan, Sichuan, China	KX811930	KX812164
96	<i>Leptobranchella oshanensis</i>	KIZ025778	Emei Shan, Sichuan, China	KX811928	KX812166

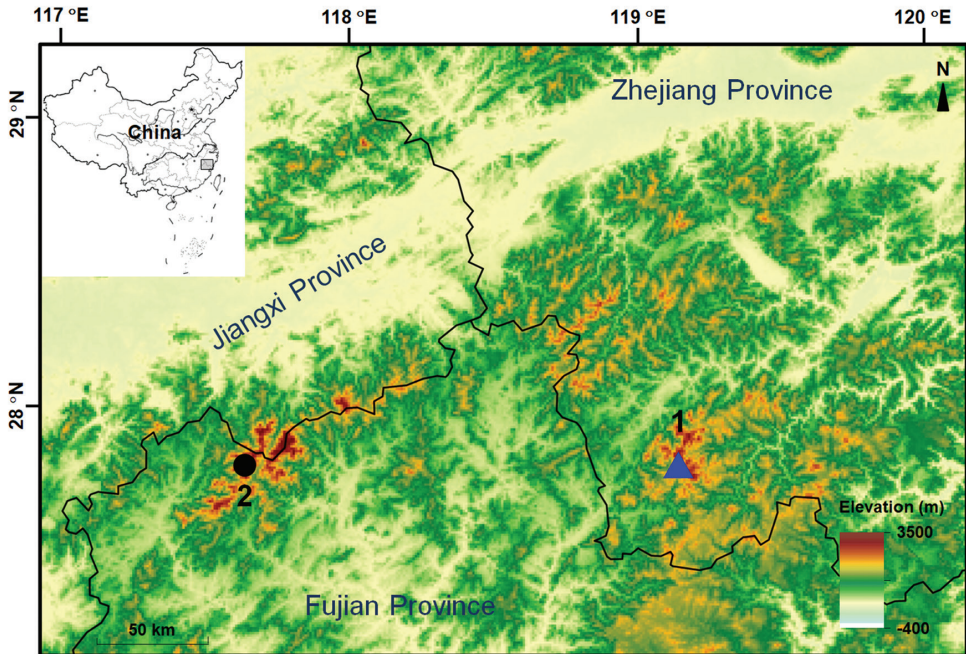


**Figure 1.** Sampling localities of *Megophrys baishanzuensis* sp. nov. and its relatives **1** Baishanzu National Park, Qingyuan County, Zhejiang Province, China, inhabited by *Megophrys baishanzuensis* sp. nov. and *M. boettgeri* **2** Wuyi Mountain, Wuyishan City, Fujian Province, China, inhabited by *M. boettgeri*, *M. kuatunensis*, and *M. ombrophila*.

## Molecular data and phylogenetic analyses

Six adult males and one tadpole of the undescribed species, two *M. kuatunensis*, one *M. ombrophila*, and two *M. boettgeri* were included in the molecular analyses (Table 1). Total DNA was extracted using a standard phenol-chloroform extraction protocol (Sambrook et al. 1989). Two fragments of the mitochondrial 16S rRNA (16S) and cytochrome oxidase subunit I (COI) genes were amplified. For 16S, the primers P7 (5'-CGC-CTGTTTACCAAAAACAT-3') and P8 (5'-CCGGTCTGAACTCAGATCACGT-3') were used following Simon et al. (1994), and for COI, Chmf4 (5'-TYTCWACWAAY-CAYAAAGAYATCGG-3') and Chmr4 (5'-ACYTCRGGRTGCCRAARAATCA-3') were used following Che et al. (2012). Gene fragments were amplified under the

following conditions: an initial denaturing step at 95 °C for 4 min; 36 cycles of denaturing at 95 °C for 30 s, annealing at 52 °C (for 16S)/47 °C (for COI) for 40 s and extending at 72 °C for 70 s. Sequencing was conducted using an ABI3730 automated DNA sequencer in Shanghai DNA BioTechnologies Co., Ltd. (Shanghai, China). New sequences were deposited in GenBank (for GenBank accession numbers see Table 1).

For molecular analyses, the available sequences for congeners of *Megophrys* were downloaded from GenBank (Table 1), primarily from previous studies (Chen et al. 2017; Liu et al. 2018). For phylogenetic analyses, corresponding sequences of one *Leptobranchella oshanensis* (Liu, 1950) and one *Leptobranchium boringii* (Liu, 1945) were also downloaded (Table 1), and used as outgroups following Mahony et al. (2017). Sequences were assembled and aligned using the Clustalw module in BioEdit v.7.0.9.0 (Hall 1999) with default settings. Alignments were checked by eye and revised manually if necessary. For phylogenetic analyses of mitochondrial DNA, the dataset concatenated with 16S and COI gene sequences. To avoid under- or over-parameterization (Lemmon and Moriarty 2004; McGuire et al. 2007), the best partition scheme and the best evolutionary model for each partition were chosen for the phylogenetic analyses using PARTITIONFINDER v. 1.1.1 (Robert et al. 2012). In this analysis, 16S gene and each codon position of COI gene were defined, and Bayesian Inference Criteria was used. As a result, the analysis suggested that the best partition scheme is 16S gene/ each codon position of COI gene, and selected GTR + G + I model as the best model for each partition. Phylogenetic analyses were conducted using maximum likelihood (ML) and Bayesian Inference (BI) methods, implemented in PhyML v. 3.0 (Guindon et al. 2010) and MrBayes v. 3.12 (Ronquist and Huelsenbeck 2003), respectively. For the ML tree, branch supports were drawn from 10,000 nonparametric bootstrap replicates. In BI, two runs each with four Markov chains were simultaneously run for 50 million generations with sampling every 1,000 generations. The first 25% trees were removed as the “burn-in” stage followed by calculations of Bayesian posterior probabilities (BPP) and the 50% majority-rule consensus of the post burn-in trees sampled at stationarity. Finally, mean genetic distance between *Megophrys* species based on uncorrected *p*-distance model was estimated respectively on 16S and COI genes using MEGA v. 6.06 (Tamura et al. 2013).

## Morphological comparisons

Six adult males and one tadpole of the undescribed species were measured (Table 1 and Suppl. material 1). For comparisons, six adult male specimens of *M. kuatunensis* were also measured (Suppl. material 1). The terminology and methodology followed Fei et al. (2009). Measurements were taken with a dial caliper to 0.1 mm. Twenty-two morphometric characters of adult specimens were measured:

- ED** eye diameter (distance from the anterior corner to the posterior corner of the eye);
- FIL** first finger length (distance from base to tip of finger I);
- FIIL** second finger length (distance from base to tip of finger II);

- FIIL** third finger length (distance from base to tip of finger III);  
**FIVL** fourth finger length (distance from base to tip of finger IV);  
**FL** foot length (distance from tarsus to the tip of fourth toe);  
**HDL** head length (distance from the tip of the snout to the articulation of jaw);  
**HDW** maximum head width (greatest width between the left and right articulations of jaw);  
**HAL** hand length (distance from tip of third digit to proximal edge of inner palmar tubercle);  
**IND** internasal distance (minimum distance between the inner margins of the external nares);  
**IOD** interorbital distance (minimum distance between the inner edges of the upper eyelids);  
**LAL** length of lower arm and hand (distance from the elbow to the distal end of the Finger IV);  
**LW** lower arm width (maximum width of the lower arm);  
**SNT** distance between the nasal the posterior edge of the vent;  
**SVL** snout-vent length (distance from the tip of the snout to the posterior edge of the vent);  
**SL** snout length (distance from the tip of the snout to the anterior corner of the eye);  
**TFL** length of foot and tarsus (distance from the tibiotarsal articulation to the distal end of the Toe IV);  
**THL** thigh length (distance from vent to knee);  
**TL** tibia length (distance from knee to tarsus);  
**TW** maximal tibia width;  
**TYD** maximal tympanum diameter;  
**UEW** upper eyelid width (greatest width of the upper eyelid margins measured perpendicular to the anterior-posterior axis).

For the single tadpole of the undescribed species, eleven morphometric characters were measured:

- BH** maximum body height;  
**BW** maximum body width;  
**IOS** interocular distance (minimum distance between eye);  
**MW** mouth width (distance between two corners of mouth);  
**SL** snout length (distance from the tip of the snout to the anterior corner of the eye);  
**SS** snout to spiraculum (distance from spiraculum to the tip of the snout);  
**SVL** snout-vent length;  
**TAH** tail height (maximum height between upper and lower edges of tail);  
**TAL** tail length (distance from base of vent to the tip of tail);  
**TBW** maximum width of tail base;  
**TOL** total length (distance from the tip of the snout to the tip of tail).

To reduce the impact of allometry, the correct value from the ratio of each character to SVL was calculated, and then was log-transformed for the following morphometric analyses. Mann-Whitney *U* tests were conducted to test the significance of differences on morphometric characters between the undescribed species and *M. kuatunensis*. The significance level was set at 0.05. Furthermore, principal component analyses (PCA) were conducted to highlight whether the different species were separated in morphometric space.

The new species was also compared with all other *Megophrys* species on morphology. Comparative data were obtained for related species as described in literature (Table 2).

## Bioacoustics analyses

The advertisement calls of the undescribed species were recorded from the holotype specimen CIBQY20200726001 in the field on 26 July 2020 from Qingyuan County, Zhejiang Province, China. When registering the male in the stream the ambient air temperature was 21.5 °C and there was air humidity of 87%. For comparisons, the advertisement calls of *M. kuatunensis* from Wuyi Mountain, Fujian Province, China were recorded from the specimens CIBWY18082410, CIBWY18082411 and CIBWY18082412 at an ambient air temperature of 22.0 °C and air humidity of 88% on 24 August 2018. SONY PCM-D50 digital sound recorder was used to record within 20 cm of the calling individual. The sound files in wave format were resampled at 48 kHz with sampling depth 24 bits. The sonograms and waveforms were generated by WaveSurfer software (Sjöander and Beskow 2000) from which all parameters and characters were measured. Ambient temperature was taken by a digital hygrothermograph.

## Results

### Phylogenetic analyses

Aligned sequence matrix of 16S+COI contains 1104 bp. ML and BI trees of the mitochondrial DNA dataset presented almost consistent topology, and as well, though relationships of many clades were unresolved (Fig. 2). In mitochondrial DNA trees, all samples of the undescribed species were clustered into one clade which was deeply clustered into the *Megophrys* clade. The species is likely sister to *M. kuatunensis* (bootstrap supports < 50% and BPP = 0.51) though the relationships between the two species and most other congeners were not resolved (all bootstrap supports < 50% and many BPP < 0.95).

Genetic distances based on 16S and COI genes with uncorrected *p*-distance model between the samples of the undescribed species were all below 0.2%. The genetic distance between the undescribed species and its closest related species *M. kuatunensis* were 2.1% and 8.1% on 16S and COI respectively, which was higher or at the same level with those among many pairs of sister species, for example, 1.7% and 3.8% on 16S and COI respectively between *M. spinata* and *M. sangzhiensis* (Suppl. materials 2 and 3).

**Table 2.** References for morphological characters for congeners of the genus *Megophrys*.

Species	Literature obtained
<i>M. aceras</i> Boulenger, 1903	Boulenger 1903
<i>M. acuta</i> Wang, Li & Jin, 2014	Li et al. 2014
<i>M. anerae</i> Mahony, Teeling & Biju, 2013	Mahony et al. 2013
<i>M. angka</i> Wu, Suwannapoom, Poyarkov, Chen, Pawangkhanant, Xu, Jin, Murphy & Che, 2019	Wu et al. 2019
<i>M. auralensis</i> Ohler, Swan & Daltry, 2002	Ohler et al. 2002
<i>M. awub</i> Mahony, Kamei, Teeling, & Biju, 2020	Mahony et al. 2020
<i>M. baluensis</i> (Boulenger, 1899)	Boulenger 1899a
<i>M. baolongensis</i> Ye, Fei & Xie, 2007	Ye et al. 2007
<i>M. binchuanensis</i> Ye & Fei, 1995	Ye and Fei 1995
<i>M. binlingensis</i> Jiang, Fei & Ye, 2009	Fei et al. 2009
<i>M. boettgeri</i> (Boulenger, 1899)	Boulenger 1899b
<i>M. brachykolos</i> Inger & Romer, 1961	Inger and Romer 1961
<i>M. carinense</i> (Boulenger, 1889)	Boulenger 1889
<i>M. caobangensis</i> Nguyen, Pham, Nguyen, Luong, & Ziegler, 2020	Nguyen et al. 2020
<i>M. caudoprocta</i> Shen, 1994	Shen. 1994
<i>M. cheni</i> (Wang & Liu, 2014)	Wang et al. 2014
<i>M. chishuiensis</i> Xu, Li, Liu, Wei & Wang, 2020	Xu et al. 2020
<i>M. chuannanensis</i> (Fei, Ye & Huang, 2001)	Fei et al. 2001
<i>M. damrei</i> Mahony, 2011	Mahony 2011
<i>M. daweimontis</i> Rao & Yang, 1997	Rao and Yang 1997
<i>M. dongguanensis</i> Wang & Wang, 2019	Wang et al. 2019b
<i>M. dringi</i> Inger, Stuebing & Tan, 1995	Inger et al. 1995
<i>M. dzukou</i> Mahony, Kamei, Teeling & Biju, 2020	Mahony et al. 2020
<i>M. edwardinae</i> Inger, 1989	Inger 1989
<i>M. elfina</i> Poyarkov, Duong, Orlov, Gogoleva, Vassilieva, Nguyen, Nguyen, Nguyen, Che & Mahony, 2017	Poyarkov et al. 2017
<i>M. fansipanensis</i> Tapley, Cutajar, Mahony, Nguyen, Dau, Luong, Le, Nguyen, Nguyen, Portway, Luong & Rowley, 2018	Tapley et al. 2018
<i>M. feae</i> Boulenger, 1887	Boulenger 1887
<i>M. feii</i> Yang, Wang & Wang, 2018	Yang et al. 2018
<i>M. flavipunctata</i> Mahony, Kamei, Teeling & Biju, 2018	Mahony et al. 2018
<i>M. gerti</i> (Ohler, 2003)	Ohler 2003
<i>M. gigantica</i> Liu, Hu & Yang, 1960	Liu et al. 1960
<i>M. glandulosa</i> Fei, Ye & Huang, 1990	Fei et al. 1990
<i>M. hansii</i> (Ohler, 2003)	Ohler 2003
<i>M. himalayana</i> Mahony, Kamei, Teeling & Biju, 2018	Mahony et al. 2018
<i>M. hoanglienensis</i> Tapley, Cutajar, Mahony, Nguyen, Dau, Luong, Le, Nguyen, Nguyen, Portway, Luong & Rowley, 2018	Tapley et al. 2018
<i>M. huangshanensis</i> Fei & Ye, 2005	Fei and Ye 2005
<i>M. insularis</i> (Wang, Liu, Lyu, Zeng & Wang, 2017)	Wang et al. 2017a
<i>M. intermedia</i> Smith, 1921	Smith 1921
<i>M. jiangii</i> Liu, Li, Wei, Xu, Cheng, Wang & Wu, 2020	Liu et al. 2020
<i>M. jingdongensis</i> Fei & Ye, 1983	Fei et al. 1983
<i>M. jinggangensis</i> (Wang, 2012)	Wang et al. 2012
<i>M. julianensis</i> Wang, Zeng, Lyu & Wang, 2019	Wang et al. 2019b
<i>M. kalimantanensis</i> Munir, Hamidy, Matsui, Iskandar, Sidik & Shimada, 2019	Munir et al. 2019
<i>M. kobayashii</i> Malkmus & Matsui, 1997	Malkmus and Matsui 1997
<i>M. koui</i> Mahony, Foley, Biju & Teeling, 2017	Mahony et al. 2017
<i>M. kuatunensis</i> Pope, 1929	Pope 1929
<i>M. lancip</i> Munir, Hamidy, Farajallah & Smith, 2018	Munir et al. 2018
<i>M. leishanensis</i> Li, Xu, Liu, Jiang, Wei & Wang, 2018	Li et al. 2018
<i>M. lekaguli</i> Stuart, Chuaynkern, Chan-ard & Inger, 2006	Stuart et al. 2006
<i>M. liboensis</i> (Zhang, Li, Xiao, Li, Pan, Wang, Zhang & Zhou, 2017)	Zhang et al. 2017
<i>M. ligayae</i> Taylor, 1920	Taylor 1920

Species	Literature obtained
<i>M. lini</i> (Wang & Yang, 2014)	Wang et al. 2014
<i>M. lishuiensis</i> (Wang, Liu & Jiang, 2017)	Wang et al. 2017b
<i>M. longipes</i> Boulenger, 1886	Boulenger 1886
<i>M. major</i> Boulenger, 1908	Boulenger 1908
<i>M. mangshanensis</i> Fei & Ye, 1990	Fei et al. 2012
<i>M. maonensis</i> Bourret, 1937	Bourret 1937
<i>M. medogensis</i> Fei, Ye & Huang, 1983	Fei et al. 1983
<i>M. megacephala</i> Mahony, Sengupta, Kamei & Biju, 2011	Mahony et al. 2011
<i>M. microstoma</i> (Boulenger, 1903)	Boulenger 1903
<i>M. minor</i> Stejneger, 1926	Stejneger 1926
<i>M. mirabilis</i> Lyu, Wang & Zhao	Lyu et al. 2020
<i>M. montana</i> Kuhl & Van Hasselt, 1822	Kuhl and Van Hasselt 1822
<i>M. monticola</i> (Günther, 1864)	Günther 1864; Mahony et al. 2018
<i>M. mufumontana</i> Wang, Lyu & Wang, 2019	Wang et al. 2019b
<i>M. nankiangensis</i> Liu & Hu, 1966	Hu and Liu 1966
<i>M. nankunensis</i> Wang, Zeng & Wang, 2019	Wang et al. 2019b
<i>M. nanlingensis</i> Lyu, Wang, Liu & Wang, 2019	Wang et al. 2019b
<i>M. nasuta</i> (Schlegel, 1858)	Schlegel 1858
<i>M. numbumaeng</i> Mahony, Kamei, Teeling, & Biju, 2020	Mahony et al. 2020
<i>M. obesa</i> Wang, Li & Zhao, 2014	Wang et al. 2014
<i>M. ombrophila</i> Messenger & Dahn, 2019	Messenger et al. 2019
<i>M. omeimontis</i> Liu, 1950	Liu 1950
<i>M. oreocrypta</i> Mahony, Kamei, Teeling & Biju, 2018	Mahony et al. 2018
<i>M. oropedion</i> Mahony, Teeling & Biju, 2013	Mahony et al. 2013
<i>M. orientalis</i> Li, Lyu, Wang & Wang, 2020	Li et al. 2020
<i>M. pachyproctus</i> Huang, 1981	Huang and Fei 1981
<i>M. palpebralespinosa</i> Bourret, 1937	Bourret 1937
<i>M. parallela</i> Inger & Iskandar, 2005	Inger and Iskandar 2005
<i>M. parva</i> (Boulenger, 1893)	Boulenger 1893
<i>M. periosa</i> Mahony, Kamei, Teeling & Biju, 2018	Mahony et al. 2018
<i>M. popei</i> (Zhao, Yang, Chen, Chen & Wang, 2014)	Zhao et al. 2014
<i>M. robusta</i> Boulenger, 1908	Boulenger 1908
<i>M. rubrimera</i> Tapley, Cutajar, Mahony, Chung, Dau, Nguyen, Luong & Rowley, 2017	Tapley et al. 2017
<i>M. sangzhiensis</i> Jiang, Ye & Fei, 2008	Jiang et al. 2008
<i>M. serchhipii</i> (Mathew & Sen, 2007)	Mathew and Sen 2007
<i>M. shapingensis</i> Liu, 1950	Liu 1950
<i>M. shimentaina</i> Lyu, Liu & Wang	Lyu et al. 2020
<i>M. shuichengensis</i> Tian & Sun, 1995	Tian and Sun 1995
<i>M. shunhuangensis</i> Wang, Deng, Liu, Wu & Liu, 2019	Wang et al. 2019a
<i>M. spinata</i> Liu & Hu, 1973	Hu et al. 1973
<i>M. stejnegeri</i> Taylor, 1920	Taylor 1920
<i>M. synoria</i> (Stuart, Sok & Neang, 2006)	Stuart et al. 2006
<i>M. takensis</i> Mahony, 2011	Mahony 2011
<i>M. tuberogranulata</i> Shen, Mo & Li, 2010	Mo et al. 2012
<i>M. vegrandis</i> Mahony, Teeling, Biju, 2013	Mahony et al. 2013
<i>M. wawuensis</i> Fei, Jiang & Zheng, 2001	Fei et al. 2012
<i>M. wugongensis</i> Wang, Lyu & Wang, 2019	Wang et al. 2019b
<i>M. wuliangshanensis</i> Ye & Fei, 1995	Ye and Fei 1995
<i>M. wushanensis</i> Ye & Fei, 1995	Ye and Fei 1995
<i>M. xianjuensis</i> Wang, Wu, Peng, Shi, Lu & Wu, 2020	Wang et al. 2020
<i>M. xiangnanensis</i> Lyu, Zeng & Wang	Lyu et al. 2020
<i>M. yangmingensis</i> Lyu, Zeng & Wang	Lyu et al. 2020
<i>M. zhangii</i> Ye & Fei, 1992	Ye and Fei 1992
<i>M. zunhebotensis</i> (Mathew & Sen, 2007)	Mathew and Sen 2007

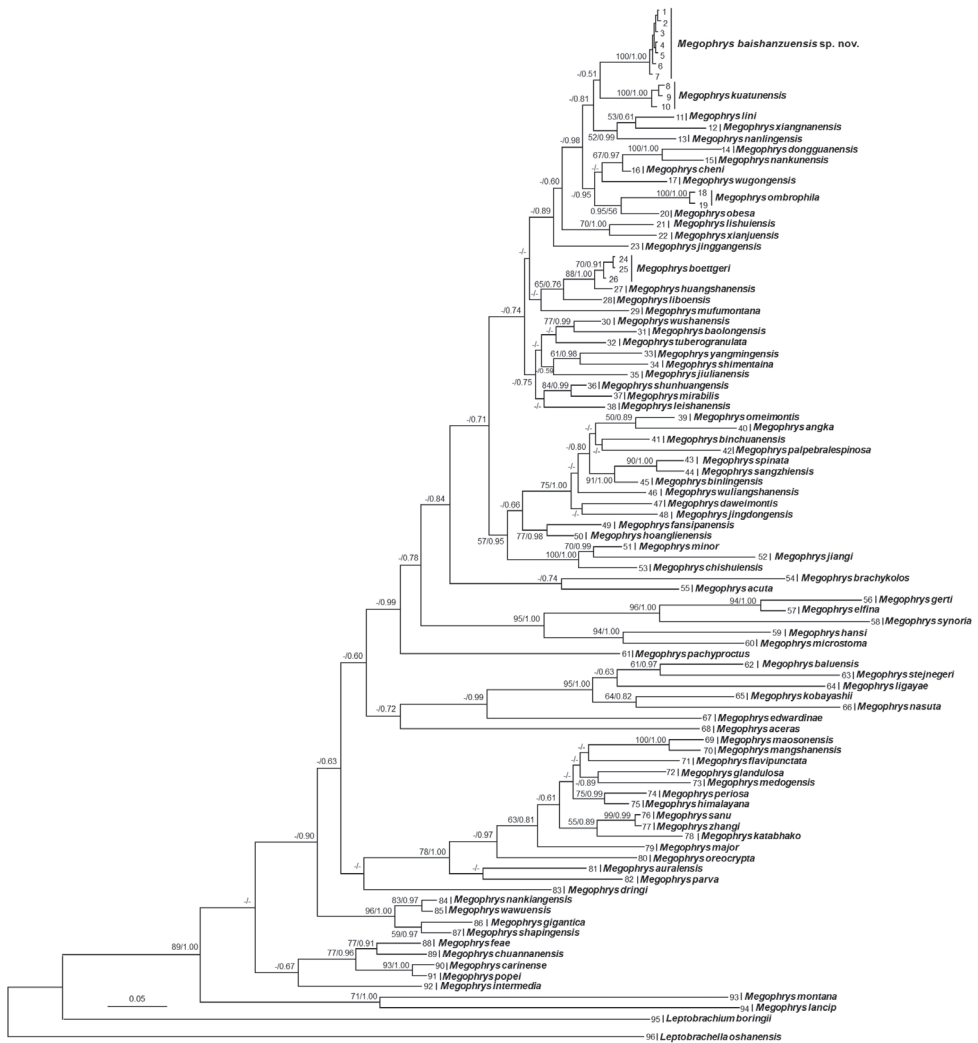


**Figure 2.** Maximum likelihood (ML) tree of the genus *Megophrys* reconstructed based on 16S rRNA and COI gene sequences. Bayesian posterior probability/ML bootstrap supports were denoted beside each node. Samples 1–96 refer to Table 1.

In PCA for male group, the total variation of the first two principal components was 47.5%. On the two-dimensional plots of PC1 vs. PC2, the undescribed species was almost separated from *M. kuatunensis* (Fig. 3). The first two principal component axes could separate *M. kuatunensis* from the undescribed species mainly based on limb and head characteristics, namely, HDL, HDW, IND, FIL, FIIL and FL. The results of Mann-Whitney *U* tests indicated that in males, the undescribed species was significantly different from *M. kuatunensis* on UEW and TFL (*p*-values < 0.05; Table 3).

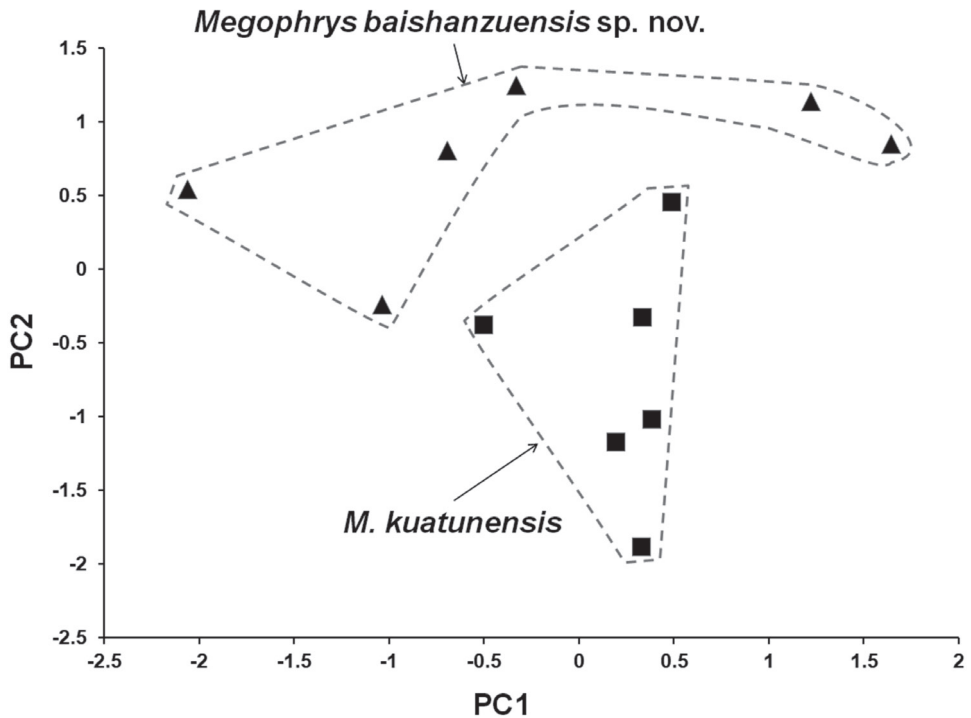


**Figure 3.** Plots of the first principal component (PC1) versus the second (PC2) for *Megophrys baishanzuensis* sp. nov. and *M. kuatunensis* from principal component analyses on male group.

There were two differences in sonograms and waveforms of calls between the undescribed species and *M. kuatunensis* (Fig. 4; Table 4). Firstly, the undescribed species had slower call repetition rate than the latter (0.79 call/s in the former vs. 1.18 call/s in the latter). Secondly, the undescribed species had lower dominant frequency (3.19–3.38 kHz in the former vs. 3.38–3.75 kHz in the latter).

Based on the molecular phylogenetic analyses, morphological comparisons (Supp. material 4), and bioacoustics differences, the specimens from Qiangyuan County, Zhejiang Province, China represent a new species which is described as follows.

### Taxonomic accounts

#### *Megophrys baishanzuensis* sp. nov.

<http://zoobank.org/563EBE4E-45FF-4956-AB3B-70467B2D338E>

Figs 4A, B, E, G, H, 5–8; Tables 1–4, Suppl. materials 1–4

**Holotype.** CIBQY20200726001 (Figs 4A, B, E, G, H, 5), adult male, from Baishanzu National Park, Qingyuan County, Zhejiang Province, China (27.76°N, 119.18°E, ca. 1537 m a.s.l.), collected by Bin Wang on 26 July 2020.

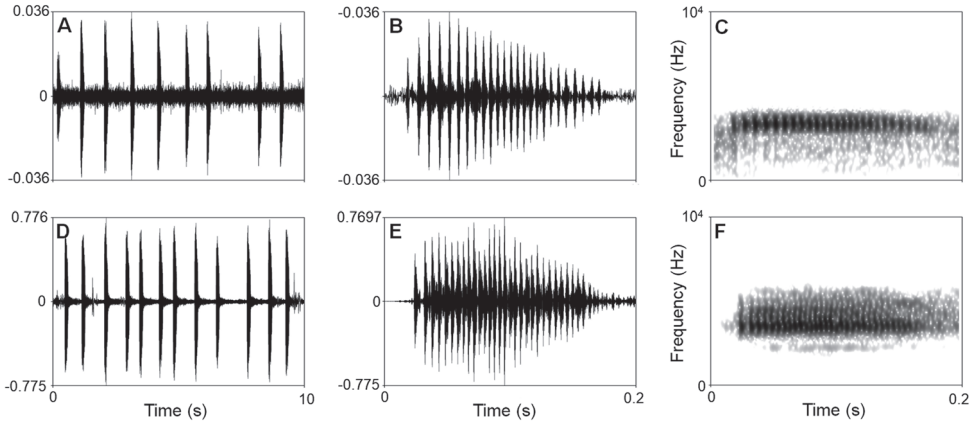


**Figure 4.** Visualization of advertisement calls of *Megophrys baishanzuensis* sp. nov. and *M. kuatunensis* **A–C** waveform showing 10 seconds, waveform showing 0.2 seconds and sonogram showing 0.2 seconds of CIBQY20200726001 of *Megophrys baishanzuensis* sp. nov. **D–F** waveform showing 10 seconds, waveform showing 0.2 seconds and sonogram showing 0.2 seconds of CIBWY18082410 of *M. kuatunensis*.

**Paratype.** Five adult males collected from the same place as holotype collected by Bin Wang. CIBQY20200719001–CIBQY20200719004 collected on 19 July 2020 by Bin Wang, and CIBQY20200726002 collected by Zhonghao Luo on 26 July 2020.

**Other material examined.** One tadpole (CIBQY20200719005; Fig. 7) collected by Bin Wang on 19 July 2020.

**Diagnosis.** *Megophrys baishanzuensis* sp. nov. is assigned to the genus *Megophrys* based on molecular phylogenetic analyses and the following generic diagnostic characters: snout shield-like; projecting beyond the lower jaw; canthus rostralis distinct; chest glands small and round, closer to the axilla than to midventral line; femoral glands on rear part of thigh; vertical pupils (Fei et al. 2009).

*Megophrys baishanzuensis* sp. nov. could be distinguished from its congeners by a combination of the following morphological characters: body size small (SVL 28.4–32.4 mm in males); vomerine teeth absent; tongue not notched behind; tympanum distinctly visible, oval; a small horn-like tubercle at the edge of each upper eyelid; two metacarpal tubercles distinctly visible in hand; toes without webbing; heels overlapping when thighs are positioned at right angles to the body; tibiotarsal articulation reaching the level to the middle of eye when leg stretched forward.

**Description of holotype.** (Figs 4A, B, E, G, H, 5). SVL 28.5 mm; head width larger than head length (HDW/HDL ratio ca. 1.3); snout obtusely pointed, protruding well beyond the margin of the lower jaw in ventral view; loreal region vertical and concave; canthus rostralis well-developed; top of head flat in dorsal view; eye large, eye diameter 46.0% of head length; pupils vertical; nostril orientated laterally, closer to snout than eye; tympanum distinct, 55.8% of eye diameter; vomerine ridges present and vomerine teeth absent; margin of tongue smooth, not notched behind.

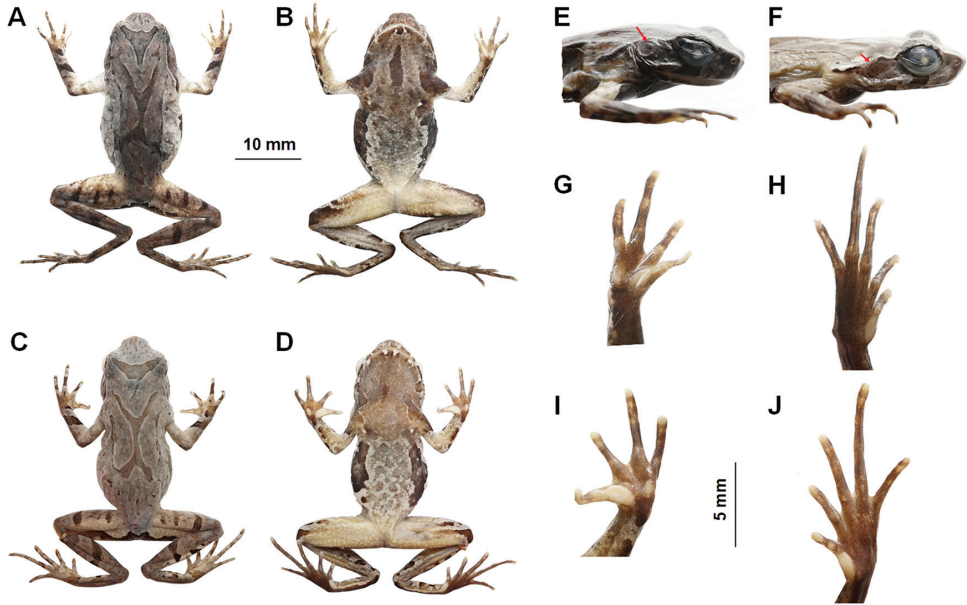


**Figure 5.** Photos of the holotype specimen CIBQY20200726001 of *Megophrys baishanzuensis* sp. nov. and topotype specimen of *M. kuatunensis* **A, B, E, G, H** dorsal view of body, ventral view of body, lateral view of head, ventral view of hand, and ventral view of foot of CIBQY20200726001, respectively **C, D, F, I, J** dorsal view of body, ventral view of body, lateral view of head, ventral view of hand, and ventral view of foot of CIBWY18082413, respectively. Red arrow points to tympanum.

Forelimbs slender, the length of lower arm and hand 47.0% of SVL; fingers slender, relative finger lengths: I < II < IV < III; tips of digits globular, without lateral fringes; subarticular tubercle distinct at the base of each finger; two metacarpal tubercles, prominent, oval-shaped, the inner one bigger than the outer one.

Hindlimbs slender, tibia length 46.5% times of SVL; heels overlapping when thighs are positioned at right angles to the body, tibiotarsal articulation reaching the middle of eye when leg stretched forward; tibia length longer than thigh length; relative toe lengths I < II < V < III < IV; tips of toes round, slightly dilated; subarticular tubercles absent on each toes; toes without webbing but with narrow lateral fringe; inner metatarsal tubercle oval-shaped; outer metatarsal tubercle absent.

Dorsal skin rough, several large warts scattered on flanks; a small horn-like tubercle at the edge of each upper eyelid; tubercles on the dorsum forming a X-shaped ridge, two dorsolateral parallel ridges on either side of the X-shaped ridges; an inverted triangular brown speckle between two upper eyelids; several tubercles scattered on dorsal, flanks and dorsal surface of thighs and tibiae; supratympanic fold distinct.

Numerous granules scattered on ventrum; pectoral and femoral glands distinct; numerous white granules on outer thighs.

**Coloration of holotype in life.** (Fig. 5). Dorsal brown, several pink tubercles scattered on dorsal, an inverted triangular brown speckle between the eyes; X-shaped ridges

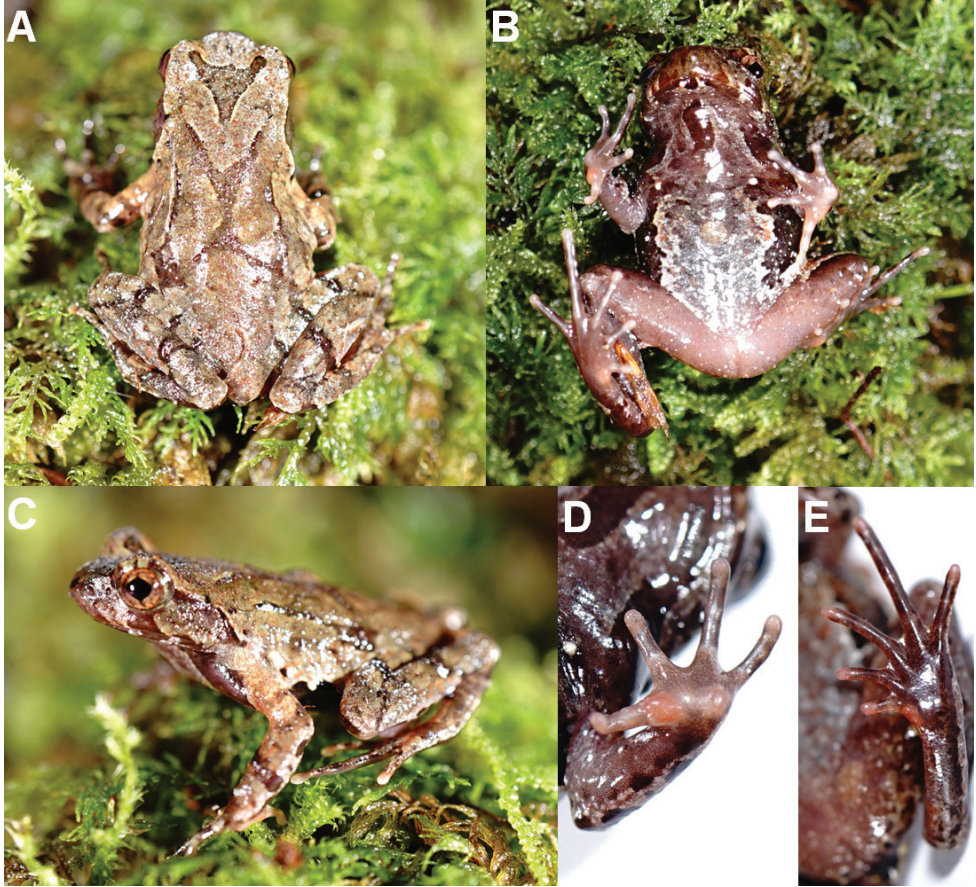


**Figure 6.** Photos of the holotype CIBQY20200726001 of *Megophrys baishanzuensis* sp. nov. in life **A** dorsal view **B** ventral view **C** lateral view **D** ventral view of hand **E** ventral view of foot.

on the dorsum brown, four dark transverse bands on the dorsal surface of the thigh and shank; ventral surface of body white with brown spots; two dark brown dark bars on the flanks, throat brown; white vertical bars on lower and upper lip; ventral surface of anterior limb dark reddish purple, posterior limb orange with numerous white granules; tip of digits pale grey; inner metatarsal tubercle and two metacarpal tubercles pinkish; soles uniform dark reddish purple; pectoral glands white.

**Coloration of holotype in preservation.** (Fig. 4A, B, E, G, H). Color of dorsal surface fades to taupe; the inverted triangular brown speckle between the eyes and brown X-shaped ridges on dorsum are more distinct; ventral surface greyish white; creamy-white substitutes the purple grey on tip of digits; the posterior of ventral surface of body, inner of thigh and upper of tibia fades to creamy-white.

**Variation.** Fig. 6. Measurements and basic statistics of adult specimens are presented in Tables 3 and Supp. material 1. All specimens were similar in morphology but some individuals different from the holotype in color pattern. In CIBQY2020200719001

**Table 3.** Morphometric comparisons between the adult specimens of *Megophrys baishanzuensis* sp. nov. and *M. kuatunensis*. Units given in mm. See abbreviations for the morphological characters in Materials and methods section. P-value resulted from Mann-Whitney *U* test. Significant level at 0.05.

Character	<i>Megophrys baishanzuensis</i> sp. nov.		<i>M. kuatunensis</i>		Mann-Whitney U value	P-value
	Male (N = 6)		Male (N = 6)			
	Ranging	Mean ± SD	Ranging	Mean ± SD		
SVL	28.4–32.4	30.5 ± 1.8	28.4–32.4	30.5 ± 1.8	13.000	0.423
HDL	8.0–9.1	8.6 ± 0.4	8.0–9.1	8.6 ± 0.4	6.000	0.055
HDW	9.3–10.5	10.2 ± 0.4	9.3–10.5	10.2 ± 0.4	8.000	0.109
SL	3.4–4.1	3.8 ± 0.3	3.4–4.1	3.8 ± 0.3	16.000	0.749
SNT	1.5–2.6	2.0 ± 0.4	1.5–2.6	2.0 ± 0.4	18.000	1.000
IND	3.1–3.7	3.4 ± 0.3	3.1–3.7	3.48 ± 0.3	16.000	0.749
IOD	2.8–3.3	3.0 ± 0.2	2.8–3.3	3.08 ± 0.2	6.000	0.055
UEW	2.3–3.0	2.6 ± 0.2	2.3–3.0	2.6 ± 0.2	2.000	<b>0.010</b>
ED	3.7–4.0	3.8 ± 0.1	3.7–4.0	3.8 ± 0.1	15.000	0.631
TYD	1.5–2.1	1.8 ± 0.2	1.5–2.1	1.8 ± 0.2	16.000	0.749
LAL	13.4–14.6	14.1 ± 0.5	13.4–14.6	14.2 ± 0.5	9.000	0.150
HAL	6.6–7.9	7.1 ± 0.5	6.6–7.9	7.1 ± 0.5	6.000	0.055
LW	2.2–2.7	2.4 ± 0.2	2.2–2.7	2.4 ± 0.2	10.000	0.200
FIL	2.2–2.8	2.5 ± 0.2	2.2–2.8	2.5 ± 0.2	17.000	0.873
FIIL	2.4–3.0	2.7 ± 0.2	2.4–3.0	2.7 ± 0.2	12.000	0.200
FIIL	4.3–5.1	4.6 ± 0.3	4.3–5.1	4.6 ± 0.3	10.000	0.200
FIVL	2.6–3.6	3.0 ± 0.4	2.6–3.6	3.0 ± 0.4	15.000	0.631
THL	12.2–13.5	12.9 ± 0.5	12.2–13.5	12.9 ± 0.5	10.000	0.200
TL	12.8–14.9	13.9 ± 0.9	12.8–14.9	13.9 ± 0.9	13.000	0.423
TW	2.7–4.2	3.3 ± 0.5	2.7–4.2	3.3 ± 0.5	13.000	0.423
TFL	17.8–20.4	19.4 ± 1.0	17.8–20.4	19.4 ± 1.0	1.000	<b>0.006</b>
FL	11.2–12.3	11.8 ± 0.4	11.2–12.3	11.8 ± 0.4	13.000	0.423

the tubercles on the dorsum forming two > shaped, disconnected ridges (Fig. 6A); in CIBQY2020200719004 the tubercles on the dorsum forming a big and distinct X-shaped speckle (Fig. 6B); in CIBQY2020200719003 ventral surface of body grey with brown spots (Fig. 6C); in CIBQY2020200726002 ventral surface of body and limbs brownish red (Fig. 6D).

**Tadpole description.** Fig. 7. The tadpole CIBQY20200719006 (Fig. 7) was confirmed as *Megophrys baishanzuensis* sp. nov by molecular phylogenetic analyses. Measurements in mm. Stage 31. Body slender, body brownish black and tail pale brown, body height greater than tail height; dorsal fin arising behind the origin of the tail, the highest fin near mid-length, tapering gradually to the narrowly pointed tip; tail approximately 1.9 times as long as snout-vent length; tail height 13.6% of tail length; body width longer than body height (BW/BH1.2); eyes large, lateral, nostril near eyes; spiracle on the left side of the body and distinct; oral disk terminal, lips expanded and directed upwardly into a umbelliform oral disk; flank of body brownish black with some white spots, tail fins lightly colored, with small white and black spots. TOL 22.7; SVL 8.7; BW 3.0; BH 2.7; SL 2.0; SS 4.0; IOS 1.8; TAL 14.7; TAH 2.2; TBD 1.5; MW 1.3.

**Advertisement call.** Fig. 4. The call description is based on recordings of the holotype CIBQY20200726001 (Fig. 4; Table 4) from a shrub leaf near the streamlet.

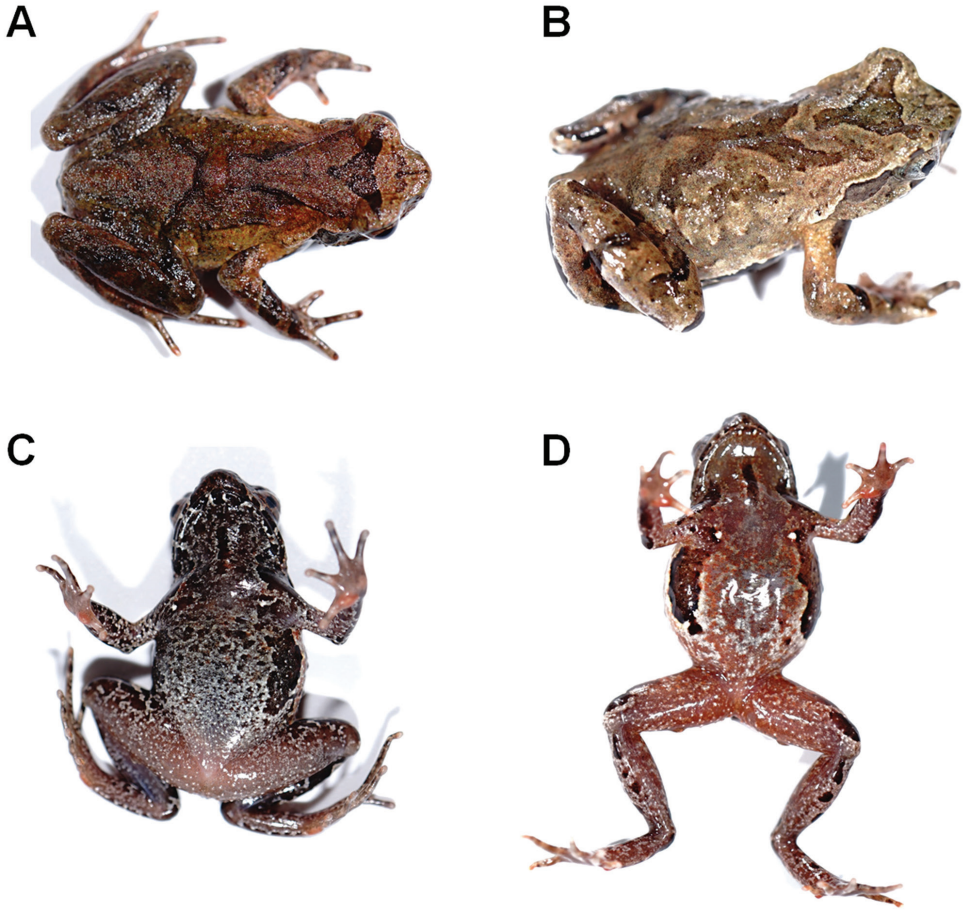


**Figure 7.** Color variation in *Megophrys baishanzuensis* sp. nov. in life **A** dorsal view of the adult male CIBQY2020200719001 **B** dorsal view of the adult male CIBQY2020200719004 **C** ventral view of the adult male CIBQY2020200719003 **D** ventral view of the adult male CIBQY2020200726002.

Call duration was 151.0–170.0 ms (mean  $162.4 \pm 5.7$ ). Inter-call interval was 682.0–1869.0 ms (mean  $936.8 \pm 349.0$ ). Pulse/call was 23.0–30.0 (mean  $26.0 \pm 2.4$ ); pulse duration was 3.0–6.0 (mean  $4.9 \pm 6.0$ ) and call repetition rate was 0.79 call/s.

Amplitude modulation within note was apparent, beginning with moderately high energy pulses, increasing to the maximum by approximately quarter, and then decreasing towards the end. The average dominant frequency was  $3.36 \pm 0.06$  (3.19–3.38 kHz).

**Secondary sexual characters.** A single subgular vocal sac present in male. In breeding season, nuptial pads are present on the dorsal base of the first two fingers in males.

**Comparisons.** Supp. material 4. By having small body size, *Megophrys baishanzuensis* sp. nov. differs from *M. ancræ*, *M. auralensis*, *M. awuh*, *M. baluensis*, *M. baolongensis*, *M. binlingensis*, *M. boettgeri*, *M. caobangensis*, *M. carinense*, *M. caudoprocta*, *M. chishuiensis*, *M. chuannanensis*, *M. damrei*, *M. daweimontis*, *M. dzukou*, *M. edwardinae*,

**Table 4.** Comparisons of characteristics of advertisement calls of *Megophrys baishanzuensis* sp. nov. and *M. kuatunensis*.

Call character	<i>Megophrys baishanzuensis</i> sp. nov.	<i>M. kuatunensis</i>		
	CIBQY20200726001	CIBWY2018082410	CIBWY2018082412	WY2018082411
Number of call groups measured	11	30	30	20
Number of notes measured	22	30	30	40
Call duration (ms)	151.0–170.0 (162.4 ± 5.7)	131.0–163.0 (147.2 ± 7.1)	131.0–163.0 (147.2 ± 7.1)	130.0–159.0 (120.9 ± 5.9)
Call repetition rate (calls/s)	0.79	1.18	1.13	1.3
Intercall interval (ms)	682.0–1869.0 (936.8 ± 349.0)	404–1548.0 (687.3 ± 206.8)	404–1548.0 (687.3 ± 206.8)	350.0–733.0 (458.4 ± 87.1)
Pulses/call	23.0–30.0 (26.0 ± 2.4)	25.0–36.0 (30.0 ± 2.3)	25.0–36.0 (30.0 ± 2.3)	32.0–40.4 (35.7 ± 2.3)
Dominant frequency (kHz)	3.19–3.38 (3.36 ± 0.06)	3.38–3.75 (3.46 ± 0.16)	3.38–3.75 (3.46 ± 0.16)	3.38–3.38 (3.38 ± 0.01)
Pulse duration (ms)	3.0–6.0 (4.9 ± 0.6)	3.0–6.0 (4.4 ± 0.7)	3.0–6.0 (4.4 ± 0.7)	3.0–6.0 (4.5 ± 0.6)

*M. feae*, *M. flavipunctata*, *M. gigantea*, *M. glandulosa*, *M. hanshi*, *M. himalayana*, *M. hoanglienensis*, *M. huangshanensis*, *M. insularis*, *M. jiangi*, *M. jingdongensis*, *M. jinggangensis*, *M. kalimantanensis*, *M. kobayashii*, *M. lancip*, *M. lekaguli*, *M. liboensis*, *M. ligayae*, *M. lini*, *M. longipes*, *M. major*, *M. mangshanensis*, *M. medogensis*, *M. megacephala*, *M. mirabilis*, *M. montana*, *M. monticola*, *M. nasuta*, *M. obesa*, *M. omeimontis*, *M. orientalis*, *M. pachyproctus*, *M. palpebralespinosa*, *M. parallela*, *M. parva*, *M. periosa*, *M. platyparietus*, *M. popei*, *M. sangzhiensis*, *M. serchhipii*, *M. shapingensis*, *M. shuichengensis*, *M. spinata*, *M. takensis*, *M. wawuensis*, and *M. xiangnanensis* (maximum SVL < 33.0 mm in the new species vs. minimum SVL > 34.0 mm in the latter).

By vomerine teeth absent, *Megophrys baishanzuensis* sp. nov. differs from *M. anerae*, *M. baluensis*, *M. carinense*, *M. caudoprocta*, *M. chuannanensis*, *M. damrei*, *M. daweimontis*, *M. dongguanensis*, *M. dzukou*, *M. fansipanensis*, *M. feae*, *M. flavipunctata*, *M. glandulosa*, *M. himalayana*, *M. hoanglienensis*, *M. insularis*, *M. intermedia*, *M. jingdongensis*, *M. jinggangensis*, *M. jiulianensis*, *M. kalimantanensis*, *M. kobayashii*, *M. lancip*, *M. lekaguli*, *M. liboensis*, *M. ligayae*, *M. longipes*, *M. mangshanensis*, *M. maosonensis*, *M. medogensis*, *M. megacephala*, *M. montana*, *M. nankunensis*, *M. nanlingensis*, *M. nasuta*, *M. numhumaeng*, *M. omeimontis*, *M. oreocrypta*, *M. orientalis*, *M. oropedion*, *M. pachyproctus*, *M. palpebralespinosa*, *M. parallela*, *M. parva*, *M. periosa*, *M. platyparietus*, *M. popei*, *M. robusta*, *M. rubrimera*, *M. serchhipii*, *M. shimentaina*, *M. stejneri*, *M. takensis*, *M. zhangii*, and *M. zunhebotensis* (vs. present in the latter).

By a small horn-like tubercle present at the edge of each upper eyelid, *Megophrys baishanzuensis* sp. nov. differs from *M. aceras*, *M. acuta*, *M. carinense*, *M. caudoprocta*, *M. chuannanensis*, *M. feae*, *M. gerti*, *M. hanshi*, *M. intermedia*, *M. intermedia*, *M. jinggangensis*, *M. kalimantanensis*, *M. kouii*, *M. lancip*, *M. liboensis*, *M. microstoma*, *M. montana*, *M. nasuta*, *M. orientalis*, *M. palpebralespinosa*, *M. platyparietus*, *M. popei*, *M. shuichengensis*, *M. stejneri*, and *M. synoria* (vs. having a prominent and elongated tubercle in the latter).

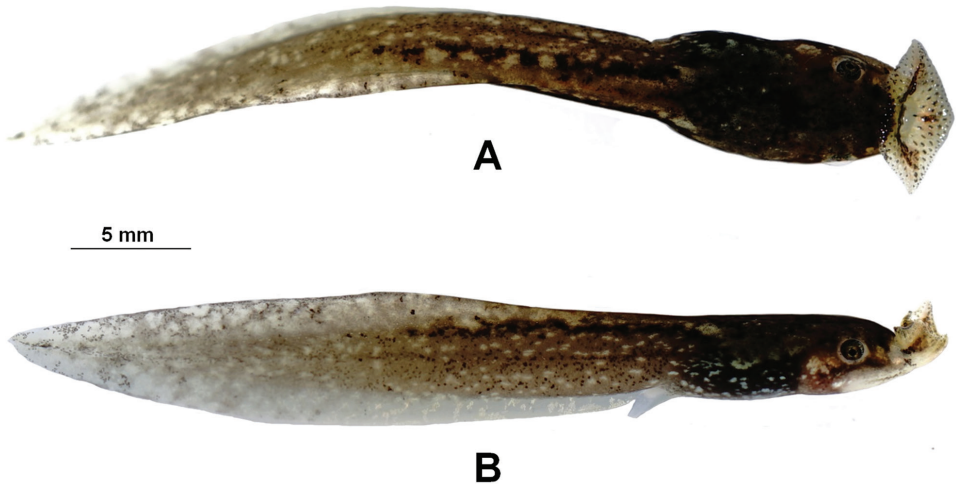


**Figure 8.** Photos of the tadpole CIBQY20200719006 of *Megophrys baishanzuensis* sp. nov. in life **A** dorsal view **B** lateral view.

By tongue not notched behind, *Megophrys baishanzuensis* sp. nov. differs from *M. ancræ*, *M. baolongensis*, *M. binlingensis*, *M. boettgeri*, *M. carinense*, *M. cheni*, *M. chuannanensis*, *M. damrei*, *M. dringi*, *M. dzukou*, *M. fansipanensis*, *M. feae*, *M. feii*, *M. flavipunctata*, *M. gerti*, *M. glandulosa*, *M. hoanglienensis*, *M. huangshanensis*, *M. insularis*, *M. jiulianensis*, *M. jingdongensis*, *M. kalimantanensis*, *M. kuatunensis*, *M. liboensis*, *M. mangshanensis*, *M. maosonensis*, *M. medogensis*, *M. minor*, *M. nankiangensis*, *M. nanlingensis*, *M. numhbumaeng*, *M. omeimontis*, *M. oropedion*, *M. pachyproctus*, *M. parallela*, *M. popei*, *M. robusta*, *M. sangzhiensis*, *M. shapingensis*, *M. shuichengensis*, *M. spinata*, *M. vegrandis*, *M. wawuensis*, *M. zhang*, and *M. zunhebotoensis* (vs. notched behind in the latter).

By toes with narrow lateral fringes, *Megophrys baishanzuensis* sp. nov. differs from *M. angka*, *M. baolongensis*, *M. brachykolos*, *M. caobangensis*, *M. chishuiensis*, *M. damrei*, *M. daweimontis*, *M. dongguanensis*, *M. fansipanensis*, *M. feae*, *M. himalayana*, *M. hoanglienensis*, *M. huangshanensis*, *M. insularis*, *M. jiangi*, *M. jiulianensis*, *M. kalimantanensis*, *M. kou*, *M. leishanensis*, *M. lekaguli*, *M. lishuiensis*, *M. major*, *M. mangshanensis*, *M. medogensis*, *M. megacephala*, *M. microstoma*, *M. minor*, *M. nankunensis*, *M. obesa*, *M. ombrophila*, *M. oreocrypta*, *M. oropedion*, *M. pachyproctus*, *M. parva*, *M. periosa*, *M. shunhuangensis*, *M. takensis*, *M. tubero granulata*, *M. wawuensis*, *M. wugongensis*, *M. wuliangshanensis* and *M. xianjuensis* (vs. lacking in the latter); and differs from *M. binchuanensis*, *M. boettgeri*, *M. carinense*, *M. cheni*, *M. chuannanensis*, *M. dringi*, *M. feii*, *M. gigantea*, *M. glandulosa*, *M. intermedia*, *M. jingdongensis*, *M. liboensis*, *M. lini*, *M. orientalis*, *M. palpebralespinosa*, *M. platyparietus*, *M. shapingensis*, *M. shuichengensis*, *M. spinata*, and *M. xiangnanensis* (vs. with wide lateral fringes in the latter).

By toes without webbing, *Megophrys baishanzuensis* sp. nov. differs from *M. brachykolos*, *M. carinense*, *M. flavipunctata*, *M. jingdongensis*, *M. jinggangensis*, *M. lini*,

*M. major*, *M. palpebralespinosa*, *M. popei*, *M. shuichengensis*, and *M. spinata* (vs. at least one-fourth webbed in the latter).

By heels overlapping when thighs are positioned at right angles to the body, *Megophrys baishanzuensis* sp. nov. differs from *M. actuta*, *M. brachykolos*, *M. dongguanensis*, *M. huangshanensis*, *M. kuatunensis*, *M. nankunensis*, *M. obesa*, *M. ombrophila*, *M. wushanensis*, and *M. wugongensis* (vs. just meeting or not meeting in the latter).

By tibiotarsal articulation reaching to the level to the middle of eye when leg stretched forward, *Megophrys baishanzuensis* sp. nov. differs from *M. daweimontis*, *M. glandulosa*, *M. lini*, *M. major*, *M. medogensis*, *M. obesa*, *M. sangzhiensis*, and *M. yangmingensis* (vs. reaching the anterior corner of the eye or beyond eye or nostril and tip of snout in the latter); differs from *M. mufumontana* (vs. reaching tympanum in males and to the eye in females in the latter); and differs from *M. chishuiensis* (vs. reaching the level between tympanum and eye in the latter).

By having an internal single subgular vocal sac in male, *Megophrys baishanzuensis* sp. nov. differs from *M. caudoprocta*, *M. shapingensis*, and *M. shuichengensis* (vs. vocal sac absent in the latter).

The congeners *M. boettgeri*, *M. lishuiensis*, *M. ombrophila*, and *M. xianjuensis* all occur in Wuyi Mountains, Fujian Province and/or Zhejiang Province, China, and probably have sympatric distribution with *Megophrys baishanzuensis* sp. nov. (Fei et al. 2012; Wang et al. 2017b; Messenger et al. 2019; Wang et al. 2020). The new species can be distinguished from these species by a series of morphological characters as follows. The new species differs from *M. boettgeri* by body size smaller (adult males with 28.4–32.4 mm vs. adult males with 34.5–37.8 mm), and in breeding male nuptial pads present on the dorsal base of the first two fingers (vs. nuptial pad only on the first finger). The new species differs from *M. lishuiensis* by vomerine ridges present (vs. absent), toes with narrow lateral fringe (vs. without), and tibiotarsal articulation reaching the middle of eye when leg stretched forward (vs. reaching the range from tympanum to eye). The new species differs from *M. ombrophila* by heels overlapping when thighs are positioned at right angles to the body (vs. not meeting), vomerine ridges present (vs. absent), and toes with narrow lateral fringe (vs. without). The new species differs from *M. xianjuensis* by tibiotarsal articulation reaching the middle of eye when leg stretched forward (vs. reaching the range from tympanum to eye), and toes with narrow lateral fringe (vs. without).

*Megophrys baishanzuensis* sp. nov. is phylogenetically closest to *M. kuatunensis*. *Megophrys baishanzuensis* sp. nov. could be identified from *M. kuatunensis* distinctly by tibiotarsal articulation reaching the middle of eye when leg stretched forward (vs. reaching the range from tympanum to eye), heels overlapping when thighs are positioned at right angles to the body (vs. not meeting), tongue not notched behind (vs. notched feebly), the supratympanic fold more expanded in dorsal view and tympanum protruding (vs. concave), and having significantly lower ratios of UEW and TFL to SVL in males (all  $p$ -values < 0.05; Table 3). On call characters, the new species has slower call repetition rate (0.79 call/s in the new species vs. 1.18 call/s in *M. kuatunensis*), and has lower dominant frequency (3.19–3.38 kHz in the new species vs. 3.38–3.75 kHz in *M. kuatunensis*).



**Figure 9.** Habitats of *Megophrys baishanzuensis* sp. nov. in the type locality, Baishanzu National Park, Qingyuan County, Zhejiang Province, China **A** landscape for forest **B** the stream under the forest inhabited by *Megophrys baishanzuensis* sp. nov.

**Distribution and habitat.** *Megophrys baishanzuensis* sp. nov. is known from the type locality, Baishanzu National Park, Qingyuan County Zhejiang Province, China, at elevations between 1400–1600 m. The individuals of the new species were frequently found in the stream surrounded by evergreen broadleaved forests (Fig. 9). *M. boettgeri* was also found in the same stream.

**Etymology.** The specific name *baishanzuensis* refers to the distribution of this species, Baishanzu National Park, Qingyuan County, Zhejiang Province, China. We propose the common name “Baishanzu horned toad” (English) and Bai Shan Zu Jiao Chan (百山祖角蟾, Chinese).

## Discussion

Although *Megophrys baishanzuensis* sp. nov. superficially resembles *M. kuatunensis*, molecular phylogenetic analyses, detailed morphological comparisons and call datas all proposed the distinct differences between them. Moreover, the breeding seasons of them are different. According to our surveys, the breeding season of *M. kuatunensis* is in April to May in Wuyi Mountain, Fujian Province, China. But in this season, we did not find any individual of *Megophrys baishanzuensis* sp. nov. in Qingyuan County,

Zhejiang Province, China. And, the breeding season of the new species should be later than June because in June, we only listened to the calls of one male in the type locality ( $< 10\text{ }^{\circ}\text{C}$ ), and, in late July, the males of the species started to call when the temperature was just higher than  $18\text{ }^{\circ}\text{C}$  (but we did not find any female individual and egg of it). Different call characteristics and breeding ecology most probably promoted separation of the two species.

During our several and extensive surveys, we only found fewer than 15 adult males of *Megalophrys baishanzuensis* sp. nov., only in a small stream near the top of the mountain in Baishanzu National Park, Zhejiang Province, China, and even then, we did not find any female, and only found four tadpoles of this species. Obviously, the population of the new species is very endemic and small. Fortunately, this population is in a preserved area in Baishanzu National Park. Of course, we still should make a reinforced plan to preserve this area for this toad species.

## Acknowledgements

We thank Zhonghao Luo, Yang Li and Shengchao Shi for their help with collecting samples and data. This work was supported by the Biodiversity Survey Project of Lishui, Zhejiang Province and the Project supported by the Biodiversity investigation, Observation and Assessment Program (2019–2023) of Ministry of Ecology and Environment of China.

## References

- Boulenger GA (1886) Description of a new frog of the genus *Megalophrys*. Proceedings of the Zoological Society of London 1885: 850–850. <https://doi.org/10.1111/j.1096-3642.1885.tb02927.x>
- Boulenger GA (1887) Description of a new frog of the genus *Megalophrys*. Annali del Museo Civico di Storia Naturale di Genova Serie 2, 4: 512–513.
- Boulenger GA (1889) Description of a new batrachian of the genus *Leptobrachium*, obtain by M. L. Burma. Annali del Museo Civico di Storia Naturale di Genova. Serie 2, 7: 748–750.
- Boulenger GA (1893) Descriptions of three new batrachians from Tonkin. Annals and Magazine of Natural History, Series 7 12: 186–188. <https://doi.org/10.1080/00222930308678835>
- Boulenger GA (1899a) Descriptions of three new reptiles and a new batrachian from Mount Kina Balu, North Borneo. Annals and Magazine of Natural History, Series 7(4):1–453. <https://doi.org/10.1080/00222939908678228>
- Boulenger GA (1899b) On a collection of reptiles and batrachians made by Mr. J. D. La Touche in N.W. Fokien, China. Proceedings of the Zoological Society of London 1899: 159–172.
- Boulenger GA (1903) Report on the batrachians and reptiles. In: N Annandale and HCRobinson (Eds) Fasciculi Malayenses. Anthropological and Zoological Results of an Expedition to Perak and the Siamese Malay States 1901–1903 undertaken by Nelson Annandale and

- Herbert C. Robinson under the auspices of the University of Edinburgh and the University of Liverpool. Volume 2, Zoology, Part 1, 131–176.
- Boulenger GA (1908) A revision of the oriental pelobatid batrachians (genus *Megophrys*). Proceedings of the Zoological Society of London 78(2): 407–430. <https://doi.org/10.1111/j.1096-3642.1908.tb01852.x>
- Bourret R (1937) Notes herpétologiques sur l'Indochine française. XIV. Les batraciens de la collection du Laboratoire des Sciences Naturelles de l'Université. Descriptions de quinze especes ou variétés nouvelles. Annexe au Bulletin Général de l'Instruction Publique Hanoi, 1937: 5–56.
- Che J, Chen HM, Yang JX, Jin JQ, Jiang K, Yuan ZY, Murphy RW, Zhang YP (2012) Universal COI primers for DNA barcoding amphibians. Molecular Ecology Resource 12: 247–258. <https://doi.org/10.1111/j.1755-0998.2011.03090.x>
- Chen JM, Zhou WW, Nikolay A, Poyarkov Jr NA, Stuart BL, Brown RM, Lathrop A, Wang YY, Yuan ZL, Jiang K, Hou M, Chen HM, Suwannapoom C, Nguyen SN, Duong TV, Papenfuss TJ, Murphy RW, Zhang YP, Che J (2017) A novel multilocus phylogenetic estimation reveals unrecognized diversity in Asia toads, genus *Megophrys* sensu lato (Anura: Megophryidae). Molecular Phylogenetics and Evolution 106: 28–43. <https://doi.org/10.1016/j.ympev.2016.09.004>
- Delorme M, Dubois A, Grosjean S, Ohler A (2006) Une nouvelle ergotaxinomie des Megophryidae (Amphibia, Anura). Alytes 24: 6–21.
- Deuti K, Grosjean S, Nicolas V, Vasudevan K, Ohler A (2017) Nomenclatural puzzle in early *Megophrys nomina* (Anura, Megophryidae) solved with description of two new species from India (Darjeeling hills and Sikkim). Alytes 34: 20–48.
- Dubois A (1987) Miscellanea taxinomica batrachologica (I). Alytes 1987[1986]: 7–95.
- Fei L, Hu SQ, Ye CY, Huang YZ (2009) Fauna Sinica. Amphibia. Volume 2. Anura. Science Press, Beijing, 328–481. [In Chinese]
- Fei L, Ye CY, Huang YZ (1983) Two new subspecies of *Megophrys omeimontis* Liu from China (Amphibia, Pelobatidae). Acta Herpetologica Sinica. New Series, Chengdu 2(2): 49–52. [In Chinese with English abstract]
- Fei L, Ye CY, Huang YZ (1990) Key to Chinese Amphibians. Publishing House for Scientific and Technological, Chongqing, 108–110. [In Chinese]
- Fei L, Ye CY, Huang YZ (2001) Colour Handbook Amph. Sichuan, Science Press, Beijing, 138–139. [In Chinese]
- Fei L, Ye CY (2005) Two new species of Megophryidae from China. In: Fei L (Ed.) The Key and Illustration of Chinese. Sichuan Publishing House of Science and Technology, Chongqing, 253–255. [In Chinese]
- Fei L, Ye CY, Jiang JP (2012) Colored atlas of Chinese Amphibians and their distributions. Sichuan Publishing House of Science and Technology, Chengdu, 135–247. [In Chinese]
- Fei L, Ye CY (2016) Genus *Liophrys* Fei, Ye and Jiang, new genus; Subgenus *Atympanophrys* (*Borealophrys*) Fei, Ye and Jiang, new subgenus; Subgenus *Atympanophrys* (*Gigantophrys*) Fei, Ye and Jiang, new subgenus; Genus *Boulenophrys* Fei, Ye and Jiang, 2016, new genus; Subgenus *Xenophrys* (*Tianophrys*) Fei, Ye and Jiang, new subgenus. In: Fei L, Ye CY (Eds) Amphibians of China. Volume (I). Science Press, Beijing, 611–735.

- Frost DR (2020) Amphibian Species of the World: an Online Reference. Version 6.0. Electronic Database. American Museum of Natural History, New York. <http://research.amnh.org/herpetology/amphibia/index.html> [Accessed on 12 Sep 2020]
- Günther ACLG (1864) The reptiles of British India. Ray Society, London, 414–415.
- Guindon S, Dufayard JF, Lefort V, Anisimova M, Hordijk W, Gascuel O (2010) New algorithms and methods to estimate maximum-likelihood phylogenies: assessing the performance of PhyML 3.0. *Systematic Biology* 59(3): 07–321. <https://doi.org/10.1093/sysbio/syq010>
- Hall TA (1999) BIOEDIT: a user-friendly biological sequence alignment editor and analysis program for Windows 95/98/NT. *Nucleic Acids Symposium Series* 41(41): 95–98.
- Hu SX, Zhao EM, Liu CZ (1966) A herpetological survey of the Tsinling and Ta-pa shan region. *Acta Zoologica Sinica* 18(1): 57–89.
- Hu SX, Zhao EM, Liu CZ (1973) A survey of amphibians and reptiles in Kweichow province, including a herpetofauna analysis. *Acta Zoologica Sinica* 19(2): 149–171.
- Huang YZ, Fei L (1981) Two new species of amphibians from Xizang. *Acta Zootaxonomica Sinica* 6: 211–215.
- Inger RF (1989) Four new species of frogs from Borneo. *Malayan Nature Journal*. Kuala Lumpur 42: 229–243.
- Inger RF, Romer JD (1961) A new pelobatid frog of the genus *Megophrys* from Hong Kong. *Fieldiana. Zoology* 39(46): 533–538. <https://doi.org/10.5962/bhl.title.3373>
- Inger RF, Stuebing RB, Lian TF (1995) New species and new records of Anurans from Borneo. *Raffles Bulletin of Zoology*, Singapore 43(1): 115–131.
- Inger RF, Iskandar DT (2005) A collection of amphibians from west Sumatra, with description of a new species of *Megophrys* (Amphibia: Anura). *Raffles Bulletin of Zoology*, Singapore 133–142.
- Jiang JP, Yuan FR, Xie F, Zheng ZH (2003) Phylogenetic relationships of some species and genera in megophryids inferred from partial sequences of mitochondrial 12S and 16S rRNA genes. *Zoological Research* 24: 241–248. [In Chinese with English abstract]
- Jiang JP, Ye CY, Fei L (2008) A new Horn Toad *Megophrys sangzhiensis* from Hunan, China (Amphibia, Anura). *Zoological Research* 29(2): 219–222. <https://doi.org/10.3724/SPJ.1141.2008.00219> [In Chinese with English abstract]
- Kuhl H, Van Hasselt JC (1822) *Uittreksels uit breieven van de Heeren Kuhl en van Hasselt, aan de Heeren C. J. Temminck, Th. van Swinderen en W. de Haan*. *Algemeene Konst-en Letter-Bode* 7: 99–104.
- Lathrop A (1997) Taxonomic review of the megophryid frogs (Anura: Pelobatoidea). *Asian Herpetological Research* 7: 68–79. <https://doi.org/10.5962/bhl.part.18857>
- Lemmon AR, Moriarty EC (2004) The importance of proper model assumption in Bayesian phylogenetics. *Systematic Biology* 53(2): 265–277. <https://doi.org/10.1080/10635150490423520>
- Li YL, Jin MJ, Zhao J, Liu ZY, Wang YY, Pang H (2014) Description of two new species of the genus *Megophrys* (Amphibia: Anura: Megophryidae) from Heishiding Natural Reserve, Fengkai, Guangdong, China, based on molecular and morphological data. *Zootaxa* 3795(4): 449–471. <https://doi.org/10.11646/zootaxa.3795.4.5>

- Li SZ, Xu N, Lv JC, Jiang JP, Wei G, Wang B (2018a) A new species of the odorous frog genus *Odorrana* (Amphibia, Anura, Ranidae) from southwestern China. PeerJ 6(e5695): 1–28. <https://doi.org/10.7717/peerj.5695>
- Li SZ, Xu N, Liu J, Jiang JP, Wei G, Wang B (2018b) A new species of the Asian toad genus *Megophrys sensu lato* (Amphibia: Anura: Megophryidae) from Guizhou Province, China. Asian Herpetological Research 9(4): 224–239.
- Li SZ, Wei G, Xu N, Cui JG, Fei L, Jiang JP, Liu J, Wang B (2019a) A new species of the Asian music frog genus *Nidirana* (Amphibia, Anura, Ranidae) from Southwestern China. PeerJ 7: e7157. <https://doi.org/10.7717/peerj.7157>
- Li SZ, Zhang MH, Xu N, Lv JC, Jiang JP, Liu J, Wei G, Wang B (2019b) A new species of the genus *Microhyla* (Amphibia: Anura: Microhylidae) from Guizhou Province, China. Zootaxa 4624: 551–575. <https://doi.org/10.11646/zootaxa.4624.4.7>
- Li Y, Zhang DD, Lyu ZT, Wang J, Li YL, Liu ZY, Chen HH, Rao DQ, Jin ZF, Zhang CY, Wang YY (2020) Review of the genus *Brachytarsophrys* (Anura: Megophryidae), with revalidation of *Brachytarsophrys platyparietus* and description of a new species from China. Zoological Research 41(2): 105–122. <https://doi.org/10.24272/j.issn.2095-8137.2020.033>
- Liu CZ (1950) Amphibians of Western China. Fieldiana. Zoology Memoires 2: 1–400. <https://doi.org/10.5962/bhl.part.4737>
- Liu CZ, Hu SQ, Yang HH (1960) Amphibian of Yunnan collected in 1958. Acta Zoologica Sinica 12(2): 149–174.
- Liu ZY, Zhu TQ, Zeng ZC, Lyu ZT, Wang J, Messenger K, Greenberg A J, Gou ZX, Yang ZH, Shi SH, Wang YY (2018) Prevalence of cryptic species in morphologically uniform taxa—Fast speciation and evolutionary radiation in Asian frogs. Molecular Phylogenetics and Evolution 127: 723–731. <https://doi.org/10.1016/j.ympev.2018.06.020>
- Liu J, Li SZ, Wei G, Xu N, Cheng YL, Wang B, Wu J (2020) A new species of the Asian toad genus *Megophrys sensu lato* (Anura: Megophryidae) from Guizhou Province, China. Asian Herpetological Research 11(1): 1–18.
- Lyu ZT, Zeng ZC, Wan H, Yang JH, Li YL, Pang H, Wang YY (2019) A new species of *Amolops* (Anura: Ranidae) from China, with taxonomic comments on *A. liangshanensis* and Chinese populations of *A. marmoratus*. Zootaxa 4609: 247–268. <https://doi.org/10.11646/zootaxa.4609.2.3>
- Lyu ZT, Li YQ, Zeng ZC, Zhao J, Liu ZL, Guo GX, Wang YY (2020) Four new species of Asian horned toads (Anura, Megophryidae, *Megophrys*) from southern China. ZooKeys 942: 105–140. <https://doi.org/10.3897/zookeys.942.47983>
- Luo T, Xiao N, Gao K, Zhou J (2020) A new species of *Leptobranchella* (Anura, Megophryidae) from Guizhou Province, China. ZooKeys 923: 115–140. <https://doi.org/10.3897/zookeys.923.47172>
- Mahony S (2011) Two new species of *Megophrys* Kuhl & van Hasselt (Amphibia: Megophryidae), from western Thailand and southern Cambodia. Zootaxa 2734: 23–39. <https://doi.org/10.11646/zootaxa.2734.1.2>
- Mahony S, Sengupta S, Kamei RG, Biju SD (2011) A new low altitude species of *Megophrys* Kuhl and van Hasselt (Amphibia: Megophryidae), from Assam, Northeast India. Zootaxa 3059: 36–46. <https://doi.org/10.11646/zootaxa.3059.1.2>

- Mahony S, Teeling EC, Biju SD (2013) Three new species of horned frogs, *Megophrys* (Amphibia: Megophryidae), from northeast India, with a resolution to the identity of *Megophrys boettgeri* populations reported from the region. *Zootaxa* 3722(2): 143–169. <https://doi.org/10.11646/zootaxa.3722.2.2>
- Mahony S, Nicole MF, Biju SD, Teeling EC (2017) Evolutionary history of the Asian Horned Frogs (Megophryinae): integrative approaches to time tree dating in the absence of a fossil record. *Molecular Phylogenetics and Evolution* 34(3): 744–771. <https://doi.org/10.1093/molbev/msw267>
- Mahony S, Kamei RG, Teeling EC, Biju SD (2018) Cryptic diversity within the *Megophrys major* species group (Amphibia: Megophryidae) of the Asian Horned Frogs: Phylogenetic perspectives and a taxonomic revision of South Asian taxa, with descriptions of four new species. *Zootaxa* 4523: 1–96. <https://doi.org/10.11646/zootaxa.4523.1.1>
- Malkmus R, Matsui M (1997) *Megophrys kobayashii*, ein neuer pelobatider Frosch vom Mount Kinabalu. *Sauria*, Berlin 19: 31–37.
- Mathew R, Sen N (2007) Description of two new species of *Megophrys* (Amphibia: Anura: Megophryidae) from North-east India. *Cobra* 1: 18–28.
- McGuire JA, Witt CC, Altshuler DL, Remsen JV (2007) Phylogenetic systematics and biogeography of hummingbirds: Bayesian and maximum likelihood analyses of partitioned data and selection of an appropriate partitioning strategy. *Systematic Biology* 56(5): 837–856. <https://doi.org/10.1080/10635150701656360>
- Messenger KR, Dahn HA, Liang YR, Xie P, Wang Y, Lu CH (2019) A new species of the genus *Megophrys* Günther, 1864 (Amphibia: Anura: Megophryidae) from Mount Wuyi, China. *Zootaxa* 4554(2): 561–583. <https://doi.org/10.11646/zootaxa.4554.2.9>
- Mo XY, Shen YH, Li HH, Wu MS (2010) A new species of *Megophrys* (Amphibia: Anura: Megophryidae) from the northwestern Hunan Province, China. *Current Zoology* 56(4): 432–436. <https://doi.org/10.1093/czoolo/56.4.432>
- Munir M, Hamidy A, Farajallah A, Smith EN (2018) A new *Megophrys* Kuhl and Van Hasselt (Amphibia: Megophryidae) from southwestern Sumatra, Indonesia. *Zootaxa* 4442: 389–412. <https://doi.org/10.11646/zootaxa.4442.3.3>
- Munir M, Hamidy A, Matsui M, Iskandar DT, Sidik I, Shimada T (2019) A new species of *Megophrys* Kuhl & Van Hasselt (Amphibia: Megophryidae) from Borneo allied to *M. nasuta*. *Zootaxa* 4679: 1–24. <https://doi.org/10.11646/zootaxa.4679.1.1>
- Myers N, Mittermeier RA, Mittermeier CG, Da Fonseca GAB, Kent J (2000) Biodiversity hotspots for conservation priorities. *Nature* 403: 853–858. <https://doi.org/10.1038/35002501>
- Nguyen TQ, Pham CT, Nguyen TT, Luong AM, Ziegler T (2020) A new species of *Megophrys* (Amphibia: Anura: Megophryidae) from Vietnam. *Zootaxa* 4722: 401–422. <https://doi.org/10.11646/zootaxa.4722.5.1>
- Ohler A, Swan SR, Daltry JC (2002) A recent survey of the amphibian fauna of the Cardamom Mountains, Southwest Cambodia with descriptions of three new species. *Raffles Bulletin of Zoology*, Singapore 50(2): 465–481.
- Ohler A (2003) Revision of the genus *Ophryophryne* Boulenger, 1903 (Megophryidae) with description of two new species. *Alytes* 21(1): 23–44.

- Pope CH (1929) Four new frogs from Fukien Province, China. *American Museum Novitates* 352: 1–5.
- Poyarkov NA, Duong Jr TV, Orlov NL, Gogoleva SI, Vassilieva AB, Nguyen LT, Nguyen VDH, Nguyen SN, Che J, Mahony S (2017) Molecular, morphological and acoustic assessment of the genus *Ophryophryne* (Anura, Megophryidae) from Langbian Plateau, southern Vietnam, with description of a new species. *ZooKeys* 672: 49–120. <https://doi.org/10.3897/zookeys.672.10624>
- R Development Core Team (2008) R: a language and environment for statistical computing. Vienna: R Foundation for Statistical Computing. <http://www.Rproject.org>
- Rao DQ, Yang DT (1997) The karyotypes of Megophryinae (Pelobatidae) with a discussion on their classification and phylogenetic relationships. *Asian Herpetological Research* 7: 93–102. <https://doi.org/10.5962/bhl.part.18858>
- Robert L, Brett C, Simon YWH, Stéphane G (2012) PartitionFinder: combined selection of partitioning schemes and substitution models for phylogenetic analyses. *Molecular Phylogenetics and Evolution* 29(6): 1695–1701. <https://doi.org/10.1093/molbev/mss020>
- Ronquist FR, Huelsenbeck JP (2003) MrBayes3: Bayesian phylogenetic inference under mixed models. *Bioinformatics* 19(12): 1572–1574. <https://doi.org/10.1093/bioinformatics/btg180>
- Sambrook J, Fritsch EF, Maniatis T (1989) *Molecular cloning: a laboratory manual*. Cold Spring Harbor Laboratory Press, New York, 1659 pp.
- Schlegel H (1858) *Handleiding tot de Beoefening der Dierkunde*. Volume 2. Koninklijke Militaire Akademie, Breda, 57 pp. <https://doi.org/10.5962/bhl.title.11648>
- Shen Y H (1994) A new pelobatid toad of the genus *Megophrys* from China (Anura: Pelobatidae). In: Zoological Society of China Editor. *The 60<sup>th</sup> Anniversary of the Foundation of the Zoological Society of China, Nanking (China), September 1994*. China Science and Technology Publishing House, Nanjing, 603–606.
- Simon C, Frati F, Beckenbach A, Crespi B, Liu H, Flook P (1994) Evolution, weighting and phylogenetic utility of mitochondrial gene sequences and a compilation of conserved polymerase chain reaction primers. *Annals of the Entomological Society of America* 87(6): 651–701. <https://doi.org/10.1093/aesa/87.6.651>
- Sjöander K, Beskow J (2000) *Wavesurfer* (Anura: Pelobatidae). In: Acoustical society of China Editor. *The International Conference on Spoken Language Processing, Beijing (China), October 2000*. Military Yiwon Publishing House, Beijing, 464–467.
- Smith MA (1921) New or little-known reptiles and batrachians from southern Annam (Indo-China). *Proceedings of the Zoological Society of London* 1921: 423–440. <https://doi.org/10.1111/j.1096-3642.1921.tb03271.x>
- Stejneger L (1926) Two new tailless amphibians from western China. *Proceedings of the Biological Society of Washington* 39: 53–54.
- Stuart BL, Chuaynkern Y, Chan-ard T, Inger RF (2006) Three new species of frogs and a new tadpole from eastern Thailand. *Fieldiana Zoology, New Series* 1543: 1–10. [https://doi.org/10.3158/0015-0754\(2006\)187\[1:TNSOFA\]2.0.CO;2](https://doi.org/10.3158/0015-0754(2006)187[1:TNSOFA]2.0.CO;2)
- Tamura K, Stecher G, Peterson D, Fiipski A, Kumar S (2013) MEGA6: molecular evolutionary genetics analysis, version 6.0. *Molecular Biology and Evolution* 30: 2725–2729. <https://doi.org/10.1093/molbev/mst197>

- Tapley B, Cutajar T, Mahony S, Nguyen CT, Dau VQ, Nguyen TT, Luong HV, Rowley JJJ (2017) The Vietnamese population of *Megophrys kuatunensis* (Amphibia: Megophryidae) represents a new species of Asian horned frog from Vietnam and southern China. *Zootaxa* 4344(3): 465–492. <https://doi.org/10.11646/zootaxa.4344.3.3>
- Tapley B, Cutajar TP, Mahony S, Nguyen CT, Dau VQ, Luong AM, Le DT, Nguyen TT, Nguyen TQ, Portway C, Luong HV, Rowley JJJ (2018) Two new and potentially highly threatened *Megophrys* Horned frogs (Amphibia: Megophryidae) from Indochina's highest mountains. *Zootaxa* 4508: 301–333. <https://doi.org/10.11646/zootaxa.4508.3.1>
- Taylor EH (1920) Philippine Amphibia. *Philippine Journal of Science* 16: 213–359. <https://doi.org/10.5962/bhl.part.4751>
- Taylor EH (1962) The amphibian fauna of Thailand. *University of Kansas Science Bulletin* 43: 265–599. <https://doi.org/10.5962/bhl.part.13347>
- Tian YZ, Sun A (1995) A new species of *Megophrys* from China (Amphibia: Pelobatidae). *Journal of Liupanshui Teachers College* 52(3): 11–15. [In Chinese]
- Tian WS, Hu QX (1983) Taxonomic study on genus *Megophrys*, with descriptions of two genera. *Acta Herpetologica Sinica* 2: 41–48.
- Wang J, Liu ZY, Lyu ZT, Wang YY (2017a) A new species of the genus *Megophrys* (Amphibia: Anura: Megophryidae) from an offshore island in Guangdong Province, southeastern China. *Zootaxa* 4324(3): 541–556. <https://doi.org/10.11646/zootaxa.4324.3.8>
- Wang YE, Liu BQ, Jiang K, Jin W, Xu JN, Wu CH (2017b) A new species of the Horn Toad of the genus *Xenophrys* from Zhejiang, China (Amphibia: Megophryidae). *Chinese Journal of Zoology* 52: 19–29. [in Chinese with English abstract]
- Wang YY, Zhang TD, Zhao J, Sung YH, Yang JH, Pang H, Zhang Z (2012) Description of a new species of the genus *Megophrys* Günther, 1864 (Amphibia: Anura: Megophryidae) from Mount Jinggang, China, based on molecular and morphological data. *Zootaxa* 3546: 53–67. <https://doi.org/10.11646/zootaxa.3546.1.4>
- Wang YY, Zhao J, Yang JH, Zhou ZM, Chen GL, Liu Y (2014) Morphology, molecular genetics, and bioacoustics support two new sympatric *Megophrys* (Amphibia: Anura Megophryidae) species in Southeast China. *PLoS ONE* 9: e93075. <https://doi.org/10.1371/journal.pone.0093075>
- Wang L, Deng XJ, Liu Y, Wu QQ, Liu Z (2019a) A new species of the genus *Megophrys* (Amphibia: Anura: Megophryidae) from Hunan, China. *Zootaxa* 4695(4): 301–330. <https://doi.org/10.11646/zootaxa.4695.4.1>
- Wang J, Lyu ZT, Liu ZY, Liao CK, Zeng ZC, Li YL, Wang YY (2019b) Description of six new species of the subgenus *Panophrys* within the genus *Megophrys* (Anura, Megophryidae) from southeastern China based on molecular and morphological data. *ZooKeys* 851: 113–164. <https://doi.org/10.3897/zookeys.851.29107>
- Wang J, Li YL, Li Y, Chen H-H, Zeng YJ, Shen JM, Wang Y-Y (2019c) Morphology, molecular genetics, and acoustics reveal two new species of the genus *Leptobrachella* from northwestern Guizhou Province, China (Anura, Megophryidae). *ZooKeys* 848: 119–154. <https://doi.org/10.3897/zookeys.848.29181>
- Wang B, Wu YQ, Peng JW, Shi SC, Lu NN, Wu J (2020) A new *Megophrys* Kuhl and Van Hasselt (Amphibia: Megophryidae) from southeastern China. *ZooKeys* 851: 113–164. <https://doi.org/10.3897/zookeys.851.29107>

- Wei G, Li SZ, Liu J, Cheng YL, Xu N, Wang B (2020) A new species of the Music frog *Nidirana* (Anura, Ranidae) from Guizhou Province, China. *ZooKeys* 904: 63–87. <https://doi.org/10.3897/zookeys.904.39161>
- Wu YH, Suwannapoom C, Poyarkov Jr NA, Chen JM, Pawangkhanant P, Xu K, Jin JQ, Murphy RW, Che J (2019) A new species of the genus *Xenophrys* (Anura: Megophryidae) from northern Thailand. *Zoological Research* 40: 564–574. <https://doi.org/10.24272/j.issn.2095-8137.2019.032>
- Xu N, Li SZ, Liu J, Wei G, Wang B (2020) A new species of the horned toad *Megophrys* Kuhl & Van Hasselt, 1822 (Anura, Megophryidae) from southwest China. *ZooKeys* 943: 119–144. <https://doi.org/10.3897/zookeys.943.50343>
- Yang JH, Wang J, Wang YY (2018) A new species of the genus *Megophrys* (Anura: Megophryidae) from Yunnan Province, China. *Zootaxa* 4413: 325–338. <https://doi.org/10.11646/zootaxa.4413.2.5>
- Ye CY, Fei L (1992) A new Pelobatid toad of the genus *Megophrys* from Xizang, China. *Acta Herpetologica Sinica* 1–2: 50–52. [In Chinese]
- Ye CY, Fei L (1995) Taxonomic studies on the small type *Megophrys* in China including descriptions of the new species (subspecies) (Pelobatidae: genus *Megophrys*). *Herpetologica Sinica* 4–5: 72–81. [In Chinese]
- Ye CY, Fei L, Xie F (2007) A new species of Megophryidae *Megophrys baolongensis* from China (Amphibia, Anura). *Herpetologica Sinica* 11: 38–41. [In Chinese]
- Zhang Y, Li G, Xiao N, Li J, Pan T, Wang H, Zhang B, Zhou J (2017) A new species of the genus *Megophrys* (Amphibia: Anura: Megophryidae) from Libo County, Guizhou, China. *Asian Herpetological Research* 8: 75–85.
- Zhao J, Yang JH, Chen GL, Chen CQ, Wang YY (2014) Description of a new species of the genus *Brachytarsophrys* Tian and Hu, 1983 (Amphibia: Anura: Megophryidae) from Southern China based on molecular and morphological data. *Asian Herpetological Research* 5(3): 150–160. <https://doi.org/10.3724/SPJ.1245.2014.00150>

## Supplementary material I

### Table S1

Authors: Bin Wang

Data type: morphological measurements

Explanation note: Measurements of the adult specimens of *Megophrys baishanzuensis* sp. nov. and *M. kuatunensis*. Units given in mm. See abbreviations for the morphological characters in Materials and methods section.

Copyright notice: This dataset is made available under the Open Database License (<http://opendatacommons.org/licenses/odbl/1.0/>). The Open Database License (ODbL) is a license agreement intended to allow users to freely share, modify, and use this Dataset while maintaining this same freedom for others, provided that the original source and author(s) are credited.

Link: <https://doi.org/10.3897/zookeys.1005.58629.suppl1>

## Supplementary material 2

### Table S2

Authors: Bin Wang

Data type: genetic distance

Explanation note: Uncorrected  $p$ -distances between the *Megophrys* species on the 16S gene.

Copyright notice: This dataset is made available under the Open Database License (<http://opendatacommons.org/licenses/odbl/1.0/>). The Open Database License (ODbL) is a license agreement intended to allow users to freely share, modify, and use this Dataset while maintaining this same freedom for others, provided that the original source and author(s) are credited.

Link: <https://doi.org/10.3897/zookeys.1005.58629.suppl2>

## Supplementary material 3

### Table S3

Authors: Bin Wang

Data type: genetic distance

Explanation note: Uncorrected  $p$ -distances between the *Megophrys* species on the COI gene.

Copyright notice: This dataset is made available under the Open Database License (<http://opendatacommons.org/licenses/odbl/1.0/>). The Open Database License (ODbL) is a license agreement intended to allow users to freely share, modify, and use this Dataset while maintaining this same freedom for others, provided that the original source and author(s) are credited.

Link: <https://doi.org/10.3897/zookeys.1005.58629.suppl3>

## Supplementary material 4

### Table S4

Authors: Bin Wang

Data type: morphological comparisons

Explanation note: Diagnostic characters separating *Megophrys baishanzuensis* sp. nov. from other species of *Megophrys*.

Copyright notice: This dataset is made available under the Open Database License (<http://opendatacommons.org/licenses/odbl/1.0/>). The Open Database License (ODbL) is a license agreement intended to allow users to freely share, modify, and use this Dataset while maintaining this same freedom for others, provided that the original source and author(s) are credited.

Link: <https://doi.org/10.3897/zookeys.1005.58629.suppl4>

# Rattlesnake (*Crotalus* spp.) distribution and diversity in Zacatecas, Mexico

Jesús Lenin Lara-Galván<sup>1</sup>, Juan Felipe Martínez-Montoya<sup>1</sup>,  
José Jesús Sigala-Rodríguez<sup>2</sup>, Citlalli Edith Esparza-Estrada<sup>2,3</sup>,  
Octavio César Rosas-Rosas<sup>1</sup>, Lucía Ávila-Herrera<sup>4</sup>, A. Márcia Barbosa<sup>5</sup>

**1** *Colegio de Postgraduados, Campus San Luis Potosí, Posgrado en Innovación en Manejo de Recursos Naturales. Iturbide 73, Salinas de Hidalgo, San Luis Potosí, CP. 78622, México* **2** *Colección Zoológica. Universidad Autónoma de Aguascalientes. Aguascalientes, Ags. CP. 20131, México* **3** *Instituto de Ecología, A.C., Red de Biología Evolutiva, Laboratorio de Macroecología Evolutiva. Carretera Antigua a Coatepec 351, El Haya, Xalapa, CP. 91070, Veracruz, México* **4** *Presidencia Municipal de Valparaíso. Constitución Sn, Capulín de la Sierra, CP. 99200. Valparaíso, Zacatecas, México* **5** *CIBIO/InBIO, Universidade de Évora. 7004-516. Évora. Portugal* **6** *CICGE – Centro de Investigação em Ciências Geo-Espaciais, Universidade do Porto, Portugal*

Corresponding authors: Jesús Lenin Lara-Galván ([phrynosomatidae17@gmail.com](mailto:phrynosomatidae17@gmail.com));

Juan Felipe Martínez-Montoya ([fmontoya@colpos.mx](mailto:fmontoya@colpos.mx));

A. Márcia Barbosa ([ana.marcia.barbosa@gmail.com](mailto:ana.marcia.barbosa@gmail.com))

---

Academic editor: R. Jadin | Received 27 July 2020 | Accepted 3 November 2020 | Published 18 December 2020

---

<http://zoobank.org/1E7EE6CD-ACCE-4942-8D46-1C94E42E9CFC>

---

**Citation:** Lara-Galván JL, Martínez-Montoya JF, Sigala-Rodríguez JJ, Esparza-Estrada CE, Rosas-Rosas OC, Ávila-Herrera L, Barbosa AM (2020) Rattlesnake (*Crotalus* spp.) distribution and diversity in Zacatecas, Mexico. In: Spence J, Casale A, Assmann T, Liebherr J, Penev L (Eds) Systematic Zoology and Biodiversity Science: A tribute to Terry Erwin (1940–2020). ZooKeys 1005: 103–132. <https://doi.org/10.3897/zookeys.1005.56964>

---

## Abstract

Mexico is home to a large number of reptile species and has one of the greatest diversities of venomous snakes, among which the rattlesnakes pertaining to the *Crotalus* genus stand out. Out of more than 40 species in the country, nine are found in Zacatecas: *C. aquilus*, *C. atrox*, *C. basiliscus*, *C. lepidus*, *C. molossus*, *C. polystictus*, *C. pricei*, *C. scutulatus* and *C. willardi*. Although these reptiles are important, due to their relevance in terms of ecology, cultural use and public health, their conservation is impacted by multiple factors, such as habitat fragmentation and indiscriminate killing. Thus, most species within this genus are found in some type of risk category at both the national and international level. The purpose of this study was to determine the potential distribution and diversity of rattlesnakes at the municipal level in the understudied state of Zacatecas. To do this, we analyzed and described the global distribution of nine rattlesnake species by building species distribution models, which determined their potential distri-

bution based on a set of ecological variables and presence records. The resulting models were used to assess the diversity of rattlesnake species potentially present in each municipality within the state. Thirty-nine (67.24 %) out of fifty-eight municipalities registered at least one rattlesnake species. Fresnillo, Sombrerete and Valparaíso were some of the municipalities showing greatest diversity. Moreover, *C. atrox*, *C. lepidus*, *C. molossus* and *C. scutulatus* were the most widely found species in the state. On the other hand, *C. basiliscus*, *C. polystictus*, *C. pricei* and *C. willardi* were rarely spotted and so, information on their distribution patterns within Zacatecas is limited. Finally, the areas having the largest potential for the distribution of these species were defined. These findings should make field work much more time- and cost-effective, facilitating the collection of in situ data that are useful for management and conservation plans of these species in Zacatecas.

### Keywords

Central northern Mexico, conservation, Geographic Information System (GIS), herpetofauna, Species Distribution Models (SDM)

## Introduction

Mexico is home to a great diversity of reptile species, including a large number of endemics, with 864 different species having been reported by 2014 (Flores-Villela and García-Vázquez 2014). The states of Oaxaca (262), Chiapas (220) and Veracruz (200) have the greatest number of species (Flores-Villela and García-Vázquez 2014), while Zacatecas has only 108 according to the most recent information gathering (Sigala-Rodríguez et al. 2020). Pitvipers stand out among all these reptiles (Jadin et al. 2011) and, particularly in this family, rattlesnakes belonging to the *Crotalus* genus are noteworthy. As of 2018, this genus is comprised of 47 species, with 42 of them found in Mexico, among which 27 are endemic (Uetz 2018). Recently, there have been several studies on the herpetofauna in the central and northern regions of Mexico, in which Zacatecas is located. This state is one of the largest and shares its borders with eight other states (Figure 1). Despite its size, the data available concerning its herpetofauna is very scarce, thereby constituting an information gap about the species distributed in the region; Flores-Villela and García-Vázquez (2014) and Lemos-Espinal et al. (2018) underlined the lack of studies and species lists of herpetofauna in Zacatecas. By contrast, neighboring states have complete works on their amphibians and reptiles, such as Aguascalientes: Vázquez-Díaz and Quintero-Díaz 2005; Coahuila: Lemos-Espinal and Smith 2016a; Durango: Valdez Lares et al. 2013, Lemos-Espinal et al. 2018a, Lemos-Espinal et al. 2019; Guanajuato: Elizalde-Arellano et al. 2014; Jalisco: Chávez-Avila et al. 2015; Nayarit: Lujá et al. 2014, Woolrich-Pina et al. 2016; Nuevo León: Lazcano-Villarreal 1997; Lazcano-Villarreal et al. 2010; Lemos-Espinal et al. 2016b; Lemos-Espinal et al. 2018b; and San Luis Potosí: Lemos-Espinal et al. 2018c.

Another problem that Zacatecas faces is the lack of publications on regional or municipal studies with venomous snakes and herpetofauna in general. There are only specific notes recorded on the state rattlesnake species of the *Crotalus* genus such as *C. aquilus* (Carbajal-Márquez et al. 2015a), *C. basiliscus* (Ahumada-Carrillo et al. 2011; Carbajal-Márquez et al. 2015b); *C. polystictus* (Campbell and Lamar 2004; Ahumada-

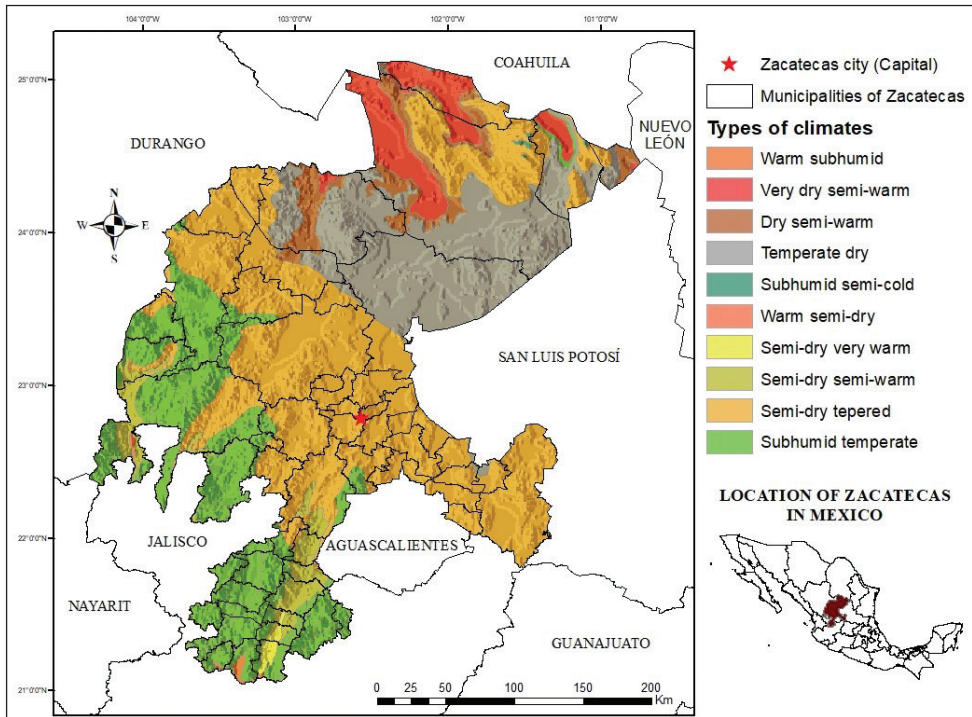


**Figure 1.** Location of the state of Zacatecas and their climate types (modified from INEGI 2008).

Carrillo 2010), *C. atrox*, *C. lepidus*, *C. molossus* and *C. scutulatus* (Campbell and Lamar 2004), *C. willardi* (Klauber 1949). Moreover, the presence of *C. pricei* in the state is inferred by using presence records compiled in several databases.

In general, the studies on Mexican rattlesnakes have focused on their distribution at a large scale or on a single species. An example of this is the study by Paredes-García et al. (2011) about the representativeness of rattlesnakes in natural protected areas (NPAs), their natural history (Arnaud et al. 2008), ecology (Secor 2016), evolution (Strickland et al. 2018) and genetic diversity (Schield et al. 2018). Despite their importance in terms of ecology, public health and culture, it is generally considered that rattlesnakes have seen their populations significantly reduced, and the Mexican government confers different levels of protection for the nine species present in Zacatecas SEMARNAT (2019). According to the Red List published by IUCN (2020), the nine species are listed in the least concern (LC) risk category. Conservation threats mainly originate from the fragmentation of their habitat derived from land use changes, as well as hunting and illegal trade (Maritz et al. 2016), and indiscriminate killing due to the perceived danger associated with them (Ávila-Villegas 2017).

One way to determine distribution patterns is using species distribution modeling techniques (SDMs). These are based on the assumption that the distribution of a given species is the result -at least within a short time frame- of a balance between undisturbed factors, i.e., a (pseudo)-equilibrium between the biotic entities and the physical characteristics (Guisan and Theurillat 2000). Therefore, the SDMs are based on the environmen-

tal conditions of the sites where species are present (Phillips et al. 2006), representing the mathematical estimation of the ecological niche of the species in question and trying to establish the relationship between species distribution and the spatial distribution of the environmental variables utilized to generate the model (Elith et al. 2006). Distribution models are commonly used in several areas of biology, including biodiversity evaluations at various levels, so as to prioritize species conservation, in addition to the fields of evolutionary biology, epidemiology and global change biology (Araújo and Peterson 2012).

Due to the lack of information on rattlesnakes of Zacatecas, their local importance and the concern by state agencies, we launched a study on the distribution patterns of the nine species of rattlesnakes in Zacatecas to be used in rattlesnake management and conservation in the state. The aim of this paper is to combine the literature, field work and Species Distribution Models or SDMs to effectively determine the known and potential presence of these species in Zacatecas, to estimate *Crotalus* diversity per municipality, to identify their environmental requirements and gain knowledge about their biology.

## Methods

### Area of study

The state of Zacatecas is located in Mexico's central northern region (Figure 1), representing 3.7 % of the country's surface area. The altitude in the state ranges from 800 to 3,120 meters above sea level (INEGI 2017). The climate in the central region of the state is cold and semi-arid, whereas the climate in the northwestern region is hot and also semi-arid (INEGI 2008). Conversely, the climate in the northeastern portion of Zacatecas is hot and arid, with a mean annual temperature of 19 °C and an annual rainfall of 289 mm. Finally, the area filled with ravines towards the southwestern region of the state has a warm, Mediterranean-like climate during the summer. This is the bioclimatic region that most highly contrasts with the rest of the state (Climate Data 2018). This climate diversity results in four biogeographical provinces that meet within the state (Figure 2): Chihuahuan Desert province, Pacific Lowlands province and Sierra Madre Occidental province (Morrone et al. 2017).

### Gathering presence records

To determine the potential distribution of rattlesnakes in Zacatecas, we gathered records on their global presence. In order to do this, we conducted queries in the databases of the Global Biodiversity Information Facility: GBIF 2016; Vertebrate Networks: Vertnet 2016 and the National Commission for the Knowledge and Use of Biodiversity: CONABIO 2016. Specialized literature also provided presence records of *Crotalus aquilus* (Carbajal-Márquez et al. 2015a) and *C. basiliscus* in Zacatecas (Ahumada-Carrillo et al. 2011; Carbajal-Márquez et al. 2015b). Finally, we incorporated the presence records reported by Ávila-Herrera (2012), Ávila-Herrera et al. (2020), Esparza-Estrada (2014) Lara-Galván (2015) and our own field work. The total num-

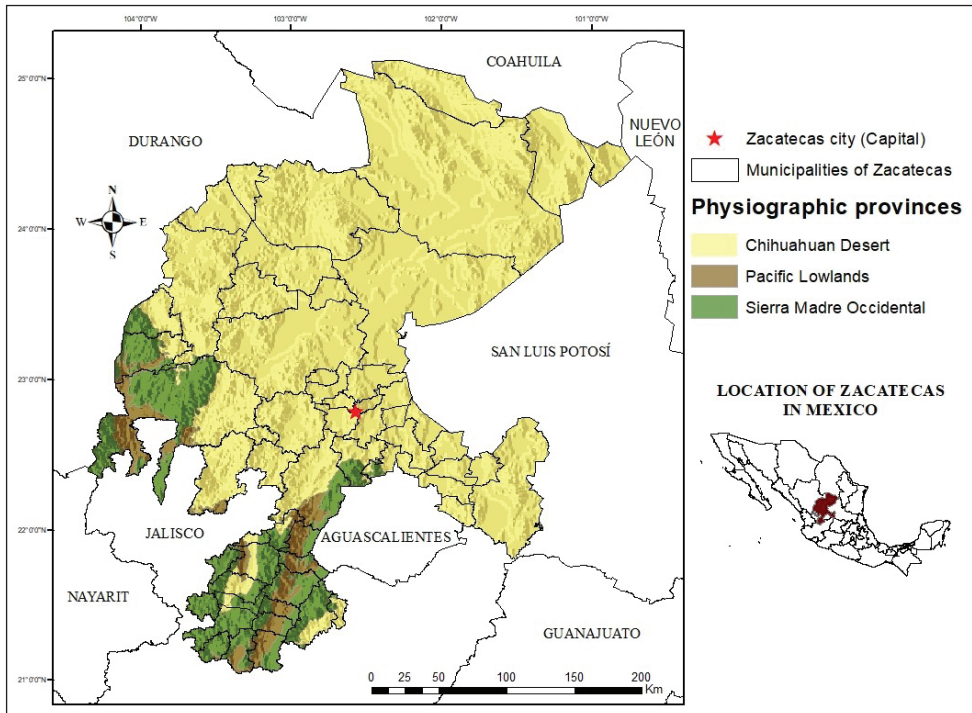


**Figure 2.** Location of Zacatecas in central-northern Mexico and Physiographic Provinces in which this state is situated (map based on Morrone et al. 2017).

ber of records was 12,113, which were subsequently reduced to 3,412 (Table 1) by eliminating duplicated, inaccurate or incomplete records. We also considered records containing complementary information, such as the location, species biology and information strictly referring to the site where organisms were observed in order to use that in the geo-referencing process. Of the total number of presence records used in the potential distribution models, 248 correspond to the state of Zacatecas.

### Definition of the spatial extent for modeling

According to Elith et al. (2011), when the study area or landscape of interest (L) is determined, it must contain a geographical area suggested and defined by the ecologist in relation to the problem, which can be delimited by geographical borders or by the knowledge of the point up to where the focal species may have spread. In addition, Merow et al. (2013) mentioned the importance of obtaining presence records for the species to be modeled, covering all the possible habitats where they might be found and the known distribution range of the species in question. Hence, the modelled presence records comprised the target species' global distributions, and two different polygons that delimited the modelling extent. Thus, based on the IUCN (2020) classification for the species in the *Crotalus* genus reported in Zacatecas, two groups of study were established: 1) species endemic to Mexico and 2) species non-endemic to Mexico (Table 1). Based on this, the

**Table 1.** Number of presence records shown by species of the *Crotalus* genus in Zacatecas included in the potential distribution modeling.

Group Studied	Species	Total occurrence records	Records pertaining to Zacatecas
Endemic to Mexico	<i>C. aquilus</i>	127	7
	<i>C. basiliscus</i>	115	3
	<i>C. polystictus</i>	90	14
Non-endemic to Mexico	<i>C. atrox</i>	999	39
	<i>C. lepidus</i>	375	52
	<i>C. molossus</i>	494	67
	<i>C. pricei</i>	117	2
	<i>C. scutulatus</i>	1,011	61
	<i>C. willardi</i>	84	3

first polygon included the entire Mexican territory and was used to model the distribution of species endemic to Mexico (*Crotalus aquilus*, *C. basiliscus* and *C. polystictus*). The second polygon comprised the entire Mexican territory together with the southernmost states of the United States of America, namely, Arizona, Arkansas, California, Colorado, Kansas, Louisiana, Nevada, New Mexico, Oklahoma, Texas and Utah. This was done to include those species whose distribution range is also present in this portion of the USA (*Crotalus atrox*, *C. lepidus*, *C. molossus*, *C. pricei*, *C. scutulatus* and *C. willardi*).

### Species Distribution Modeling (SDM)

We prepared distribution models using package *sdm*, version 1.0.46, implemented in the R software, which assembles and evaluates models using 15 algorithms: BIOCLIM, BIOCLIM.DISMO, BRT, CART, FDA, GAM, GLM, GLMNET, MARS, MAXENT, MAXLIKE, MDF, RF, RPART and SVM. This provides the potential distribution of a given species or community. For each species, we used all available presence points, in addition to several background points created randomly within the modelling extent, so that the proportion of presence points was 30 % for all species (Naimi and Araújo 2016).

### Predictor variable selection

We utilized a set of environmental variables that are typically associated with the presence of the species, the 19 bioclimatic variables from the WorldClim, version 2.0 database (Fick and Hijmans 2017). These data refer to the minimum, median and maximum temperature, as well as to the rainfall records from 1970 to 2000 and any deviations associated with these data. These variables have a spatial resolution of 30" or approximately 1 km<sup>2</sup>. For the Mexican endemic species polygon, in addition to environmental variables, we included information on the land use, series V vegetation and edaphology (CONABIO 2017), rock types, topofom systems and the Mexican digital elevation continuum 3.0 (CEM 3.0). Further data was obtained from the National Statistics and Geography Institute (INEGI 2017), from which the slope and exposure were calculated. As for the non-endemic species polygon (Mexico and southern USA),

**Table 2.** Variables selected by the *multGLM* function in the *fuzzySim* R package and used in distribution modeling per species of rattlesnake present in Zacatecas, Mexico.

Group Studied	Species	Variables used in SDM
Endemic	<i>C. aquilus</i>	bio_04, bio_09, bio_18, rock types and topoform systems.
	<i>C. basiliscus</i>	bio_07, bio_14, bio_15, bio_19, topoform systems and slope.
	<i>C. polystictus</i>	bio_04, bio_10, bio_15, bio_16, slope and topoform systems.
Non-Endemic	<i>C. atrox</i>	bio_01, bio_02, bio_03, bio_05, bio_08, bio_09, bio_12, bio_14, bio_15, bio_19, altitude, human influence and land cover.
	<i>C. lepidus</i>	bio_02, bio_03, bio_05, bio_08, bio_11, bio_14, bio_15, human influence, land cover and slope.
	<i>C. molossus</i>	bio_02, bio_08, bio_11, bio_12, bio_14, bio_15, bio_18, bio_19, altitude, human influence and land cover.
	<i>C. pricei</i>	bio_02, bio_08, bio_14, bio_19, altitude, human influence and land cover.
	<i>C. scutulatus</i>	bio_01, bio_05, bio_07, bio_09, bio_12, bio_14, bio_19, altitude, human influence, slope and land cover.
	<i>C. willardi</i>	bio_01, bio_08, bio_09, bio_12, bio_14, bio_18, bio_19, altitude and human influence.

**Abbreviation notes:** (bio\_01) annual mean temperature, (bio\_02) mean diurnal range, (bio\_03) isothermality, (bio\_04) temperature seasonality, (bio\_05) max temperature of warmest month, (bio\_06) min temperature of coldest month, (bio\_07) temperature annual range, (bio\_08) mean temperature of wettest quarter, (bio\_09) mean temperature of driest quarter, (bio\_10) mean temperature of warmest quarter, (bio\_11) mean temperature of coldest quarter, (bio\_12) annual precipitation, (bio\_13) precipitation of wettest month, (bio\_14) precipitation of driest month, (bio\_15) precipitation seasonality, (bio\_16) precipitation of wettest quarter, (bio\_17) precipitation of driest quarter, (bio\_18) precipitation of warmest quarter, and (bio\_19) precipitation of coldest quarter.

we also included soil cover, human influence and the digital elevation continuum, downloaded from the Commission for Environmental Cooperation (CEC 2017), where the slope and exposure were also computed. Cartographic data was re-projected into the WGS\_1984 world geographical coordinate system. The data of each predictor variable was cut out and retrieved. Map images were processed using ArcGIS 10.5 (ESRI 2016), QGIS 2.18.14 (QGIS 2009) and R 3.5.0 (R Core Team 2016).

Regarding variable selection (Table 2), we determined the most suitable variables for each species distribution model using the *multGLM* function in the *fuzzySim* R package (Barbosa 2015), where for each pair of correlated variables above  $|r| = 0.8$ , the function excludes the variable having the least significant relationship with the distribution of the species in question. The remaining variables are then subject to a stepwise selection process using the Akaike Information Criterion (AIC), to keep only informative variables in the models. Finally, any non-significant variables that might remain in the model after this process were eliminated (Reino et al. 2017; Gutiérrez-Rodríguez et al. 2017). The variables selected for each species were subsequently used to create models using the 15 algorithms applied in the *sdm* package. Afterwards, we calculated the mean and variance for each model's predictions. The mean was used to show the potential distribution for each species of *Crotalus*, while the variance was used to estimate the agreement between predictions of different algorithms (Naimi and Araújo 2016). Finally, a potential distribution map was created based on the mean, cutting out the data to the surface of the region of interest, i.e. the state of Zacatecas.

## Model evaluation

Model evaluation was based on the criterion of area under the curve (AUC), which is considered a standard method to evaluate the discrimination capacity (i.e. differentiating the locations where presence and non-presence has been recorded) of predictive

distribution models, avoiding the subjectivity of choosing a classification threshold. The value of AUC depends on the ratio of presence and the size of the area to be modeled, as pinpointed by (Lobo et al. 2008), but we used a constant prevalence value of 30 % for all species (Naimi and Araújo 2016).

### Species at the municipal level

To determine the rattlesnake number at the municipal level, we used the available presence records and prepared a list of the species observed at each municipality. Likewise, the list included the results of potential distribution models (Figures 3–11) that identified the areas bearing a higher suitability for these organisms. This implied overlapping the layer of municipalities over the potential distribution maps.

### Field verification of models

Based on the potential distribution models for each rattlesnake species found in Zacatecas, two localities per municipality were selected (three in the case of the Pinos, Loreto and Valparaíso municipalities). Thus, the field work in this study comprised a total of 48 localities throughout 22 municipalities within the state. These 22 municipalities were chosen randomly to include various regions throughout the state. Moreover, in these municipalities, we selected localities situated within the areas of greatest suitability as predicted by the models. A map of Mexican localities was overlapped to the potential distribution maps to conduct this geographical selection (CONABIO 2017). Field work was carried out in the areas surrounding the chosen localities in order to verify the presence of these species. To gather further information about these organisms, interviews were conducted to five individuals per locality, chosen randomly. Two of the five interviews targeted individuals who were believed to have closer contact with these organisms, i.e. individuals who engage in farming, cattle raising or rodent hunting. The other three interviews were carried out randomly, trying to include different age ranges and sexes. Finally, field verification was conducted in those areas having the most suitable habitats for the presence of these organisms based on the recommendations by Campbell and Lamar (2004), where the main criteria are related to land use, vegetation at elevation, including night driving along secondary roads, dirt roads and paths. At each location, we took into consideration visual records, skin sheds in good state, road kills and personal communications that could be confirmed (e.g. photographs and hunted specimens). A minimum sampling effort of 2 hours per location was considered, thus having a total of 243 hours of field work in a time period spanning from May to September of 2019, representing 22.09 field work hours/man.

### Results

There was significant variation on the number of records for the rattlesnakes present in Zacatecas, ranging from 1,011 records for *C. scutulatus* to 84 records for *C. willardi*

throughout their distribution range. The latter species, along with *C. basiliscus* and *C. pricei*, had the lowest number of available presence records, as opposed to *C. molossus*, which was the species with the greatest number of records in Zacatecas (Table 1).

In the species distribution modeling, the most informative environmental variables for the models were bio\_08 (mean temperature of wettest quarter), bio\_14 (precipitation of driest month), bio\_19 (precipitation of coldest quarter), altitude, land cover and slope. Anthropogenic influence, which intuitively includes the direct influence of human beings on ecosystems (based on population density, built-up area, highways, railroads, navigable rivers, land use and night-time illumination), impacted the presence of *C. atrox*, *C. lepidus*, *C. molossus* and *C. scutulatus*. Rock types and edaphology were less relevant at the time of model preparation. On the other hand, variables such as bio\_06 (min temperature of coldest month) or bio\_10 (mean temperature of warmest quarter) were not selected in any of the distribution models.

### Species Distribution Models -SDM-

In Zacatecas, the potential areas for the distribution of *C. aquilus* (Figure 3) are mainly found in the municipalities of Atolinga, Tepechitlán and Tlaltenango de Sánchez

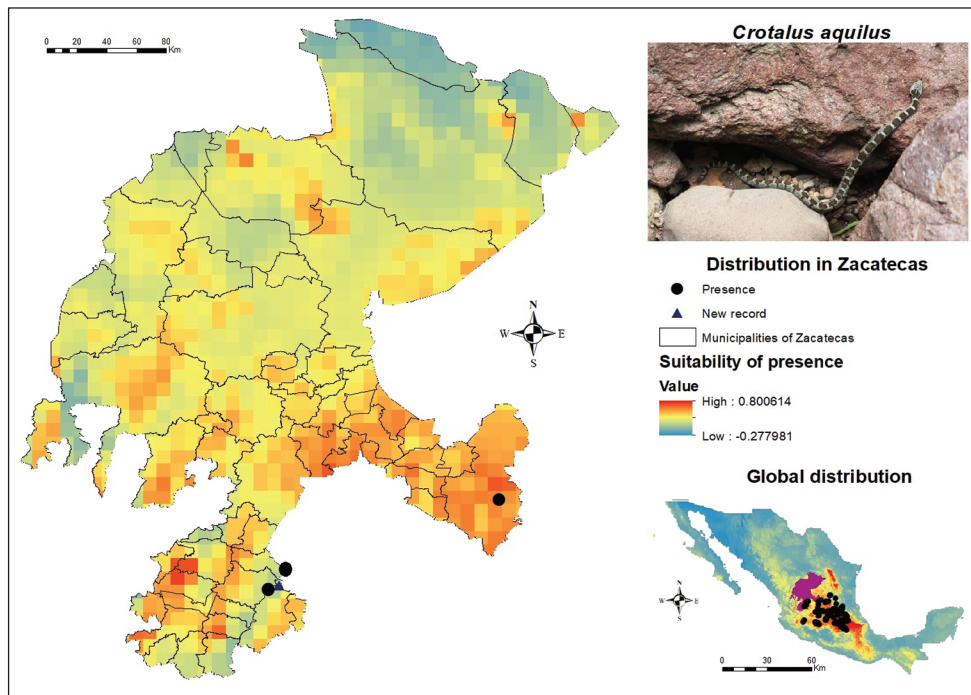


**Figure 3.** Presence and global potential distribution of *Crotalus aquilus* in Zacatecas, Mexico. Insert includes a *C. aquilus* from Tlachichila in the municipality of Nochistlán de Mejía (photo provided by Juan Felipe Martínez Montoya). The occurrence records used as input for the models are symbolized with dots, new records found during post-modeling field work are symbolized with triangles and the potential distribution is shown with warmer colors (red) identifying high potential for predicted presence for the species.

Román in the southwest. The distribution modeling also indicates areas in Genaro Codina, Cuauhtémoc and the municipality of Pinos, the latter in the southeastern region of the state. According to the distribution presented here, more organisms could be found in the border region between Aguascalientes and Zacatecas, since it presents a high degree of suitability for its occurrence, in addition to the municipalities of General Pánfilo Natera, Noria de Ángeles, Villa González Ortega and Villa Hidalgo that also present moderately high values. Regarding its global distribution, the largest number of records are located in the states of Guanajuato, Hidalgo and Querétaro, as well as specific records in Mexico City.

The western diamondback rattlesnake, *Crotalus atrox* is present in a large portion of the territory of Zacatecas (Figure 4), mainly along the northern region, which includes the municipalities of Concepción del Oro (where a record gathered during previous work is added), El Salvador and Mazapil. This species also showed records in the central and northern regions of the state, in the municipalities of Fresnillo and Río Grande, which exhibit distribution potential for the species. *C. atrox* has an extensive distribution in Zacatecas. During our post-modeling field work, many more individuals of this species were found in the municipalities of Concepción del Oro and Mazapil. The eastern region of Zacatecas has a low and medium suitability for this spe-

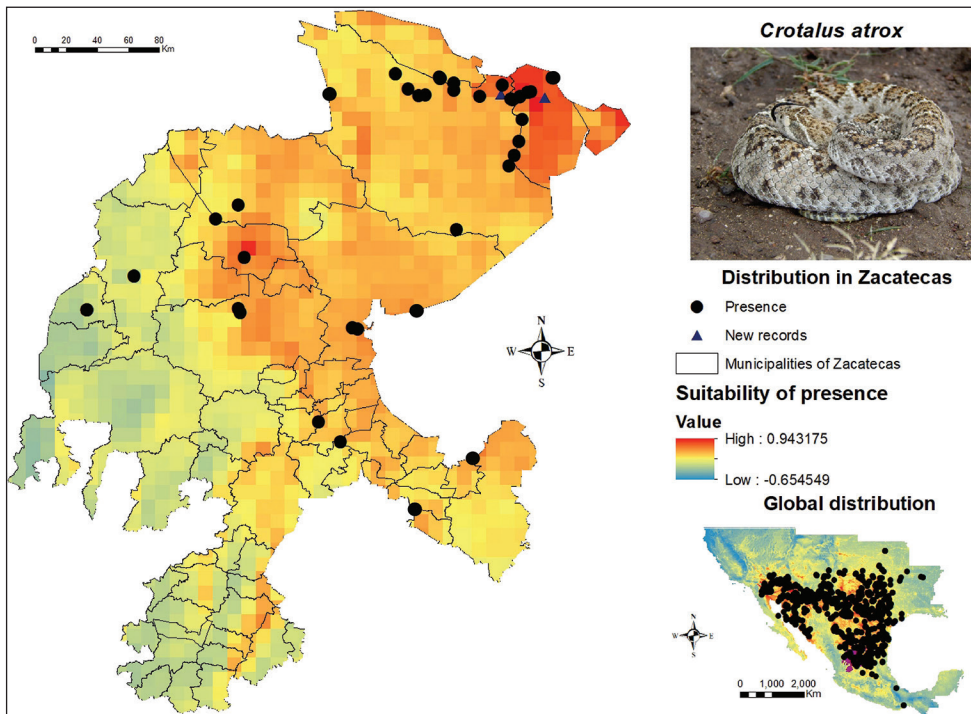


**Figure 4.** Presence and global potential distribution of *Crotalus atrox* in Zacatecas, Mexico. Insert includes a *C. atrox* from the municipality of Concepción del Oro (photo provided by Lenin Lara Galván). For explanation of the symbols and legend, see Figure 3.

cies, although a presence point is registered in the municipality of Chalchihuites. The southwestern region of Zacatecas stands out as the area having the lowest suitability throughout the entire state.

The known distribution of *C. basiliscus* in Zacatecas is limited to the western and southwestern parts of the state (Figure 5). This species has presence records in the municipalities of El Plateado de Joaquín Amaro, Moyahua de Estrada and Valparaíso. However, the SDM indicates the following municipalities as medium suitability areas: Apozol, Atolinga, Jalpa, Juchipila, Mezquital del Oro, Momax, Monte Escobedo, Nochistlán de Mejía, Tepechitlán, Tlaltenango de Sánchez Román and Trinidad García de la Cadena. Two presence records were added by post-modelling field work, including a live specimen caught and released, which was provided by Bañuelos-Alamillo (pers. comm. 2018), as well as the record of a dead specimen provided by a resident from the locality of San Rafael de las Tablas. Both records are located within the municipality of Valparaíso and the zones in question are included in the delimited areas with the greatest distribution potential.

The rock rattlesnake *Crotalus lepidus* is one of the species with most presence records in the state. The global potential distribution model for this species (Figure 6) contained a total of 375 occurrence records. Among these, 52 records are located in

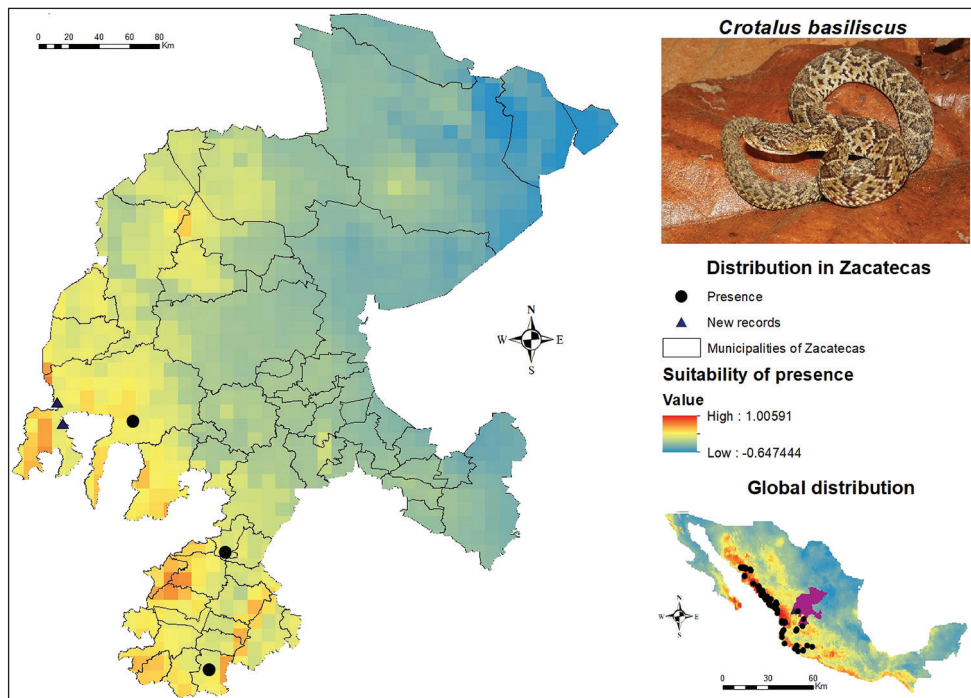


**Figure 5.** Presence and global potential distribution of *Crotalus basiliscus* in Zacatecas, Mexico. Insert includes a *C. basiliscus* from the municipality of Moyahua de Estrada (photo provided by Ivan Ahumada Carrillo). For explanation of the symbols and legend, see Figure 3.

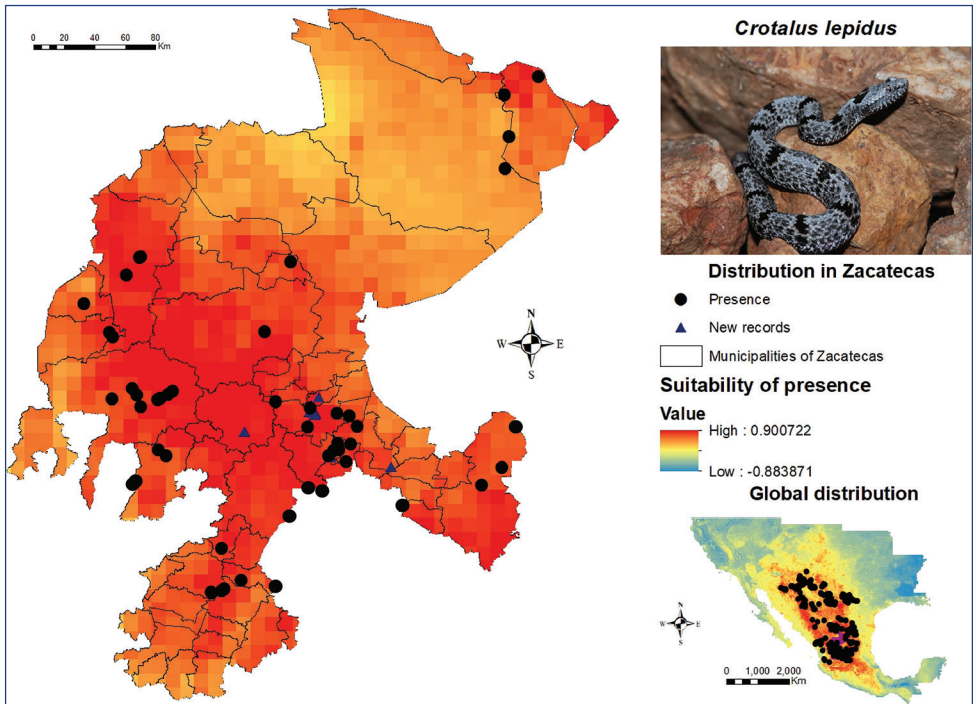


**Figure 6.** Presence and global potential distribution of *Crotalus lepidus* in Zacatecas, Mexico. Insert includes a *C. lepidus* from the semi-urban locality of Santa Monica in the municipality of Guadalupe (photo provided by Jesús Sigala Rodríguez). For explanation of the symbols and legend, see Figure 3.

Zacatecas, mainly concentrating within the state's central region, which is home to the largest urban areas and is composed of the municipalities of Guadalupe and Zacatecas. This species shows presence records primarily in the municipalities of Cuauhtémoc, Genaro Codina and Valparaíso. According to its global distribution model, its potential presence extends throughout the entire state of Zacatecas, from the municipalities of Pinos in the central region, where a significant number of records were identified, to the municipalities of Genaro Codina, Vetagrande and Villanueva. A few records were similarly identified in the northern region of the municipalities of Concepción del Oro, El Salvador, Cañitas de Felipe Pescador, General Francisco R. Murguía, Juan Aldama, Mazapil, Melchor Ocampo and Miguel Auza, in spite of showing a low suitability in the model. According to the SDM, the environment with the most suitable conditions for the presence of this species is located in the municipalities of Guadalupe, Jerez, Fresnillo, Monte Escobedo, Valparaíso, Vetagrande and Zacatecas. These rattlesnakes were found during post-modelling field work in the former two and the latter two municipalities. Two specimens were also spotted in the municipalities of Genaro Codina and Ojocaliente.

The black-tailed rattlesnake (*C. molossus*) exhibits an extensive potential distribution within Zacatecas (Figure 7). This species spreads throughout the whole state, from

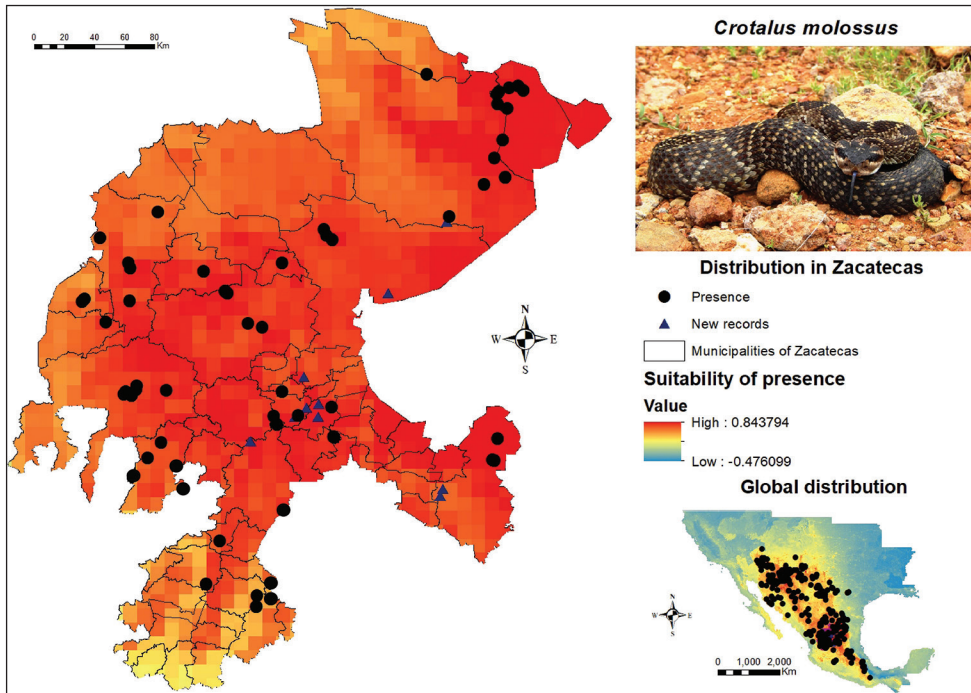


**Figure 7.** Presence and global potential distribution of *Crotalus molossus* in Zacatecas, Mexico. Insert includes a *C. molossus* from the municipality of Pinos (photo provided by Lenin Lara Galván). For explanation of the symbols and legend, see Figure 3.

the municipality of Pinos in the southeastern region to Sombrerete in the western region, with a substantial number of records along the northern region, particularly in the municipalities of Concepción del Oro and El Salvador. Specimens of this species were discovered in the municipalities of Guadalupe, Mazapil, Pánuco, Villanueva, Villa de Cos and Zacatecas during field work. One more organism and a clearly identifiable record of a skin shed of this species were found in Pinos. When inhabitants from different localities in some municipalities of Zacatecas were interviewed, they mentioned the black-tailed rattlesnake as the most abundant and most commonly observed species in parcels, dirt roads and paved roads. This species, together with *C. atrox*, are usually sold for food in the state capital. Conversely, Mezquital del Oro, Moyahua de Estrada and Trinidad García were some of the municipalities presenting a medium suitability for *C. molossus*, although the possibility of finding them in these areas cannot be ruled out.

In the case of *C. polystictus*, the presence records (Figure 8) are concentrated in the western and southwestern region of the state, precisely in the municipalities Atolinga, Chalchihuites, El Plateado de Joaquín Amaro, Fresnillo, Jerez, Monte Escobedo, Sombrerete, Tabasco, Teúl de González Ortega and Valparaíso. Additional sources for *Crotalus polystictus* were consulted (Meik et al. 2012; Santiago-Pérez et al. 2017) to obtain a greater number of presence records. These zones also coincide with a high potential of

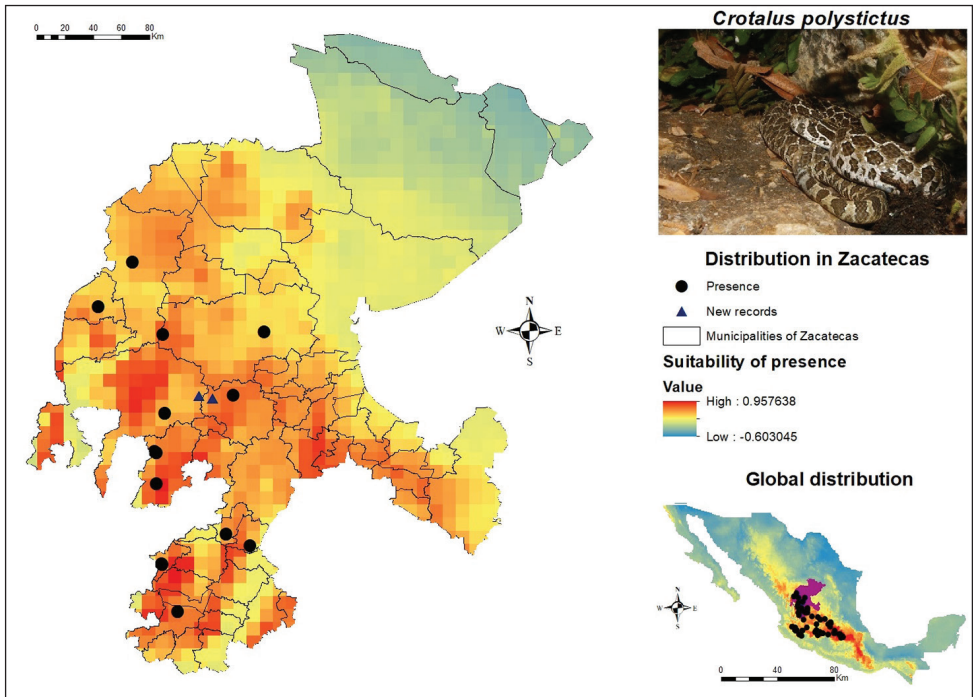


**Figure 8.** Presence and global potential distribution of *Crotalus polystictus* in Zacatecas, Mexico. Insert includes a *C. polystictus* from the municipality of Atolina (photo provided by Iván Ahumada Carrillo). For explanation of the symbols and legend, see Figure 3.

suitability for their presence, according to the SDM. Besides, other regions of the municipalities of Apozol, Apulco, Juchipila, Tepechitlán and Genaro Codina were highlighted, the latter in the center-south of Zacatecas. On the other hand, the northern zone shows a low potential for its presence, so it is recommended to apply a greater sampling effort in the regions presented in red. In the central portion of the state, two new records for this species can be seen, which were provided by Bañuelos-Alamillo (2018). One is located in the municipality of Jerez and the other one in the nearby municipality of Valparaíso, both coinciding with an area of high suitability for *C. polystictus*.

Regarding its global distribution, it extends from Zacatecas to Mexico City and it is similarly reported in the states of Aguascalientes, Jalisco, Guanajuato, Michoacán, Querétaro and the State of Mexico, all of them exhibiting a significant number of records. In the southwestern portion of its known distribution, the record which is found closest to Colima was in the municipality of Tuxpan in Jalisco. Several authors mentioned that this species *probably occurs* Campbell and Lamar (2004) and is *likely to occur* Lemos-Espinal et al. (2020) in Colima. However, no presence records for this area were registered.

Unlike other species with a greater number of records, there were only two presence records of *Crotalus pricei* in Zacatecas, which are located in the municipalities of Genaro Codina and Villanueva. According to the SDM (Figure 9), the western region of Za-

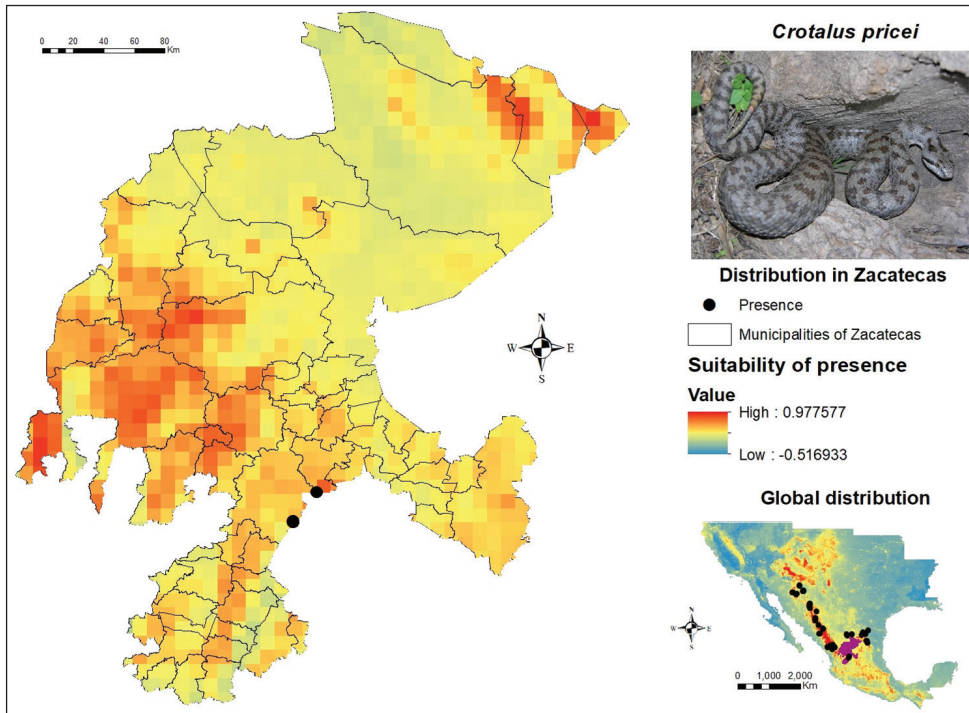


**Figure 9.** Presence and global potential distribution of *Crotalus pricei* in Zacatecas, Mexico. Insert includes a *C. pricei* from Durango state (photo provided by Jesús Sigala Rodríguez). For explanation of the symbols and legend, see Figure 3.

catecas presents the minimum essential ecological conditions for the presence of this species, mainly in the municipalities of Chalchihuites, the western portion of Fresnillo, Jerez, Jiménez del Teul, Monte Escobedo, the south of Sombrerete, Susticacán, the northern area of Tepetongo and especially the municipality of Valparaíso, which shows a high potential for its development. On the other hand, in the northern region of Zacatecas, these parameters were found in Concepción del Oro, El Salvador and Mazapil, which could be due to the occurrence records in the northeast region of its global distribution. This extends from Arizona in the southern United States, down to Mexico throughout the states of Sonora, Chihuahua and Durango, with the latter two being the states where the largest number of *C. pricei* records were concentrated, together with those located in the state of Nuevo León. In the center of Mexico, it is possible to find two specific records in San Luis Potosí, one mentioned by Grünwald et al. (2012) and an additional one included in the personal field work database of Jesús Sigala.

During the field work, no direct observations or skin sheddings were identified for this species, although there are two records a few kilometers from the Zacatecas border. One of them is located in the municipality of Mezquitic, Durango (Grünwald et al. 2012) and a more recent one is situated in Mezquitil, also in the state of Durango, and included in the personal database of Jesús Sigala. In Zacatecas, this species can be con-

sidered rare, which evidences the necessity for increased field work efforts, especially at high altitudes, since the records hereby presented were found in areas > 2,500 m., thus lying within the altitude range reported by Campbell and Lamar (2004), precisely 1,850 – 3,203 m. Therefore, it is recommended to sample high elevation areas that coincide with the greatest potential for the distribution of this species in order to confirm its presence, as well as to increase the number of records and carry out a modeling based on the presence of this organism.

*Crotalus scutulatus* is one of the species with the greatest number of records for the construction of the SDM (Figure 10). The points of occurrence gathered are mainly located in the municipalities of Guadalupe and Zacatecas, spreading their distribution range both northwards into the municipalities of General Francisco R. Murguía, Fresnillo, Río Grande and Sain Alto, and southwards, starting from Ojocaliente and finishing in Pinos. Valparaíso concentrates a substantial amount of records for this species, which is also found on the other side of the state, namely, in the municipality of Concepción del Oro. During field work, this species was identified in the municipality of Pánfilo Natera in an area of abundant plateaus and barren soil. *C. scutulatus* is es-

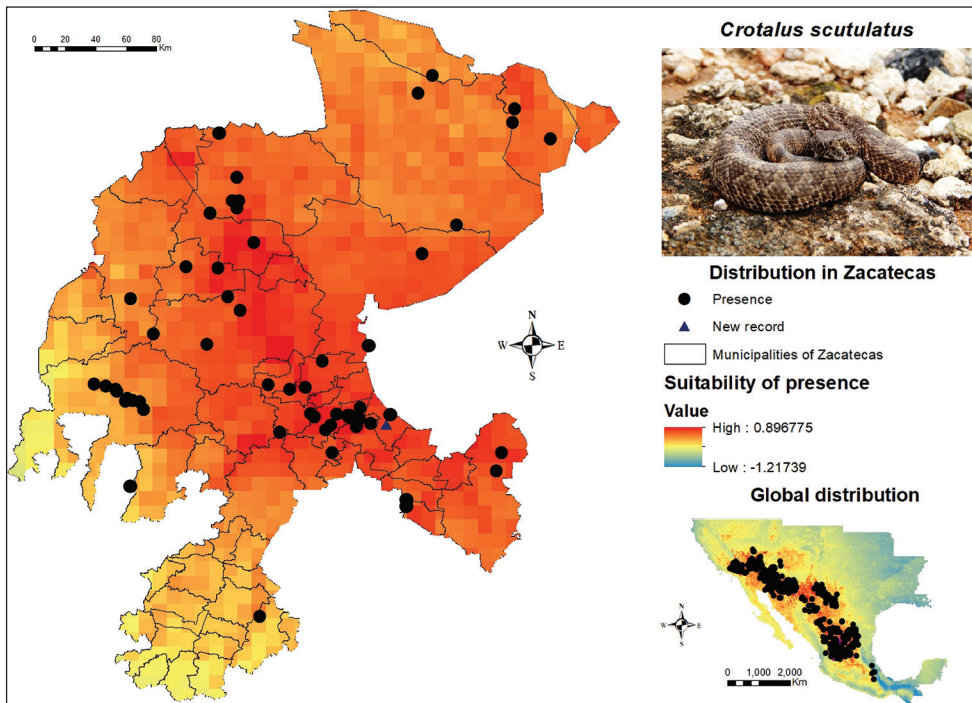


**Figure 10.** Presence and global potential distribution of *Crotalus scutulatus* in Zacatecas, Mexico. Insert includes a *C. scutulatus* from Pedregoso in the municipality of Pinos (photo provided by Lenin Lara Galván). For explanation of the symbols and legend, see Figure 3.

essentially present throughout the entire state, although the southern and southwestern regions have a medium potential suitability.

Finally, the occurrence data and the potential distribution map of *C. willardi* are shown in Figure 11. To prepare the modelling of this species throughout its known distribution range, 84 geo-referenced points were available. Among these, two were registered in Sombrerete and one in Valparaíso and according to the SDM, they are also the municipalities of Zacatecas that exhibit the greatest potential for their distribution. In addition, specific areas with high potential for its presence are shown in Fresnillo, Jiménez del Teul, Monte Escobedo and a series of municipalities in the southwestern region of the state. Along with *C. pricei*, this is one of the species with the lowest number of occurrence records in Zacatecas. Regarding their global distribution, the presence records are spread in the western region of Mexico, mainly in the states of Durango, Chihuahua and Sonora, as well as in Arizona and New Mexico in the United States. It is recommended to apply greater sampling efforts in Valparaíso and Sombrerete, especially in the Durango-Zacatecas border area in order to increase the number of localities for this species in the region.

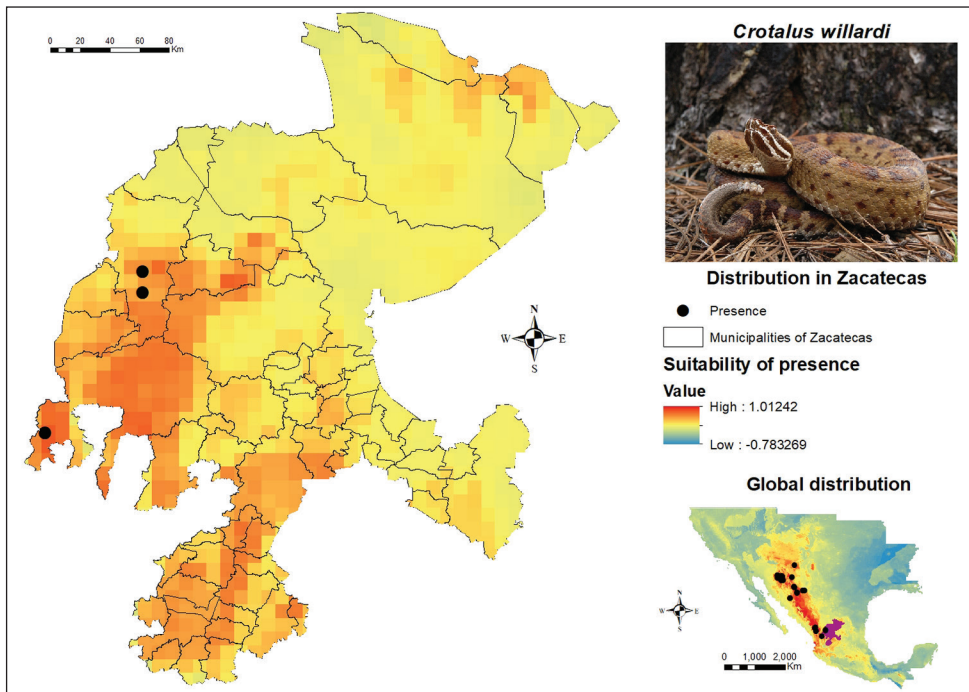


**Figure 11.** Presence and global potential distribution of *Crotalus willardi* in Zacatecas, Mexico. Insert includes a *C. willardi* from the state of Durango (photo provided by Joseph E. Forks). For explanation of the symbols and legend, see Figure 3.

**Table 3.** Rattlesnake diversity per municipality in Zacatecas, Mexico, based on published records, collection records and field work *Ca*: *Crotalus aquilus*, *Cax*: *C. atrox*, *Cb*: *C. basiliscus*, *Cl*: *C. lepidus*, *Cm*: *C. molossus*, *Cp*: *C. polystictus*, *Cpr*: *C. pricei*, *Cs*: *C. scutulatus*, and *Cw*: *C. willardi*.

Municipality	<i>Ca</i>	<i>Cax</i>	<i>Cb</i>	<i>Cl</i>	<i>Cm</i>	<i>Cp</i>	<i>Cpr</i>	<i>Cs</i>	<i>Cw</i>	Species
Apozol										–
Apulco										–
Atolinga						x				1
Benito Juárez										–
Calera de Víctor Rosales								x		1
Cañitas de Felipe Pescador				x	x					2
Concepción del Oro		x		x	x			x		4
Cuauhtémoc				x						1
Chalchihuites		x		x	x	x				4
El Plateado de Joaquín Amaro			x	x	x	x				4
El Salvador										–
Fresnillo		x		x	x	x		x		5
Genaro Codina				x	x		x	x		4
General Enrique Estrada										–
General Francisco R. Murguía		x						x		2
General Pánfilo Natera								x		1
Guadalupe		x		x	x			x		4
Huanusco	x			x	x					3
Jalpa				x	x					2
Jerez				x		x				2
Jiménez del Téul				x	x					2
Juan Aldama										–
Juchipila										–
Loreto		x								1
Luis Moya				x						1
Mazapil		x		x	x			x		4
Melchor Ocampo		x			x			x		3
Mezquital del Oro										–
Miguel Auza										–
Momax										–
Monte Escobedo				x	x	x		x		4
Morelos					x			x		2
Moyahua de Estrada			x							1
Nochistlán de Mejía	x				x			x		3
Noria de Ángeles										–
Ojocaliente		x		x				x		3
Pánuco					x			x		2
Pinos	x			x	x			x		4
Río Grande		x						x		2
Santa María de la Paz										–
Sain Alto					x			x		2
Sombrerete		x		x	x	x		x	x	6
Susticacán										–
Tabasco						x				1
Tepechitlán										–
Tepetongo										–
Teúl de González Ortega						x				1
Tlaltenago de Sánchez Román				x	x					2
Trancoso				x				x		2
Trinidad García de la Cadena										–
Valparaíso			x	x	x	x		x	x	6
Vegetrande				x						1
Villa de Cos		x			x			x		3

Municipality	<i>Ca</i>	<i>Cax</i>	<i>Cb</i>	<i>Cl</i>	<i>Cm</i>	<i>Cp</i>	<i>Cpr</i>	<i>Cs</i>	<i>Cw</i>	Species
Villa García										–
Villa González Ortega										–
Villa Hidalgo										–
Villanueva					x		x	x		3
Zacatecas				x	x			x		3
Total municipalities with presence per species:	3	12	3	23	24	10	2	23	2	

## Species at the municipal level

Thirty-nine (67.24 %) out of the fifty-eight municipalities (Table 3) have at least one record of rattlesnake species. During the field verification performed in the potential distribution areas for these organisms in Zacatecas, twenty-seven new occurrence records belonging to six species (*Crotalus atrox*, *C. basiliscus*, *C. lepidus*, *C. molossus*, *C. polysticus* and *C. scutulatus*) and one more unpublished record for *C. aquilus* were added. According to the compilation of total records, Sombrerete and Valparaíso were the municipalities exhibiting the highest rattlesnake diversity, with six different species being reported, followed by Fresnillo, with five different species. The municipalities of Chalchihuites, Concepción del Oro, El Plateado de Joaquín Amaro, Genaro Codina, Guadalupe, Mazapil, Monte Escobedo and Pinos reported four species each. The municipality of Zacatecas, where the state capital is located, has the presence of three species of this genus. Although there are no occurrence records for rattlesnakes in 19 municipalities, according to the SDM, all municipalities have the minimum conditions for the presence of rattlesnakes. It is noteworthy that *C. molossus* has reported presence in 24 municipalities and *C. lepidus* and *C. scutulatus* in 23 municipalities, as opposed to *C. pricei* and *C. willardi*, reported in only two municipalities.

## Discussion

The model building area spanned the entire known distribution range of these species, so as to cover all possible habitats where the species might be found (Merow et al. 2013). However, the discussion on results focuses on the area of interest, i.e. the state of Zacatecas, as done by Elith et al. (2011), who refer to the study area as that one having the problem or interest for the ecologist. All this aimed at gathering a greater number of occurrence records for species as *C. aquilus*, *C. pricei* and *C. willardi*.

*C. aquilus* exhibited presence records in Huanusco, Nochistlán de Mejía and Pinos. Likewise, the SDM identified the municipalities of Cuauhtémoc and Genaro Codina as potential areas for the occurrence of this species and the municipality of Pinos was also indicated as a potential area of occurrence, which is demonstrated with the presence record reported for this area.

During our post-modelling field work, further occurrence records were collected. Moreover, when interviews were applied to individuals from different communities,

*C. basiliscus* was pointed out as a frequently spotted species in the region. Given that this organism is easily mistaken for *C. molossus*, we only considered records backed up with specimens and the knowledge that *C. basiliscus* prefers zones around 1,000 meters above sea level, which are the sites where georeferencing data were obtained. This is in agreement with the information reported by Campbell and Lamar (2004), who stated that this species prefers ecotone zones between tropical deciduous forests and pine-oak forests. Our results suggest that the slope is one of the most important variables for the construction of the distribution model for this species.

Human influence was one of the most widely used variables for the construction of potential distribution models for *C. atrox*, *C. lepidus*, *C. molossus*, *C. scutulatus*, *C. pricei* and *C. willardi*, which is consistent with the literature and data obtained, since the first four species do not seem to have any problem to occupy habitats in close proximity to both urban and rural areas. In relation to this, presence records of *C. atrox* and *C. molossus* were obtained within populated areas, sightings of *C. lepidus* and *C. molossus* were also registered in the hills of Los Alamitos and La Virgen, which are located next to the largest and most populated urban area in the state. Sightings of *C. lepidus* in the aforementioned regions occurred in steep slopes and predominantly rocky soils, being the first variable (i.e. slope) among the ones selected for the construction of the SDM. Human presence is not an obstacle for the sighting of *C. atrox* and *C. scutulatus*, or at least for their transit in the vicinity of noisy urban areas with dense housing and transportation infrastructures. Indeed, some of the documented records for *C. atrox* are in paved and dirt roads. Moreover, Tay-Zavala et al. (2002) mentioned *C. atrox* and *C. scutulatus* as two of the most important species in medical terms in Mexico, due to the large amount of snakebites caused by them. Those two species presented the greatest number of presence records and their distribution range is extensive across the USA and Mexico, including the state of Zacatecas.

Records of *C. pricei* in Zacatecas are scarce and Campbell and Lamar (2004) did not mention the distribution of this species in Zacatecas. However, it is reported in the historical records of Klauber (1949) and in this same study, very nearby localities in the state of Durango are mentioned. In the neighboring state of Aguascalientes, this species is extremely rare according to Sigala-Rodríguez (2008). However, Bañuelos-Alamillo (pers. comm. 2018) mentioned a new record in 2017. The SDM points out regions in northeastern Zacatecas, specifically the municipalities of Concepción del Oro, El Salvador and Mazapil, as those with a high distribution potential. This may be due to the fact that these municipalities have mountain ranges whose altitudes are higher than 2,900 meters above sea level (INEGI 2017), with altitude being one of the variables used to construct the model of the species in question, which agrees with Campbell and Lamar (2004), who mentioned the preference of this species for high elevations. Another potential reason why these areas turned out to be potential for this species could be the occurrence records of *C. pricei* in northeastern Mexico.

*C. scutulatus* has a wide distribution throughout the state. However, there are areas in southwestern Zacatecas which, according to the SDM, have a medium potential for the development of this species. This may be due to the type of vegetation preferred by these organisms and, consequently, the type of climate, given that these regions are usu-

ally more humid, as they lie within the Juchipila and Tlaltenango canyons. This results in a topography that greatly differs from that in most of Zacatecas, which, according to Campbell and Lamar (2004), are the most suitable habitats for the settling of this species. In the case of the specimen found in the municipality of General Pánfilo Natera, the sampled area exhibited a rocky, eroded soil, where *Opuntia* spp. was the predominant crop.

No specimens were recorded for *C. willardi* during post-modelling field work. Yet, all the individuals who were interviewed to gather further location data, when being shown photographs of rattlesnakes from Zacatecas, mentioned having seen this species in the mountainous regions within the municipality of Valparaíso. The physical characteristics of this species, such as its color and the shape of its head, rattle and scales, is what allowed the locals to immediately discriminate it from the rest of species reported in the state. Although field sampling failed to provide additional presence records for this species, the habitat, environment and altitudinal range in those regions in Valparaíso are coincident with the characteristics that Campbell and Lamar (2004) mention for this species.

There are no occurrence records for any rattlesnake species in 19 of the municipalities in Zacatecas (Table 3). However, it is important to point out that this does not mean that no records might be found in these zones, since according to the outputs produced by the distribution models for these species, all the municipalities in the state have appropriate conditions for the presence of at least one rattlesnake species. Zacatecas is one of the most extensive states in the central-northern part of Mexico; hence, additional sampling efforts are required to report new records within the state and SDM predictions can be a valuable tool to guide sampling effort in an efficient and cost-effective manner.

## Conclusions

Based on the obtained records and the field work, the distribution of nine rattlesnake species (*Crotalus* genus) was confirmed in the state of Zacatecas: *C. aquilus*, *C. atrox*, *C. basiliscus*, *C. lepidus*, *C. molossus*, *C. polystictus*, *C. pricei*, *C. scutulatus* and *C. willardi*. In addition to the confirmed records, there is available indirect information on their presence in many areas, including personal communications, unverified sightings and detailed descriptions of specimens matching the physical characteristics and ecological requirements of the species. However, it is necessary to confirm their presence in these zones.

We recommend applying greater field work efforts in areas where no occurrence records have yet been identified for these species, as well as for organisms that showed the lowest number of records, particularly in the areas with a higher potential for presence. Likewise, we strongly advise conducting field work during the July-October period, since this will increase the sighting probability. We also suggest updating models once additional occurrence records have been registered.

Results obtained from the distribution modeling of these species generally agree with field work verification, making it possible to prioritize field efforts more effectively in different localities. During field work verification, multiple night sightings of rattlesnakes

were noted, both alive or run over by vehicles on the roads, being the latter one of the major causes of death of these species in the state. This piece of information was merely gathered for *Crotalus molossus* and *C. atrox*, species, which were found in these areas.

This paper represents substantial contribution to the knowledge on rattlesnakes in Zacatecas. Their occurrence records are shown and zones with greatest diversity within the state are inferred. Moreover, this study indicates the potential distribution areas of these organisms. This material will be of major help for the implementation of strategies on public health issues, as well as for the proposal of management and conservation plans for these species.

## Suggestions

We believe that this study could be used by individuals wishing to conduct future projects related to rattlesnake conservation in Zacatecas. We also encourage the publication and incorporation of new occurrence records that contribute to gather further information on these organisms in the state.

## Acknowledgements

All authors thank the reviewers, whose comments and suggestions provided great input and enriched this manuscript.

J.L.L.G. would like to thank the National Science, Technology and Innovation Council for the grant awarded to study the Graduate Degree in Natural Resource Management Innovation, from which this research arose. I similarly thank Jorge Bañuelos-Alamillo for having provided occurrence records. Further, to Iván Ahumada Carrillo and Joseph E. Forks for the outstanding photographs included within this manuscript; to Eric Centenero Alcalá for generously lending valuable photographic material that was used in the catalog during the interviews and a special thanks to Xabier Herrero for helping to improve the translation of this document.

A.M.B. was funded by Fundação para a Ciência e a Tecnologia, Portugal (Contract No. IF/00266/2013 related to the exploratory project CP1168/CT0001).

J.J.S.R. was funded by PRODEP-SEP and by institutional resources, initially from Universidad Autónoma de Zacatecas and currently from the Universidad Autónoma de Aguascalientes.

Finally, the authors would like to thank Jesús Lara Rayos, Paulo Sergio Haro Galván, Mónica Díaz Teniente, Emmeth Rodríguez Pérez, Guillermo Alatorre de Alba, Delia Hernández Juárez, Rodolfo Zacarías Alvarado, Jorge Bañuelos Alamillo, Violeta Bañuelos Frías, as well as the individuals from the various localities visited, for their field work collaboration aiming at the verification of the SDMs.

Collecting permits needed to conduct field work were issued to Jesús Sigala-Rodríguez: SGPA/DGVS/ 06292/06, SGPA/DGVS/ 09453/14, SGPA/DGVS/

05874/17, and scientific collector permit FAUT-0110 SGPA/DGVS/ 04324 and to David Lazcano-Villarreal SGPA/DGVS/ 011906/17.

## References

- Ahumada-Carrillo IT (2010) Herpetofauna del municipio de Atolinga, Zacatecas. Tesis de licenciatura, Guadalajara, Jalisco: Universidad de Guadalajara. <http://biblioteca.cucba.udg.mx:8080/xmlui/handle/123456789/4927>
- Ahumada-Carrillo IT, Vázquez-Huizar O, Vázquez-Díaz J, García UO (2011) Noteworthy records of amphibians and reptiles from Mexico. *Herpetological Review*, 42(2): 397–398.
- Araújo M, Peterson A (2012) Uses and misuses of bioclimatic envelope models. *Ecology* 93(7): 1527–1539. <https://doi.org/10.1890/11-1930.1>
- Arnaud G, Trujillo LB, Hernández I, Avila H, Murillo R, Quijada A (2008) Natural history of the rattlesnake *Crotalus catalinensis*, endemic of Santa Catalina Island, Gulf of California, Mexico. *Estudios de Las islas del Golfo de California*, 2001: 93–100.
- Ávila-Herrera L (2012) Serpientes venenosas del estado de Zacatecas, México. Tesis de licenciatura, Zacatecas, Zacatecas: Universidad Autónoma de Zacatecas.
- Ávila-Herrera L, Esparza-Estrada CE, Sigala-Rodríguez JJ (2020) Serpientes venenosas. En: La biodiversidad en Zacatecas. Estudio de Estado. CONABIO, México, 246–248.
- Ávila-Villegas H (2017) Serpiente de Cascabel. Entre el peligro y la conservación. (Primera ed.) Comisión Nacional para el Conocimiento y Uso de la Biodiversidad. ISBN: 978-607-8328-96-3.
- Bañuelos-Alamillo JA (personal communication, 2018) Personal database of presence records for species in the *Crotalus* genus in Zacatecas. Mention *Crotalus basiliscus* y *Crotalus pricei* in Zacatecas.
- Barbosa M (2015) fuzzySim: applying fuzzy logic to binary similarity indices in ecology. *Methods in Ecology and Evolution* 6: 853–858. <https://doi.org/10.1111/2041-210X.12372>
- Campbell JA, Lamar WW (2004) *The Venomous Reptiles of the Western Hemisphere*. Comstock, Cornell University Press. <https://doi.org/10.1016/j.jrstmh.2004.12.001>
- Carbajal-Márquez RA, González-Saucedo ZY, Arenas-Monroy JC (2015a) *Crotalus aquilus* Klauber, 1952 (Squamata: Viperidae), a New State Record for Zacatecas, Mexico. *Acta Zoológica Mexicana* 0065–1737(31): 131–133. <https://doi.org/10.21829/azm.2015.311528>
- Carbajal-Márquez RA, Bañuelos-Alamillo JA, Rivas-Mercado EA, Quintero-Díaz GE, Dominguez de la Riva MA (2015b) *Crotalus basiliscus* (Mexican west coast rattlesnake). Geographic distribution: Zacatecas. *Herpetological Review* 46(3): 1–385.
- CEC [Commission for Environmental Cooperation] (2017) *North America Environmental Atlas*. <http://www.cec.org/> [accessed in November 14, 2016]
- Chávez-Avila S, Casas-Andreu G, García-Aguayo A, Cifuentes-Lemus JL, Cupul-Magaña P (2015) Anfibios y Reptiles del estado de Jalisco: Análisis espacial, distribución y conservación. Universidad de Guadalajara.
- Climate Data (2018) Climate data for North America. <https://en.climate-data.org> [accessed in April 23, 2018]

- CONABIO [Comisión Nacional para el Conocimiento y Uso de la Biodiversidad] (2016) Red Mundial de Información sobre Biodiversidad. Acceso a la información: *Crotalus* <https://www.conabio.gob.mx> [accessed in November 09, 2016]
- CONABIO [Comisión Nacional para el Conocimiento y Uso de la Biodiversidad] (2017) Portal de Geoinformación. <http://www.conabio.gob.mx/informacion/gis/> [accessed in December 04, 2017]
- Elith J, Graham C, Anderson R, Dudík M, Ferrier S, Guisan A, Hijmans R, Huettmann F, Leathwick J, Lehmann A, Li J, Lohmann L, Loiselle B, Manion G, Moritz C, Nakamura M, Nakazawa Y, Overton J, Peterson A, Zimmermann N (2006) Novel methods improve prediction of species distributions from occurrence data. *Ecography* 29: 129–151. <https://doi.org/10.1111/j.2006.0906-7590.04596.x>
- Elith J, Phillips SJ, Hastie T, Dudík M, Chee YE, Yates CJ (2011) A statistical explanation of MaxEnt for ecologists. *Diversity and Distributions* 17(1): 43–57. <https://doi.org/10.1111/j.1472-4642.2010.00725.x>
- Elizalde-Arellano C, López-Vidal J, Hernández-Arciga R, Villegas-Ruiz J (2018) Los Anfibios y Reptiles del estado de Guanajuato. Secretaría de Medio Ambiente y Ordenamiento Territorial Estado de Guanajuato.
- Esparza-Estrada CE (2014) Distribución de las serpientes de cascabel en México mediante el uso de modelado de nicho ecológico. Tesis de licenciatura, Zacatecas, Zacatecas: Universidad Autónoma de Zacatecas.
- ESRI [Environmental Systems Research Institute] (2016) ArcGIS 10.5.1 [Computer software]. Esri Inc., Redlands.
- Fick SE, Hijmans RJ (2017) WorldClim 2: new 1-km spatial resolution climate surfaces for global land areas. *International Journal of Climatology* 37(12): 4302–4315. <https://doi.org/10.1002/joc.5086>
- Flores-Villela O, García-Vázquez UO (2014) Biodiversidad de reptiles en México. *Revista Mexicana de Biodiversidad* 85(SUPPL.): 467–475. <https://doi.org/10.7550/rmb.43236>
- GBIF [Global Biodiversity Information Facility] (2016) Custom data export. Get data, occurrences: *Crotalus*. <https://www.gbif.org> [accessed in October 10, 2016 and September 2020]
- Grünwald CI, Pérez-Rivera N, Ahumada-Carrillo IT, Franz-Chávez H, La Forest BT (2012) New distributional records for the herpetofauna of Mexico. *Herpetological Review* 47(1): 85–90.
- Guisan A, Theurillat JP (2000) Equilibrium modeling of alpine plant distribution: how far can we go? *Phytocoenologia* 30(3–4): 353–384. <https://doi.org/10.1127/phyto/30/2000/353>
- Gutiérrez-Rodríguez J, Barbosa M, Martínez-Solano Í (2017) Integrative inference of population history in the Ibero-Maghrebian endemic *Pleurodeles waltl* (Salamandridae). *Molecular Phylogenetics and Evolution* 112: 122–137. <https://doi.org/10.1016/j.ympev.2017.04.022>
- INEGI [Instituto Nacional de Estadística y Geografía] (2008) Conjunto de datos vectoriales de la carta de la Carta de Unidades Climáticas. Scale, 1:1 000 000. <https://www.inegi.org.mx> [accessed in November 16, 2019]
- INEGI [Instituto Nacional de Estadística y Geografía] (2017) Continuo de Elevaciones Mexicano: Modelo de Elevación Digital (MED). <https://www.inegi.org.mx/app/geo2/elevacionesmex/> [accessed in November 17, 2017]

- IUCN [International Union for Conservation of Nature] (2017) The IUCN Red List of Threatened Species, Version 2020-2. <http://www.iucn.org>
- Jadin RC, Smith EN, Campbell JA (2011) Unravelling a tangle of Mexican serpents: A systematic revision of highland pitvipers. *Zoological Journal of the Linnean Society* 163(3): 943–958. <https://doi.org/10.1111/j.1096-3642.2011.00748.x>
- Klauber LM (1949) The subspecies of the ridge-nosed rattlesnake, *Crotalus willardi*. *Transactions of the San Diego Society of Natural History* 11(8): 121–140. <https://doi.org/10.5962/bhl.part.28859>
- Lara-Galván JL (2015) Serpientes venenosas de Aguascalientes y Zacatecas: Patrones de distribución y riqueza de especies. Tesis de Licenciatura, Zacatecas, Zacatecas: Universidad Autónoma de Zacatecas.
- Lazcano-Villarreal D (1997) Anfibios y reptiles del estado de Nuevo León. Universidad Autónoma de Nuevo León. Facultad de Ciencias. Informe final SNIB-CONABIO. proyecto No. B099. México.
- Lazcano-Villarreal D, Banda-Leal J, Jacobo-Galván RD (2010) Serpientes de Nuevo León. Universidad Autónoma de Nuevo León.
- Lemos-Espinal JA, Smith GR (2016a) Amphibians and reptiles of the state of Coahuila, Mexico, with comparison with adjoining states. *Zookeys* 593: 117–137. <https://doi.org/10.3897/zookeys.593.8484>
- Lemos-Espinal JA, Smith GR, Cruz A (2016b) Amphibians and Reptiles of the state of Nuevo León, Mexico. *Zookeys* 594: 123–141. <https://doi.org/10.3897/zookeys.594.8289>
- Lemos-Espinal JA, Smith GR, Gadsden-Esparza H, Valdez-Lares R, Woolrich-Piña GA (2018a) Amphibians and reptiles of the state of Durango, Mexico, with comparisons with adjoining states. *ZooKeys* (748): 65–87. <https://doi.org/10.3897/zookeys.748.22768>
- Lemos-Espinal JA, Smith GR, Cruz A (2018b) Amphibians and Reptiles of Nuevo León, México. *Rodeo New Mexico: ECO-Herpetological Publishing and Distribution, Rodeo New Mexico*, 370 pp.
- Lemos-Espinal JA, Smith GR, Woolrich-Piña GA (2018c) Amphibians and reptiles of the state of San Luis Potosí, Mexico, with comparisons with adjoining states. *ZooKeys* 753: 83–106. <https://doi.org/10.3897/zookeys.753.21094>
- Lemos-Espinal JA, Smith GR, Valdez-Lares R (2019) Amphibians and Reptiles of Durango, México. *ECO-Herpetological Publishing and Distribution, Rodeo New Mexico*, 414 pp.
- Lemos-Espinal JA, Smith GR, Pierce LJS, Painter CW (2020) The amphibians and reptiles of Colima, Mexico, with a summary of their conservation status. *ZooKeys* 927: 99–125. <https://doi.org/10.3897/zookeys.927.50064>
- Lobo JM, Jiménez-Valverde A3, Real R (2008) AUC: A misleading measure of the performance of predictive distribution models. *Global Ecology and Biogeography* 17(2): 145–151. <https://doi.org/10.1111/j.1466-8238.2007.00358.x>
- Luja VH, Ahumada-Carrillo IT, Ponce-Campos P, Figueroa-Esquivel E (2014) Checklist of amphibians of Nayarit, western Mexico. *Check List* 10(6): 1336–1341. <https://doi.org/10.15560/10.6.1336>
- Maritz B, Penner J, Martins M, Crnobrnja-Isailović J, Spear S, Alencar L, Sigala-Rodríguez J, Messenger K, Clark R, Soorae P, Luiselli L, Jenkins C, Greene H (2016) Identifying global

- priorities for the conservation of vipers. *Biological Conservation* 204: 94–102. <https://doi.org/10.1016/j.biocon.2016.05.004>
- Meik JM, Streicher JW, Mociño-Deloya E, Setser K, Lazcano-Villarreal D (2012) Shallow phylogeographic structure in the declining Mexican Lance-headed Rattlesnake, *Crotalus poly-stictus* (Serpentes: Viperidae). *Phyllomedusa: Journal of Herpetology* 11(1): 3–11. <https://doi.org/10.11606/issn.2316-9079.v11i1p3-11>
- Merow C, Smith MJ, Silander JA (2013) A practical guide to MaxEnt for modeling species' distributions: What it does, and why inputs and settings matter. *Ecography* 36(10): 1058–1069. <https://doi.org/10.1111/j.1600-0587.2013.07872.x>
- Morrone JJ, Escalante T, Rodríguez-Tapia G (2017) Mexican biogeographic provinces: Map and shapefiles. *Zootaxa* 4277(2): 277–279. <https://doi.org/10.11646/zootaxa.4277.2.8>
- Naimi B, Araújo M (2016) Sdm: A reproducible and extensible R platform for species distribution modelling. *Ecography* 39(4): 368–375. <https://doi.org/10.1111/ecog.01881>
- Paredes-García MD, Ramírez-Bautista A, Martínez-Morales MA (2011) Distribución y representatividad de las especies del género *Crotalus* en las áreas naturales protegidas de México. *Revista Mexicana de Biodiversidad* 82: 689–700. <https://doi.org/10.22201/ib.20078706e.2011.2.464>
- Phillips SJ, Anderson RP, Schapire RE (2006) Maximum entropy modeling of species geographic distributions. *Ecological Modeling* 190: 231–259. <https://doi.org/10.1016/j.ecol-model.2005.03.026>
- QGIS Development Team (2009) QGIS 2.18.24. QGIS Geographic Information System. Open Source Geospatial Foundation Project. <http://qgis.osgeo.org>
- Reino L, Ferreira M, Martínez-Solano Í, Segurado P, Xu C, Barbosa M (2017) Favourable areas for co-occurrence of parapatric species: niche conservatism and niche divergence in Iberian tree frogs and midwife toads. *Journal of Biogeography* 44: 88–98. <https://doi.org/10.1111/jbi.12850>
- R Core Team (2016) A language and environment for statistical computing. R Foundation for Statistical Computing, Vienna. <http://www.R-project.org/>
- Santiago-Pérez AL, Rosas-Espinoza VC, Domínguez-Laso M, Rodríguez-Canseco JM (2017) First record of *Crotalus poly-stictus* (Squamata: Viperidae) in the protected natural area of Sierra de Quila, Jalisco, Mexico. *Acta Zoológica Mexicana* 33(1): 108–112. <https://doi.org/10.21829/azm.2017.3311017>
- Schild D, Adams R, Card D, Corbin A, Jezkova T, Hales N, Meik J, Perry B, Spencer C, Smith L, Campillo-García G, Bouzid N, Strickland J, Parkinson C, Borja M, Castañeda-Gaytán G, Bryson R, Flores-Villela O, Mackessy S, Castoe T (2018) Cryptic genetic diversity, population structure, and gene flow in the Mojave rattlesnake (*Crotalus scutulatus*). *Molecular Phylogenetics and Evolution* 127: 669–681. <https://doi.org/10.1016/j.ympev.2018.06.013>
- Secor SM (2016) Ecological Significance of Movements and Activity Range for the Sidewinder, *Crotalus cerastes*. *American Society of Ichthyologists and Herpetologists (ASIH) Vol. 1994, No. 3 (Aug. 17, 1994), 631–645.* <https://doi.org/10.2307/1447179>
- SEMARNAT [Secretaría de Medio Ambiente y Recursos Naturales] (2019) Modificación al anexo normativo III, lista de especies en riesgo de la Norma Oficial Mexicana NOM-059-Ecol-(2010) Protección ambiental-Especies nativas de México de flora y fauna silvestres-

Categorías de riesgo y especificaciones para su inclusión, exclusión o cambio-Lista de especies en riesgo, publicado el 30 de diciembre del 2010.

- Sigala-Rodríguez JJ (2008) La serpiente de cascabel *Crotalus pricei* (Serpentes: Viperidae) en Aguascalientes: ¿Especie rara o en peligro de extinción?. En La Biodiversidad en Aguascalientes: Estudio de Estado. 2008. Comisión Nacional para el Conocimiento y Uso de la Biodiversidad (CONABIO), Instituto del Medio Ambiente del Estado de Aguascalientes (IMAE), Universidad Autónoma de Aguascalientes (UAA). ISBN: 978-970-9000-45-0. México, 147 pp.
- Sigala-Rodríguez JJ, Quintero-Díaz GE, Ahumada-Carrillo IT, Carbajal-Márquez RA, Enríquez ED, Vacio de la Torre MR (2020) Reptiles. En: La biodiversidad en Zacatecas. Estudio de Estado. CONABIO, México, 235–240.
- Strickland J, Smith C, Mason A, Schield D, Borja M, Castañeda-Gaytán G, Spencer C, Smith L, Trápaga A, Bouzid N, Campillo-García G, Flores-Villela O, Antonio-Rangel D, Mackessy S, Castoe T, Rokyta D, Parkinson C (2018) Evidence for divergent patterns of local selection driving venom variation in Mojave Rattlesnakes (*Crotalus scutulatus*). Scientific Reports 8(1): 1–15. <https://doi.org/10.1038/s41598-018-35810-9>
- Tay-Zavala J, Díaz-Sánchez JG, Sánchez-Vega JT, Ruiz-Sánchez D, Castillo L (2002) Serpientes y reptiles de importancia médica en México. Rev Fac Med UNAM, 45(No. 5 Septiembre-October), 212–219.
- Uetz P, Hošek J (2018) The Reptile Database. <http://www.reptile-database.org> [accessed on January 25, 2018]
- Valdez-Lares R, Muñoz-Martínez R, Gadsden H, Aguirre-León G, Castañeda-Gaytán G, González-Trápaga R (2013) Checklist of amphibians and reptiles of the state of Durango, México. Check List 9(4): 714–724. <https://doi.org/10.15560/9.4.714>
- Vázquez-Díaz J, Quintero-Díaz GE (2005) Anfibios y Reptiles de Aguascalientes. CONABIO. CIEMA, A.C. México.
- Vertnet [Vertebrate Networks] (2016) Database: *Crotalus*. <https://www.vرتnet.org> [accessed in October 12, 2016]
- Woolrich-Pina GA, Ponce-Campos P, Loc-Barragan J, Ramirez-Silva JP, Mata-Silva V, Johnson JD, Garcia-Padilla E, Wilson LD (2016) The herpetofauna of Nayarit, Mexico: composition, distribution, and conservation. Mesoamerican Herpetology 3: 376–448.

## Supplementary material I

### SF1 *Crotalus aquilus* global distribution

Authors: Jesús Lenin Lara-Galván, Juan Felipe Martínez-Montoya, A. Márcia Barbosa

Data type: Image

Explanation note: Global model of potential distribution.

Copyright notice: This dataset is made available under the Open Database License (<http://opendatacommons.org/licenses/odbl/1.0/>). The Open Database License (ODbL) is a license agreement intended to allow users to freely share, modify, and use this Dataset while maintaining this same freedom for others, provided that the original source and author(s) are credited.

Link: <https://doi.org/10.3897/zookeys.1005.56964.suppl1>

## Supplementary material 2

### SF2 *Crotalus atrox* global distribution

Authors: Jesús Lenin Lara-Galván, Juan Felipe Martínez-Montoya, A. Márcia Barbosa

Data type: Image

Explanation note: Global model of potential distribution.

Copyright notice: This dataset is made available under the Open Database License (<http://opendatacommons.org/licenses/odbl/1.0/>). The Open Database License (ODbL) is a license agreement intended to allow users to freely share, modify, and use this Dataset while maintaining this same freedom for others, provided that the original source and author(s) are credited.

Link: <https://doi.org/10.3897/zookeys.1005.56964.suppl2>

## Supplementary material 3

### SF3 *Crotalus basiliscus* global distribution

Authors: Jesús Lenin Lara-Galván, Juan Felipe Martínez-Montoya, A. Márcia Barbosa

Data type: Image

Explanation note: Global model of potential distribution.

Copyright notice: This dataset is made available under the Open Database License (<http://opendatacommons.org/licenses/odbl/1.0/>). The Open Database License (ODbL) is a license agreement intended to allow users to freely share, modify, and use this Dataset while maintaining this same freedom for others, provided that the original source and author(s) are credited.

Link: <https://doi.org/10.3897/zookeys.1005.56964.suppl3>

## Supplementary material 4

### SF4 *Crotalus lepidus* global distribution

Authors: Jesús Lenin Lara-Galván, Juan Felipe Martínez-Montoya, A. Márcia Barbosa

Data type: Image

Explanation note: Global model of potential distribution.

Copyright notice: This dataset is made available under the Open Database License (<http://opendatacommons.org/licenses/odbl/1.0/>). The Open Database License (ODbL) is a license agreement intended to allow users to freely share, modify, and use this Dataset while maintaining this same freedom for others, provided that the original source and author(s) are credited.

Link: <https://doi.org/10.3897/zookeys.1005.56964.suppl4>

## Supplementary material 5

### SF5 *Crotalus molossus* global distribution

Authors: Jesús Lenin Lara-Galván, Juan Felipe Martínez-Montoya, A. Márcia Barbosa

Data type: Image

Explanation note: Global model of potential distribution.

Copyright notice: This dataset is made available under the Open Database License (<http://opendatacommons.org/licenses/odbl/1.0/>). The Open Database License (ODbL) is a license agreement intended to allow users to freely share, modify, and use this Dataset while maintaining this same freedom for others, provided that the original source and author(s) are credited.

Link: <https://doi.org/10.3897/zookeys.1005.56964.suppl5>

## Supplementary material 6

### SF6 *Crotalus polystictus* global distribution

Authors: Jesús Lenin Lara-Galván, Juan Felipe Martínez-Montoya, A. Márcia Barbosa

Data type: Image

Explanation note: Global model of potential distribution.

Copyright notice: This dataset is made available under the Open Database License (<http://opendatacommons.org/licenses/odbl/1.0/>). The Open Database License (ODbL) is a license agreement intended to allow users to freely share, modify, and use this Dataset while maintaining this same freedom for others, provided that the original source and author(s) are credited.

Link: <https://doi.org/10.3897/zookeys.1005.56964.suppl6>

## Supplementary material 7

### SF7 *Crotalus pricei* global distribution

Authors: Jesús Lenin Lara-Galván, Juan Felipe Martínez-Montoya, A. Márcia Barbosa

Data type: Image

Explanation note: Global model of potential distribution.

Copyright notice: This dataset is made available under the Open Database License (<http://opendatacommons.org/licenses/odbl/1.0/>). The Open Database License (ODbL) is a license agreement intended to allow users to freely share, modify, and use this Dataset while maintaining this same freedom for others, provided that the original source and author(s) are credited.

Link: <https://doi.org/10.3897/zookeys.1005.56964.suppl7>

## Supplementary material 8

### SF8 *Crotalus scutulatus* global distribution

Authors: Jesús Lenin Lara-Galván, Juan Felipe Martínez-Montoya, A. Márcia Barbosa

Data type: Image

Explanation note: Global model of potential distribution.

Copyright notice: This dataset is made available under the Open Database License (<http://opendatacommons.org/licenses/odbl/1.0/>). The Open Database License (ODbL) is a license agreement intended to allow users to freely share, modify, and use this Dataset while maintaining this same freedom for others, provided that the original source and author(s) are credited.

Link: <https://doi.org/10.3897/zookeys.1005.56964.suppl8>

## Supplementary material 9

### SF9 *Crotalus willardi* global distribution

Authors: Jesús Lenin Lara-Galván, Juan Felipe Martínez-Montoya, A. Márcia Barbosa

Data type: Image

Explanation note: Global model of potential distribution.

Copyright notice: This dataset is made available under the Open Database License (<http://opendatacommons.org/licenses/odbl/1.0/>). The Open Database License (ODbL) is a license agreement intended to allow users to freely share, modify, and use this Dataset while maintaining this same freedom for others, provided that the original source and author(s) are credited.

Link: <https://doi.org/10.3897/zookeys.1005.56964.suppl9>

# *Tetramesa amica* and its parasitoid *Eurytoma amicophaga* (Hymenoptera, Eurytomidae): two new species associated with medusahead, *Taeniatherum caput-medusae* (Poaceae)

Hossein Lotfalizadeh<sup>1</sup>, Jean-Yves Rasplus<sup>2</sup>,  
Massimo Cristofaro<sup>3,4</sup>, Francesca Marini<sup>4</sup>

**1** Plant Protection Research Department, East Azarbaijan Agricultural and Natural Resources Research & Education Center, AREEO, Tabriz, Iran **2** CBGP, Univ. Montpellier, CIRAD, INRA, IRD, Montpellier SupAgro, Montpellier, France **3** Centro di Ricerca Casaccia, Agenzia Nazionale Nuove Tecnologie, Energia, e Sviluppo Economico (ENEA), Via Anguillarese, 301, I-00123, Rome, Italy **4** Biotechnological and Biological Control Agency (BBCA) onlus, Rome, Italy

Corresponding author: Hossein Lotfalizadeh ([hlotfalizadeh@gmail.com](mailto:hlotfalizadeh@gmail.com))

Academic editor: A. Köhler | Received 10 July 2020 | Accepted 1 December 2020 | Published 18 December 2020

<http://zoobank.org/FB01F523-32C8-455C-A7BD-C0FE4F00EC08>

**Citation:** Lotfalizadeh H, Rasplus J-Y, Cristofaro M, Marini F (2020) *Tetramesa amica* and its parasitoid *Eurytoma amicophaga* (Hymenoptera, Eurytomidae): two new species associated with medusahead, *Taeniatherum caput-medusae* (Poaceae). ZooKeys 1005: 133–149. <https://doi.org/10.3897/zookeys.1005.56353>

## Abstract

Medusahead, *Taeniatherum caput-medusae* (Poales: Poaceae), is an annual grass native to central Asia and the Mediterranean region. It is a noxious, invasive weed in much of western North America. During field explorations carried out in Greece in 2017, the new phytophagous eurytomid *Tetramesa amica* Lotfalizadeh, **sp. nov.** and its parasitoid *Eurytoma amicophaga* Lotfalizadeh, **sp. nov.**, also new to science, were recorded for the first time on medusahead. These new species are described and characters that enable to recognize them from their closest relatives are summarized. *Tetramesa* species are generally species-specific gall-inducers. They induce damages that may have a significant impact on the physiology of infested plants by reducing the productivity of flowering heads and seed weight. Based on these data, *T. amica* Lotfalizadeh, **sp. nov.** is currently being investigated as a candidate biological control agent of medusahead.

## Keywords

Biological control, Chalcidoidea, parasitoid, phytophagous, weeds

## Introduction

Medusahead, *Taeniatherum caput-medusae* (L.) Nevski (Poaceae), is a self-pollinating annual grass, native of the Mediterranean region. It has been introduced in northern and north-western Europe, Chile, Australia, as well as in the Americas (Major et al. 1960; Peters 2013; Kyser et al. 2014). This grass is currently listed as a noxious, invasive weed in many states of Western USA, with a 12% spreading rate per year (Rice 2005). In most cases, it becomes quickly established in the localities where it was introduced (Archer 2001). *Taeniatherum caput-medusae* is highly competitive and replaces more desirable annual grasses and forbs (Sharp et al. 1957), but it is almost worthless as forage.

In the past, a few pathogens, such as *Fusarium arthrosporioides*, *Pseudomonas fluorescens*, *Ustilago phrygica* were reported as natural enemies of *T. caput-medusae* (Sforza et al. 2004). A species of eriophyid mite, *Aculodes altamurgiensis*, which is highly specific to medusahead, is currently under investigation as a candidate for biological control (Cristofaro et al. 2020). However, until now no phytophagous insect has been reported to develop on this weed.

Eurytomidae (Hymenoptera, Chalcidoidea) includes 1400–1500 species distributed in 88 genera worldwide (Noyes 2020) and they are mostly parasitoids. In the Palaearctic region, the family includes phytophagous species, mostly in the genera *Tetramesa*, *Bruchophagus* and *Systole*. Most of the 202 described species of *Tetramesa* are known to be species-specific and their host-range is generally restricted to a single grass species, a genus or, in a few cases, on closely related genera (Phillips 1936; Claridge 1961; Dawah 1987). Eggs are laid in the stems of the host plants and the larvae are stem galling and borers, whereas adults feed on nectar (Claridge 1961; Claridge and Dawah 1994; Al-Barrak et al. 2004). Galls induced by the larvae can reduce the productivity of flowering heads and seed weight (Claridge 1961; Spears 1978) and a few *Tetramesa* spp. are sometimes considered pests of crops (Phillips 1927; Spears 1978; Spears and Barr 1985). Claridge (1958, 1961), Szelényi (1968), and Zerova (1965, 1967, 1976, 1978) extensively revised the Palaearctic species of *Tetramesa*, and Graham (1974) studied the species fauna of England.

The significant impact on their host and their high host-specificity make *Tetramesa* species interesting candidates for biological control of weeds. Some species of *Tetramesa* have already been used against invasive grasses such as *Arundo donax* in the USA (Goolsby and Moran 2009) and *Sporobolus* spp. in Australia (Witt and McConnachie 2003).

Until now and despite numerous surveys, no *Tetramesa* has been found associated with the genus *Taeniatherum* (Noyes 2020). Our study presents the first record of a phytophagous eurytomid wasps associated with *T. caput-medusae*. We describe *Tetramesa amica* Lotfalizadeh, sp. nov. and its parasitoid, *Eurytoma amicophaga* Lotfalizadeh, sp. nov. (Hymenoptera: Eurytomidae).

## Materials and methods

Infested samples of *T. caput-medusae* were collected near the town Alexandroupoli (Greece) close to Greek-Turkish border, from 2017 to 2019 and examined in the labo-

ratory. The site was visited once a month, from May to July, and stem galls were collected. Insects were obtained by natural emergence to adults from spikes kept under controlled conditions (24–26 °C, 80% RH, 16L:12D), or by dissecting dry stem galls. Specimens were desiccated using HMDS (Heraty and Hawks 1998) and glued on point cards. Terminology follows Harris (1979) for cuticular sculpture and Lotfalizadeh et al. (2007) for morphology.

The following keys were used to identify *Tetramesa* species: Claridge (1958, 1961) and Zerova (1965, 1967, 1976, 1978). Identification of *Eurytoma* species was performed using keys by Zerova (1976, 1977, 1978, 2010). Images were performed with a Keyence digital microscope (VHX-5000) and were edited in Adobe Photoshop CS6 software. Holotype and paratypes are deposited at **HMIM** (Hayk Mirzayans Insect Museum, Tehran, Iran) and paratypes at **CBGP** (Centre de Biologie pour la Gestion des Populations, Montferrier-sur-Lez, France).

Abbreviations used in the text:

- C1–3** first to third clavomere;  
**F1, F2, etc.** first funiculars, second funiculars, etc.;  
**Gt1-n** Gastral terga 1-n;  
**OOL** ocular–ocellar line (= the shortest distance between posterior ocellus and adjacent eye margin);  
**POL** posterior ocellar line (= the shortest distance between the posterior ocelli).

## Results

Two eurytomid species belonging to *Tetramesa* and *Eurytoma* were obtained from stem galls on *T. caput-medusae*. These two species appeared to be new and are described hereafter

### *Tetramesa amica* Lotfalizadeh, sp. nov.

<http://zoobank.org/A116AC65-D628-4F3D-AB44-B3766C9F1DB7>

Figures 1, 2

**Type material.** *Holotype*: female, ex *Taeniatherum caput-medusae*, 8 May 2017, 27 July 2018, and 21 May 2019 (galls collection dates), by F. Marini (deposited in HMIM); Paratypes: 20♀♀ & 3♂♂, same data as holotype (deposited in HMIM & CBGP).

**Type locality.** Highway E90, between E0 Ardaniou Orestiadass and E0 Alexandroupoli Kipon, ca. 5 km west of the border of Greece-Turkey and 1.3 km northeast of Vrysoùla (40°56'58"N, 26°14'59"E), 40 m above sea level, Dimos Alexandroupoli, Greece.

**Diagnosis.** *Tetramesa amica* Lotfalizadeh, sp. nov. differs from other species of *Tetramesa* by the combination of the following characters: in female, F1–2 longer than broad, F3–5 as long as broad; fore wing with an obscure black spot under marginal

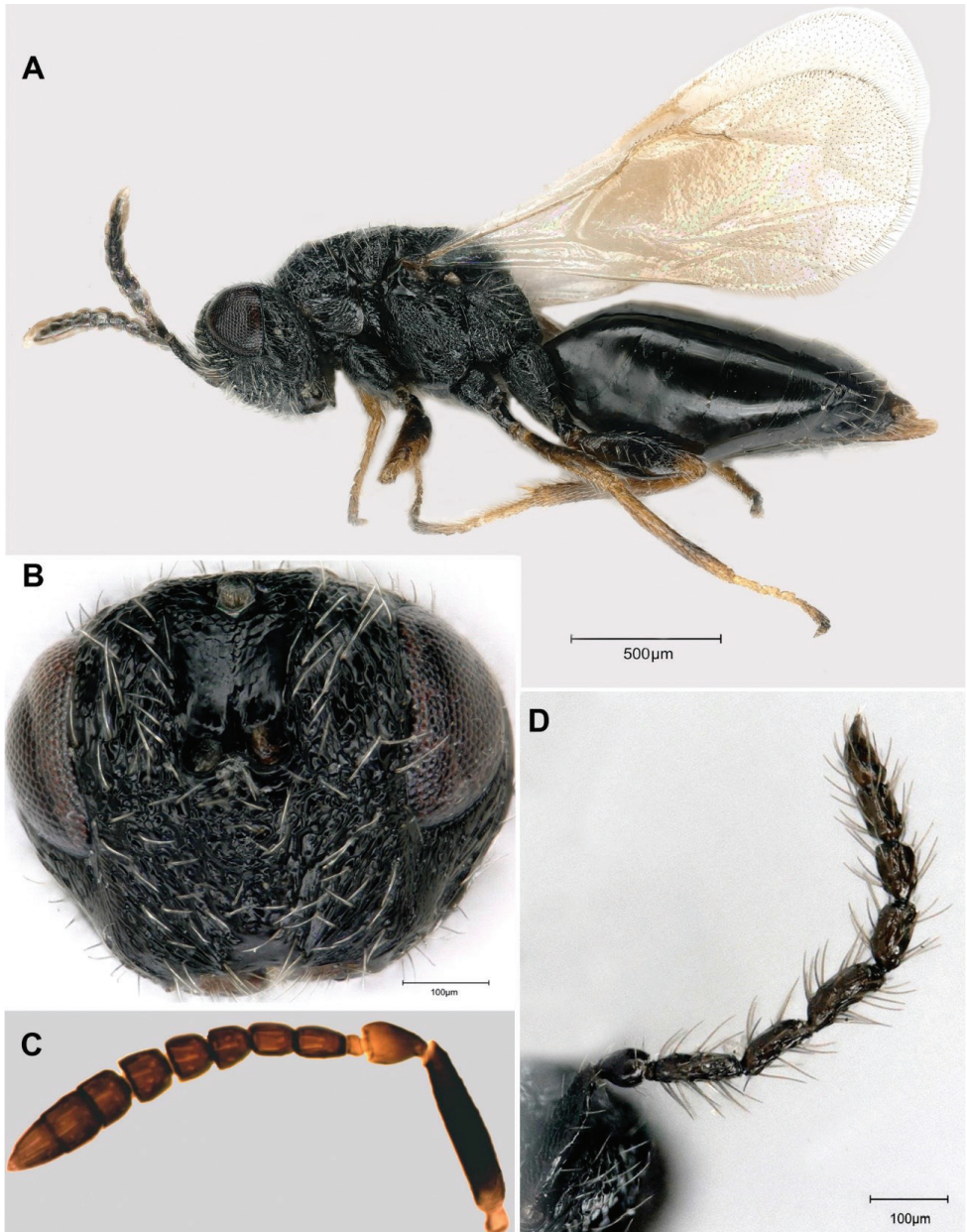


**Figure 1.** *Tetramesa amica* Lotfalizadeh, sp. nov. **A** female habitus in lateral view **B** head of female in frontal view **C** female antenna **D** male antenna.

vein; gaster longer than head+ mesosoma; marginal vein much longer than postmarginal and stigmal veins; in male all funiculars longer than wide, with long setae, longer than width of funiculus; F1–3 as same as long.

**Description. Holotype Female.** *Body* length 2.4 mm. Black, coxae black, pro- and mesofemur brown with a median dark band, metafemur dark brown at apex, all

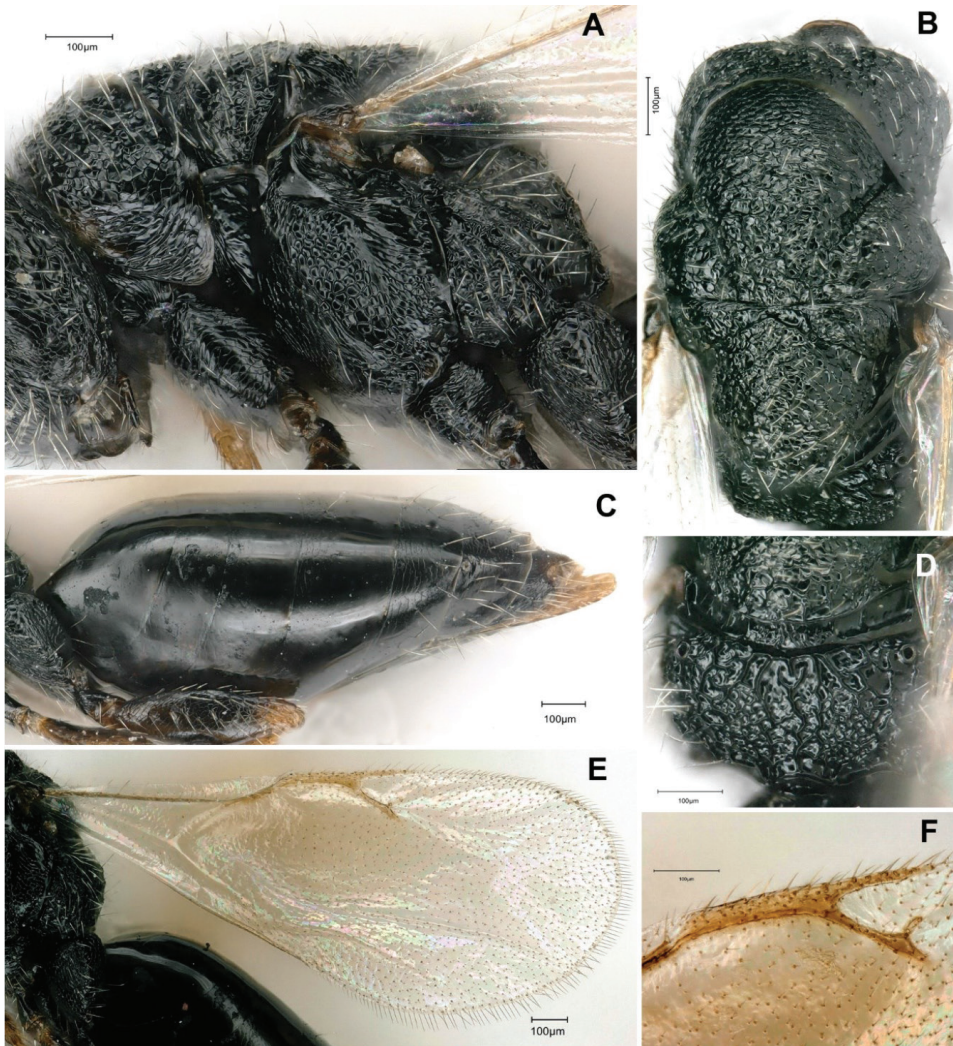


**Figure 2.** *Tetramesa amica* Lotfalizadeh, sp. nov., female **A** mesosoma in lateral view **B** mesosoma in dorsal view **C** metasoma in lateral view **D** propodeum in dorsal view **E** fore wing **F** fore wing venation.

tibiae brown with a faint dark brown median band, tarsi bright yellow, except last tarsomere; tegula dark medially and brown in margin; pronotum with pair of small yellow spots antero-laterally; fore wing hyaline, slightly infuscate below marginal vein; veins yellowish brown. Antenna mainly dark, except scape basally, pedicel in distal half and anellus brownish; ovipositor brown. Setae on body whitish, those on wings blackish.

**Head** in dorsal view stout,  $1.7 \times$  as broad as long, distinctly wider than pronotum; temple rounded laterally, very short,  $2.0 \times$  shorter than eye. POL  $2.1 \times$  OOL (13:6). Head in frontal view, wider than height (18:14); malar space shorter than longitudinal eye diameter (6:8). Ventral margin of clypeus slightly emarginated (Fig. 1B), dorsally smooth, laterally strigose. Scrobe relatively deep, unclearly bordered, with subparallel edges, tapering only slightly basally. Eye glabrous; cheek shorter than longitudinal di-

iameter of eye (60:80). Face sculpture distinct, reticulated-cellular, with very short and sparse pubescence. Head, in lateral view, ca.  $1.3 \times$  as long as wide.

**Antenna** (Fig. 1C) inserted distinctly above middle of face; scape long (100:22), not convex, reaching level of anterior ocellus; pedicel  $1.36 \times$  as long as wide (34:25); with 5 funiculars, anellus small, ca.  $1.5 \times$  as broad as long (8:14); F1 long,  $1.5 \times$  as long as wide (32:16), F2 longer than broad (27:20), F3 as long as broad (24:24), F4 slightly wider (24:25), F5 wider than long (25:28); with three clavomeres, clavomeres clearly separated, C1 (24: 30), C2 (27:30), C3 (33:30), width of clava exceeding width of flagellum (30:28).

**Mesosoma** in lateral view elongated (Fig. 2A), relatively convex, with mesonotum and mesoscutellum at the same level. Propodeum  $2.0 \times$  as wide as long (14:7), with slight median depression, three longitudinally irregular rugae, peripherally coarsely rugose (Fig. 2D), slightly inclined relative to mesonotum (ca.  $70^\circ$ ), in dorsal view ca.  $0.7 \times$  as long as mesoscutellum (70:105), almost half as long as mesoscutum (70:140). Mesoscutellum as long as wide medially. Pronotum and mesonotum reticulate, with scattered and inconspicuous umbilicate sculpture, more distinct on mesoscutellum and pronotum. Metacoxa elongate, weakly reticulated.

**Fore wing** (Fig. 2E) ca.  $2.2 \times$  as long as its maximum width, infusate under marginal vein. Marginal vein relatively long and slightly expanded; ratio of marginal, postmarginal and stigmal veins: 70:55:55 (Fig. 2F).

**Metasoma** elongated, narrowed apically (in lateral view) (Fig. 2C), longer than head + mesosoma, with extremely short petiole, Gt1 longest, shorter than Gt2 and Gt3 combined; relative measurements Gt1–7: 26, 23, 17, 10, 13, 5, 7. All terga shiny, Gt5–7 weakly reticulated.

**Male.** Length of body 2.1–2.3 mm. Coloration and sculpture as in females, but yellow spots smaller and predominant on face and upper corners of pronotum. Antenna (Fig. 1D) with seven flagellomeres and long pubescence. Petiole of first tergum short, at most twice longer than its width. Metasoma long,  $0.5$ – $0.65 \times$  as long as mesosoma.

**Comparative notes.** *Tetramesa amica* is closely related to *Tetramesa inermis* Erdős, 1963, *T. matrana* Erdős, 1969, and *T. cylindrica*. Diagnostic characters that enable one to discriminate *T. amica* sp. nov. from these species are presented in Tables 1–3.

The antenna of *T. amica* sp. nov. resembles that of *T. fumipennis* except F1 that is not constricted basally (Fig. 1C) (conical in *T. fumipennis*), with five funiculars, with three clavomeres (respectively six and two in *T. fumipennis*), head in its lower part wider than in *T. fumipennis* and gaster more flattened dorsally than in *T. fumipennis*.

**Etymology.** The specific epithet derives from the Latin noun *amicus* (i.e., friendship) and refers to the friendship between entomologists from different countries (France, Iran, and Italy), which made possible the sampling, discovery, and description of this new species.

**Host.** Medusahead, *Taeniatherum caput-medusae* (L.) Nevski (Poaceae). Adults are phytophagous and lay eggs into medusahead stems. Oviposition and larval development induce a response of the plant, which produces stem galls, from which adults emerge.

**Table 1.** Features distinguishing *Tetramesa amica* Lotfalizadeh, sp. nov. from *Tetramesa inermis* Erdős, 1963.

Characters	<i>Tetramesa amica</i> Lotfalizadeh, sp. nov.	<i>Tetramesa inermis</i> Erdős, 1963†
Pronotal antero-lateral yellow spots	With a pair of small yellow spots, hardly seen dorsally	With a pair of relatively large spots, well seen dorsally
Frons sculpture in the lower part	Laterally straight and medially smooth (Fig. 1B)	Entirely straight
Antennal anellus in female	Wider than long (Fig. 1C)	Longer than wide
Length of funiculars in female	F1 ca. 1.5 × as long as wide, F2 longer than broad, F3–5 as long as broad (Fig. 1C)	F1 ca. 1.5 × as long as wide, F2–3 square, F4–5 transverse
Length of clava in female	Longer than the three pre-claval funiculars together (83:72) (Fig. 1C)	Equal to the three pre-claval funiculars together
Male antenna	Funicule thick, funiculars constricted basally and apically (Fig. 1D)	Funicule filiform, funiculars without basal and apical constriction
Sculpture of mesoscutellum	Identical to pronotum (Fig. 2B)	Coarser than pronotum
Uncus of stigma	Distinct and long (Fig. 2F)	As usual (not especially long)
Host plant	<i>Taeniatherum caput-medusae</i>	<i>Bromus</i> spp.

† See figures in Erdős (1963) and Zerova (1976).

**Table 2.** Features distinguishing *Tetramesa amica* Lotfalizadeh, sp. nov. from *Tetramesa matrana* Erdős, 1969.

Characters	<i>Tetramesa amica</i> Lotfalizadeh, sp. nov.	<i>Tetramesa matrana</i> Erdős, 1969
Funiculars in female	F2 longer than broad, F3–5 as long as broad (Fig. 1C)	F2–3 as long as broad, F4–5 transverse
Length of clava	Longer than the three pre-claval funiculars together (83:72) (Fig. 1C)	Equal to the three pre-claval funiculars together
Sculpture of mesoscutellum	Identical to pronotum (Fig. 2B)	Coarser than pronotum.
Propodeum	coarsely rugose (Fig. 2D)	almost non-sloping, highly shiny, densely reticulate
Host plant	<i>Taeniatherum caput-medusae</i>	<i>Arrhenatherum elatius</i> L.

**Table 3.** Features distinguishing *Tetramesa amica* Lotfalizadeh, sp. nov. from *Tetramesa cylindrica* (Schlechtendal, 1891).

Characters	<i>Tetramesa amica</i> Lotfalizadeh, sp. nov.	<i>Tetramesa cylindrica</i> (Schlechtendal, 1891)†
Width of the head (frontal view)	1.2 × wider than long (Fig. 1B)	0.8 × wider than long
Length of funiculars of the female	F1–2 longer than wide, F3–5 quadrate (Fig. 1C)	Only F1 longer than wide, F2–5 quadrate
Male antenna	Funiculars non-depressed medially (Fig. 1D)	F2–4 depressed medially
Gastral sculpture	Mainly smooth (Fig. 2C)	Finely alutaceous dorsally
Length of metasoma	1.1 × as long as mesosoma + head (Fig. 1A)	As long as mesosoma + head
Postmarginal vein	1.4 × the length of marginal vein (Fig. 2F)	As long as marginal vein
Stigma vein	As long as postmarginal vein (Fig. 2F)	0.7 × the length of postmarginal vein
Host plant	<i>Taeniatherum caput-medusae</i>	<i>Stipa capillata</i>

† See figures in Zerova (1965, 1967).

***Eurytoma amicophaga* Lotfalizadeh, sp. nov.**

<http://zoobank.org/1FB6F92C-A988-4BCE-AEEB-3FD6627F0FFE>

Figures 3, 4

**Type material.** *Holotype:* female, ex *Tetramesa amica* Lotfalizadeh, sp. nov. on *Taeniatherum caput-medusae*, 28 May 2017, 27 July 2018, and 21 May 2019 (galls collection dates), F. Marini leg. (deposited in HMIM). *Paratypes:* same data as holotype, 1♀ & 5♂♂ (deposited in HMIM & CBGP).

**Type locality.** Highway E90, between E0 Ardaniou Orestiadass and E0 Alexandroupoli Kipon, ca. 5 km west of the border of Greece-Turkey and 1.3 km northeast of Vrysoùla (40°56'58"N, 26°14'59"E), 40 m above sea level, Dimos Alexandroupoli, Greece.

**Diagnosis.** All funiculars longer than broad, with F1 ca. 2.5 × as long as wide (Fig. 3A). Pro- and mesonotum densely punctured (Fig. 4B), and narrow interspaces coriaceous sculpture. Gaster long, as long as mesosoma + head. Gt4 longest tergum, ovipositor horizontal.

**Description. Holotype. Female. Body** length 3.3 mm. Coloration: body black; following areas yellow to reddish brown: profemur apically and interiorly, protibia interiorly, mid femur and tibia basally and apically, metafemur apically and metatibia basally, three basal tarsomeres, distal spurs of tibiae; wing veins brown. Valvulae mostly dark brown.

**Head** 1.3 × as wide as long (164:125) (Fig. 4F). Relative measurements: head width 158, head length 130, width of frontovertex 100, length of eye 62, length of temple 12, ocellar diameter 15, distance between lateral and median ocelli 18, POL 35, OOL 20, malar space 45, height of eye 72. Head relatively transverse in dorsal view (140:85) (Fig. 4E). Anterior outline of frons slightly convex. Temple with straight lateral outline, hardly converging back-wards and strongly angulate with occiput. Clypeus hardly emarginated. Lower face mostly strigose laterally, ridges not reaching antennal toruli above, face punctured latero-dorsally (Fig. 3C). Frons covered with piliferous punctures. Malar carina raised near oral fossa, curved, incomplete, not reaching lower margin of eye above (Fig. 3C). Gena entirely punctured, inter-punctures finely reticulate, gena without area of fine sculpture behind malar carina. Genal carina raised; outline of carina forming blunt angle above oral fossa. Inter-torular space deeply sulcate, bearing one row of hairs. Inner margins of antennal toruli raised. Lateral margin of antennal scrobes carinate, forming a raised lobe above toruli. Postgenal laminae expanded, visible in lateral view as a small tooth (Fig. 3C). Scape 55, slightly swelling ventrally, straight dorsally. Pedicel + flagellum as long as width of head (130). Pedicel short, 2 × as long as wide (20:10) with a basal bottleneck (Fig. 3C). With five funiculars, all funiculars longer than wide, F4–5 as long as broad (Fig. 3C). F1 longer than pedicel (25:20) (Fig. 3C), 2.5 × as long as wide (25:10), following segments progressively decreasing in length (20, 17, 17, 15, 15). With three clavomeres (38), slightly tapering to apex, and narrowly rounded (Fig. 3C).

Relative measurements of mesosoma: length 205, width 120, length of pronotal collar 105, mesoscutum as long as mesoscutellum 70; width of mesoscutellum 75. Pro- and mesonotum densely punctured (Fig. 4B), inter-punctures coriaceous. Notauli impressed but obliterated by sculpture of mesoscutum, especially in posterior part. Axillar grooves obliterated by sculpture anteriorly, not reaching transscutal line. Dorsal outline of mesoscutellum strongly convex. Frenal arms visible laterally. Propodeum slightly sloping, slightly inclined with main axis of mesonotum (Fig. 4D), broadly concave in middle, with an areolate median groove, not delimited by submedian ridges and visible through change in sculpture only, generally reticulate-areolate. Adscrobal carina of mesopleuron distinctly raised ventrally (Fig. 4A); femoral depression mostly

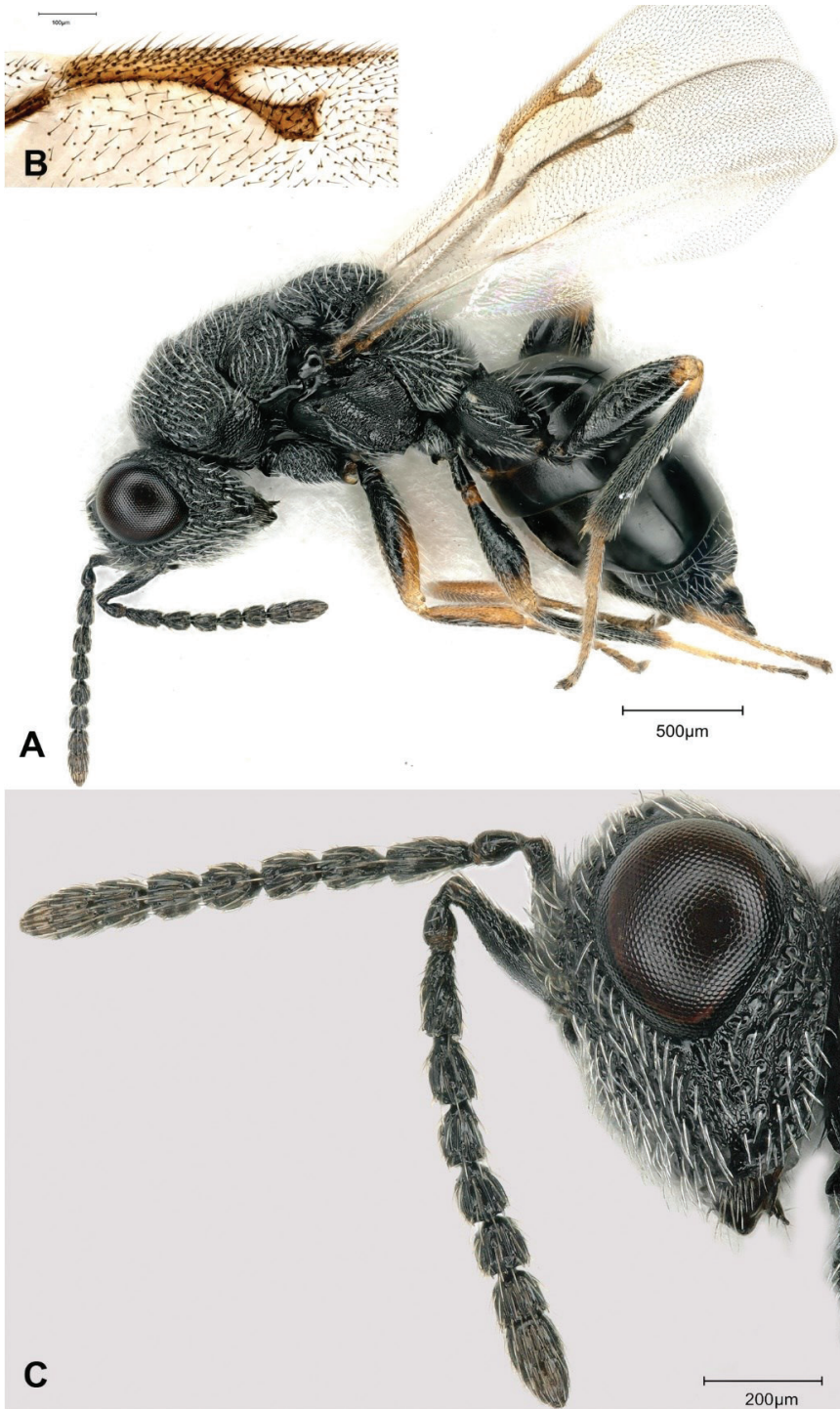


**Figure 3.** *Eurytoma amicophaga* Lotfalizadeh, sp. nov., female **A** female habitus in lateral view **B** fore wing venation **C** head and antennae in lateral view.

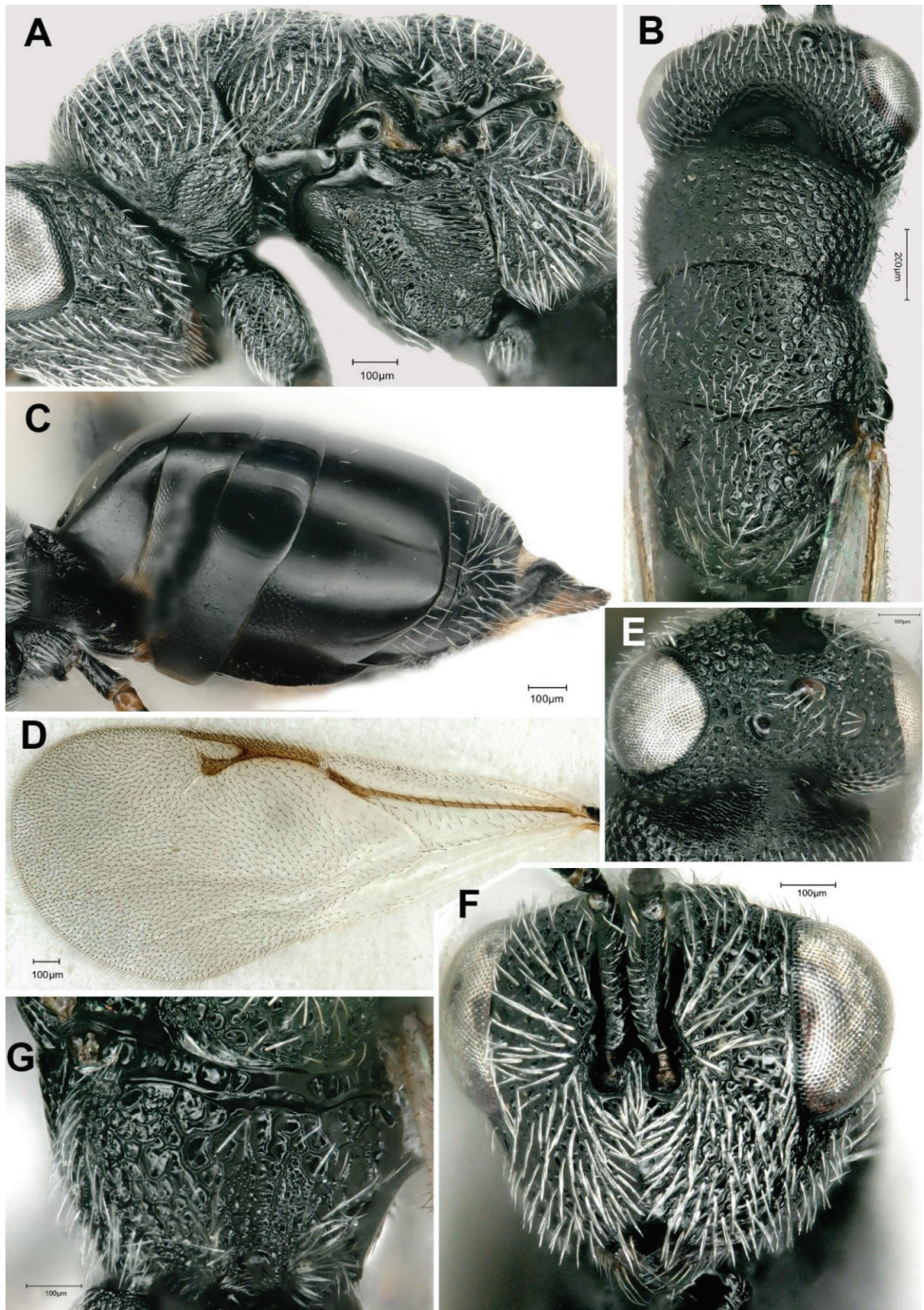


**Figure 4.** *Eurytoma amicophaga* Lotfalizadeh, sp. nov., female **A** mesosoma in lateral view **B** mesosoma in dorsal view **C** metasoma in lateral view **D** fore wing **E** head in dorsal view **F** head in frontal view **G** propodeum in dorsal view.

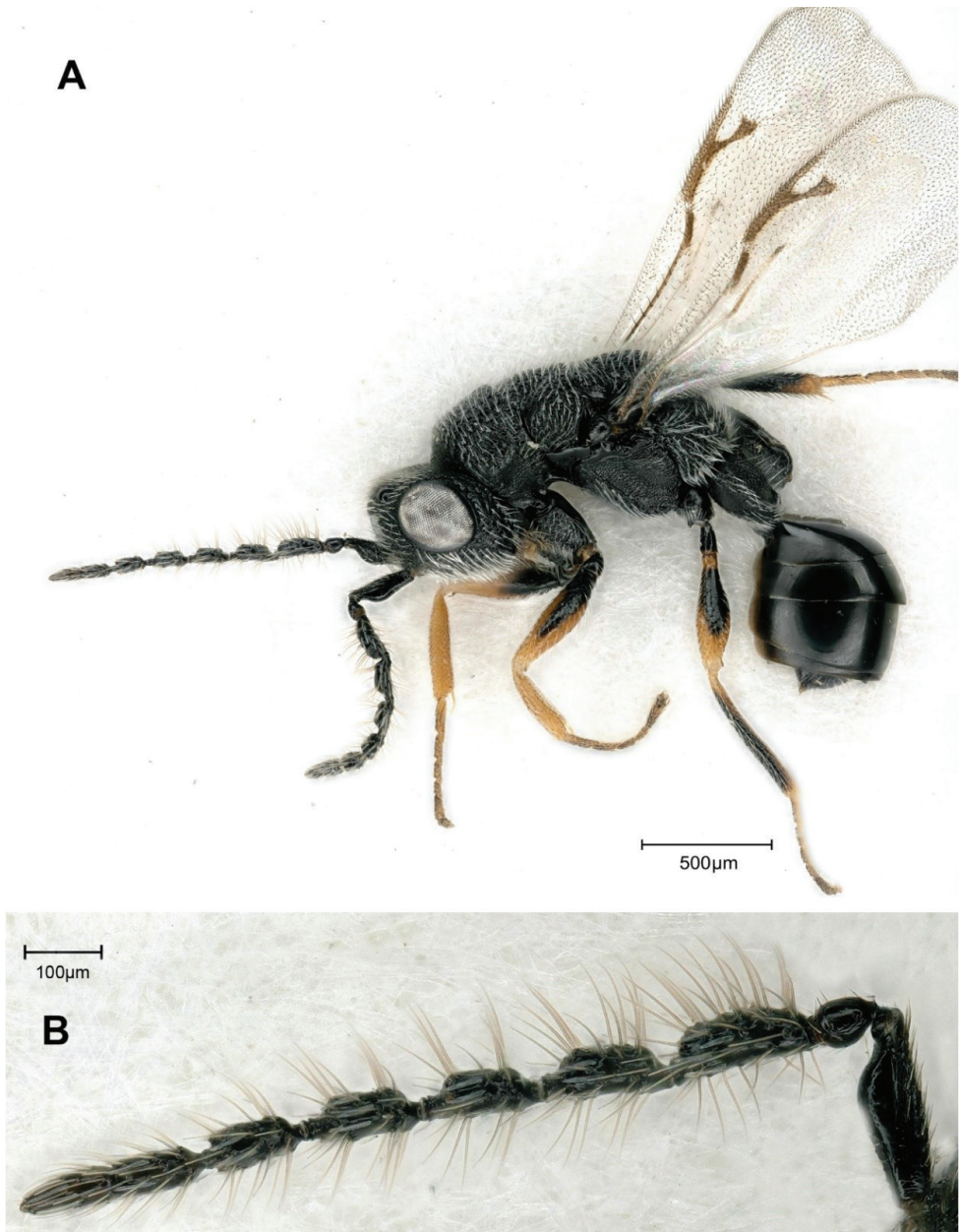


**Figure 5.** *Eurytoma amicophaga* Lotfalizadeh, sp. nov., male **A** male in lateral habitus, **B** antenna.

reticulate, with some carinulae. Mesepimeron mostly reticulate ventrally, striolate dorsally, with usual longitudinal rugae originating from its posterior margin, finely reticulate ventrally. Procoxae with usual oblique groove and S-like basal ridge of *Eurytoma*. Mesocoxae with well-developed lamella distally, striolate on anterodorsal surface. Metacoxa entirely reticulate, bare dorsally at base. Fore wing ca.  $2.3 \times$  longer than wide

(175:75) (Fig. 4D), marginal vein  $1.2 \times$  as long as stigmal vein (80:65); postmarginal vein (75) slightly shorter than marginal vein (Fig. 3B). Basal cell partly sparsely hairy; speculum reduced to a narrow stripe behind parastigma; dorsal surface of costal cell with three or four rows of setae.

**Petiole.** Gastral petiole transverse, bearing usual dorso-median and lateral teeth, which are acute. Gaster longer than mesosoma (105:90) (Fig. 4C), height 48, respective lengths of Gt1–6 on median line as 26, 15, 12, 24, 18 and 28; syntergum 30; maximal lateral length of Gt4: 75. Gt1 with usual basal submedian pits. Posterior margins of Gt5 diverging ventrally, margin of Gt4 convex dorsally. Gt2 and Gt3 basally (in lateral view) and Gt4 ventrally with a well delimited area showing reticulate sculpture. Gt4 not completely overlapping Gt5 laterally and emarginate on posterior margin dorsally. Gt5 not punctulate dorsally. Gt6 not carinate dorsally. Valvulae not ascending backwards with main axis of gaster (Fig. 4C).

**Male** (Fig. 5A). Body length 1.6 mm. Characters distinctive from female: Scape distinctly swollen anteriorly and ventrally (Fig. 5B). With 7 flagellomeres, basally wider and longer than distal, segments pedunculate with at least 2 rows of erect setae on F2–F5 and ca.  $1.5\text{--}2 \times$  as long as wide, last two flagellomeres definitely separated. Relative measurements of scape 75:25, of pedicel 28:27. Gastral petiole elongate, as long as metacoxa, evenly reticulate, cylindrical in lateral view, lateral length ca.  $1.4 \times$  as long as greatest width, with slight ventral carina (Fig. 5A).

**Variations.** Body length ranges from 2.5 to 3.6 mm. Pro and mesofemora, scape sometimes nearly entirely black. Marginal vein slightly to distinctly longer than stigmal vein.

**Comparative notes.** *Eurytoma amicophaga* Lotfalizadeh, sp. nov. is distinct from other species of this species group. It is characterized by elongated funiculars, although *E. steffani* Claridge, 1959 and *E. pollux* Claridge, 1959 share similar funicular segments. However, *E. steffani* has all funicular segments longer than broad (F4–5 quadrate in *E. amicophaga* Lotfalizadeh, sp. nov.). *Eurytoma pollux* obviously differs from *E. amicophaga* in the longer head in frontal view, less than  $1.2 \times$  longer than broad (wider head, more than  $1.3 \times$  longer than broad in *E. amicophaga* Lotfalizadeh, sp. nov.) and marginal vein more than  $1.5 \times$  as long as stigmal vein (less than  $1.5 \times$  as long as stigmal vein in *E. amicophaga* Lotfalizadeh, sp. nov.). *Eurytoma amicophaga* Lotfalizadeh, sp. nov. is also closely related to *E. festucae* Zerova, 1977 and may be separated by characters summarized in Table 4.

**Table 4.** Features distinguishing *Eurytoma amicophaga* Lotfalizadeh, sp. nov. from *Eurytoma festucae* Zerova, 1977.

Characters	<i>Eurytoma amicophaga</i> Lotfalizadeh, sp. nov.	<i>Eurytoma festucae</i> Zerova, 1977†
Width of head (frontal view)	$1.2 \times$ as wide as long (Fig. 4F)	$1.9 \times$ as wide as long
Male antenna	Funiculars long, F1 more than $2 \times$ as long as wide (Fig. 5B)	Funiculars short, F1 distinctly $< 2 \times$ as long as wide
Scape in male antenna	long, $2.8 \times$ as long as wide	short, $2.2 \times$ as long as wide
F1 length	$2.5 \times$ as long as wide (Fig. 3A)	$2 \times$ as long as wide
Marginal vein	Long, more than $1.5 \times$ as long as stigmal vein (Fig. 3A)	Short, as long as stigmal vein
Host	<i>Tetramesa amica</i> Lotfalizadeh, sp. nov. on <i>Taeniatherum caput-medusae</i>	<i>Tetramesa brevicollis</i> on <i>Festuca</i> spp.

† See figures in Zerova (2010).

**Etymology.** The specific name refers to the host species (*Tetramesa amica* Lotfalizadeh, sp. nov.) with which holotype is associated.

**Host.** *Tetramesa amica* Lotfalizadeh, sp. nov. (Hymenoptera: Eurytomidae). Larvae feed on *T. amica* larvae and adults emerge from the stem galls caused by *T. amica* larvae on medusahead plants.

## Discussion

Several studies have been carried out on the taxonomy and biology of species of *Eurytoma* and *Tetramesa* associated with grasses in the Palaearctic region. However, no revision of these genera has been published so far and the identification of species remains difficult. This is also due to the rather uniform morphology of these wasps that renders their identification challenging (Henneicke et al. 1992; Lotfalizadeh et al. 2007). *Tetramesa amica* Lotfalizadeh, sp. nov. belongs to the *cylindrica* species group of *Tetramesa*. This distinctive group of species is characterized by the alutaceous sculpture of head and thorax, without distinct umbilicate punctures, and with small pronotal yellow spots (Claridge 1961). The *cylindrica* species group includes *T. aciculata* (Schlechtendal, 1891), *T. cylindrica* (Schlechtendal, 1891), *T. dispar* Zerova, 1965, *T. ukrainica* Zerova, 1965, *T. punctata* Zerova, 1965 and *T. scheppigi* (Schlechtendal, 1891) (Claridge 1961; Zerova 1976).

Several species of *Tetramesa* have been shown to efficiently affect the populations of their host plants. Substantial reduction in seed weight was reported for an undescribed *Tetramesa* on *Aristida longiseta* Steud., *Sitanion hystrix* (Nutt.), *Sporobolus cryptandrus* (Torr.) and *Stipa comata* Trin. & Rupr. (i.e., 47, 33, 46, and 60%, respectively), with consequent reduction in seed germination (e.g., up to 99% of *A. longiseta* seeds not germinating) (Spears and Barr 1985). Witt and Mc Connachie (2003) collected a stem-boring *Tetramesa* species on *Sporobolus pyramidalis* P. Beauv., *S. africanus* Poir. A. Robyns and Tournay and *S. natalensis* (Steud.) in South Africa. They reported a high rate of prevalence of *Tetramesa* in stems with up to 33% of *S. pyramidalis* infested by *Tetramesa* larvae. Inflorescences of approximately 60% of the infested culms were malformed and significantly shorter than non-infested one. Finally, the stem-galling wasp *T. romana* is considered one of the best biological control agents released in USA to control giant reed (*Arundo donax*) (Goolsby and Moran 2009; Goolsby et al. 2016; Moran et al. 2017). Therefore, based on our current knowledge on *Tetramesa* spp., *T. amica* exhibits characteristics to be considered a prospective biocontrol agent against *T. caput-medusae*. Since few biological and ecological informations are currently available on this phytophagous species, more studies are needed to better characterize biological traits, host specificity, duration of immature stages, number of generations, fecundity, and longevity of adults. More information is also needed on its natural distribution in the Western Palaearctic region.

Species of *Tetramesa* are frequently parasitized by other chalcid wasps or exploited by inquilines. These antagonistic species appear to be also highly specialized on one or a few host species (Dawah et al. 1995, 2002; Dubbert et al. 1998; Matsumoto

and Saigusa 2001). During our field surveys, we discovered that *T. amica* is parasitized by *E. amicophaga* Lotfalizadeh, sp. nov. Females of this species exhibits fusiform flagellomeres (Fig. 3C), a relatively long marginal vein ( $1.2 \times$  as long as stigmal vein) (Fig. 3B), and a horizontal ovipositor (Fig. 4C) which indicate that *Eurytoma amicophaga* Lotfalizadeh, sp. nov. belongs to the *appendigaster* species group as outlined in Claridge (1959) and Lotfalizadeh et al. (2007) (named the *phragmiticola* species group by Zerova (2010)). This species group contains parasitoids of *Tetramesa* species developing in grass stems. The exact biology of this parasitoid remains to be discovered, and studies are requested to better evaluate parasitism rates of *E. amicophaga* and how it may affect the performance of *T. amica* to control medusahead.

## Acknowledgements

The authors are grateful to all colleagues and friends who contributed to the study in some way. Many of them supported our activities: Francesca Di Cristina and Silvia Barlattani (BBCA onlus, Rome, Italy) with technical support; Emilio Guerrieri (IPSP-CNR, Portici, Naples, Italy); Raffaele Sasso (ENEA, Casaccia, Rome, Italy) with their scientific support; Celso Azevedo and Anelia M. Stojanova for review of the manuscript, and the subject editor Andreas Köhler for his valuable help to improve this article.

## References

- Al-Barrak M, Loxdale Fls HD, Brookes CP, Dawah HA, Biron DG, Alsagair O (2004) Molecular evidence using enzyme and RAPD markers for sympatric evolution in British species of *Tetramesa* (Hymenoptera: Eurytomidae). *Biological Journal of the Linnean Society* 83: 509–525. <https://doi.org/10.1111/j.1095-8312.2004.00408.x>
- Archer A (2001) *Taeniatherum caput-medusae*. In: Fire Effects Information System. U.S. Department of Agriculture, Forest Service, Rocky Mountain Research station, Fire Sciences Laboratory. [www.fs.fed.us/database/feis/](http://www.fs.fed.us/database/feis/)
- Casagrande RA, Häfliger P, Hinz HL, Tewksbury L, Blossey B (2018) Grasses as appropriate targets in weed biocontrol: is the common reed, *Phragmites australis*, an anomaly? *BioControl* 63: 391–403. <https://doi.org/10.1007/s10526-018-9871-y>
- Claridge MF (1958) *Tetramesa* Walker 1848, a valid name for *Isosoma* Walker 1832 in place of *Harmolita* Motschulsky 1863, with a short discussion of some eurytomid genera (Hym., Eurytomidae). *The Entomologist's Monthly Magazine* 94: 81–85.
- Claridge MF (1959) The identity of *Eurytoma appendigaster* (Swederus, 1795) (Hym., Eurytomidae), together with descriptions of some closely allied species from Gramineae. *Entomologist's Monthly Magazine* 95: 2–13.
- Claridge MF (1961) A contribution to the biology and taxonomy of some Palaearctic species of *Tetramesa* Walk. (*Isosorna* Walk.; *Harmolita* Motsch.) (Hymenoptera: Eurytomidae) with

- particular reference to the British fauna. Transactions of the Entomological Society of London 113: 175–217. <https://doi.org/10.1111/j.1365-2311.1961.tb00807.x>
- Claridge MF, Dawah HA (1994) Assemblages of herbivorous chalcid wasps and their parasitoids associated with grasses – problems of species and specificity. In: Williams MAJ (Ed.) Plant galls: organisms, interactions, populations. Systematics Association Special Volume no. 49. Clarendon Press, Oxford, 313–329.
- Cristofaro M, Roselli G, Marini F, de Lillo E, Petanovic RU, Vidovic B, Augé M, Rector BG (2020) Open field evaluation of *Aculodes altamurgensis*, a recently described eriophyid species associated with medusahead (*Taeniatherum caput-medusae*). Biocontrol Science and Technology 30(4): 339–350. <https://doi.org/10.1080/09583157.2019.1711021>
- Dawah HA (1987) Biological species problems in some *Tetramesa* (Hymenoptera: Eurytomidae). Biological Journal of the Linnean Society 32: 237–245. <https://doi.org/10.1111/j.1095-8312.1987.tb00431.x>
- Dawah HA, Hawkins BA, Claridge MF (1995) Structure of the parasitoid communities of grass-feeding chalcid wasps. Journal of Animal Ecology 64: 708–720. <https://doi.org/10.2307/5850>
- Dawah HA, Al-Haddah FH, Jervis MA (2002) Morphological and biological characterization of three closely related species of *Pediobius* Walker (Hymenoptera: Eulophidae). Journal of Natural History 36: 423–433. <https://doi.org/10.1080/00222930010023501>
- Dubbert M, Tschartnke T, Vidal S (1998) Stem-boring insects of fragmented *Calamagrostis* habitats: herbivore-parasitoids community structure and the unpredictability of grass shoot abundance. Ecological Entomology 23: 271–280. <https://doi.org/10.1046/j.1365-2311.1998.00126.x>
- Erdős J (1969) Aliquot species novae Hungariae in familia Eurytomidarum (Hym., Chalcidoidea). Annales Historico-Naturalis Musei Nationalis Hungarici 61: 337–449.
- Graham MWR de V (1974) New species of *Tetramesa* Walk. and *Eurytoma* Illig. from England (Hymenoptera: Eurytomidae). Folia Entomologica Hungarica 27: 73–80.
- Goolsby JA, Moran P (2009) Host range of *Tetramesa romana* Walker (Hymenoptera: Eurytomidae), a potential biological control of giant reed, *Arundo donax* L. in North America. Biological Control 49(2): 160–168. <https://doi.org/10.1016/j.biocontrol.2009.01.019>
- Goolsby JA, Moran PJ, Racelis AE, Summy KR, Jimenez MM, Lacewell RD, Perez de Leon A, Kirk AA (2016) Impact of the biological control agent *Tetramesa romana* (Hymenoptera: Eurytomidae) on *Arundo donax* (Poaceae: Arundinoideae) along the Rio Grande River in Texas. Biocontrol Science and Technology 26: 47–60. <https://doi.org/10.1080/09583157.2015.1074980>
- Harris RA (1979) A glossary of the surface sculpturing. Occasional Papers in Entomology of the California Department of Food and Agriculture 28: 1–31. <http://doi.org/10.5281/zenodo.26215>
- Henneicke K, Dawah HA, Jervis MA (1992) Taxonomy and biology of final-instar larvae of some Eurytomidae (Hymenoptera: Chalcidoidea) associated with grasses in the UK. Journal of Natural History 26(5): 1047–1087. <https://doi.org/10.1080/00222939200770621>
- Heraty J, Hawks D (1998) Hexamethylsilazane—a chemical alternative for drying insects. Entomological News 109: 369–374.

- Hilken TO, Miller RF (1980) Medusahead (*Taenia-therum asperum* Nevski): A review and annotated bibliography. Oregon State University Agricultural Experiment Station Bulletin 644, Corvallis.
- Kyser GB, DiTomaso JM, Davies KW, Davy JS, Smith BS (2014) Medusahead management guide for the Western States. University of California: Weed Research and Information Center, Davis, 68 pp. <https://wric.ucdavis.edu> [Accessed on 10 Jan 2019]
- Lotfalizadeh H, Delvare G, Rasplus J-Y (2007) Phylogenetic analysis of Eurytominae based on morphological characters (Chalcidoidea: Eurytomidae). Zoological Journal of the Linnean Society 151: 441–510. <https://doi.org/10.1111/j.1096-3642.2007.00308.x>
- Major JC, McKell CM, Berry LJ (1960) Improvement of medusahead-infested rangeland. California Agricultural Experiment Station Extension Service Leaflet 123: 1–8.
- Matsumoto R, Saigusa T (2001) The biology and immature stages of *Thrybius togashii* Kusigemati (Hymenoptera: Ichneumonidae: Cryptinae), with a description of male. Journal of Natural History 35: 1507–1516. <https://doi.org/10.1080/002229301317067656>
- Moran PJ, Vacek AT, Racelis AE, Pratt PD, Goolsby JA (2017) Impact of the *Arundo* wasp, *Tetramesa romana* (Hymenoptera: Eurytomidae), on biomass of the invasive weed, *Arundo donax* (Poaceae: Arundinoideae), and on revegetation of riparian habitat along the Rio Grande in Texas. Biocontrol Science and Technology 27: 96–114. <https://doi.org/10.1080/09583157.2016.1258453>
- Noyes JS (2020) Universal Chalcidoidea Database. <http://www.nhm.ac.uk/chalcidoids> [Accessed on 10 Jan 2019]
- Peters ML (2013) Genetic and Morphological Variation in *Taeniatherum caput-medusae* (Medusahead): Taxonomic Diversity, Geographic Origins, Multiple Introductions and Founder Effects. Boise State University Theses and Dissertations, 717 pp.
- Phillips WJ (1927) *Eurytoma parva* (Giraud) Phillips and its biology as a parasite of wheat jointworm, *Harmolita tritici* (Fitch). Journal of Agricultural Research Washington 34: 743–758.
- Phillips WJ (1936) A second revision of Chalcid-flies of the genus *Harmolita* (*Isosoma*) of America north of Mexico, with descriptions of twenty new species. Technical Bulletin. United States Department of Agriculture 518: 1–25.
- Rice PM (2005) Grass family: Poaceae. Medusahead, *Taeniatherum caput-medusae* (L.) Nevski. In: Duncan CA, Clark JK (Eds) Invasive plants of range and wildlands and their environmental, economic, and societal impacts. Weed Science Society of America, Lawrence, 171–178 pp.
- Sforza R, Eken C, Hayat R, Widmer TL (2004) First evaluation of *Ustilago phrygica* for the biological control of *Taeniatherum caput-medusae* (Triticeae). XII<sup>ème</sup> Colloque International sur la Biologie des Mauvaises Herbes, Dijon, 31 août – 2 septembre 2004, 1–8.
- Sharp LA, Hironaka M, Tisdale EW (1957) Viability of medusahead seed collected in Idaho. Journal of Range Management 10: 123–126. <https://doi.org/10.2307/3894201>
- Simmonds NW (1976) Evolution of crop plants. Longman, London, 339 pp.
- Spears BM (1978) Taxonomy and bionomics of *Tetramesa* (Hymenoptera: Eurytomidae) associated with certain native grasses of Idaho. PhD Thesis. University of Idaho, USA.

- Spears BM, Barr WF (1985) Effect of jointworms on the growth and reproduction of four native range grasses of Idaho. *Journal of Range Management* 38: 44–46. <https://doi.org/10.2307/3899331>
- Sutton GF, Canavan K, Day MD, Den Breeyen A, Goolsby JA, Cristofaro M, McConnachie AJ, Paterson ID (2019) Grasses as suitable targets for classical weed biological control. *BioControl* 64: 605–622. <https://doi.org/10.1007/s10526-019-09968-8>
- Szelényi G (1968) On some new species of *Tetramesa* Walk., with notes on their parasites (Hymenoptera: Chalcidoidea). *Acta Zoologica Academiae Scientiarum Hungaricae* 1–2: 213–224.
- Witt ABR, McConnachie AJ (2003) The potential for classical biological control of invasive grass species with special reference to invasive *Sporobolus* spp. (Poaceae) in Australia. In: Cullen JM, Briese DT, Kriticos DJ, Lonsdale WM, Morin L, Scott JK (Eds) *Proceedings of the XI International Symposium on Biological Control of Weeds*. CSIRO Entomology, Canberra, 198–202.
- Zerova MD (1965) Species of the genus *Tetramesa* Wlk. (Hymenoptera, Eurytomidae) that damage *Stipa*, *Bromus* and *Zerna* in the Ukraine. *Entomologicheskoe Obozrenie* 44(3): 632–648.
- Zerova MD (1967) Species of *Tetramesa* Walk (Hymenoptera: Eurytomidae) in the Ukrainian fauna. *Vestnik Zoologii* 3: 29–37.
- Zerova MD (1976) Hymenoptera. Part 6. Family Eurytomidae; subfamilies Rileyinae and Harmolitinae. *Fauna SSSR*. Vol. 110. Academy of Science of the USSR, Zoological Institute, St. Petersburg, 230 pp.
- Zerova MD (1977) New species of the genus *Eurytoma* Illiger (Hymenoptera, Chalcidoidea, Eurytomidae) from the European part of the USSR. *Novye i Malozvestnye Vid Nasekomich Evropeyskoy Chasti SSSR* 1977: 89–93.
- Zerova MD (1978) Hymenoptera Parasitica. Chalcidoidea – Eurytomidae. *Fauna Ukrainy*. Vol. 11, is. 9. Academy of Science of Ukraine SSR, Institute of Zoology, Kiev, 465 pp.
- Zerova MD (2010) Palearctic species of the genus *Eurytoma* (Hymenoptera, Chalcidoidea, Eurytomidae): morphological and biological peculiarities, trophic associations and key to determination. *Vestnik Zoologii, Kiev Supplement* 24: 1–203.



# Corrigenda: The first survey of the beetles (Coleoptera) of the Farasan Archipelago of the southern Red Sea, Kingdom of Saudi Arabia. ZooKeys 959: 17–86. <https://doi.org/10.3897/zookeys.959.51224>

Mahmoud S. Abdel-Dayem<sup>1</sup>, Jiří Háva<sup>2</sup>

**1** King Saud University Museum of Arthropods (KSMA), Plant Protection Department, College of Food and Agriculture Sciences, King Saud University, Riyadh, 11451, Saudi Arabia **2** Forestry and Game Management Research Institute, Strnady 136, CZ-252 02 Praha 5 - Zbraslav, Czech Republic

Corresponding author: Mahmoud S. Abdel-Dayem ([mseleem@ksu.edu.sa](mailto:mseleem@ksu.edu.sa))

---

Academic editor: L. Penev | Received 8 December 2020 | Accepted 9 December 2020 | Published 18 December 2020

---

<http://zoobank.org/2E2DB5FB-005E-4E5E-A6C4-017C0BE4DCCA>

---

**Citation:** Abdel-Dayem MS, Háva J (2020) Corrigenda: The first survey of the beetles (Coleoptera) of the Farasan Archipelago of the southern Red Sea, Kingdom of Saudi Arabia. ZooKeys 959: 17–86. <https://doi.org/10.3897/zookeys.959.51224>. ZooKeys 1005: 151–152. <https://doi.org/10.3897/zookeys.1005.61812>

---

In Abdel-Dayem MS, Abu El-Ghiet UM, Elsheikh TM, Elgharbawy AA, Al-Fifi ZIA, Aldhafer HM (2020) The first survey of the beetles (Coleoptera) of the Farasan Archipelago of the southern Red Sea, Kingdom of Saudi Arabia. ZooKeys 959: 17–86.

After the publication of the work referenced above, our attention was drawn to misidentified species of Dermestidae *Attagenus obtusus* (Gyllenhal in Schönherr, 1808). The correct identification for this species is *Orbeola hirsutululum* (Reiche in Mulsant et Rey, 1868). Other corrections are as follows:

**Page 1, “Abstract” line 13:** “... Arabian and Afrotropical elements (74 spp., 41.0%).” should be

“..... Arabian and Afrotropical elements (75 spp., 41.9%).”

**Page 34, line 25:** “41. *Attagenus obtusus* (Gyllenhal in Schönherr, 1808)” should be “41. *Orbeola hirsutululum* (Reiche in Mulsant et Rey, 1868)”

**Page 34, line 28:** The paragraph under “Literature records” should read:  
“Riyadh (Mroczkowski 1979).”

**Page 34–35, line 32:** The paragraph under “General distribution” should read:  
“AFR-SAR species, distributed in East Africa (Eritrea); Levant, Turkmenistan and Arabian Peninsula (KSA, United Arab Emirates, Yemen).”

**Page 77, line 10:** “that 41.3% of the species belong to Saharo-Arabian .....” should be  
“that 41.9% of the species belong to Saharo-Arabian ....”

**Page 79, lines 4–6:** “... whereas only 28 of Farasan Archipelago’s 179 species (15.6%) are shared with the 645 species currently known from the Socotran fauna, half (50%, 14 spp.) of which ....” should be

“... whereas only 29 of Farasan Archipelago’s 179 species (16.2%) are shared with the 645 species currently known from the Socotran fauna, about half (50%, 15 spp.) of which ....”

**Page 79, line 16:** “Only 15.6% of its species are shared .....” should be  
“Only 16.2% of its species are shared ....”

**Page 79, Table 1:** In 20<sup>th</sup> row 20 “Dermestidae”: 4<sup>th</sup> column: “1 (3)” should be “2 (3)” and 5<sup>th</sup> column: “0.6% (2.1%)” should be “1.1% (2.1%)”

## References

Abdel-Dayem MS, Abu El-Ghiet UM, Elsheikh TM, Elgharbawy AA, Al-Fifi ZIA, Aldhaffer HM (2020) The first survey of the beetles (Coleoptera) of the Farasan Archipelago of the southern Red Sea, Kingdom of Saudi Arabia. *ZooKeys* 959: 17–86. <https://doi.org/10.3897/zookeys.959.51224>